Characterization of an ADP-ribosylation factor family member involved in endomembrane system and iron acquisition regulation

Inaugural-Dissertation

zur Erlangung des Doktorgrades
der Mathematisch-Naturwissenschaftlichen Fakultät
der Heinrich-Heine-Universität Düsseldorf

vorgelegt von

Inga Mohr
aus Oberhausen

Düsseldorf, Oktober 2021

aus dem Institut für Botanik
der Heinrich-Heine-Universität Düsseldorf

Gedruckt mit der Genehmigung der
Mathematisch-Naturwissenschaftlichen Fakultät der
Heinrich-Heine-Universität Düsseldorf

Berichterstatter:

1. Prof. Dr. Petra Bauer

2. Prof. Dr. Kai Stühler

Tag der mündlichen Prüfung:
17.12.2021

Eidesstattliche Erklärung

Ich versichere an Eides Statt, dass die Dissertation von mir selbständig und ohne unzulässige fremde Hilfe unter Beachtung der „Grundsätze zur Sicherung guter wissenschaftlicher Praxis an der Heinrich-Heine-Universität“ erstellt worden ist.

Ich habe die Dissertation in dieser oder ähnlicher Form bisher keiner anderen Fakultät vorgelegt.

Ich habe bisher keine erfolglosen Promotionsversuche unternommen.

Inga Mohr

Düsseldorf, 28.10.2021

Table of Contents

1. Preface

This work is divided into three parts. First of all, the work is summarized, both in English and in German. This is followed by an introduction about iron deficiency in plants and its transcriptional regulation, as well as the post-transcriptional regulation of the iron transporter IRT1 as a model system for plasma membrane protein trafficking in the endomembrane system. This part ends with the presentation of the thesis objectives. The second part represents the main part of this work and consists of three manuscripts.

1. **ARF and ARF-like GTPases and their respective GEFs and GAPs in *Arabidopsis thaliana***

   Inga Mohr, Rumen Ivanov and Petra Bauer *-in preparation*

The first manuscript, a review, gives a glance on small GTPases in general and describes structural aspects of the GTPase activation cycle with respect to their guanine nucleotide exchange factors (GEF) and GTPase-activating proteins (GAPs). It summarizes the current knowledge of the ARF-like GTPases and the ARF-GEFs and -GAPs in *Arabidopsis thaliana*.

2. **The small ARF-like GTPase TTN5 is linked to IRT1 within the endomembrane system**

   Inga Mohr, Regina Gratz, Kalina Angrand, Monique Eutebach, Lara Genders, Karolin Montag, Merina Rubek Basgaran, Tzvetina Brumbarova, Petra Bauer and Rumen Ivanov *-in preparation*

In the second manuscript we identified the small ARF-like GTPase TITAN 5 (TTN5) as a novel interactor of the cytosolic loop with a variable and regulatory region of IRT1. We located TTN5 in endomembrane compartments where it colocalized with IRT1. Additional interactions with the IRT1 regulators ENHANCED BENDING 1 (EHB1) and SORTING NEXIN 1 (SNX1) led to the suggestion of TTN5 being a coordinator of IRT1 sorting and cycling between the plasma membrane and the vacuole.

3. **Interactomics of IRT1 regulators in the iron homeostasis**

   Inga Mohr, Pichaporn Chuenban, Monique Eutebach, Claudia von der Mark, Gereon Poschmann, Daniel Waldera-Lupa, Kai Stühler, Petra Bauer and Rumen Ivanov *-in preparation*

The third manuscript consists of an IP-MS-based interactome study of TTN5, in comparison with the IRT1-regulators EHB1 and PATELLIN 2 (PATL2) and the Fe-related IRON DEFICIENCY-INDUCED 1 (IDI1). We obtained several interconnections between the interactomes and to Fe-related processes, like Fe chelation and distribution as well as oxidative stress responses. Identification of H^+-ATPases 1 (AHA1) as interactor of TTN5 and their colocalization in vesicle-like structures, promoting TTN5 role in PM protein trafficking.

The last part contains the concluding remarks that we can draw from the findings of this work.

2. Summary

To avoid iron-related stresses, the main Arabidopsis iron importer, IRON-REGULATED TRANSPORTER 1 (IRT1), undergoes a multi-level post-translational regulation ensuring its controlled activity and abundance at the plasma membrane. A major factor in IRT1 regulation is its dynamic trafficking away from and towards the plasma membrane, achieved through cycles of endocytosis and endosomal recycling. The IRT1 regulatory network is a model system of plasma membrane protein trafficking, but large parts of the endomembrane cycling machinery remain elusive and are of great interest in the field of IRT1-related iron homeostasis and intracellular trafficking. The small ADP-ribosylation factor (ARF) GTPases are key signaling regulators of vesicle-mediated protein trafficking by switching between an active GTP-bound and an inactive GDP-bound conformation, with the help of guanine nucleotide exchange factors (GEFs) and GTPase-activating proteins. Though closely related to ARF GTPases, the ARF-likes and their functions are poorly understood, especially in plants. We identified the small ARF-like GTPase TITAN 5 (TTN5) as a novel IRT1 interactor. Colocalization analysis with compartment markers, combined with pharmacological treatments, enabled us to pinpoint the TTN5 localization in the endomembrane system. Together with IRT1, TTN5 colocalized in vesicles of the *trans*-Golgi network and multivesicular bodies, implying a role of TTN5 in IRT1 trafficking. TTN5 interacted with the IRT1-regulators ENHANCED BENDING 1 (EHB1), SORTING NEXIN 1 (SNX1) and PATELLIN 2 (PATL2) as well, suggesting an important coordinating function in iron uptake. At the same time, physiological data indicated a positive influence of TTN5 on iron homeostasis.

To obtain a better understanding of TTN5 and the events influencing its function, we employed immunoprecipitation-mass spectrometry to investigate the interactome of TTN5 in comparison with the IRT1 regulators EHB1 and PATL2 and the iron-related protein IRON DEFICIENCY-INDUCED 1 (IDI1). The plasma membrane H^+-ATPases AHA1 and AHA2 were identified as TTN5 interactors. Fluorescence microscopy revealed, similarly to IRT1, a colocalization of TTN5 together with AHA1 in vesicle-like structures of the endomembrane system. We propose a potential function of TTN5 in plasma membrane protein trafficking. We also identified SEC12, an ER-anchored GEF protein involved in vesicle trafficking and potentially a GEF for TTN5.

Our findings on the function of TTN5 and its interactome are important new information for both the regulation of plant nutrient import and the role of the understudied ARF-like GTPases in Arabidopsis endomembrane trafficking. The data focuses the spotlight on the endomembrane system as an important factor for studies on plant breeding and biofortification.

3. Zusammenfassung

Um eisenbedingten Stress zu vermeiden, unterliegt der wichtigste Eisenimporter in Arabidopsis, IRON-REGULATED TRANSPORTER 1 (IRT1), einer mehrstufigen posttranslationalen Regulierung, die seine kontrollierte Aktivität und Menge an der Plasmamembran gewährleistet. Ein wichtiger Faktor bei der Regulierung von IRT1 ist dessen dynamischer Transport von der Plasmamembran weg und zu ihr hin, der durch Zyklen der Endozytose und des endosomalen Recyclings erfolgt. Das IRT1-Regulierungsnetzwerk ist ein Modellsystem für den Plasmamembran-Proteintransport, aber große Teile der Endomembran-Zyklusmaschinerie sind nach wie vor nicht bekannt oder eindeutig geklärt und von großem Interesse im Bereich der IRT1-bezogenen Eisenhomöostase und des intrazellulären Transports. Die kleinen ADP-Ribosylierungsfaktor (ARF)-GTPasen sind wichtige Signalregulatoren des Vesikel-vermittelten Proteintransports, indem sie mit Hilfe von Guaninnukleotid-Austauschfaktoren (GEFs) und GTPase-aktivierenden Proteinen zwischen einer aktiven GTP-gebundenen und einer inaktiven GDP-gebundenen Konformation wechseln. Obwohl sie eng mit den ARF-GTPasen verwandt sind, sind die ARF-ähnlichen GTPasen und ihre Funktionen insbesondere in Pflanzen kaum erforscht. Wir identifizierten die kleine ARF-ähnliche GTPase TITAN 5 (TTN5) als einen neuen IRT1-Interaktor. Durch eine Kolokalisierungsanalyse mit Kompartimentmarkern in Kombination mit pharmakologischen Behandlungen konnten wir die Lokalisierung von TTN5 im Endomembransystem bestimmen. Zusammen mit IRT1 kolokalisierte TTN5 in Vesikeln des *trans*-Golgi-Netzwerks und in multivesikulären Körperchen, was auf eine Rolle von TTN5 beim IRT1-Transport hindeutet. TTN5 interagierte auch mit den IRT1-Regulatoren ENHANCED BENDING 1 (EHB1), SORTING NEXIN 1 (SNX1) und PATELLIN 2 (PATL2) und lässt auf eine wichtige koordinierende Funktion bei der Eisenaufnahme schließen. Gleichzeitig weisen physiologische Daten auf einen positiven Einfluss von TTN5 auf die Eisenhomöostase hin. Um TTN5 und dessen funktionsbeeinflussende Ereignisse, besser zu verstehen, untersuchten wir mit Hilfe der Immunpräzipitations-Massenspektrometrie das Interaktom von TTN5. Dies geschah im Vergleich mit den IRT1-Regulatoren EHB1 und PATL2 und dem eisenregulierten Protein IRON DEFICIENCY-INDUCED 1 (IDI1). Die Plasmamembran H^+-ATPasen AHA1 und AHA2 wurden dabei als TTN5-Interaktoren identifiziert. Fluoreszenzmikroskopie zeigte, ähnlich wie bei IRT1, eine Kolokalisierung von TTN5 zusammen mit AHA1 in vesikelartigen Strukturen des Endomembransystems. Wir vermuten eine mögliche Funktion von TTN5 beim Transport von Plasmamembranproteinen. Wir identifizierten auch SEC12, ein ER-verankertes GEF-Protein, das am Vesikel-Transport beteiligt ist und möglicherweise ein GEF für TTN5 ist.

Unsere Erkenntnisse über die Funktion von TTN5 und sein Interaktom sind wichtige neue Informationen sowohl für die Regulierung des pflanzlichen Nährstoffimports als auch für die Rolle der bisher wenig untersuchten ARF-ähnlichen GTPasen im Endomembran-Transport von Arabidopsis. Die Daten rücken dabei das Endomembransystem als wichtigen Faktor für Studien zur Pflanzenzüchtung und Biofortifikation in den Fokus.

4. Introduction

Proper nutrition is the prerequisite for healthy and fertile plant development. The basic essential building blocks are macro- and micronutrients. Primary macronutrients are nitrogen, phosphorus and potassium, whereas typical micronutrients are metals like zinc, manganese, copper and iron (Fe). Fe belongs to the four most abundant elements in the earth crust, only oxygen, silicon and aluminum are more enriched (Wedepohl, 1995). It is of great importance as a typical cofactor for many enzymes due to its ability to change redox state. In mitochondria, Fe is present in iron-sulfur clusters or heme proteins of the respiratory chain complexes, whereas in chloroplasts these are essential in the photosystems (Nouet et al., 2011; Balk and Schaedler, 2014). A disturbed photosynthesis due to lack of Fe leads to leaf chlorosis, a phenotypical symptom of Fe deficiency. But also an oversupply has toxic effects for plants and is visible by leaf bronzing. Accumulating Fe can lead to the formation of reactive oxygen species (ROS) in the Fenton reaction resulting in cellular damages, like lipid peroxidation in the membranes (Halliwell and Gutteridge, 1992; Distéfano et al., 2020; Gratz et al., 2021). Due to plants sessile nature, they need to cope with their direct environmental conditions. Though quite abundant, soil Fe is mostly present in its ferric (Fe^{3+}) form due to oxidation induced by the rise of atmospheric oxygen in the Great Oxidation Event (Kump, 2008). Especially in calcareous soils or at high pH, it is present mostly in insoluble complexed Fe^{3+}. Plants evolved two main root uptake strategies to cope with the lack of iron. Typical for dicotyledonous plants and non-graminaceous monocots is a reduction-based strategy, also called Strategy I, Strategy II, which is based on chelation, is present in grasses (Römheld and Marschner, 1986; Ivanov et al., 2012; Kobayashi and Nishizawa, 2012; Brumbarova et al., 2015; Riaz and Guerinot, 2021).

4.1. Strategy I in Arabidopsis - a reduction-based strategy

Arabidopsis, a non-graminaceous plant, is using Strategy I for Fe uptake. Strategy I takes place mainly by a process of three major steps carried out by plasma membrane (PM) proteins in the root epidermis (Figure 1). At first, the complexed soil Fe^{3+} is solubilized by an acidification of the local rhizosphere. This is carried out by one member of the Arabidopsis H^+-ATPase family, AHA2. It extrudes protons from the inside and leads to the essential lowering of the pH for Fe^{3+} solubilization (Santi and Schmidt, 2009; Brumbarova et al., 2015). The metal ions are present in their Fe^{3+} state and need to be reduced to ferrous Fe (Fe^{2+}). The reduction is catalyzed by the FERRIC REDUCTASE-OXIDASE (FRO) family protein, FRO2. This step of Fe acquisition is assumed to be the rate-limiting one of Fe uptake (Eide et al., 1996; Yi and Guerinot, 1996; Robinson et al., 1999). The last step is the actual uptake of the reduced Fe^{2+} into the root. Fe^{2+} is imported by the divalent metal ion transporter IRON-REGULATED

TRANSPORTER 1 (IRT1) (Eide et al., 1996; Vert et al., 2002). Recent data is indicating a complex formation of AHA2, FRO2 and IRT1, suggesting an optimization of the Fe uptake (Martín-Barranco et al., 2020).

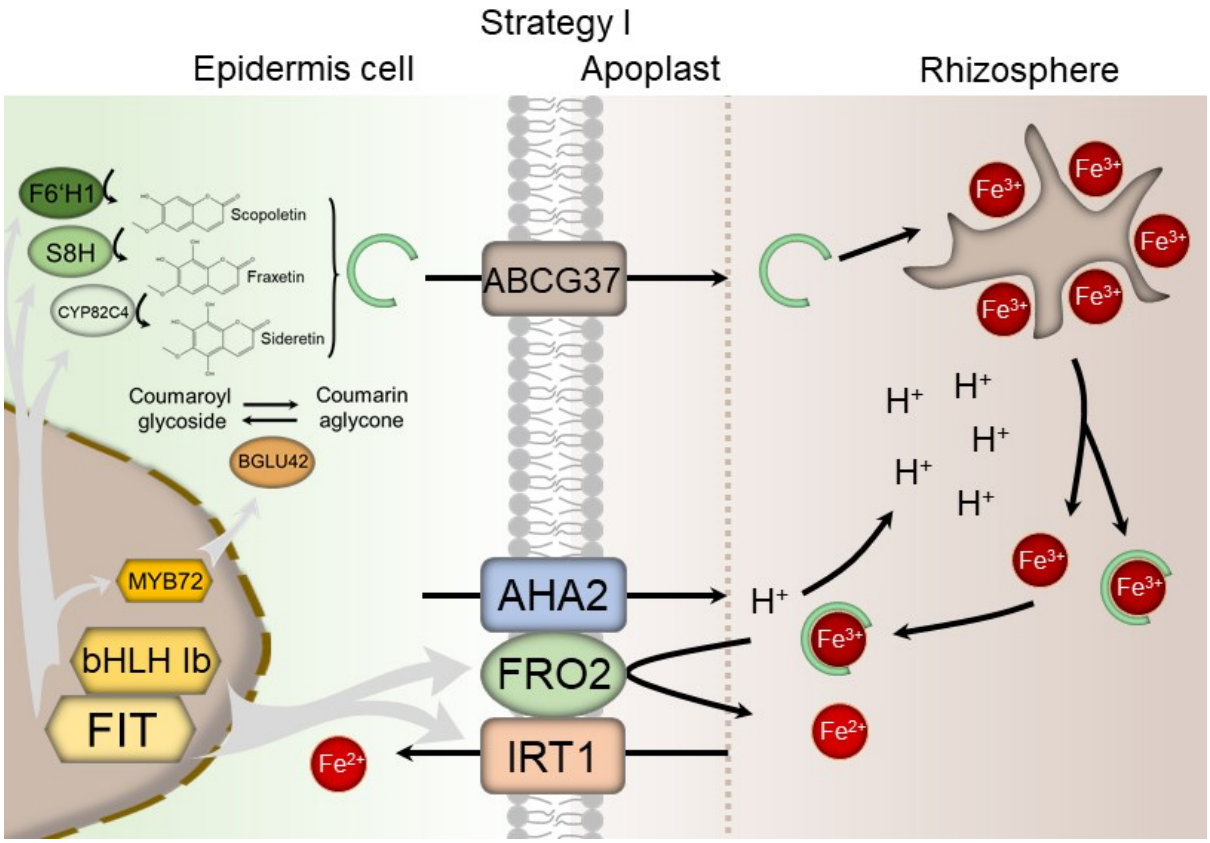

Figure 1. Plant iron uptake strategy I.
Model plant *Arabidopsis thaliana* is using Strategy I for Fe uptake. It is a mainly three major steps process of PM proteins in the root epidermis. Complexed soil Fe is solubilized by local rhizosphere acidification carried out by AHA2. Ferric Fe (Fe^{3+}) is reduced to ferrous Fe (Fe^{2+}) by FRO2. Fe^{2+} is imported by IRT1. Fe deficiency is leading to the secretion of fluorescent phenolic compounds, coumarins (green circles), by ABCG37. These compounds, like scopoletin, fraxetin and sideretin can chelate Fe^{3+} facilitating the reduction and subsequent Fe import. The production of scopolin and scopoletin is MYB72-dependent and the activity of BGLU42 is needed for scopolin deglycosylation and the following secretion into the rhizosphere. *IRT1* and *FRO2* and the genes *F6'H1*, *S8H*, *CYP82C4* and *MYB72*, related to coumarin secretion are transcriptionally up-regulated (grey arrows) upon Fe deficiency by a FIT-bHLH Ib-heterodimer.

Next to this three-step process, Fe deficiency is also leading to the secretion of fluorescent phenolic compounds. These compounds, coumarins, can chelate and reduce Fe^{3+} (Fourcroy et al., 2014; Tsai et al., 2018). The ATP-BINDING CASSETTE G37/PLEIOTROPIC DRUG RESISTANCE 9 (ABCG37/PDR9, from here on only called ABCG37) transporter is a key player in Arabidopsis coumarin secretion, like scopoletin, esculetin, sideretin and fraxetin, into the rhizosphere (Fourcroy et al., 2014). Coumarin biosynthesis initiates from produced feruloyl-CoA. This is further processed to 6'-hydroxyferuloyl-CoA by the FERULOYL-CoA 6'-HYDROXYLASE, F6'H1 and the coumarin scopoletin emerges by spontaneous *trans/cis* isomerization and lactonization (Kai et al., 2008). Scopoletin can be further converted to fraxetin

by SCOPOLETIN 8-HYDROXYLASE (S8H) and then to sideretin by the Cytochrome P450 CYP82C4 (Rajniak et al., 2018). The Fe chelation is assumed to greatly facilitate the reduction and subsequent Fe import (Schmid et al., 2014; Tsai and Schmidt, 2017) and indicating similarities between both Fe uptake strategies.

4.2. Strategy II – chelation-based

Grasses take up Fe by the chelation-based mechanism, called Strategy II. They bypass the need of reducing Fe^{3+} to Fe^{2+} by the ability of importing complexed Fe^{3+}. Under Fe deficiency, grasses release small organic compounds, more precisely phytosiderophores of the mugineic acid family. These compounds are secreted by the TRANSPORTER OF MUGINEIC ACID (TOM1) (Nozoye et al., 2011). The phytosiderophore-Fe^{3+} complexes are taken up by the YELLOW STRIPE (YS) transporter family, like YS1 in maize or YS-LIKE15 (OsYSL15) in rice (Curie et al., 2001; Inoue et al., 2009). IRT1 homologs in *Oryza sativa*, OsIRT1 and OsIRT2, are able to directly take up Fe^{2+} similar to Strategy I and make the two strategies seem less distinctive from each other (Bughio et al., 2002; Ishimaru et al., 2006). Similar was proposed for other *Oryza* species on transcriptomic data making the so called Combined Strategy a typical *Oryza* feature (Wairich et al., 2019). A possible explanation, especially with respect to the lack of acidification and reduction processes, can be the adaption to flooded rice paddies, containing high amounts of soluble Fe^{2+} (Walker and Connolly, 2008).

4.3. Transcriptional regulation of Fe acquisition

A regulatory network of the Fe uptake machinery is indispensable with regard to essential and toxic Fe properties. Identification of transcription factor FER in tomato was a first step in the identification of transcriptional regulation in iron deficiency response (Ling et al., 2002; Ivanov et al., 2012). A homolog in Arabidopsis was identified as the basic helix-loop-helix (bHLH) protein 029 (bHLH029) and named FER-LIKE IRON DEFICIENCY INDUCED TRANSCRIPTION FACTOR (FIT) (Ling et al., 2002; Bauer et al., 2004; Colangelo and Guerinot, 2004; Jakoby et al., 2004). It belongs to bHLH subgroup IIIa and can form heterodimers with another bHLH protein of subgroup Ib, bHLH038, bHLH039, bHLH100 or bHLH101 (Yuan et al., 2008; Wang et al., 2013). Under Fe deficiency, FIT heterodimer is up-regulating the expression of the main Strategy I genes, *FRO2* and *IRT1*, to promote Fe uptake (Colangelo and Guerinot, 2004; Jakoby et al., 2004; Yuan et al., 2008; Ivanov et al., 2012).

FIT itself as well as *bHLH038*, *bHLH039*, *bHLH100* and *bHLH101* are induced upon Fe deficiency (Wang et al., 2007). Indeed, bHLH transcription factors of clade IVc, bHLH034, bHLH104, bHLH105/ILR3 and bHLH115, form homo- and heterodimers and thereby regulating the induction of subgroup Ib, with subsequent up-regulation of the Fe deficiency response

(Zhang et al., 2015; Li et al., 2016; Liang et al., 2017; Gao et al., 2019). Recently, the probably phosphorylated bHLH121/UPSTREAM REGULATOR OF IRT1 (URI) of subgroup IVb was identified as part of heterodimers with IVc bHLHs for *bHLH Ib* up-regulation and their targets *IRT1* and *FRO2* (Gao et al., 2019; Kim et al., 2019; Lei et al., 2020). Next to it, it seems to be important for the induction of another IVc bHLHs target, *bHLH047*/*POPEYE* (PYE), which is up-regulated due to Fe deficiency as well (Long et al., 2010; Gao et al., 2019; Kim et al., 2019). PYE is repressing the expression of several Fe deficiency-induced genes, such as *NAS4* and *FRO3*. Together with PYE, bHLH105/ILR3 is inhibiting the expression of Fe homeostasis genes, being both an activator and repressor.

A transcriptional regulation of *FIT* requires FIT. The heterodimer bHLH039-FIT is up-regulating *FIT* expression (Wang et al., 2007; Naranjo-Arcos et al., 2017), but FIT activity is further regulated by post-translational modification. As one example, FIT protein was described to be present in inactive and active pools, whereas the active one is phosphorylated at Ser-272 by CBL-INTERACTING PROTEIN KINASE 11 (CIPK11) in Fe-deficient conditions (Gratz et al., 2019).

Additionally, transcriptional regulation is also a key point in coumarin synthesis and secretion. The production of scopolin and scopoletin is MYB72-dependent and the activity of BETA-GLUCOSIDASE 42 (BGLU42) is needed for scopolin deglycosylation and the following secretion into the rhizosphere (Stringlis et al., 2018). *MYB72* belongs to the highly induced transcription factors upon Fe deficiency in a FIT-dependent manner (Colangelo and Guerinot, 2004; Dinneny et al., 2008; Sivitz et al., 2012). *ABCG37* and *F6'H1* are up-regulated under Fe deficiency in a FIT-dependent manner as well (Colangelo and Guerinot, 2004; Yang et al., 2010; Schmid et al., 2014).

4.4. Plasma membrane protein cycling in the endomembrane system

PM proteins undergo a constant turnover to regulate their activity (Figure 2). They are synthesized at the endoplasmic reticulum (ER) and then transported via the Golgi to the PM. Their activity at the PM is regulated by different approaches with one being the removal from the PM which is achieved by endocytosis. Endocytosis has different reasons. It leads either to the protein degradation or is a necessary step in the constitutive regulation of PM proteins abundance. Once endocytosed they can follow two different routes. They can be either targeted to the vacuole and degraded or sorted for recycling back to the PM (Schwihla and Korbei, 2020; Ivanov and Vert, 2021).

4.4.1. Clathrin-mediated endocytosis

Endocytosis of cargo proteins is carried out by either clathrin-mediated endocytosis (CME) or clathrin-independent endocytosis, e.g. the flotillin-regulated endocytosis, with CME being the

most commonly used pathway (Valencia et al., 2016). CME comprises five steps: nucleation, cargo selection, formation of the clathrin coat, vesicle release by membrane scission and uncoating (McMahon and Boucrot, 2011). During nucleation, a clathrin-coated pit is formed by PM-bending towards the cytoplasm. This formation depends on the recruitment of adaptor and accessory proteins. Such proteins are able to interact with specific membrane lipids and sorting motifs of the cargo and are responsible for the clathrin recruitment from the cytoplasm to the PM. One adaptor protein complex involved in CME is AP-2. It can bind to phosphatidylinositol-4,5-bisphosphate ($PI(4,5)P_2$) at the PM, to the selected cargo and to clathrin (Höning et al., 2005; McMahon and Boucrot, 2011). Another important adaptor complex in Arabidopsis is the TPLATE complex (Gadeyne et al., 2014).

Cargo selection is carried out by endocytic sorting signals, which can be linear amino acid motifs, conformational motifs and posttranslational modifications (Traub and Bonifacino, 2013). One important sorting feature is the posttranslational modification by ubiquitin attachment. Ubiquitination usually happens at Lys residues and can be ranging from a single or several monoubiquitinations to polyubiquitination. The latter is formed by ubiquitin chains of the ubiquitin Lys residues especially of Lys-48 and Lys-63 (Tanno and Komada, 2013).

The cargo recognition leads to the clathrin coat formation. Clathrin consists of three heavy and three light chains, which are arranged in a triskelion (Pearse, 1976). Such triskelia are recruited from the cytoplasm to the PM by the adaptor complexes and form the clathrin coat (Valencia et al., 2016). The final vesicle release is then achieved by membrane scission by dynamin-related proteins. They assemble into a multimeric structure around the neck of the clathrin-coated pit (Chappie and Dyda, 2013). When the mature vesicle is detached from the PM, the clathrin-coat is released to make the vesicle able to fuse with endosomes (Valencia et al., 2016).

4.4.2. Endosomal sorting for recycling or vacuolar degradation

The endocytosed cargo is transported via vesicle-mediated trafficking to the *trans*-Golgi network (TGN), which is the plant equivalent of early endosomes. The TGN is a Golgi-derived compartment and matures from the *trans*-most cisterna and is important for cargo recycling (Dettmer et al., 2006; Lam et al., 2007). The TGN membranes are rich of phosphatidylinositol-4-phosphate (PI4P), but contain nearly no phosphatidylinositol-3-phosphate (PI3P), a typical feature of animal early endosomes (Vermeer et al., 2006; Singh et al., 2014). One component of cargo recycling at the TGN is ADP-ribosylation factor (ARF) -signaling. The ARF family is a subfamily of Ras small GTPases which function is dependent on the interaction with guanine nucleotide exchange factors (GEFs) and GTPase-activating proteins (GAPs), essential for nucleotide exchange and hydrolysis. The ARF-GEF GNOM can localize to the Golgi and the

TGN, functioning in the recycling of PM proteins, like auxin efflux carrier PIN-FORMED 1 (PIN1) and boron transporter BOR1 (Steinmann et al., 1999; Geldner et al., 2003; Yoshinari et al., 2021). GNOM is also functioning in the maintenance of the TGN being indirectly involved in protein recycling (Naramoto et al., 2014). Next to GNOM, the BFA-inhibited GEF (BIG) family is also located and functions at the TGN in protein recycling.

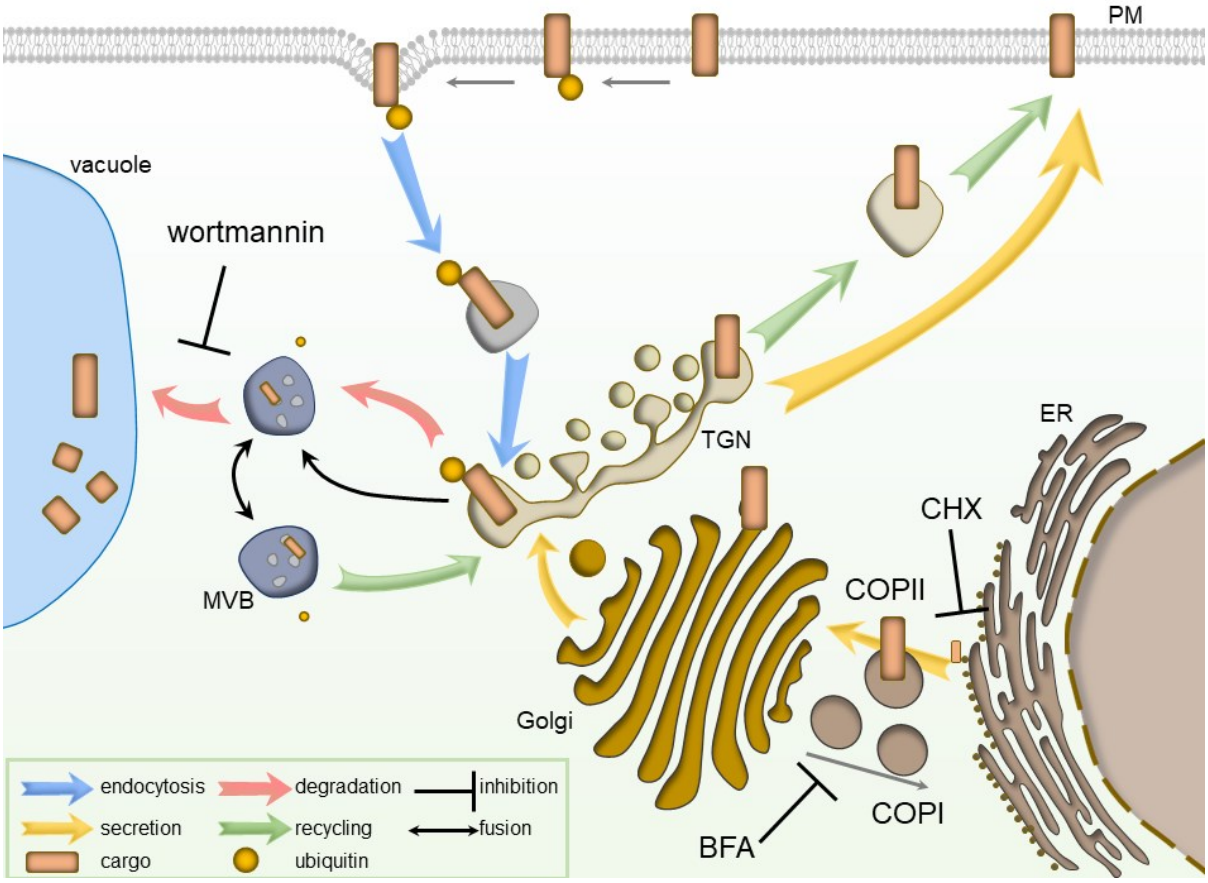

Figure 2. Plasma membrane protein cycling in the endomembrane system.
Plasma membrane (PM) proteins are synthesized at the ER and then secreted to the PM. They are constitutively regulated by a cycle of endocytosis with subsequent degradation in the vacuole or recycling back to the PM. Cargo selection is carried out by endocytic sorting signals, like ubiquitination, a posttranslational modification. The ubiquitinated cargo is endocytosed (blue arrows), mainly by clathrin-mediated endocytosis and transported to the *trans*-Golgi network (TGN). At the TGN, the cargo can be sorted for degradation in the vacuole (red arrows) or for recycling back to the PM (green arrows). In the lytic pathway, the cargo is internalized into intraluminal vesicles of maturing multivesicular bodies (MVBs), which are able to fuse with the vacuole. For the recycling pathway, ubiquitin is removed and cargo-containing vesicles are transported to the PM.
Pharmacological treatments can interfere with pathways of the endomembrane system and facilitate their visualization. Cycloheximide (CHX) blocks the protein synthesis at the ribosomes and allows detection of only endocytic trafficking. Brefeldin A (BFA), inhibits BFA-sensitive ARF-GEFs at the Golgi and interferes with COPI vesicles and the proper TGN maintenance. It leads to the formation of BFA bodies. Wortmannin is blocking function of phosphatidylinositol-3-kinases and prevents vacuolar degradation. It leads to homotypic fusion of MVBs or fusion with the TGN, visible as swollen MVBs.

From the Ras superfamily another subfamily is taken place in vesicle-mediated trafficking, the Ras-like proteins in brain (RABs) (Minamino and Ueda, 2019). They are located at the TGN and additionally, an indicator of another endosomal compartment which arises from the TGN,

the multivesicular bodies (MBVs) (Scheuring et al., 2011; Minamino and Ueda, 2019). MVBs mature from late endosomes by forming intraluminal vesicles (ILV) as a result of internalized membrane-bound cargo. An indicator of late endosomes is next to RAB GTPases the loosening of PI4P with simultaneous enrichment of PI3P (Singh et al., 2014). The recycling of endocytosed cargo in plants is happening in the TGN and the MVBs, with the latter being the last step of sorting fate as they are capable of fusion with the vacuole. The RAB GTPase RABG3F is interacting with another sorting complex, the core retromer, which can thereby bind MVBs. In yeast, the retromer consists of several VACUOLAR PROTEIN SORTING (VPS) proteins and SORTING NEXINS (SNX) (Simonetti and Cullen, 2018). Though SNX proteins are also present in Arabidopsis and take place in the sorting fate of endocytosed cargo, the retromer complex probably acts separately and at a later step in endosomal sorting from the SNX proteins (Heucken and Ivanov, 2018).

MVB maturation depends on the involvement of Endosomal Sorting Complexes Required for Transport (ESCRT). They take place in the sorting of ubiquitinated cargo into intraluminal vesicles to form MVBs (MacDonald et al., 2012). Plants only contain homologs of the ESCRT complexes I-III and lacking ESCRT-0. The function of ESCRT-0 is taken over by TOM1-LIKE (TOL) protein complexes and SRC-HOMOLOGY-3 DOMAIN-CONTAINING PROTEIN 2 (SH3P2) (Korbei et al., 2013; Nagel et al., 2017). They are needed for the recognition of ubiquitinated cargo at the PM and the recruitment of the following steps. ESCRT-I is binding the ubiquitinated cargo at the TGN and recruits the ESCRT-II. The two subunits of ESCRT-I, FYVE1/FYVE DOMAIN PROTEIN REQUIRED FOR ENDOSOMAL SORTING 1 (FREE1) and VPS23A/ELC, and the ESCRT-II complex take place in the maturation of MVBs by forming ILV (Spitzer et al., 2006; Gao et al., 2014). Whereas ESCRT-II can still bind the ubiquitinated cargo, ESCRT-III lacks this ability. This complex is organized and recruited by its upstream components and needed for the membrane scission of intraluminal vesicles (Henne et al., 2012). The final scission step could be missing in plants, leaving a small connection between the intraluminal vesicles, with ESCRT-III functioning as a barrier to keep the cargo internalized (Buono et al., 2017). Depending of the sorting fate of the endocytosed cargo, MVBs either fuse with the tonoplast for cargo degradation or regulate the recycling back to the PM.

4.4.3. Studying endosomal trafficking using pharmacological treatments

Endocytosis and the related sorting and degradation processes are essential for cell survival. Typical knock-out approaches lead to embryo or seedling lethality, making endocytosis more complicated to study. To cope with such problems, transient inhibition of different steps of endocytosis increased importance.

4.4.3.1 Brefeldin A (BFA)

Brefeldin A (BFA) is a fungal metabolite which is commonly used to investigate intracellular transport within the endomembrane system, especially between the ER and the Golgi. It is inhibiting ARF-GEF activity in a reversible process as an uncompetitive inhibitor (Mansour et al., 1999; Peyroche et al., 1999; Jackson and Casanova, 2000). ARF GTPase activation depends on the nucleotide exchange from GDP to GTP, which is achieved by interaction with a respective GEF. Upon binding, a conserved residue, the glutamic finger of the GEF Sec7 domain is inserted in the nucleotide-binding pocket of the GTPase and leads to the release of bound GDP, opening the possibility to bind GTP (Béraud-Dufour et al., 1998; Mossessova et al., 1998; Casanova, 2007). BFA is inhibiting this process by binding to the ARF-GDP-Sec7 intermediate and preventing the nucleotide release (Renault et al., 2003). Five of the eight ARF-GEFs in Arabidopsis are BFA-sensitive, namely, GNOM, GNL1, BIG1, BIG2 and BIG4 and treatment leads to formation of BFA bodies (Geldner et al., 2003).

4.4.3.2 Wortmannin

Wortmannin is a fungal metabolite that inhibits phosphatidylinositol-3-kinase (PI3K) function by covalent binding to a conserved residue of the kinase. At higher concentrations it can also inhibit phosphatidylinositol-4-kinases. It is affecting vacuolar trafficking. Wortmannin treatment lead to fusion, swelling and vacuolization of MBVs, which appear in a typical wortmannin-induced doughnut-like shape (Jaillais et al., 2008; Cui et al., 2016).

4.4.3.3 Cycloheximide (CHX)

Cycloheximide (CHX) is an antibiotic produced by *Streptomyces griseus* and functions as inhibitor of protein synthesis. It inhibits the activity of the peptidyltransferase at the ribosomes and thereby prevents translation (Pestka, 1971; Park et al., 2019). CHX is commonly used to distinguish endocytosed from newly synthesized proteins, the endocytic and the secretion pathways (De Caroli et al., 2020).

4.5. Posttranslational regulation of IRT1 in the endomembrane system

One key model protein of endosomal PM trafficking is the main iron transporter IRT1 (Figure 3). Next to transcriptional regulation, posttranslational modifications and regulation based on direct protein-protein interactions play a great role in the Fe uptake machinery. Additionally to its primary substrate Fe, it can also transport other divalent metal ions such as manganese, zinc, cadmium and cobalt (Eide et al., 1996; Korshunova et al., 1999; Vert et al., 2002). Apart from its Fe deficiency-induced FIT-dependent up-regulation, IRT1 activity and its stability depends on its constant turnover (Ivanov and Vert, 2021). IRT1 presence was detected in vesicle-positive structures located to the TGN/early endosomes and at the PM, indicating the

endocytosis of the transporter for targeted degradation in the vacuole but with possible recycling in the TGN back to the PM (Barberon et al., 2011). The regulation of IRT1 is not dependent on its main substrate Fe, but excess of its secondary metal substrates can trigger degradation. Upon moderate non-Fe metal concentrations, the degradation is promoted by the action of IRT1 DEGRADATION FACTOR 1 (IDF1) a RING E3 ubiquitin ligase. It leads to multimonoubiquitination resulting in the formation of IRT1-Ub complexes at the PM, with subsequent ubiquitin-mediated endocytosis (Kerkeb et al., 2008; Barberon et al., 2011; Shin et al., 2013). Fe-deficient but excessive non-Fe metal conditions lead to IRT1 phosphorylation by CIPK23. Potentially phosphorylated residues are present in the large cytosolic loop containing the variable region of IRT1, next to its ubiquitination sites. The CIPK23-dependent IRT1 phosphorylation results in IDF1 recruitment to the PM and a shift of IRT1 multimonoubiquitination pattern to K63-polyubiquitination. The reaction to non-Fe metals seems to be thereby induced by their binding to a histidine-rich stretch in IRT1 variable region.

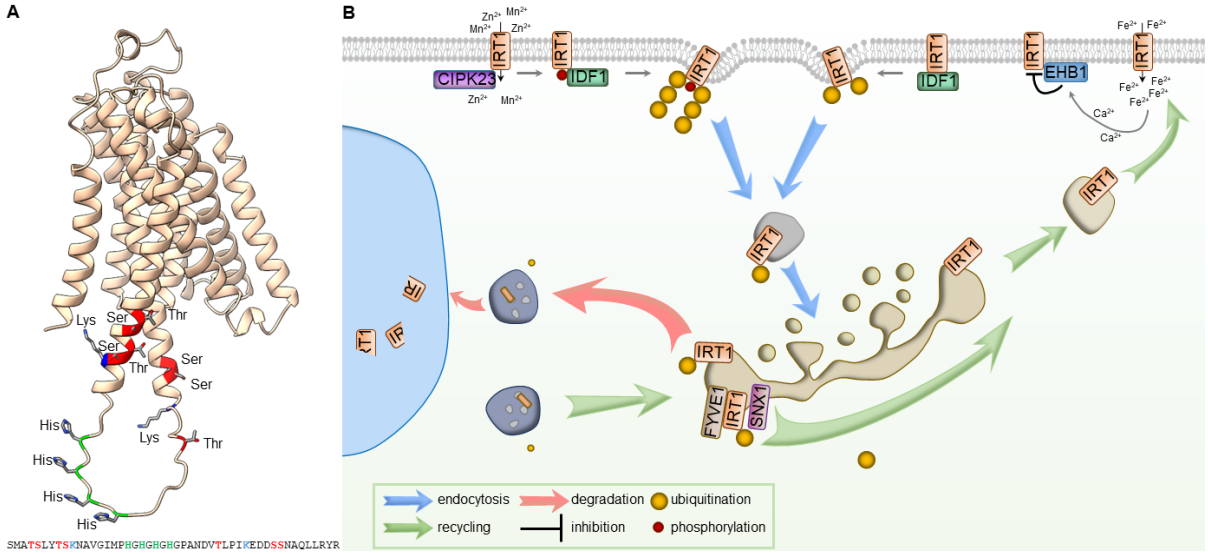

Figure 3. Regulation of IRT1.
(A), Schematic representation of IRT1 structure with its large cytosolic loop containing the variable region. The latter consists of several amino acids being target for post-translational modifications. Thr and Ser are potential phosphorylation sites (red). Lys are ubiquitinated (blue). A histidine-rich stretch (green) is needed for non-Fe metal binding. The sequence of the cytosolic loop is depicted below. (B), IRT1 undergoes constant cycling in the cell, being endocytosed from the PM for degradation in the vacuole or recycled for secretion in the sorting endosomes. The degradation is promoted by IDF1 multimonoubiquitination. Fe-deficient but excessive non-Fe metal conditions lead to IRT1 phosphorylation by CIPK23 resulting in IDF1-dependent K63-polyubiquitination. IRT1 function at the PM is inhibited by EHB1 in a Ca^{2+}-dependent manner. IRT1 recycling to the PM is promoted by FYVE1 and SNX1.

IRT1 was introduced with the potential function as transporter and receptor, a so-called transceptor (Dubeaux et al., 2018). IRT1 function at the PM is inhibited by the C2-domain containing protein ENHANCED BENDING 1 (EHB1). The interaction depends on EHB1 CAR signature domain and increases upon Ca^{2+} presence. EHB1 can bind to the membrane via its Ca^{2+}-binding site in the presence of Ca^{2+} and does not need the CAR signature domain (Khan et al., 2019). Positive effects on IRT1 cycling were identified by the interaction with the PI3P-

binding protein FYVE1/FREE1. Its PI3P-binding ability leads to FYVE1/FREE1 localization at MVBs but also the TGN where it is responsible for IRT1-sorting back to the PM (Barberon et al., 2014). Another important protein for IRT1 recycling is SNX1. SNX1-loss of function lines show a reduced amount of IRT1 protein under Fe deficiency with an altered endosome to PM ratio indicating SNX1 importance in endocytosed IRT1 recycling in sorting endosomes (Ivanov et al., 2014).

Though many components of IRT1 regulation and endosomal trafficking are already known, large parts remain still elusive and provide a variety of approaches to investigate the transporter and endosomal trafficking in general.

5. Thesis Objectives

IRT1 activity is highly regulated at multiple levels, such as gene expression, protein stability and endosomal trafficking. It contains a large cytosolic loop with a variable region, which is essential for its regulation by non-iron metal sensing, posttranslational modifications and protein-protein interactions. Several interactors and regulators are already known but our knowledge is still incomplete (Cointry and Vert, 2019). Previous data in our group identified three novel potential interactors of IRT1 variable region in an Arabidopsis root cDNA-based yeast two-hybrid screen, one of them being the ARF-like small GTPase TTN5. Loss of TTN5 results in embryo lethality, implying an essential function. This identification resulted in the following questions: 1) What is the current state of knowledge of the ARF family and their regulatory proteins? 2) How is TTN5 functioning in the cell and does it have a role in Fe homeostasis with regard to IRT1 regulation? And 3) how does the TTN5 interactome look like and what does it reveal about the function?

In order to address these questions, the following thesis objectives were formulated:

1. Overview of ARF and ARF-like proteins.
   The structural features and conformational characteristics of the ARF and ARF-like proteins were described. The current state of knowledge of the ARF-likes and the ARF-GEFs and -GAPs was summarized.

2. Investigation of the interaction between IRT1 and TTN5 and the role of TTN5 in IRT1 regulation and Fe homeostasis.
   Fluorescence-based interaction methods were performed to confirm TTN5-IRT1 interaction. Pharmacological treatments in combination with fluorescent compartment markers were used to decipher TTN5 subcellular localization and the colocalization profile with IRT1. A heterozygous knock-out line of TTN5 was tested for its impact in iron uptake, by ferric reductase assay and seed iron content and its influence on transcription levels of several iron-regulated genes was tested. Complementation studies were carried out to investigate potential interactions between TTN5 and IRT1 regulators.

3. Investigation of the TTN5 interactome in comparison with IRT1 regulators.
   Stable expressing HA_3-tagged TTN5 Arabidopsis line was used for interactome generation by immunoprecipitation with subsequent mass spectrometry analysis. The interactomes of known IRT1 regulators and iron-related genes were investigated in comparison. The data sets obtained were analyzed and examined for possible links in relation to iron

homeostasis. Two promising candidates of the TTN5 interactome, AHA1 and SEC12, were verified by Bimolecular Fluorescence Complementation (BiFC).

References

Balk J, Schaedler TA (2014) Iron Cofactor Assembly in Plants. Annual Review of Plant Biology **65:** 125-153

Barberon M, Dubeaux G, Kolb C, Isono E, Zelazny E, Vert G (2014) Polarization of IRON-REGULATED TRANSPORTER 1 (IRT1) to the plant-soil interface plays crucial role in metal homeostasis. Proceedings of the National Academy of Sciences **111:** 8293-8298

Barberon M, Zelazny E, Robert S, Conéjéro G, Curie C, Friml J, Vert G (2011) Monoubiquitin-dependent endocytosis of the IRON-REGULATED TRANSPORTER 1 (IRT1) transporter controls iron uptake in plants. Proceedings of the National Academy of Sciences **108:** E450-E458

Bauer P, Thiel T, Klatte M, Bereczky Z, Brumbarova T, Hell R, Grosse I (2004) Analysis of Sequence, Map Position, and Gene Expression Reveals Conserved Essential Genes for Iron Uptake in Arabidopsis and Tomato. Plant Physiology **136:** 4169-4183

Béraud-Dufour S, Robineau S, Chardin P, Paris S, Chabre M, Cherfils J, Antonny B (1998) A glutamic finger in the guanine nucleotide exchange factor ARNO displaces Mg^{2+} and the β-phosphate to destabilize GDP on ARF1. The EMBO Journal **17:** 3651-3659

Brumbarova T, Bauer P, Ivanov R (2015) Molecular mechanisms governing Arabidopsis iron uptake. Trends Plant Sci **20:** 124-133

Bughio N, Yamaguchi H, Nishizawa NK, Nakanishi H, Mori S (2002) Cloning an iron-regulated metal transporter from rice. Journal of Experimental Botany **53:** 1677-1682

Buono RA, Leier A, Paez-Valencia J, Pennington J, Goodman K, Miller N, Ahlquist P, Marquez-Lago TT, Otegui MS (2017) ESCRT-mediated vesicle concatenation in plant endosomes. J Cell Biol **216:** 2167-2177

Casanova JE (2007) Regulation of Arf Activation: the Sec7 Family of Guanine Nucleotide Exchange Factors. Traffic **8:** 1476-1485

Chappie JS, Dyda F (2013) Building a fission machine--structural insights into dynamin assembly and activation. Journal of cell science **126:** 2773-2784

Cointry V, Vert G (2019) The bifunctional transporter-receptor IRT1 at the heart of metal sensing and signalling. New Phytologist **223:** 1173-1178

Colangelo EP, Guerinot ML (2004) The Essential Basic Helix-Loop-Helix Protein FIT1 Is Required for the Iron Deficiency Response. The Plant Cell **16:** 3400-3412

Cui Y, Shen J, Gao C, Zhuang X, Wang J, Jiang L (2016) Biogenesis of Plant Prevacuolar Multivesicular Bodies. Molecular Plant **9:** 774-786

Curie C, Panaviene Z, Loulergue C, Dellaporta SL, Briat J-F, Walker EL (2001) Maize yellow stripe1 encodes a membrane protein directly involved in Fe(III) uptake. Nature **409:** 346-349

De Caroli M, Manno E, Perrotta C, De Lorenzo G, Di Sansebastiano G-P, Piro G (2020) CesA6 and PGIP2 Endocytosis Involves Different Subpopulations of TGN-Related Endosomes. Frontiers in plant science **11:** 350-350

Dettmer J, Hong-Hermesdorf A, Stierhof Y-D, Schumacher K (2006) Vacuolar H^+-ATPase Activity Is Required for Endocytic and Secretory Trafficking in Arabidopsis. The Plant Cell **18:** 715-730

Dinneny JR, Long TA, Wang JY, Jung JW, Mace D, Pointer S, Barron C, Brady SM, Schiefelbein J, Benfey PN (2008) Cell Identity Mediates the Response of Arabidopsis Roots to Abiotic Stress. Science **320:** 942-945

Distéfano AM, López GA, Setzes N, Marchetti F, Cainzos M, Cascallares M, Zabaleta E, Pagnussat GC (2020) Ferroptosis in plants: triggers, proposed mechanisms, and the role of iron in modulating cell death. Journal of Experimental Botany **72:** 2125-2135

Dubeaux G, Neveu J, Zelazny E, Vert G (2018) Metal Sensing by the IRT1 Transporter-Receptor Orchestrates Its Own Degradation and Plant Metal Nutrition. Molecular Cell **69:** 953-964.e955

Eide D, Broderius M, Fett J, Guerinot ML (1996) A novel iron-regulated metal transporter from plants identified by functional expression in yeast. Proceedings of the National Academy of Sciences of the United States of America **93:** 5624-5628

Fourcroy P, Sisó-Terraza P, Sudre D, Savirón M, Reyt G, Gaymard F, Abadía A, Abadia J, Álvarez-Fernández A, Briat J-F (2014) Involvement of the ABCG37 transporter in secretion of scopoletin and derivatives by Arabidopsis roots in response to iron deficiency. New Phytologist **201:** 155-167

Gadeyne A, Sánchez-Rodríguez C, Vanneste S, Di Rubbo S, Zauber H, Vanneste K, Van Leene J, De Winne N, Eeckhout D, Persiau G, Van De Slijke E, Cannoot B, Vercruysse L, Mayers Jonathan R, Adamowski M, Kania U, Ehrlich M, Schweighofer A, Ketelaar T, Maere S, Bednarek Sebastian Y, Friml J, Gevaert K, Witters E, Russinova E, Persson S, De Jaeger G, Van Damme D (2014) The TPLATE Adaptor Complex Drives Clathrin-Mediated Endocytosis in Plants. Cell **156:** 691-704

Gao C, Luo M, Zhao Q, Yang R, Cui Y, Zeng Y, Xia J, Jiang L (2014) A Unique Plant ESCRT Component, FREE1, Regulates Multivesicular Body Protein Sorting and Plant Growth. Current Biology **24:** 2556-2563

Gao F, Robe K, Bettembourg M, Navarro N, Rofidal V, Santoni V, Gaymard F, Vignols F, Roschzttardtz H, Izquierdo E, Dubos C (2019) The Transcription Factor bHLH121 Interacts with bHLH105 (ILR3) and Its Closest Homologs to Regulate Iron Homeostasis in Arabidopsis. The Plant Cell **32:** 508-524

Geldner N, Anders N, Wolters H, Keicher J, Kornberger W, Muller P, Delbarre A, Ueda T, Nakano A, Jürgens G (2003) The Arabidopsis GNOM ARF-GEF mediates endosomal recycling, auxin transport, and auxin-dependent plant growth. Cell **112:** 219-230

Gratz R, Manishankar P, Ivanov R, Köster P, Mohr I, Trofimov K, Steinhorst L, Meiser J, Mai HJ, Drerup M, Arendt S, Holtkamp M, Karst U, Kudla J, Bauer P, Brumbarova T (2019) CIPK11-Dependent Phosphorylation Modulates FIT Activity to Promote Arabidopsis Iron Acquisition in Response to Calcium Signaling. Dev Cell **48:** 726-740.e710

Gratz R, von der Mark C, Ivanov R, Brumbarova T (2021) Fe acquisition at the crossroad of calcium and reactive oxygen species signaling. Curr Opin Plant Biol **63:** 102048

Halliwell B, Gutteridge JMC (1992) Biologically relevant metal ion-dependent hydroxyl radical generation An update. FEBS Letters **307:** 108-112

Henne William M, Buchkovich Nicholas J, Zhao Y, Emr Scott D (2012) The Endosomal Sorting Complex ESCRT-II Mediates the Assembly and Architecture of ESCRT-III Helices. Cell **151:** 356-371

Heucken N, Ivanov R (2018) The retromer, sorting nexins and the plant endomembrane protein trafficking. J Cell Sci **131**

Höning S, Ricotta D, Krauss M, Späte K, Spolaore B, Motley A, Robinson M, Robinson C, Haucke V, Owen DJ (2005) Phosphatidylinositol-(4,5)-Bisphosphate Regulates Sorting Signal Recognition by the Clathrin-Associated Adaptor Complex AP2. Molecular Cell **18:** 519-531

Inoue H, Kobayashi T, Nozoye T, Takahashi M, Kakei Y, Suzuki K, Nakazono M, Nakanishi H, Mori S, Nishizawa NK (2009) Rice OsYSL15 Is an Iron-regulated Iron(III)-Deoxymugineic Acid Transporter Expressed in the Roots and Is Essential for Iron Uptake in Early Growth of the Seedlings*. Journal of Biological Chemistry **284:** 3470-3479

Ishimaru Y, Suzuki M, Tsukamoto T, Suzuki K, Nakazono M, Kobayashi T, Wada Y, Watanabe S, Matsuhashi S, Takahashi M, Nakanishi H, Mori S, Nishizawa NK (2006) Rice plants take up iron as an Fe^{3+}-phytosiderophore and as Fe2+. The Plant Journal **45:** 335-346

Ivanov R, Brumbarova T, Bauer P (2012) Fitting into the Harsh Reality: Regulation of Iron-deficiency Responses in Dicotyledonous Plants. Molecular Plant **5:** 27-42

Ivanov R, Brumbarova T, Blum A, Jantke A-M, Fink-Straube C, Bauer P (2014) SORTING NEXIN1 is required for modulating the trafficking and stability of the Arabidopsis IRON-REGULATED TRANSPORTER1. The Plant cell **26:** 1294-1307

Ivanov R, Vert G (2021) Endocytosis in plants: Peculiarities and roles in the regulated trafficking of plant metal transporters. Biology of the Cell **113:** 1-13

Jackson CL, Casanova JE (2000) Turning on ARF: the Sec7 family of guanine-nucleotide-exchange factors. Trends Cell Biol **10:** 60-67

Jaillais Y, Fobis-Loisy I, Miège C, Gaude T (2008) Evidence for a sorting endosome in Arabidopsis root cells. The Plant Journal **53:** 237-247

Jakoby M, Wang H-Y, Reidt W, Weisshaar B, Bauer P (2004) FRU (BHLH029) is required for induction of iron mobilization genes in *Arabidopsis thaliana*. FEBS Letters **577:** 528-534

Kai K, Mizutani M, Kawamura N, Yamamoto R, Tamai M, Yamaguchi H, Sakata K, Shimizu B-i (2008) Scopoletin is biosynthesized via ortho-hydroxylation of feruloyl CoA by a 2-oxoglutarate-dependent dioxygenase in *Arabidopsis thaliana*. The Plant Journal **55:** 989-999

Kerkeb L, Mukherjee I, Chatterjee I, Lahner B, Salt DE, Connolly EL (2008) Iron-induced turnover of the Arabidopsis IRON-REGULATED TRANSPORTER1 metal transporter requires lysine residues. Plant physiology **146:** 1964-1973

Khan I, Gratz R, Denezhkin P, Schott-Verdugo SN, Angrand K, Genders L, Basgaran RM, Fink-Straube C, Brumbarova T, Gohlke H, Bauer P, Ivanov R (2019) Calcium-Promoted Interaction between the C2-Domain Protein EHB1 and Metal Transporter IRT1 Inhibits Arabidopsis Iron Acquisition. Plant Physiology **180:** 1564-1581

Kim SA, LaCroix IS, Gerber SA, Guerinot ML (2019) The iron deficiency response in *Arabidopsis thaliana* requires the phosphorylated transcription factor URI. Proceedings of the National Academy of Sciences **116:** 24933-24942

Kobayashi T, Nishizawa NK (2012) Iron Uptake, Translocation, and Regulation in Higher Plants. Annual Review of Plant Biology **63:** 131-152

Korbei B, Moulinier-Anzola J, De-Araujo L, Lucyshyn D, Retzer K, Khan Muhammad A, Luschnig C (2013) Arabidopsis TOL Proteins Act as Gatekeepers for Vacuolar Sorting of PIN2 Plasma Membrane Protein. Current Biology **23:** 2500-2505

Korshunova YO, Eide D, Clark WG, Guerinot ML, Pakrasi HB (1999) The IRT1 protein from *Arabidopsis thaliana* is a metal transporter with a broad substrate range. Plant Mol Biol **40:** 37-44

Kump LR (2008) The rise of atmospheric oxygen. Nature **451:** 277-278

Lam SK, Siu CL, Hillmer S, Jang S, An G, Robinson DG, Jiang L (2007) Rice SCAMP1 defines clathrin-coated, *trans*-golgi-located tubular-vesicular structures as an early endosome in tobacco BY-2 cells. The Plant cell **19:** 296-319

Lei R, Li Y, Cai Y, Li C, Pu M, Lu C, Yang Y, Liang G (2020) bHLH121 Functions as a Direct Link that Facilitates the Activation of FIT by bHLH IVc Transcription Factors for Maintaining Fe Homeostasis in Arabidopsis. Mol Plant **13:** 634-649

Li X, Zhang H, Ai Q, Liang G, Yu D (2016) Two bHLH Transcription Factors, bHLH34 and bHLH104, Regulate Iron Homeostasis in *Arabidopsis thaliana* Plant Physiology **170:** 2478-2493

Liang G, Zhang H, Li X, Ai Q, Yu D (2017) bHLH transcription factor bHLH115 regulates iron homeostasis in *Arabidopsis thaliana*. Journal of Experimental Botany **68:** 1743-1755

Ling H-Q, Bauer P, Bereczky Z, Keller B, Ganal M (2002) The tomato fer gene encoding a bHLH protein controls iron-uptake responses in roots. Proceedings of the National Academy of Sciences **99:** 13938-13943

Long TA, Tsukagoshi H, Busch W, Lahner B, Salt DE, Benfey PN (2010) The bHLH transcription factor POPEYE regulates response to iron deficiency in Arabidopsis roots. The Plant cell **22:** 2219-2236

MacDonald C, Buchkovich NJ, Stringer DK, Emr SD, Piper RC (2012) Cargo ubiquitination is essential for multivesicular body intralumenal vesicle formation. EMBO reports **13:** 331-338

Mansour SJ, Skaug J, Zhao XH, Giordano J, Scherer SW, Melançon P (1999) p200 ARF-GEP1: a Golgi-localized guanine nucleotide exchange protein whose Sec7 domain is targeted by the drug brefeldin A. Proceedings of the National Academy of Sciences of the United States of America **96:** 7968-7973

Martín-Barranco A, Spielmann J, Dubeaux G, Vert G, Zelazny E (2020) Dynamic Control of the High-Affinity Iron Uptake Complex in Root Epidermal Cells1. Plant Physiology **184:** 1236-1250

McMahon HT, Boucrot E (2011) Molecular mechanism and physiological functions of clathrin-mediated endocytosis. Nature Reviews Molecular Cell Biology **12:** 517-533

Minamino N, Ueda T (2019) RAB GTPases and their effectors in plant endosomal transport. Current Opinion in Plant Biology **52:** 61-68

Mossessova E, Gulbis JM, Goldberg J (1998) Structure of the Guanine Nucleotide Exchange Factor Sec7 Domain of Human Arno and Analysis of the Interaction with ARF GTPase. Cell **92:** 415-423

Nagel MK, Kalinowska K, Vogel K, Reynolds GD, Wu Z, Anzenberger F, Ichikawa M, Tsutsumi C, Sato MH, Kuster B, Bednarek SY, Isono E (2017) Arabidopsis SH3P2 is an ubiquitin-binding

protein that functions together with ESCRT-I and the deubiquitylating enzyme AMSH3. Proc Natl Acad Sci U S A **114:** E7197-e7204

Naramoto S, Otegui MS, Kutsuna N, de Rycke R, Dainobu T, Karampelias M, Fujimoto M, Feraru E, Miki D, Fukuda H, Nakano A, Friml J (2014) Insights into the Localization and Function of the Membrane Trafficking Regulator GNOM ARF-GEF at the Golgi Apparatus in Arabidopsis The Plant Cell **26:** 3062-3076

Naranjo-Arcos MA, Maurer F, Meiser J, Pateyron S, Fink-Straube C, Bauer P (2017) Dissection of iron signaling and iron accumulation by overexpression of subgroup Ib bHLH039 protein. Scientific Reports **7:** 10911

Nouet C, Motte P, Hanikenne M (2011) Chloroplastic and mitochondrial metal homeostasis. Trends in Plant Science **16:** 395-404

Nozoye T, Nagasaka S, Kobayashi T, Takahashi M, Sato Y, Sato Y, Uozumi N, Nakanishi H, Nishizawa NK (2011) Phytosiderophore Efflux Transporters Are Crucial for Iron Acquisition in Graminaceous Plants*. Journal of Biological Chemistry **286:** 5446-5454

Park Y, Koga Y, Su C, Waterbury AL, Johnny CL, Liau BB (2019) Versatile Synthetic Route to Cycloheximide and Analogues That Potently Inhibit Translation Elongation. Angewandte Chemie International Edition **58:** 5387-5391

Pearse BM (1976) Clathrin: a unique protein associated with intracellular transfer of membrane by coated vesicles. Proc Natl Acad Sci U S A **73:** 1255-1259

Pestka S (1971) Inhibitors of ribosome functions. Annu Rev Microbiol **25:** 487-562

Peyroche A, Antonny B, Robineau S, Acker J, Cherfils J, Jackson CL (1999) Brefeldin A Acts to Stabilize an Abortive ARF–GDP–Sec7 Domain Protein Complex: Involvement of Specific Residues of the Sec7 Domain. Molecular Cell **3:** 275-285

Rajniak J, Giehl RFH, Chang E, Murgia I, von Wirén N, Sattely ES (2018) Biosynthesis of redox-active metabolites in response to iron deficiency in plants. Nature Chemical Biology **14:** 442-450

Renault L, Guibert B, Cherfils J (2003) Structural snapshots of the mechanism and inhibition of a guanine nucleotide exchange factor. Nature **426:** 525-530

Riaz N, Guerinot ML (2021) All together now: regulation of the iron deficiency response. Journal of Experimental Botany **72:** 2045-2055

Robinson NJ, Procter CM, Connolly EL, Guerinot ML (1999) A ferric-chelate reductase for iron uptake from soils. Nature **397:** 694-697

Römheld V, Marschner H (1986) Evidence for a Specific Uptake System for Iron Phytosiderophores in Roots of Grasses 1. Plant Physiology **80:** 175-180

Santi S, Schmidt W (2009) Dissecting iron deficiency-induced proton extrusion in Arabidopsis roots. New Phytologist **183:** 1072-1084

Scheuring D, Viotti C, Krüger F, Künzl F, Sturm S, Bubeck J, Hillmer S, Frigerio L, Robinson DG, Pimpl P, Schumacher K (2011) Multivesicular Bodies Mature from the *Trans*-Golgi Network/Early Endosome in Arabidopsis The Plant Cell **23:** 3463-3481

Schmid NB, Giehl RFH, Döll S, Mock H-P, Strehmel N, Scheel D, Kong X, Hider RC, von Wirén N (2014) Feruloyl-CoA 6′-Hydroxylase1-Dependent Coumarins Mediate Iron Acquisition from Alkaline Substrates in Arabidopsis. Plant Physiology **164:** 160-172

Schwihla M, Korbei B (2020) The Beginning of the End: Initial Steps in the Degradation of Plasma Membrane Proteins. Frontiers in Plant Science **11**

Shin L-J, Lo J-C, Chen G-H, Callis J, Fu H, Yeh K-C (2013) IRT1 DEGRADATION FACTOR1, a RING E3 Ubiquitin Ligase, Regulates the Degradation of IRON-REGULATED TRANSPORTER1 in Arabidopsis. The Plant Cell **25:** 3039-3051

Simonetti B, Cullen PJ (2018) Endosomal Sorting: *Archi*tecture of the Retromer Coat. Current Biology **28:** R1350-R1352

Singh Manoj K, Krüger F, Beckmann H, Brumm S, Vermeer Joop EM, Munnik T, Mayer U, Stierhof Y-D, Grefen C, Schumacher K, Jürgens G (2014) Protein Delivery to Vacuole Requires SAND Protein-Dependent Rab GTPase Conversion for MVB-Vacuole Fusion. Current Biology **24:** 1383-1389

Sivitz AB, Hermand V, Curie C, Vert G (2012) Arabidopsis bHLH100 and bHLH101 control iron homeostasis via a FIT-independent pathway. PLoS One **7:** e44843

Spitzer C, Schellmann S, Sabovljevic A, Shahriari M, Keshavaiah C, Bechtold N, Herzog M, Müller S, Hanisch F-G, Hülskamp M (2006) The Arabidopsis elch mutant reveals functions of an ESCRT component in cytokinesis. Development **133:** 4679-4689

Steinmann T, Geldner N, Grebe M, Mangold S, Jackson CL, Paris S, Gälweiler L, Palme K, Jürgens G (1999) Coordinated polar localization of auxin efflux carrier PIN1 by GNOM ARF GEF. Science **286:** 316-318

Stringlis IA, Yu K, Feussner K, de Jonge R, Van Bentum S, Van Verk MC, Berendsen RL, Bakker PAHM, Feussner I, Pieterse CMJ (2018) MYB72-dependent coumarin exudation shapes root microbiome assembly to promote plant health. Proceedings of the National Academy of Sciences of the United States of America **115:** E5213-E5222

Tanno H, Komada M (2013) The ubiquitin code and its decoding machinery in the endocytic pathway. J Biochem **153:** 497-504

Traub LM, Bonifacino JS (2013) Cargo recognition in clathrin-mediated endocytosis. Cold Spring Harbor perspectives in biology **5:** a016790-a016790

Tsai H-H, Rodríguez-Celma J, Lan P, Wu Y-C, Vélez-Bermúdez IC, Schmidt W (2018) Scopoletin 8-Hydroxylase-Mediated Fraxetin Production Is Crucial for Iron Mobilization. Plant Physiology **177:** 194-207

Tsai HH, Schmidt W (2017) Mobilization of Iron by Plant-Borne Coumarins. Trends in Plant Science **22:** 538-548

Valencia JP, Goodman K, Otegui MS (2016) Endocytosis and Endosomal Trafficking in Plants. Annual Review of Plant Biology **67:** 309-335

Vermeer JEM, van Leeuwen W, Tobeña-Santamaria R, Laxalt AM, Jones DR, Divecha N, Gadella Jr TWJ, Munnik T (2006) Visualization of PtdIns3P dynamics in living plant cells. The Plant Journal **47:** 687-700

Vert G, Grotz N, Dédaldéchamp F, Gaymard F, Guerinot ML, Briat J-F, Curie C (2002) IRT1, an Arabidopsis Transporter Essential for Iron Uptake from the Soil and for Plant Growth. The Plant Cell **14:** 1223-1233

Wairich A, de Oliveira BHN, Arend EB, Duarte GL, Ponte LR, Sperotto RA, Ricachenevsky FK, Fett JP (2019) The Combined Strategy for iron uptake is not exclusive to domesticated rice (Oryza sativa). Scientific Reports **9:** 16144

Walker EL, Connolly EL (2008) Time to pump iron: iron-deficiency-signaling mechanisms of higher plants. Current Opinion in Plant Biology **11:** 530-535

Wang HY, Klatte M, Jakoby M, Bäumlein H, Weisshaar B, Bauer P (2007) Iron deficiency-mediated stress regulation of four subgroup Ib BHLH genes in *Arabidopsis thaliana*. Planta **226:** 897-908

Wang N, Cui Y, Liu Y, Fan H, Du J, Huang Z, Yuan Y, Wu H, Ling H-Q (2013) Requirement and Functional Redundancy of Ib Subgroup bHLH Proteins for Iron Deficiency Responses and Uptake in *Arabidopsis thaliana*. Molecular Plant **6:** 503-513

Wedepohl HK (1995) The composition of the continental crust. Geochimica et Cosmochimica Acta **59:** 1217-1232

Yang TJW, Lin W-D, Schmidt W (2010) Transcriptional Profiling of the Arabidopsis Iron Deficiency Response Reveals Conserved Transition Metal Homeostasis Networks. Plant Physiology **152:** 2130-2141

Yi Y, Guerinot ML (1996) Genetic evidence that induction of root Fe(III) chelate reductase activity is necessary for iron uptake under iron deficiency. Plant J **10:** 835-844

Yoshinari A, Toda Y, Takano J (2021) GNOM-dependent endocytosis maintains polar localisation of the borate exporter BOR1 in Arabidopsis. Biology of the Cell **113:** 264-269

Yuan Y, Wu H, Wang N, Li J, Zhao W, Du J, Wang D, Ling HQ (2008) FIT interacts with AtbHLH38 and AtbHLH39 in regulating iron uptake gene expression for iron homeostasis in Arabidopsis. Cell Res **18:** 385-397

Zhang J, Liu B, Li M, Feng D, Jin H, Wang P, Liu J, Xiong F, Wang J, Wang H-B (2015) The bHLH Transcription Factor bHLH104 Interacts with IAA-LEUCINE RESISTANT3 and Modulates Iron Homeostasis in Arabidopsis. The Plant Cell **27:** 787-805

6. Manuscript I

ARF and ARF-like GTPases and their respective GEFs and GAPs in *Arabidopsis thaliana*

ARF and ARF-like GTPases and their respective GEFs and GAPs in *Arabidopsis thaliana*

Inga Mohr[1], Petra Bauer[1,2] and Rumen Ivanov[1]

[1]Institute of Botany, Heinrich Heine University, Universitätsstr. 1, 40225 Düsseldorf, Germany.
[2]Cluster of Excellence on Plant Sciences, Heinrich-Heine University, 40225 Düsseldorf, Germany

Author contributions: I.M. and R.I. designed the outline; I.M. wrote the manuscript; I.M., P.B. and R.I. edited the manuscript; P.B. acquired funding. P.B and R.I. agreed to serve as the author responsible for contact and communication.

Abstract

The members of the ADP-ribosylation factor (ARF) family of Ras small GTPases are key proteins in signal transduction and function by their conformational switching ability between GTP- or GDP-bound states. They are best known for its involvement in coat protein complex vesicle trafficking but take place in a diverse subset of cellular functions, via interaction with their respective guanine nucleotide exchange factors (GEFs) and GTPase-activating proteins (GAPs). Though well conserved, the number of members of ARF and ARF-likes as well as GEFs and GAPs differ a lot between different organisms and allows scope for unique functions. In this review, we will provide an overview of the conformational changes of the switching mechanism upon interaction with the GEFs and GAPs and discuss the specifics of the ARF family. Additionally, we will take a closer look on the ARF family in Arabidopsis and summarize the current state of knowledge of the ARF-likes and the ARF-GEFs and -GAPs, representing an understudied field in plant signaling.

Keywords: small GTPases, ARF, ARL, SAR, GEF, GNOM, BIG, GAP, AGD

Abbreviations:

ARF	ADP-ribosylation factor
AGD	ARF-GAP domain
ARL	ARF-like
AUX1	AUXIN 1
BAR	Bin1-amphiphysin-Rvs167p/Rvs161p
BFA	Brefeldin A
BIG	BFA-inhibited GEF
GAP	GTPase-activating protein
GBF1	Golgi BFA-resistance factor 1

GDI	GDP dissociation inhibitors
GEF	guanine nucleotide exchange factors
GNL	GNOM-LIKE
PH	pleckstrin homology
PIN1	PIN FORMED 1
RAB	Ras-like proteins in brain
RAN	Ras-related nuclear proteins
RAS	Ras sarcoma
RHO	Ras homologues
ROP	Rho of plants
SAR	SECRETION-ASSOCIATED RAS

Several classes of guanine-nucleotide binding proteins, which belong to the family of GTPases, are known. They take place in a broad range of regulatory events of signal transduction. One common feature of all classes is the conformational change, switching from the active GTP-bound to the inactive GDP-bound state, and *vice versa*. Identification of the Ras genes (*H-Ras, K-Ras* and *N-Ras*) in the cancer research field was the beginning of the validation of a new class of guanine-nucleotide binding proteins, the Ras superfamily of small GTPases (Bos, 1988; Hall, 1990; Kahn et al., 1992). The family is highly conserved, and homologs can be found in *Saccharomyces cerevisiae, Schizosaccharomyces pombe*, *Caenorhabditis elegans*, Drosophila, mammals and plants, among others. This superfamily consists of five subfamilies in mammals: the Ras sarcoma (RAS), Ras homologues (RHO), Ras-like proteins in brain (RAB), Ras-related nuclear proteins (RAN) and ADP-ribosylation factor (ARF) subfamilies (Kahn et al., 1992; Ahmadi et al., 2017). In *Arabidopsis thaliana* (Arabidopsis) only four families are represented, the ROP (Rho of plants), RAB, RAN and the ARF (Vernoud et al., 2003). In this review, we want to give a short overview of the Ras superfamily of small GTPases in general and we will take a closer look on the ARF family and their regulators, especially in the plant Arabidopsis, summarizing the current knowledge.

The Ras superfamily of small GTPases

Classification of the Ras superfamily into the different subfamilies is based on different criteria. All members exhibit consensus motifs for GTP-binding proteins. They exist in a mostly monomeric form with an almost entirely molecular mass around 20 to 29 kDa (Kahn et al., 1992; Ahmadi et al., 2017). More recent data revealed the ability of self-assembling for several Ras superfamily members into homodimers, oligomers or nanoclusters and also ARF1 was identified in homodimers (Brumm et al., 2020; Mima, 2021). Grouping into the different subfamilies is due to sequence identity and characteristic sequence motifs. They have well-

conserved motifs at their termini. The RAS and RHO proteins end with a CAAX motif for farnesyl or geranylgeranyl isoprenylation exclusively, while it is either CC or CXC modified with geranylgeranyl lipids for RAB proteins. The ARF proteins exhibit a conserved Gly-2 (Figure 2), which is necessary for the mostly typical N-myristoylation. Only RAN GTPases do not encode any N- or C-terminal lipid modification signal sequences (Kahn et al., 1992; Ahmadi et al., 2017). Next to this, the function of each subfamily is evolutionary well-conserved. The RAS proteins in yeast and mammals are important for the regulation of cell proliferation. RHO GTPases control next to the actin reorganization also signal transduction pathways which, are associated with MAP kinases. Membrane dynamics by vesicular trafficking is regulated by the RAB and ARF families and RAN proteins are involved in the regulation of the transport of proteins and RNA across the nuclear envelope (Vernoud et al., 2003).

Small GTPases as molecular switches

The members of the small GTPases function as a molecular switch typical for GTP-binding proteins. They change structurally by switching between the inactive GDP-bound and active GTP-bound states. This happens with the help of additional proteins due to the low intrinsic nucleotide exchange and hydrolysis activity of most of the small GTPases (Figure 1). Their activation is facilitated by guanine nucleotide exchange factors (GEF), which decrease the affinity of small GTPases for the bound GDP (Vernoud et al., 2003). For the hydrolysis of the bound GTP, GTPase-activating proteins (GAP) come into play (further details on GEFs and GAPs are described in the specific paragraphs below). The RAB and RHO GTPases also need the help of another class of proteins, the GDP dissociation inhibitors (GDI). They catalyze the GTPase detachment from membranes and their stabilization in the cytosol. This is carried out by masking of their post-translational lipid modifications. ARF proteins do not need GDIs (Nielsen, 2020).

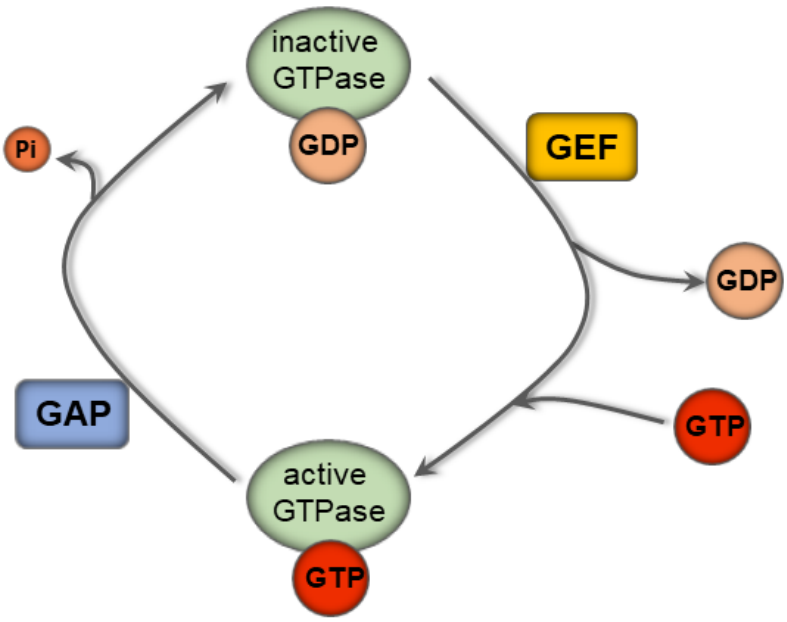

Figure 1. Small GTPases cycle between an inactive and active state with the help of GEFs and GAPs.
All GTPases exist in an inactive GDP-bound or an active GTP-bound state. Due to low internal dissociation and hydrolysis rate the help of special proteins is needed. Guanine nucleotide exchange factors (GEF) help to release the bound GDP to lead to the exchange to GTP. GTPase-activating proteins (GAP) catalyze GTP hydrolysis.

The nucleotide binding is achieved by five conserved guanine nucleotide binding motifs, namely G1 to G5. We will highlight here the individual G motifs in the sequences of the Arabidopsis ARF family members (Figure 2A, B). The G1 motif GXXXXGKS/T (also called P loop) follows a region mostly out of four hydrophobic residues. It is involved in the interaction with the nucleotide by binding of the β- and γ-phosphate groups of GTP. The conserved Lys residue is thereby of great importance. The G2 motif is a conserved Thr and needed for Mg^{2+}-binding. The third G motif, G3, is defined by DXXG. The G3 motif is involved in both Mg^{2+}-, via the Asp, and γ-phosphate-binding, via a hydrogen bond with the Gly. In the G4 motif N/TKXD, Lys and Asp bind directly to nucleotide. And the last region, G5, T/GC/SA is involved in guanine base recognition (X representing any amino acid) (Vetter and Wittinghofer, 2001; Wittinghofer and Vetter, 2011).

Important for GTP-binding is the conformational change of the two switch regions (Figure 2C), switch I around the G2 motif and switch II which contains the G3 motif. The movement allows the formation of two hydrogen bonds between the γ-phosphate and the Thr in switch I and the Gly in switch II. GTP-hydrolysis leads to the relaxation of these two regions (Pai et al., 1989; Vetter and Wittinghofer, 2001). Most ARF proteins differ a bit in their structure during the switching process from the known RAS mechanism, identified by crystal structures of mammalian and yeast ARF proteins (Figure 2C). In the GTP-bound form ARF1 shows a very similar conformation to RAS-GTP, whereas the GDP-bound form varies due to its N-terminal extension, the amphipathic helix with the post-translation myristoylation modification, needed for membrane anchoring (Goldberg, 1998). This difference between RAS-GTP and ARF1-GTP is achieved by another unique conformational change, next to the typical switch I and II changes. It happens at the connection between the two switches, β2-β3 strands in detail, and the N-terminal amphipathic helix, and is called the interswitch toggle. In the GDP-bound conformation, the N-terminal helix, with its modification, lies in a shallow groove resulting from an inward movement of the interswitch. The interswitch is like switch II part of the G3. In this conformation the conserved Trp fixes a conformation of these two switch regions, in which the Asp and the two Gly cannot bind GTP. The GTP-bound conformation is achieved by reorganization of the Trp, the two Gly and the Arg, resulting in stabilization of switch II by the formation of a network of hydrogen bonds. The two switch regions are pulled up and the N-terminal helix is pushed from its binding pocket by the interswitch (Pasqualato et al., 2002). When GTP is bound, the γ-phosphate oxygen is coordinated via hydrogen bonds with Thr and Gly of switch I and II respectively. Thr is also involved in Mg^{2+}-binding by its side chain (Vetter and Wittinghofer, 2001; Wittinghofer and Vetter, 2011).

ARF family and their conserved function in vesicle trafficking

Identification of the ARF family happened first by its stimulating activity on ADP-ribosylation by the cholera toxin A (Enomoto and Gill, 1980; Kahn and Gilman, 1984; Vernoud et al., 2003). They are well conserved over many different species from mammals over yeast to plants. The ARF family is divided into ARF and ARF-like (ARL) proteins. ARL share 40-60 % sequence similarity with ARF, but, unlike ARF, they are not able to activate cholera toxin A or rescue *S. cerevisiae* mutants (Tamkun et al., 1991; Vernoud et al., 2003; Humphreys et al., 2012; Labbaoui et al., 2017; Dautt-Castro et al., 2021). The family size differs between different species. The human genome encodes for six *ARF* and 20 *ARL* genes, whereas only six genes, divided evenly into *ARF* and *ARL*, are present in *S. cerevisiae*. In Arabidopsis, twelve *ARFs* and seven *ARLs* can be identified. Additionally, the secretion-associated and Ras-related (SAR) proteins are grouped to the ARF family (Vernoud et al., 2003; Memon, 2004; Just and Peränen, 2016). The first ARF cloned from Arabidopsis was ARF1 (Regad et al., 1993).

The ARF family is described as a key player in vesicle-mediated protein transport by recruiting coat proteins. They are involved in controlling organelle structures and cell behavior as well and can interact and activate several enzymes like PI kinases to regulate lipid composition of different types of membranes (Hwang and Robinson, 2009; Jackson and Bouvet, 2014; Yorimitsu et al., 2014; Just and Peränen, 2016).

Diverse mutations are already known to mimic the different activity conformations of small GTPases (Figure 2A). They are well conserved between the subfamilies. The family of GTPases have conserved residues which are essential for their activity such as Thr-31 (residue position is determined for ARF1) for inactivity, Gln-71 for activity. Mutating the Thr-31 to an Asn leads to an inhibition of the interaction with its respective GEF and the GDP will not dissociate from its binding pocket (Hall, 1990; Dascher and Balch, 1994). To keep ARF1 in its active state, Gln-71 has to be changed into a Leu. This position was first described for RAS as a critical catalytic residue. It is essential for the correct orientation of the water molecule, needed for nucleotide hydrolysis (Dascher and Balch, 1994; Scheffzek et al., 1997). Another conserved amino acid is essential for GTPase homo-dimerization. Mutating Tyr-35 in *S. cerevisiae* led to a reduced *in vitro* vesicle formation and also complementing ability, which could be rescued by cross-linking these mutants (Beck et al., 2009; Beck et al., 2011). More recent data in Arabidopsis, also revealed a disturbed dimer formation as a result of this mutation (Brumm et al., 2020).

To the best described functions of the ARF family belongs the anterograde and retrograde vesicle transport between the endoplasmic reticulum (ER) and the Golgi. SAR1 is involved in the COPII trafficking from the ER to the Golgi whereas ARF1 takes place in the opposite COPI

pathway. SAR1 is essential for COPII vesicle formation at the ER. It is recruited to the membrane by its GEF SEC12.

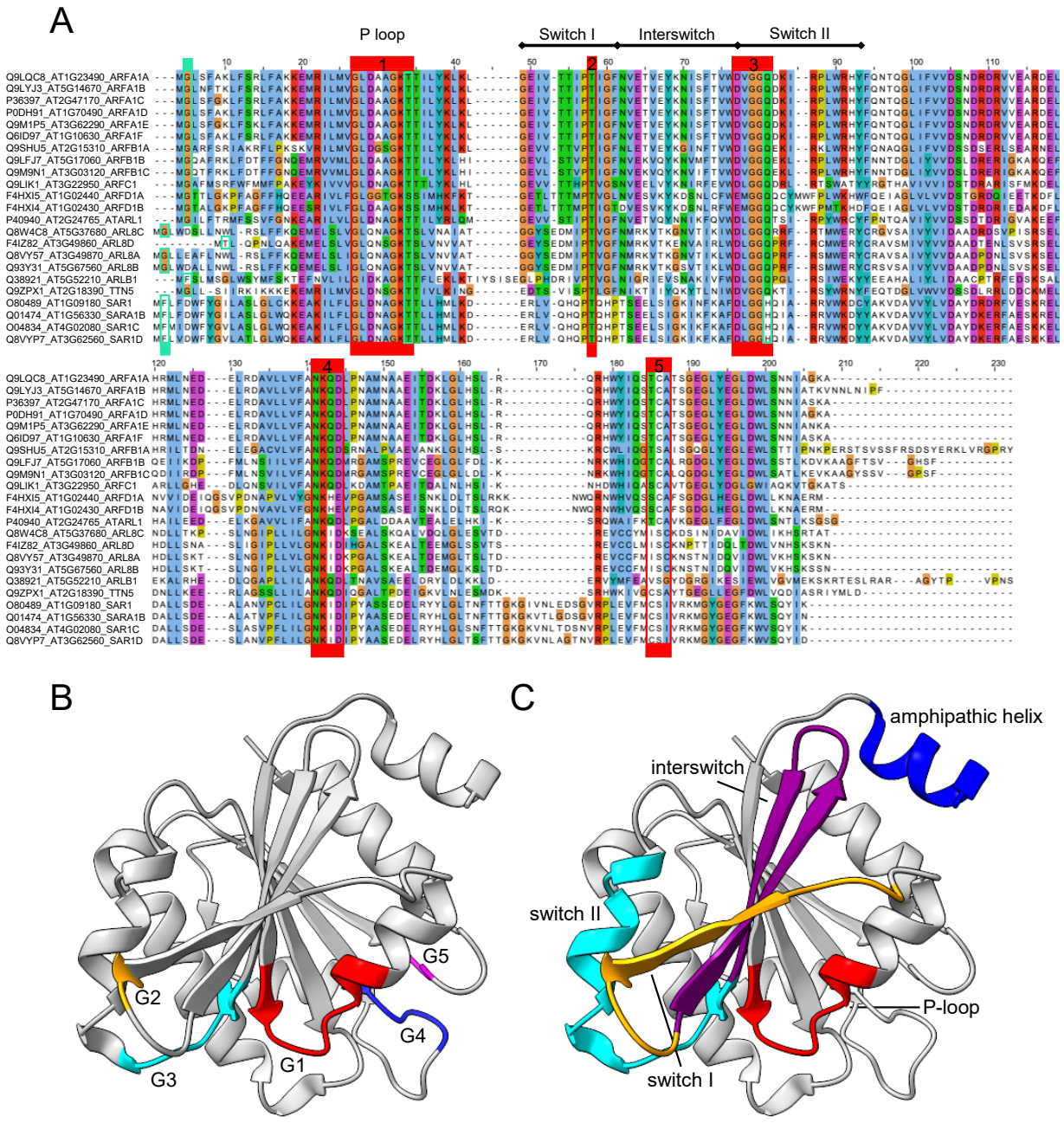

Figure 2. The Arabidopsis ARF family.
(A), Alignment of ARF, ARL and SAR proteins with their conserved G-binding motifs G1 to G5 (highlighted with red boxes). Motifs are involved in the typical switching motifs and are essential for nucleotide binding. Most possess a conserved Gly at position 2 (turquoise), as a potential myristoylation site. Mutations at specific conserved residues lead to the GTPase inactivity or activity. Inactivity: Thr to Asn (turquoise in G1 motif), activity: Gln to Lys (turquoise in G3 motif). (B, C), Crystal structure of HsARF6 (1E0S, Ménétrey et al., 2000) edited with ChimeraX (1.2.5, Goddard et al., 2018). (B), The G-binding motifs, G1 (red), G2 (orange), G3 (cyan), G4 (blue) and G5 (magenta) are highlighted. (C), The switching regions, switch I (orange), interswitch (purple), switch II (cyan), the P loop (red) and the amphipathic helix (blue) are highlighted.

This interaction is of great interest, because SEC12 is an ER-integral membrane protein without the typical Sec7 domain (for further details about Sec7 domain see respective

paragraph below), in contrast to the other known peripheral membrane ARF-GEFs. SEC12 then activates SAR1 by exchanging bound GDP to GTP and leads to the formation of COPII vesicles by recruiting of the other coat proteins (Jensen and Schekman, 2011; Brandizzi, 2018). Recent crystallography data based on *S. cerevisiae* proteins provided more detailed information how SEC12 can activate SAR1 (Joiner and Fromme, 2021). SEC12 structure is arranged in a β-propeller, consisting of seven β-sheets. Its structure does not undergo significant conformational changes upon binding to SAR1 (McMahon et al., 2012; Joiner and Fromme, 2021). An extended loop was identified as being part of the direct contact site in the SAR1-SEC12 complex in its nucleotide-free intermediate state (Joiner and Fromme, 2021). This loop is called K-loop due to its ability to bind K^+-ions and is essential for GEF activity (McMahon et al., 2012). In contrast, SAR1 undergoes conformational changes by binding to SEC12, which are different from the known structures in its GDP- or GTP-bound form. These changes lead to the loss of the nucleotide binding pocket, with special regard to Mg^{2+}-binding. The SAR1-binding site is very similar within complexes with SEC12 or the COPII-coat protein SEC23, leading to a suggested prevention of repeated SEC12-binding in the COPII pre-budding complex (Bi et al., 2002; Joiner and Fromme, 2021). It was proposed that the K-loop of SEC12 is disrupting the nucleotide-binding site by pushing the SAR1 switch II region. SAR1 Asp-73 is thereby displaced and its Mg^{2+}-binding function is disrupted. Electrostatic surface potential analyses imply SEC12-dependent positioning of SAR1 for its membrane anchoring via its amphipathic helix (Joiner and Fromme, 2021).

ARF-like (ARL) proteins in Arabidopsis

Compared to ARF1 and SAR1, only little is known about the ARL proteins.

ARL1

The first ARL in Arabidopsis was identified as an ARF homolog and described as ARF3. Homology comparisons showed the Drosophila ARL as the closest relative and led to the classification of ARF3 into the ARL class (Lebas and Axelos, 1994) and later renamed as ARL1 (Latijnhouwers et al., 2005). ARL1 is localized to the Golgi independently of GDP- or GTP-loading (Latijnhouwers et al., 2005; Stefano et al., 2006), but requires the myristoylation site, the Gly-2 (Stefano et al., 2006). ARL1 interacts with GRIP (golgin-97, RanBP2a, Imh1p, and p230/golgin-245) and is important for the targeting to the Golgi/*trans*-Golgi network (TGN) and resembles the function of mammalian and yeast ARL1 (Latijnhouwers et al., 2005). Glutathione-agarose affinity chromatography also revealed that binding of ARL1 to GRIP is independent of its activity-dependent conformation but has a preference for the active form. An *in vitro* repetition with *E. coli* expressed samples excluded the need of other proteins for this

binding. The interaction of ARL1 and GRIP is dependent on the residues Phe-51 and Trp-81, as previously predicted (Panic et al., 2003; Wu et al., 2004; Stefano et al., 2006).

ARLA1a/ARL8c

ARLA1a/ARL8c is expected to localize at the vacuole based on barley tonoplast proteome analysis by MS, which revealed the homolog of ARLA1a (Endler et al., 2006). Similar studies in Arabidopsis identified ARLA1c/ARL8a and ARLA1d/ARL8b at the tonoplast (Carter et al., 2004). The *Nicotiana tabacum* homolog NtARL8 interacts with NtTOM1 in *Tobamovirus* infected cells. Affinity purification experiments resulted in copurification of NtARL8 with NtTOM1, and the tobamoviral proteins 130K and 180K. The creation of double and triple mutants in Arabidopsis revealed that the ARF-likes from class A (ARLA1a/ARL8c, ARLA1c/ARL8a and ARLA1d/ARL8b) seem to have a function in the replication of *Tobamovirus*. *arla1c/arla1d* and *arla1c/arla1d/arla1a* plants were not able to accumulate the coat protein of *Youcai mosaic virus* (TMV-Cg) and *Tomato mosaic virus* (ToMV) (Nishikiori et al., 2011).

TITAN 5/HALLIMASCH

TITAN 5/HALLIMASCH (TTN5/HAL) was identified in screens for abnormal embryo-mutants. Homozygous *ttn5/hal* embryos consist of only a few enlarged cells with enlarged nuclei in embryo and endosperm which leads to embryo lethality. It is suggested that the cell division defect is caused by a disturbed cytokinesis and not a general arrest of the cell cycle. KNOLLE and α-tubulin antibody staining showed a failed formation of the cell plate, the mitotic spindle in anaphase or the phragmoplast in the telophase (Mayer et al., 1999; McElver et al., 2000). Based on sequence similarities it is a homolog of HsARL2 (McElver et al., 2000).

TTN5 homologs participate in the tubulin folding process by interacting with Cofactor D (respective names for the homologs: Arabidopsis *TTN5* & *TTN1*, mammalian *ARL2* & *Cofactor D*, *S. cerevisiae Cin1* & *Cin4*, *S. pombe Alp1* & *Alp41*) and similar is expected based on its mutant phenotype in Arabidopsis (Hoyt et al., 1990; Bhamidipati et al., 2000; Radcliffe et al., 2000; Tzafrir et al., 2002; Francis et al., 2017). Interesting for TTN5 is the presence of Gly-2 but it does not seem to be substrate for *N*-myristoyltransferases, based on *in vitro* N-terminal methionine excision assay, which is also the case for HsARL2 and HsARL3 (Boisson et al., 2003; Kahn et al., 2006).

We recently identified TTN5 being linked to Fe homeostasis as an IRT1vr interactor. Together they localized to endosomes/multivesicular bodies (MVBs) (Mohr et al., unpublished, Manuscript II). Additionally, TTN5 interacts with other IRT1 interactors and regulators, ENHANCED BENDING 1 (EHB1), PATELLIN 2 (PATL2) and SORTING NEXIN 1 (SNX1),

suggesting a coordinating role of TTN5 in IRT1 regulation. We hypothesized another function of TTN5 in PM protein trafficking (Mohr et al., unpublished, Manuscript II and Manuscript III). Next to IRT1, TTN5 interacts with the H^+-ATPases AHA1 and AHA2. Colocalization studies revealed coexpression of AHA1 and TTN5 in endosomes/MVBs, similar to TTN5-IRT1 colocalization. Excitingly, we identified the SAR1-GEF SEC12 as another TTN5 interactor, promoting a potential GEF activity on TTN5 (Mohr et al., unpublished, Manuscript III). Up to date, no specific ARL-GEF or -GAP proteins are identified in Arabidopsis and emphasize the noteworthiness of this special finding.

ARF-exchange factors in plants (ARF-GEFs)

GTPases have a very high affinity for GDP resulting in a slow intrinsic rate of nucleotide dissociation. GEF come into action to increase the ability of nucleotide exchange (Klebe et al., 1995; Béraud-Dufour et al., 1998).

In mammalians, five subfamilies of ARF-GEFs are classified, while only two types of ARF-GEFs exist in Arabidopsis. They belong to the family of large ARF-GEFs, the Golgi Brefeldin A (BFA)-resistance factor 1 (GBF/GNOM) and BFA-inhibited GEF (BIG) family (Memon, 2004; Wright et al., 2014; Brandizzi, 2018). The two ARF-GEF subfamilies consist of eight members in total, GNOM and GNOM-LIKE (GNL) 1 and 2, and BIG1 to BIG5. They all exhibit the characteristic feature of ARF-GEFs, the Sec7 domain (Figure 3). It is a 200 amino acid domain which is needed for the facilitation of the GDP to GTP exchange (Chardin et al., 1996; Vernoud et al., 2003). The Sec7 domain forms two subdomains, consisting of ten helices in total, seven N-terminal helices forming a superhelix and the other three packed to a dense bundle directly at the C-terminus of the superhelix (Wright et al., 2014). The superhelix, at the hydrophilic-loop-tip between helix 6 and 7, comprises a highly conserved motif, the glutamic finger (Casanova, 2007). This Glu residue is essential for GEF activity. Tested mutations of this residue to Lys or Leu abolishes ARF nucleotide-exchange activity (Béraud-Dufour et al., 1998; Cherfils et al., 1998).

The presumed mechanism of ARF-GEF-catalyzed nucleotide exchange is the following: Upon ARF-GDP interaction with its respective GEF, the switch regions of the GTPase bind to the hydrophobic groove of the Sec7 domain between the two subdomains (Wright et al., 2014). Then the glutamic finger inserts into the nucleotide-binding fold (into or in close proximity to the ARF P loop and Mg^{2+}-binding site) forced to the nucleotide phosphate by its negative charge (Béraud-Dufour et al., 1998; Mossessova et al., 1998). It leads to destabilization of the coordinating Mg^{2+} and the bound GDP due to steric and electrostatic repulsive effects with the ion and the β-phosphate (Mossessova et al., 2003; Renault et al., 2003; Casanova, 2007). Based on affinity studies, the interaction between the β-phosphate and the P loop seems to be

of utmost importance for tight nucleotide binding. The interference of the GEF and the concomitant structural change of the P loop is suggested to be the main reason for the reduced nucleotide affinity and its release from the GTPase (Vetter and Wittinghofer, 2001). When nucleotide free, ARF switches to its GTP-bound conformation and opens up the possibility of GTP-binding. The Sec7 domain is released from the ARF-interaction upon GTP-binding (Goldberg, 1998; Shin and Nakayama, 2004).

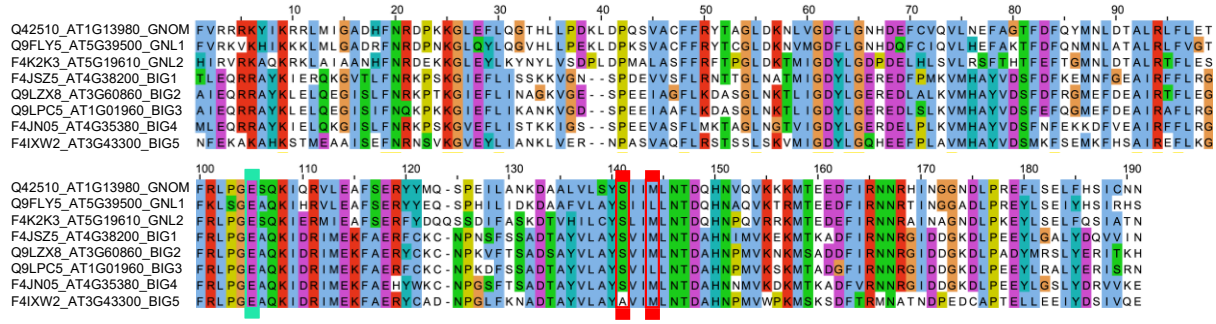

Figure 3. Alignment of the Sec7 domain of Arabidopsis ARF-GEF family.
Alignment of the Sec7 domain of GNOM (-LIKE) and BIG proteins. They possess a conserved glutamic finger (highlighted with turquoise boxes), essential for their GEF-activity. They exhibit different sensitivity against BFA, based on their sequence. GNL1, BIG3 and BIG5 are BFA-resistant whereas the rest is BFA-sensitive. Two residues crucial for BFA-sensitivity or -resistance are highlighted in red.

The fungal GEF inhibitor BFA can block the catalytic activity by acting as an uncompetitive inhibitor on the enzyme-substrate complex. BFA is forming a quaternary complex consisting of ARF-GDP-BFA-Sec7 domain and thereby stabilizing the usually short-lived ARF-GDP-Sec7 intermediate (Mansour et al., 1999; Peyroche et al., 1999; Jackson and Casanova, 2000). Crystal structures opened up the mechanism behind. When the ARF-GDP-Sec7 domain intermediate is formed, a hydrophobic cavity is created between ARF switch I and II region and the hydrophobic groove of the Sec7 domain. BFA integrates itself into this pocket and thereby inhibits the conformational changes needed for contact between the bound nucleotide and the catalytic Glu of the GEF (Renault et al., 2003).

The Arabidopsis ARF-GEFs have different sensitivity to BFA treatment (Geldner et al., 2003; Cox et al., 2004; Memon, 2004; Brandizzi, 2018). GNOM, GNL2, BIG1, BIG2 and BIG4 are sensitive to BFA treatment and the disruption of their activity leads to the formation of BFA bodies, whereas GNL1, BIG3 and BIG5 are BFA-resistant. This resistance depends on specific amino acids in their conserved Sec7 domain, making it possible to create BFA-sensitive GNL1, BIG3 or BIG5 or to induce resistance in the other ARF-GEFs. Mutating Met-696 in GNOM to Lys leads to a BFA-resistant GNOM (Peyroche et al., 1999; Geldner et al., 2003).

GNOM

GNOM is the best characterized ARF-GEF in Arabidopsis. It was identified in a defective embryo-mutant screen (Mayer et al., 1991; Mayer et al., 1993). Described *gnom* mutants have

a disturbed root and shoot apical meristem and lack the bilateral symmetry (Mayer et al., 1993). GNOM localizes to endosomal compartments. It can colocalize with the endocytosed dye FM4-64 and BFA-treatment leads to the formation of FM4-64 and GNOM-positive BFA bodies (Geldner et al., 2003). GNOM is involved in auxin transport, by regulating the intracellular cycling of auxin efflux carrier PIN-FORMED 1 (PIN1) (Steinmann et al., 1999; Geldner et al., 2003). Thereby, it is important for the recycling and its polarized localization at the PM of PIN1, which is also the case for the boron transporter BOR1 (Steinmann et al., 1999; Geldner et al., 2003; Yoshinari et al., 2021). Additionally, it is indirectly involved in protein recycling, by playing a role in proper TGN maintenance (Naramoto et al., 2014).

GNOM together with GNL1 can localize to the Golgi for recruiting and activating ARF1 in COPI vesicle trafficking from the Golgi to the ER (Richter et al., 2007; Singh et al., 2018). Recently, interaction of GNOM and BIG3 with the flippase ALA3 was investigated with a proposed role in PIN1 regulation (Zhang et al., 2020). Similar results were previously obtained in *S. cerevisiae* and *Caenorhabditis elegans*, supporting a conserved function based on such interactions (Chantalat et al., 2004; Wicky et al., 2004; Tsai et al., 2013; McGough et al., 2018; Zhang et al., 2020).

GNOM was also identified as part of the driving machinery of root hair development (Tanaka et al., 2009; Naramoto et al., 2010; Naramoto et al., 2014). It is acting in the primary hook formation phase (Jonsson et al., 2017). GNOM is expressed in trichoblasts in the early phase of bulge formation (Richter et al., 2011). Together with GNL1 it has an essential role in the planar polarity of root hair (Fischer et al., 2006).

GNOM-LIKE 1 and GNOM-LIKE 2

GNOM-LIKE 1 is predominantly located and functions at Golgi stacks, being part of the formation of COPI-coated vesicles (Richter et al., 2007). Though GNOM can compensate a loss of GNL1, GNL1 cannot act in the other way in GNOM-dependent endosomal recycling, indicating the combined activity in Golgi to ER trafficking, with an additional essential role of GNOM (Richter et al., 2007).

In contrary, GNL2 expression is specifically located in pollen with a potential role in pollen germination (Jia et al., 2009).

BIG 1 to BIG4

BIG1 to BIG4 are located at the TGN and show functional redundancy to each other. They are involved in the vesicle trafficking originating from the TGN to the vacuole, the PM or the cell division plane. The cell division plane-located protein KNOLLE accumulates in BIG4-positive BFA bodies in a *big3* mutant background, indicating its proper targeting being dependent on the activity of BIG3 (Richter et al., 2014). The four BIGs are needed for localization of ARF1 at

the TGN like GNOM, whereas GNOM acts in ARF1 recycling and BIG1 to BIG4 more in the secretion pathway (Geldner et al., 2003; Richter et al., 2014). The AP-1 adaptor protein complex is recruited by BIG1 to BIG4 to the TGN as well (Richter et al., 2014).

BIG1 to BIG4 act like GNOM in the auxin signaling, by regulating the transport of newly synthesized AUXIN 1 (AUX1), one of the major auxin influx carriers, to the PM, but independently of GNOM function. In this context, colocalization of BIG4 with ECHIDNA, the latter also involved in transport of auxin carriers, and ARF1 was detected at the TGN, thereby both proteins seem to be important for ARF1 localization. Knockouts of ARF1 or the BIGs display the same phenotypical defects in AUX1 trafficking and the hook maintenance as in *ech* mutants (Bennett et al., 1996; Boutté et al., 2013; Richter et al., 2014; Jonsson et al., 2017). Whereas GNOM is involved in the primary hook formation, the BIGs may play a role in the following steps in the hook development, being more important in the ethylene-mediated maintenance (Jonsson et al., 2017). They work in a GNOM-independent way in the lateral root formation (Richter et al., 2014). *In vitro* studies proofed GEF-activity for BIG3 on ARF1 (Nielsen et al., 2006).

For BIG2 another localization was identified. Next to its functioning at the TGN it can be also detected at recycling endosomes (Shin et al., 2004).

BIG 5

Also, BIG5/BEN1/MIN7 is involved in vesicle trafficking. It is localized at the TGN/early endosomes (EE) and takes place in the endocytosis of PM proteins and transport to the TGN. It regulates trafficking steps at the TGN/EE (Nomura et al., 2006; Tanaka et al., 2009; Nomura et al., 2011; Tanaka et al., 2013). Like GNOM, BIG5 is involved in PIN1 recycling, but BIG5 acts in an earlier step in sorting PIN1 from EE to recycling endosomes (Anders et al., 2008; Tanaka et al., 2009). Next to it, BIG5 has a role in the pathogen response, by being an inactivation target by bacterial effector HopM1 of *Pseudomonas syringae* pathovar tomato (Nomura et al., 2006; Tanaka et al., 2009; Nomura et al., 2011; Tanaka et al., 2013). Transmission and scanning electron microscopy revealed a disturbed cuticle and stomatal development in *big5* mutant leaves, which was accompanied by a reduced amount of cutin monomer content identified by GC-MS. A connection between the altered cuticle and the reduced immune response was suggested (Zhao et al., 2020). Recent data found evidence of BIG5 also relevant in the pathogen response against fungus *Fusarium graminearum* which is also conserved in crop plants (Machado Wood et al., 2021).

Like GNOM, BIG5 potentially takes place in root hair development. Loss-of-function *big5* leads to defects in root hair shape (Nomura et al., 2006; Tanaka et al., 2009; Naramoto et al., 2010; Naramoto et al., 2014; Sparks et al., 2016).

Our current knowledge of ARF-GEFs clearly shows their interplay in a wide variety of vesicle transport-dependent cellular functions. In this context, the unequal ratio of GEFs to GTPases also suggests that a GEF can recruit and activate multiple GTPases to its ancestral site of action.

ARF-activating proteins in plants (ARF-GAPs)

ARF-GAP proteins were identified by their ARF-GAP domain (AGD). In Arabidopsis, 15 ARF-GAPs are identified. They can be categorized into four classes based on their domain organization and phylogenetic analysis (Figure 4). The class I, consists of AGD1 to AGD4 and is classified by a pleckstrin homology (PH) domain and two or three ankyrin repeat domains. AGD1 to AGD3 contain an additional Bin1-amhiphysin-Rvs167p/Rvs161p (BAR) domain. Class II ARF-GAPs, AGD5 to AGD10, only possess an N-terminal AGD domain. Their sequence and domain organization are similar to Golgi-localized ARF-GAPs in yeast and mammals (Cukierman et al., 1995; Poon et al., 1999). AGD11 to AGD13 build the third class of AGDs. They contain an additional C2 domain, which is responsible for a variety of binding events, such as phospholipids or other proteins, in a Ca^{2+}-dependent manner (Vernoud et al., 2003; Dümmer et al., 2016). Class IV comprises the last two AGDs, AGD14 and AGD15, which consist almost exclusively of the AGD (Vernoud et al., 2003).

AGDs localize to different cellular compartments in the endomembrane system. All GAPs contain their name-giving 70 amino acids large GAP-domain. This domain has a conserved zinc finger motif of CXXCX(16-17)CXXC (where X representing any amino acid) close to its N-terminus and essential for their GAP-activity. Additionally, mutant-based activity assays of conserved residues identified an Arg, being also critical for hydrolysis of the third phosphate of GTP (Vitale et al., 1998; Randazzo et al., 2000; Memon, 2004).

AGD1 to AGD4

AGD1 was identified at the PM, by binding to phosphatidylinositol-4-phosphate (PI4P), and there regulating parts of polarized membrane trafficking in root hair. This is achieved by taking an impact on the cytoskeletal organization (Yoo et al., 2018). Thereby, its membrane location depends on its PH domain. A stabilizing function of AGD1 on the trafficking apparatus, needed for normal root tip growth, is proposed (Yoo et al., 2018). It is closely related to AGD2 to AGD4 and all functioning in the regulation of vasculature development, influenced by auxin signaling and transport. Loss of AGD3 leads to discontinuous leaf venation patterns (Koizumi et al., 2005; Sieburth et al., 2006). AGD3, is also called VASCULAR NETWORK DEFECTIVE 3 (VAN3) or SCARFACE (SCF). Like AGD1, AGD3 can bind PI4P, but is located to the TGN/EE and the PM (Jackson and Casanova, 2000; Koizumi et al., 2005; Naramoto et al., 2009; Naramoto et al., 2010). The ANK and PH domain of class I AGDs are needed for fully functional GAP activity,

deletions of these domains, led to a reduced or the full loss of activity (Ha et al., 2008; Naramoto et al., 2009). AGD3 can interact with ARF1 (Koizumi et al., 2005; Song et al., 2006; Min et al., 2007).

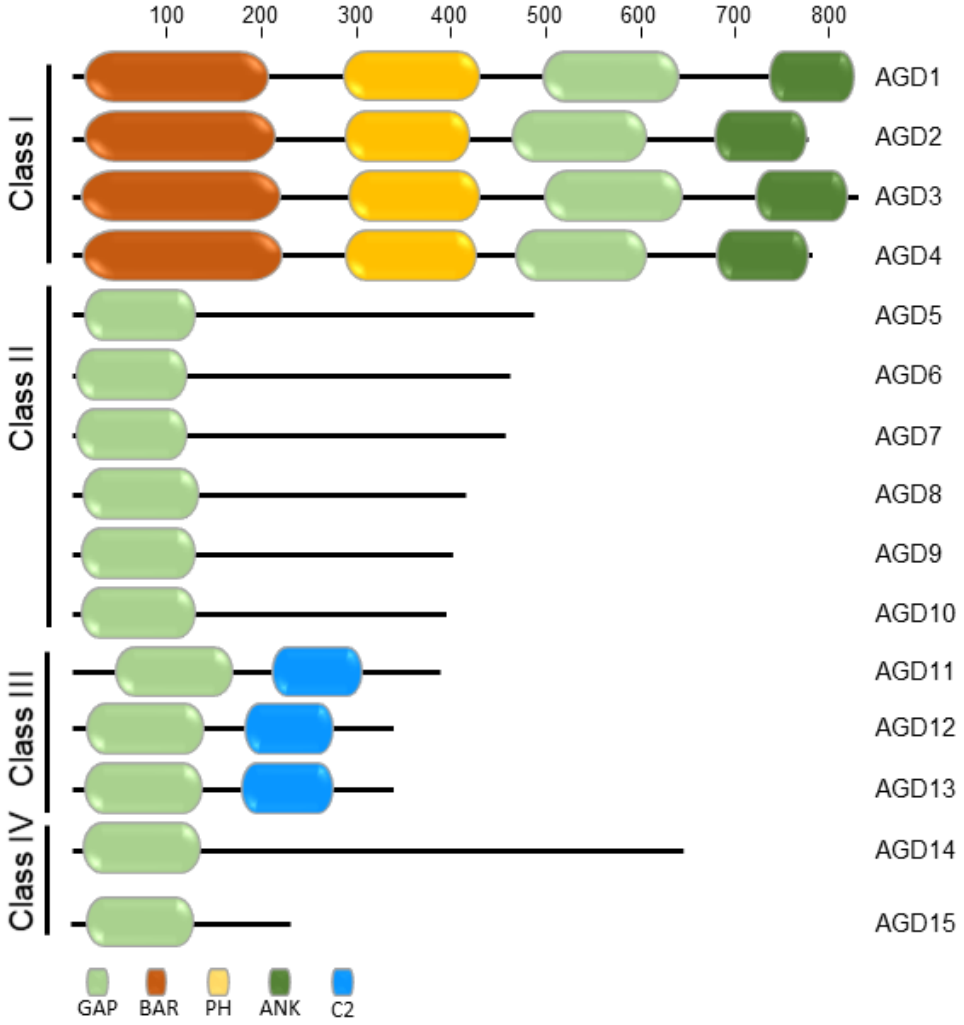

Figure 4. Domain prediction of Arabidopsis ARF-GAP family.
AGDs can be categorized into four different classes, based on their domain-structure. Class I (AGD1-AGD4) consists of a BAR, PH, GAP and ANK domain. Class II exhibit only a GAP-domain and are similar to Golgi-localized Arf-GAPs in yeast and mammals. Class III have next to its GAP-domain an additional C2 domain. Class IV possess only a GAP domain.

AGD5

AGD5, also called NEVERSHED (NEV) is a plant-specific ARF-GAP, being located at the TGN and endosomal compartments eventually the recycling ones. Loss of AGD5 activity leads to a delay in floral organ abscission, suggesting a role in membrane trafficking in the separation stage of organ abscission (Liljegren et al., 2009; Stefano et al., 2010).

AGD7 to AGD10

AGD7 to AGD10 are all located at the Golgi. They take place in the regulation of COPI vesicle trafficking, between the Golgi and the ER or in intra-Golgi trafficking or both transport

pathways (Min et al., 2007; Min et al., 2013). AGD7 and AGD10 can interact with ARF1 (Koizumi et al., 2005; Song et al., 2006; Min et al., 2007).

AGD8 and AGD9 probably possess redundant functions and are essential for plant development. Knock-out of just one of them does not lead to any specific phenotype, but crosses of these mutant lines failed to produce homozygous double-knock-out seedlings, assuming embryo lethality. They colocalize with ST-GFP and γ-COP at the Golgi (Min et al., 2013).

AGD10, also called ROOT AND POLLEN ARF-GAP (RPA) is involved in the polarized tip growth in pollen tubes and root hair (Song et al., 2006). *AGD10* expression is induced when AGD9 is lacking, suggesting a compensatory effect of AGD10 (Min et al., 2013).

AGD12

AGD12 was investigated with the C2-domain containing protein C2-DOMAIN ABA-RELATED 6/ENHANCED BENDING 1 (CAR6/EHB1). They possess some structural similarities by their C2-domain, which is involved in Ca^{2+}-binding (Dümmer et al., 2016). Together they could be involved in plant-specific functions as EHB1 is only present in plants.

Our current knowledge of the ARF family and its GEF and GAP proteins clearly reflects the importance of their interplay in the regulation of vesicle-mediated transport pathways. They take place in a broad range of cellular signaling events, ranging from protein trafficking, phytohormone-regulated or essential plant developmental processes. At the same time, many aspects of the mechanisms of direct interaction between them, as well as interaction partners and coregulations in general, remain unclear or even unidentified and offer a variety of extremely interesting opportunities for future studies. Especially, research in *S. cerevisiae* and humans has shown that ARF and ARL proteins have conserved structures among many organisms and are subject to the same molecular mechanisms. The plant ARF family also exhibits conserved functions, however, many plant-specific functions have also been developed and are of great interest. Here, the different family sizes of ARF proteins in yeast, mammals, and plants, with particular attention to the different ratio of their GEFs and GAPs, may play a crucial role. Arabidopsis possess more ARF and ARL GTPases than AGDs and especially ARF-GEFs, suggesting competing relations between the GTPases and highlighting the importance of further research to identify the role of small GTPases and in particular, of the little-studied ARL GTPases.

Acknowledgements

This work was supported by the Deutsche Forschungsgemeinschaft (DFG, German Research Foundation Project no. 267205415–SFB 1208 and project B05 to P.B.):

References

Ahmadi Y, Ghorbanihaghjo A, Argani H (2017) The balance between induction and inhibition of mevalonate pathway regulates cancer suppression by statins: A review of molecular mechanisms. Chem Biol Interact **273:** 273-285

Anders N, Nielsen M, Keicher J, Stierhof YD, Furutani M, Tasaka M, Skriver K, Jürgens G (2008) Membrane association of the Arabidopsis ARF exchange factor GNOM involves interaction of conserved domains. Plant Cell **20:** 142-151

Beck R, Adolf F, Weimer C, Bruegger B, Wieland FT (2009) ArfGAP1 Activity and COPI Vesicle Biogenesis. Traffic **10:** 307-315

Beck R, Prinz S, Diestelkötter-Bachert P, Röhling S, Adolf F, Hoehner K, Welsch S, Ronchi P, Brügger B, Briggs JAG, Wieland F (2011) Coatomer and dimeric ADP ribosylation factor 1 promote distinct steps in membrane scission. The Journal of cell biology **194:** 765-777

Bennett MJ, Marchant A, Green HG, May ST, Ward SP, Millner PA, Walker AR, Schulz B, Feldmann KA (1996) Arabidopsis AUX1 gene: a permease-like regulator of root gravitropism. Science **273:** 948-950

Béraud-Dufour S, Robineau S, Chardin P, Paris S, Chabre M, Cherfils J, Antonny B (1998) A glutamic finger in the guanine nucleotide exchange factor ARNO displaces Mg^{2+} and the β-phosphate to destabilize GDP on ARF1. The EMBO Journal **17:** 3651-3659

Bhamidipati A, Lewis SA, Cowan NJ (2000) ADP ribosylation factor-like protein 2 (Arl2) regulates the interaction of tubulin-folding cofactor D with native tubulin. Journal of Cell Biology **149:** 1087-1096

Bi X, Corpina RA, Goldberg J (2002) Structure of the Sec23/24-Sar1 pre-budding complex of the COPII vesicle coat. Nature **419:** 271-277

Boisson B, Giglione C, Meinnel T (2003) Unexpected Protein Families Including Cell Defense Components Feature in the N-Myristoylome of a Higher Eukaryote*. Journal of Biological Chemistry **278:** 43418-43429

Bos JL (1988) The ras gene family and human carcinogenesis. Mutation Research/Reviews in Genetic Toxicology **195:** 255-271

Boutté Y, Jonsson K, McFarlane HE, Johnson E, Gendre D, Swarup R, Friml J, Samuels L, Robert S, Bhalerao RP (2013) ECHIDNA-mediated post-Golgi trafficking of auxin carriers for differential cell elongation. Proceedings of the National Academy of Sciences **110:** 16259-16264

Brandizzi F (2018) Transport from the endoplasmic reticulum to the Golgi in plants: Where are we now? Semin Cell Dev Biol **80:** 94-105

Brumm S, Singh MK, Nielsen ME, Richter S, Beckmann H, Stierhof YD, Fischer AM, Kumaran M, Sundaresan V, Jürgens G (2020) Coordinated Activation of ARF1 GTPases by ARF-GEF GNOM Dimers Is Essential for Vesicle Trafficking in Arabidopsis. Plant Cell **32:** 2491-2507

Carter C, Pan S, Zouhar J, Avila EL, Girke T, Raikhel NV (2004) The vegetative vacuole proteome of *Arabidopsis thaliana* reveals predicted and unexpected proteins. Plant Cell **16:** 3285-3303

Casanova JE (2007) Regulation of Arf Activation: the Sec7 Family of Guanine Nucleotide Exchange Factors. Traffic **8:** 1476-1485

Chantalat S, Park SK, Hua Z, Liu K, Gobin R, Peyroche A, Rambourg A, Graham TR, Jackson CL (2004) The Arf activator Gea2p and the P-type ATPase Drs2p interact at the Golgi in Saccharomyces cerevisiae. J Cell Sci **117:** 711-722

Chardin P, Paris S, Antonny B, Robineau S, Béraud-Dufour S, Jackson CL, Chabre M (1996) A human exchange factor for ARF contains Sec7- and pleckstrin-homology domains. Nature **384:** 481-484

Cherfils J, Ménétrey J, Mathieu M, Le Bras G, Robineau S, Béraud-Dufour S, Antonny B, Chardin P (1998) Structure of the Sec7 domain of the Arf exchange factor ARNO. Nature **392:** 101-105

Cox R, Mason-Gamer RJ, Jackson CL, Segev N (2004) Phylogenetic Analysis of Sec7-Domain–containing Arf Nucleotide Exchangers. Molecular Biology of the Cell **15:** 1487-1505

Cukierman E, Huber I, Rotman M, Cassel D (1995) The ARF1 GTPase-activating protein: zinc finger motif and Golgi complex localization. Science **270:** 1999-2002

Dascher C, Balch WE (1994) Dominant inhibitory mutants of ARF1 block endoplasmic reticulum to Golgi transport and trigger disassembly of the Golgi apparatus. J Biol Chem **269:** 1437-1448

Dautt-Castro M, Rosendo-Vargas M, Casas-Flores S (2021) The Small GTPases in Fungal Signaling Conservation and Function. Cells **10**

Dümmer M, Michalski C, Essen LO, Rath M, Galland P, Forreiter C (2016) EHB1 and AGD12, two calcium-dependent proteins affect gravitropism antagonistically in *Arabidopsis thaliana*. J Plant Physiol **206:** 114-124

Endler A, Meyer S, Schelbert S, Schneider T, Weschke W, Peters SW, Keller F, Baginsky S, Martinoia E, Schmidt UG (2006) Identification of a vacuolar sucrose transporter in barley and Arabidopsis mesophyll cells by a tonoplast proteomic approach. Plant physiology **141:** 196-207

Enomoto K, Gill DM (1980) Cholera toxin activation of adenylate cyclase. Roles of nucleoside triphosphates and a macromolecular factor in the ADP ribosylation of the GTP-dependent regulatory component. J Biol Chem **255:** 1252-1258

Fischer U, Ikeda Y, Ljung K, Serralbo O, Singh M, Heidstra R, Palme K, Scheres B, Grebe M (2006) Vectorial information for Arabidopsis planar polarity is mediated by combined AUX1, EIN2, and GNOM activity. Curr Biol **16:** 2143-2149

Francis JW, Goswami D, Novick SJ, Pascal BD, Weikum ER, Ortlund EA, Griffin PR, Kahn RA (2017) Nucleotide Binding to ARL2 in the TBCD·ARL2·β-Tubulin Complex Drives Conformational Changes in β-Tubulin. J Mol Biol **429:** 3696-3716

Geldner N, Anders N, Wolters H, Keicher J, Kornberger W, Muller P, Delbarre A, Ueda T, Nakano A, Jürgens G (2003) The Arabidopsis GNOM ARF-GEF mediates endosomal recycling, auxin transport, and auxin-dependent plant growth. Cell **112:** 219-230

Goddard TD, Huang CC, Meng EC, Pettersen EF, Couch GS, Morris JH, Ferrin TE (2018) UCSF ChimeraX: Meeting modern challenges in visualization and analysis. Protein Sci **27:** 14-25

Goldberg J (1998) Structural Basis for Activation of ARF GTPase: Mechanisms of Guanine Nucleotide Exchange and GTP–Myristoyl Switching. Cell **95:** 237-248

Ha VL, Bharti S, Inoue H, Vass WC, Campa F, Nie Z, de Gramont A, Ward Y, Randazzo PA (2008) ASAP3 is a focal adhesion-associated Arf GAP that functions in cell migration and invasion. J Biol Chem **283:** 14915-14926

Hall A (1990) The cellular functions of small GTP-binding proteins. Science **249:** 635-640

Hoyt MA, Stearns T, Botstein D (1990) Chromosome instability mutants of *Saccharomyces cerevisiae* that are defective in microtubule-mediated processes. Molecular and Cellular Biology **10:** 223-234

Humphreys D, Liu T, Davidson AC, Hume PJ, Koronakis V (2012) The Drosophila Arf1 homologue Arf79F is essential for lamellipodium formation. J Cell Sci **125:** 5630-5635

Hwang I, Robinson DG (2009) Transport vesicle formation in plant cells. Curr Opin Plant Biol **12:** 660-669

Jackson CL, Bouvet S (2014) Arfs at a Glance. Journal of Cell Science **127:** 4103-4109

Jackson CL, Casanova JE (2000) Turning on ARF: the Sec7 family of guanine-nucleotide-exchange factors. Trends in Cell Biology **10:** 60-67

Jensen D, Schekman R (2011) COPII-mediated vesicle formation at a glance. Journal of Cell Science **124:** 1-4

Jia DJ, Cao X, Wang W, Tan XY, Zhang XQ, Chen LQ, Ye D (2009) GNOM-LIKE 2, encoding an adenosine diphosphate-ribosylation factor-guanine nucleotide exchange factor protein homologous to GNOM and GNL1, is essential for pollen germination in Arabidopsis. J Integr Plant Biol **51:** 762-773

Joiner AMN, Fromme JC (2021) Structural basis for the initiation of COPII vesicle biogenesis. Structure **29:** 859-872.e856

Jonsson K, Boutté Y, Singh RK, Gendre D, Bhalerao RP (2017) Ethylene Regulates Differential Growth via BIG ARF-GEF-Dependent Post-Golgi Secretory Trafficking in Arabidopsis. The Plant cell **29:** 1039-1052

Just WW, Peränen J (2016) Small GTPases in peroxisome dynamics. Biochimica et Biophysica Acta (BBA) - Molecular Cell Research **1863:** 1006-1013

Kahn RA, Cherfils J, Elias M, Lovering RC, Munro S, Schurmann A (2006) Nomenclature for the human Arf family of GTP-binding proteins: ARF, ARL, and SAR proteins. The Journal of cell biology **172:** 645-650

Kahn RA, Der CJ, Bokoch GM (1992) The ras superfamily of GTP-binding proteins: guidelines on nomenclature. The FASEB Journal **6:** 2512-2513

Kahn RA, Gilman AG (1984) ADP-ribosylation of Gs promotes the dissociation of its alpha and beta subunits. J Biol Chem **259:** 6235-6240

Klebe C, Prinz H, Wittinghofer A, Goody RS (1995) The Kinetic Mechanism of Ran-Nucleotide Exchange Catalyzed by RCC1. Biochemistry **34:** 12543-12552

Koizumi K, Naramoto S, Sawa S, Yahara N, Ueda T, Nakano A, Sugiyama M, Fukuda H (2005) VAN3 ARF–GAP-mediated vesicle transport is involved in leaf vascular network formation. Development **132:** 1699-1711

Labbaoui H, Bogliolo S, Ghugtyal V, Solis NV, Filler SG, Arkowitz RA, Bassilana M (2017) Role of Arf GTPases in fungal morphogenesis and virulence. PLoS Pathog **13:** e1006205

Latijnhouwers M, Hawes C, Carvalho C, Oparka K, Gillingham AK, Boevink P (2005) An Arabidopsis GRIP domain protein locates to the trans-Golgi and binds the small GTPase ARL1. The Plant Journal **44:** 459-470

Lebas M, Axelos M (1994) A cDNA encoding a new GTP-binding protein of the ADP-ribosylation factor family from Arabidopsis. Plant Physiol **106:** 809-810

Liljegren SJ, Leslie ME, Darnielle L, Lewis MW, Taylor SM, Luo R, Geldner N, Chory J, Randazzo PA, Yanofsky MF, Ecker JR (2009) Regulation of membrane trafficking and organ separation by the NEVERSHED ARF-GAP protein. Development **136:** 1909-1918

Machado Wood AK, Panwar V, Grimwade-Mann M, Ashfield T, Hammond-Kosack KE, Kanyuka K (2021) The vesicular trafficking system component MIN7 is required for minimizing *Fusarium graminearum* infection. J Exp Bot **72:** 5010-5023

Mansour SJ, Skaug J, Zhao XH, Giordano J, Scherer SW, Melançon P (1999) p200 ARF-GEP1: a Golgi-localized guanine nucleotide exchange protein whose Sec7 domain is targeted by the drug brefeldin A. Proceedings of the National Academy of Sciences of the United States of America **96:** 7968-7973

Mayer U, Buttner G, Jurgens G (1993) Apical-basal pattern formation in the Arabidopsis embryo: studies on the role of the gnom gene. Development **117:** 149-162

Mayer U, Herzog U, Berger F, Inzé D, Jürgens G (1999) Mutations in the PILZ group genes disrupt the microtubule cytoskeleton and uncouple cell cycle progression from cell division in Arabidopsis embryo and endosperm. European Journal of Cell Biology **78:** 100-108

Mayer U, Ruiz RAT, Berleth T, Miséra S, Jürgens G (1991) Mutations affecting body organization in the Arabidopsis embryo. Nature **353:** 402-407

McElver J, Patton D, Rumbaugh M, Liu C-m, Yang LJ, Meinke D (2000) The TITAN5 Gene of Arabidopsis Encodes a Protein Related to the ADP Ribosylation Factor Family of GTP Binding Proteins. The Plant Cell **12:** 1379-1392

McGough IJ, de Groot REA, Jellett AP, Betist MC, Varandas KC, Danson CM, Heesom KJ, Korswagen HC, Cullen PJ (2018) SNX3-retromer requires an evolutionary conserved MON2:DOPEY2:ATP9A complex to mediate Wntless sorting and Wnt secretion. Nature Communications **9:** 3737

McMahon C, Studer SM, Clendinen C, Dann GP, Jeffrey PD, Hughson FM (2012) The structure of Sec12 implicates potassium ion coordination in Sar1 activation. J Biol Chem **287:** 43599-43606

Memon AR (2004) The role of ADP-ribosylation factor and SAR1 in vesicular trafficking in plants. Biochim Biophys Acta **1664:** 9-30

Ménétrey J, Macia E, Pasqualato S, Franco M, Cherfils J (2000) Structure of Arf6–GDP suggests a basis for guanine nucleotide exchange factors specificity. Nature Structural Biology **7:** 466-469

Mima J (2021) Self-assemblies of Rab- and Arf-family small GTPases on lipid bilayers in membrane tethering. Biophys Rev **13:** 531-539

Min MK, Jang M, Lee M, Lee J, Song K, Lee Y, Choi KY, Robinson DG, Hwang I (2013) Recruitment of Arf1-GDP to Golgi by Glo3p-type ArfGAPs is crucial for golgi maintenance and plant growth. Plant Physiol **161:** 676-691

Min MK, Kim SJ, Miao Y, Shin J, Jiang L, Hwang I (2007) Overexpression of Arabidopsis AGD7 causes relocation of Golgi-localized proteins to the endoplasmic reticulum and inhibits protein trafficking in plant cells. Plant Physiol **143:** 1601-1614

Mossessova E, Corpina RA, Goldberg J (2003) Crystal Structure of ARF1•Sec7 Complexed with Brefeldin A and Its Implications for the Guanine Nucleotide Exchange Mechanism. Molecular Cell **12:** 1403-1411

Mossessova E, Gulbis JM, Goldberg J (1998) Structure of the Guanine Nucleotide Exchange Factor Sec7 Domain of Human Arno and Analysis of the Interaction with ARF GTPase. Cell **92:** 415-423

Naramoto S, Kleine-Vehn J, Robert S, Fujimoto M, Dainobu T, Paciorek T, Ueda T, Nakano A, Van Montagu MC, Fukuda H, Friml J (2010) ADP-ribosylation factor machinery mediates endocytosis in plant cells. Proc Natl Acad Sci U S A **107:** 21890-21895

Naramoto S, Otegui MS, Kutsuna N, de Rycke R, Dainobu T, Karampelias M, Fujimoto M, Feraru E, Miki D, Fukuda H, Nakano A, Friml J (2014) Insights into the Localization and Function of the Membrane Trafficking Regulator GNOM ARF-GEF at the Golgi Apparatus in Arabidopsis The Plant Cell **26:** 3062-3076

Naramoto S, Sawa S, Koizumi K, Uemura T, Ueda T, Friml Jri, Nakano A, Fukuda H (2009) Phosphoinositide-dependent regulation of VAN3 ARF-GAP localization and activity essential for vascular tissue continuity in plants. Development **136:** 1529-1538

Nielsen E (2020) The Small GTPase Superfamily in Plants: A Conserved Regulatory Module with Novel Functions. Annual Review of Plant Biology **71:** 247-272

Nielsen M, Albrethsen J, Larsen FH, Skriver K (2006) The Arabidopsis ADP-ribosylation factor (ARF) and ARF-like (ARL) system and its regulation by BIG2, a large ARF–GEF. Plant Science **171:** 707-717

Nishikiori M, Mori M, Dohi K, Okamura H, Katoh E, Naito S, Meshi T, Ishikawa M (2011) A Host Small GTP-binding Protein ARL8 Plays Crucial Roles in Tobamovirus RNA Replication. PLOS Pathogens **7:** e1002409

Nomura K, DebRoy S, Lee YH, Pumplin N, Jones J, He SY (2006) A Bacterial Virulence Protein Suppresses Host Innate Immunity to Cause Plant Disease. Science **313:** 220-223

Nomura K, Mecey C, Lee Y-N, Imboden LA, Chang JH, He SY (2011) Effector-triggered immunity blocks pathogen degradation of an immunity-associated vesicle traffic regulator in Arabidopsis. Proceedings of the National Academy of Sciences **108:** 10774-10779

Pai EF, Kabsch W, Krengel U, Holmes KC, John J, Wittinghofer A (1989) Structure of the guanine-nucleotide-binding domain of the Ha-ras oncogene product p21 in the triphosphate conformation. Nature **341:** 209-214

Panic B, Whyte JR, Munro S (2003) The ARF-like GTPases Arl1p and Arl3p act in a pathway that interacts with vesicle-tethering factors at the Golgi apparatus. Curr Biol **13:** 405-410

Pasqualato S, Renault L, Cherfils J (2002) Arf, Arl, Arp and Sar proteins: a family of GTP-binding proteins with a structural device for 'front-back' communication. EMBO Rep **3:** 1035-1041

Peyroche A, Antonny B, Robineau S, Acker J, Cherfils J, Jackson CL (1999) Brefeldin A Acts to Stabilize an Abortive ARF–GDP–Sec7 Domain Protein Complex: Involvement of Specific Residues of the Sec7 Domain. Molecular Cell **3:** 275-285

Poon PP, Cassel D, Spang A, Rotman M, Pick E, Singer RA, Johnston GC (1999) Retrograde transport from the yeast Golgi is mediated by two ARF GAP proteins with overlapping function. Embo j **18:** 555-564

Radcliffe PA, Vardy L, Toda T (2000) A conserved small GTP-binding protein Alp41 is essential for the cofactor-dependent biogenesis of microtubules in fission yeast. FEBS Letters **468:** 84-88

Randazzo PA, Nie Z, Miura K, Hsu VW (2000) Molecular aspects of the cellular activities of ADP-ribosylation factors. Sci STKE **2000:** re1

Regad F, Bardet C, Tremousaygue D, Moisan A, Lescure B, Axelos M (1993) cDNA cloning and expression of an Arabidopsis GTP-binding protein of the ARF family. FEBS Lett **316:** 133-136

Renault L, Guibert B, Cherfils J (2003) Structural snapshots of the mechanism and inhibition of a guanine nucleotide exchange factor. Nature **426:** 525-530

Richter S, Geldner N, Schrader J, Wolters H, Stierhof YD, Rios G, Koncz C, Robinson DG, Jürgens G (2007) Functional diversification of closely related ARF-GEFs in protein secretion and recycling. Nature **448:** 488-492

Richter S, Kientz M, Brumm S, Nielsen ME, Park M, Gavidia R, Krause C, Voss U, Beckmann H, Mayer U, Stierhof YD, Jürgens G (2014) Delivery of endocytosed proteins to the cell-division plane requires change of pathway from recycling to secretion. Elife **3:** e02131

Richter S, Müller LM, Stierhof YD, Mayer U, Takada N, Kost B, Vieten A, Geldner N, Koncz C, Jürgens G (2011) Polarized cell growth in Arabidopsis requires endosomal recycling mediated by GBF1-related ARF exchange factors. Nat Cell Biol **14:** 80-86

Scheffzek K, Ahmadian MR, Kabsch W, Wiesmüller L, Lautwein A, Schmitz F, Wittinghofer A (1997) The Ras-RasGAP Complex: Structural Basis for GTPase Activation and Its Loss in Oncogenic Ras Mutants. Science **277:** 333-339

Shin H-W, Nakayama K (2004) Guanine Nucleotide-Exchange Factors for Arf GTPases: Their Diverse Functions in Membrane Traffic. The Journal of Biochemistry **136:** 761-767

Shin HW, Morinaga N, Noda M, Nakayama K (2004) BIG2, a guanine nucleotide exchange factor for ADP-ribosylation factors: its localization to recycling endosomes and implication in the endosome integrity. Mol Biol Cell **15:** 5283-5294

Sieburth LE, Muday GK, King EJ, Benton G, Kim S, Metcalf KE, Meyers L, Seamen E, Van Norman JM (2006) SCARFACE encodes an ARF-GAP that is required for normal auxin efflux and vein patterning in Arabidopsis. Plant Cell **18:** 1396-1411

Singh MK, Richter S, Beckmann H, Kientz M, Stierhof Y-D, Anders N, Fäßler F, Nielsen M, Knöll C, Thomann A, Franz-Wachtel M, Macek B, Skriver K, Pimpl P, Jürgens G (2018) A single class of ARF GTPase activated by several pathway-specific ARF-GEFs regulates essential membrane traffic in Arabidopsis. PLOS Genetics **14:** e1007795

Song XF, Yang CY, Liu J, Yang WC (2006) RPA, a class II ARFGAP protein, activates ARF1 and U5 and plays a role in root hair development in Arabidopsis. Plant Physiol **141:** 966-976

Sparks JA, Kwon T, Renna L, Liao F, Brandizzi F, Blancaflor EB (2016) HLB1 Is a Tetratricopeptide Repeat Domain-Containing Protein That Operates at the Intersection of the Exocytic and Endocytic Pathways at the TGN/EE in Arabidopsis. Plant Cell **28:** 746-769

Stefano G, Renna L, Hanton SL, Chatre L, Haas TA, Brandizzi F (2006) ARL1 plays a role in the binding of the GRIP domain of a peripheral matrix protein to the Golgi apparatus in plant cells. Plant Mol Biol **61:** 431-449

Stefano G, Renna L, Rossi M, Azzarello E, Pollastri S, Brandizzi F, Baluska F, Mancuso S (2010) AGD5 is a GTPase-activating protein at the *trans*-Golgi network. Plant J **64:** 790-799

Steinmann T, Geldner N, Grebe M, Mangold S, Jackson CL, Paris S, Gälweiler L, Palme K, Jürgens G (1999) Coordinated polar localization of auxin efflux carrier PIN1 by GNOM ARF GEF. Science **286:** 316-318

Tamkun JW, Kahn RA, Kissinger M, Brizuela BJ, Rulka C, Scott MP, Kennison JA (1991) The arflike gene encodes an essential GTP-binding protein in Drosophila. Proc Natl Acad Sci U S A **88:** 3120-3124

Tanaka H, Kitakura S, De Rycke R, De Groodt R, Friml J (2009) Fluorescence imaging-based screen identifies ARF GEF component of early endosomal trafficking. Curr Biol **19:** 391-397

Tanaka H, Kitakura S, Rakusová H, Uemura T, Feraru MI, De Rycke R, Robert S, Kakimoto T, Friml J (2013) Cell Polarity and Patterning by PIN Trafficking through Early Endosomal Compartments in *Arabidopsis thaliana*. PLOS Genetics **9:** e1003540

Tsai P-C, Hsu J-W, Liu Y-W, Chen K-Y, Lee F-JS (2013) Arl1p regulates spatial membrane organization at the *trans*-Golgi network through interaction with Arf-GEF Gea2p and flippase Drs2p. Proceedings of the National Academy of Sciences **110:** E668-E677

Tzafrir I, McElver JA, Liu C-m, Yang LJ, Wu JQ, Martinez A, Patton DA, Meinke DW (2002) Diversity of TITAN Functions in Arabidopsis Seed Development. Plant Physiology **128:** 38-51

Vernoud V, Horton AC, Yang Z, Nielsen E (2003) Analysis of the small GTPase gene superfamily of Arabidopsis. Plant Physiol **131:** 1191-1208

Vetter IR, Wittinghofer A (2001) The guanine nucleotide-binding switch in three dimensions. Science **294:** 1299-1304

Vitale N, Moss J, Vaughan M (1998) Molecular characterization of the GTPase-activating domain of ADP-ribosylation factor domain protein 1 (ARD1). J Biol Chem **273:** 2553-2560

Wicky S, Schwarz H, Singer-Krüger B (2004) Molecular interactions of yeast Neo1p, an essential member of the Drs2 family of aminophospholipid translocases, and its role in membrane trafficking within the endomembrane system. Mol Cell Biol **24:** 7402-7418

Wittinghofer A, Vetter IR (2011) Structure-Function Relationships of the G Domain, a Canonical Switch Motif. Annual Review of Biochemistry **80:** 943-971

Wright J, Kahn RA, Sztul E (2014) Regulating the large Sec7 ARF guanine nucleotide exchange factors: the when, where and how of activation. Cellular and molecular life sciences : CMLS **71:** 3419-3438

Wu M, Lu L, Hong W, Song H (2004) Structural basis for recruitment of GRIP domain golgin-245 by small GTPase Arl1. Nat Struct Mol Biol **11:** 86-94

Yoo CM, Naramoto S, Sparks JA, Khan BR, Nakashima J, Fukuda H, Blancaflor EB (2018) Deletion analysis of AGD1 reveals domains crucial for plasma membrane recruitment and function in root hair polarity. Journal of Cell Science **131**

Yorimitsu T, Sato K, Takeuchi M (2014) Molecular mechanisms of Sar/Arf GTPases in vesicular trafficking in yeast and plants. Front Plant Sci **5:** 411

Yoshinari A, Toda Y, Takano J (2021) GNOM-dependent endocytosis maintains polar localisation of the borate exporter BOR1 in Arabidopsis. Biology of the Cell **113:** 264-269

Zhang X, Adamowski M, Marhava P, Tan S, Zhang Y, Rodriguez L, Zwiewka M, Pukyšová V, Sánchez AS, Raxwal VK, Hardtke CS, Nodzyński T, Friml J (2020) Arabidopsis Flippases Cooperate with ARF GTPase Exchange Factors to Regulate the Trafficking and Polarity of PIN Auxin Transporters. The Plant Cell **32:** 1644-1664

Zhao Z, Yang X, Lü S, Fan J, Opiyo S, Yang P, Mangold J, Mackey D, Xia Y (2020) Deciphering the Novel Role of AtMIN7 in Cuticle Formation and Defense against the Bacterial Pathogen Infection. International Journal of Molecular Sciences **21:** 5547

Author contributions to manuscript I

Inga Mohr

Conceived the study, wrote the original draft and prepared figures, reviewed/edited the manuscript.

Rumen Ivanov

Conceived the study, reviewed/edited the manuscript.

Petra Bauer

Acquired funding, reviewed/edited the manuscript.

7. Manuscript II

The small ARF-like GTPase TTN5 is linked to IRT1 within the endomembrane system

The small ARF-like GTPase TTN5 is linked to IRT1 within the endomembrane system

Inga Mohr[1], Regina Gratz[1], Kalina Angrand[2], Monique Eutebach[1], Lara Genders[1], Karolin Montag[1], Merina Rubek Basgaran[1], Tzvetina Brumbarova[1], Petra Bauer[1,3] and Rumen Ivanov[1]

[1]Institute of Botany, Heinrich Heine University, Universitätsstr. 1, 40225 Düsseldorf, Germany.
[2]Department of Biosciences-Plant Biology, Saarland University, 66123 Saarbrücken, Germany.
[3]Cluster of Excellence on Plant Sciences, Heinrich-Heine University, 40225 Düsseldorf, Germany.

Author contributions: P.B. and R.I. conceived the project; I.M., T.B., P.B. and R.I. designed experiments, supervised the research and analyzed data; I.M., R.G., K.A. and M.E. performed experiments; L.G., K.M. and M.R.B contributed key materials; I.M. wrote the manuscript; I.M., P.B. and R.I. edited the manuscript; P.B. acquired funding. P.B. and R.I. agreed to serve as the author responsible for contact and communication.

Highlights

- The small GTPase TTN5 is a novel interactor of the large intracellular loop and variable region of IRT1 and has a positive effect on Fe acquisition
- TTN5 shows dynamic association with the vesicle transport system
- TTN5 interacts with EHB1 and SNX1 suggesting a coordinating role in IRT1 regulation

Abstract

Iron (Fe) acquisition is a prerequisite for plant survival. The root iron transporter IRON-REGULATED TRANSPORTER 1 (IRT1), a member of the evolutionarily conserved ZIP multi-membrane-spanning divalent metal transporter family, is crucial for iron uptake in *Arabidopsis thaliana*. IRT1 activity is tightly controlled through regulation of protein stability and via endomembrane trafficking towards the plasma membrane (PM) to balance the demands for iron and toxic excess iron effects. Here, we report that the small ARF-like GTPase TITAN 5/HALLIMASCH (hereafter termed TTN5) interacts with IRT1vr, the large cytoplasmic loop with a variable region and regulatory domain of IRT1. Physiological data indicate a positive impact of TTN5 on iron acquisition. We show that TTN5 is present in dynamic fashion at different sites of the endomembrane system. As it colocalizes with IRT1 in endosomes/multivesicular bodies, TTN5 may function in IRT1 transport. In addition, IRT1 regulators EHB1 and SNX1 also interact with TTN5. Our results suggest that TTN5 coordinates IRT1 sorting and cycling between the PM and the vacuole. The identification of the small

GTPase opens a possibility to understand the mechanism of the IRT1 cycling route within the cell and integrate the fundamental role of TTN5 in the endomembrane system.

Abbreviations

ABA	abscisic acid
AD	activation domain
AHA2	Arabidopsis H^+-ATPase 2
Arabidopsis	*Arabidopsis thaliana*
ARF-like / ARL	ADP-ribosylation factor-like
BAR	Bin-Amphiphysin-Rvs
BART	Binder of ARL2
BD	binding domain
BFA	brefeldin A
bHLH	basis helix-loop-helix
BiFC	Bimolecular Fluorescence Complementation
BLOC-1	biogenesis of lysosome-related organelles complex 1
BPDS	bathophenanthrolinedisulfonic acid
Ca^{2+}	calcium
CBL	CALCINEURIN B-LIKE PROTEIN
CIPK	CBL-INTERACTING PROTEIN KINASE
EE	early endosomes
EHB1	ENHANCED BENDING 1
ER	endoplasmic reticulum
Fe	iron
FRET-APB	Förster Resonance Energy Transfer-Acceptor Photobleaching
FRO2	FERRIC REDUCTION OXIDASE 2
GAP	GTPase-activating protein
GEF	guanine nucleotide exchange factor
GmMan1	*Glycine max* α-1,2 mannosidase 1
HAL	HALLIMASCH
ICQ	intensity correlation quotient
IDF1	IRT1 DEGRADATION FACTOR 1
IRT1vr	IRON-REGULATED TRANSPORTER 1 variable region
MVB	multivesicular body
PDE6δ	delta subunit of phosphodiesterase
PI3K	Phosphatidylinositol-3-kinase
PI3P	phosphatidylinositol-3-phosphate
PIN	PIN FORMED
PM	plasma membrane
PVC	prevacuolar compartment
PX	PHOX
PYR1/PYL	PYRABACTIN RESISTANCE 1 /-LIKE
RAB	Ras-like proteins in brain

ROI	region of interest
SNX1	SORTING NEXIN 1
TBC	tubulin folding cofactor
TGN	*trans*-Golgi network
TTN5	TITAN 5
Y2H	yeast two-hybrid
ZIP	ZRT/IRT-LIKE PROTEIN

Keywords: EHB1, IRT1, SNX1, TTN5, vesicle, plasma membrane, ZIP

Introduction

Plants, due to their sessile nature, need to react and adapt when exposed to environmental changes, such as variations of soil nutrient availability. This is achieved through a network of complex regulatory responses. One essential element is iron (Fe), which is abundant in the soil but mostly present in insoluble ferric Fe (Fe^{3+}) complexes at neutral or basic pH. Plants have evolved two Fe acquisition strategies to mobilize Fe in the soil and render it bioavailable. Grasses use mostly phytosiderophore-Fe^{3+} chelation-based Strategy II, whereas dicotyledonous plants like *Arabidopsis thaliana* (Arabidopsis), follow Fe^{3+} reduction-based Strategy I (Römheld and Marschner, 1986). In Strategy I plants, under Fe deficiency, the H^+-ATPase 2 (AHA2) acidifies the rhizosphere (Santi and Schmidt, 2009; Brumbarova et al., 2015), which releases Fe^{3+} from the insoluble soil complexes. With the aid of small secreted Fe-chelating organic compounds such as coumarins in Arabidopsis, Fe^{3+} is reduced via FERRIC REDUCTION OXIDASE 2 (FRO2) to the more soluble and reactive ferrous iron (Fe^{2+}) (Robinson et al., 1999). Fe^{2+} is taken up by IRON-REGULATED TRANSPORTER 1 (IRT1) (Eide et al., 1996; Vert et al., 2002).

IRT1 is one of the founding members of the ZIP (ZRT, IRT-LIKE PROTEIN) family, with members in bacteria, archaea, fungi, plants and animals (Eide et al., 1996; Guerinot, 2000). It is the main Fe transporter in Arabidopsis roots but is also capable of transporting zinc, manganese, cobalt and cadmium (Eide et al., 1996; Korshunova et al., 1999; Rogers et al., 2000; Vert et al., 2002). *IRT1* is induced under Fe deficiency in the root epidermis and central cylinder in conjunction with *FRO2* and other genes for Fe acquisition, root metal homeostasis and root cell elongation processes that are targets of a bHLH factor cascade, namely the bHLH proteins FIT and bHLH proteins of the subgroup Ib such as bHLH039 (Vert et al., 2002; Jakoby et al., 2004; Naranjo-Arcos et al., 2017; Schwarz and Bauer, 2020). IRT1 forms a protein complex with AHA2 and FRO2 at the plasma membrane (PM) (Martín-Barranco et al., 2020), and protein stability and activity of the whole complex are likely targets of the same machinery. IRT1 protein activity depends on protein synthesis, transport from the *trans*-Golgi network/early

endosomes (TGN/EE) to the PM, degradation via the lytic pathway and recycling back to the PM (Barberon et al., 2011). The large partly variable cytosolic region between transmembrane domains three and four is a characteristic regulatory feature of ZIP proteins (Guerinot, 2000; Gaither and Eide, 2001). In IRT1, this regulatory variable region, IRT1vr, is composed of a histidine-rich metal-ion-binding stretch, several phosphorylation and two ubiquitination sites and is a scaffold for protein-protein interactions (Grossoehme et al., 2006; Kerkeb et al., 2008; Dubeaux et al., 2018; Cointry and Vert, 2019; Khan et al., 2019). Common for PM proteins, IRT1 follows the ubiquitination-dependent degradation pathway (Barberon et al., 2011; Shin et al., 2013; Barberon et al., 2014; Foot et al., 2017). Remarkably, IRT1 protein degradation is initiated by excessive zinc and manganese uptake and binding to the cytosolic His-stretch. This is causing the recruitment and phosphorylation of IRT1vr by CBL-INTERACTING PROTEIN KINASE 23 (CIPK23) and subsequent K63-polyubiquitination and vacuolar degradation with involvement of RING E3 ubiquitin ligase IRT1 DEGRADATION FACTOR 1 (IDF1) (Shin et al., 2013; Dubeaux et al., 2018). On the other hand, phosphatidylinositol-3-phosphate (PI3P)-binding protein FYVE1/FREE1, as well as the sorting nexin SNX1 promote recycling of endocytosed IRT1 and its transport from the endosomes back to the PM (Barberon et al., 2014; Ivanov et al., 2014; Ivanov and Vert, 2021). C2 domain protein ENHANCED BENDING 1 (EHB1, also known as CAR6) has inhibitory effects on IRT1 and FRO2. EHB1 attaches to the PM in a calcium (Ca^{2+})-dependent manner and inhibits IRT1 by interacting through a CAR protein-specific signature domain (EHB1sig) with IRT1vr close to the membrane (Khan et al., 2019). Clearly, intracellular trafficking affects Fe uptake drastically by IRT1 turnover, however, regulation of the transport mechanism and protein turnover still remain largely elusive.

Cycling of PM proteins is an important function of endomembrane trafficking. To keep a balanced level of active proteins at the PM, they are internalized via endocytosis and transported to the TGN/EE. Here, they can be sorted for degradation and targeted to the vacuole by the lytic pathway or recycled back to the PM. The different transporting routes accomplished by several vesicle types derived from the diverse cellular compartments clearly indicate the need of well-organized protein networks (Valencia et al., 2016; Ivanov and Vert, 2021). Not to neglect the specific influence of the interactome of each protein itself. One protein family highly involved in vesicle-mediated endomembrane trafficking is the Ras superfamily of small GTPases, especially their Ras-like proteins in brain (RAB) and ADP-ribosylation factor (ARF) subfamilies. They function as molecular switch via its GDP-bound or GTP-bound activity state in vesicle-related processes, like their formation and their tethering to the target membrane. Small GTPases have low intrinsic nucleotide exchange and hydrolysis activity and therefore, require the support of guanine nucleotide exchange factors (GEFs) and GTPase-

activating proteins (GAPs). GEFs recruit the inactive, GDP-bound, GTPase to their site of action and lead to nucleotide exchange by GDP release. GTP binding occurs through a conformational change of two regions referred to as switch I and II. The active, GTP-loaded, GTPases then exert their function, e.g. the recruiting and subsequent assembly of coat proteins by ARF1 or SAR1, until hydrolysis of the GTP by GAPs. Most of the known interactions occur in the active conformation of the GTPases (Sztul et al., 2019; Nielsen, 2020; Adarska et al., 2021). One well-established example of ARF-GTPases in PM protein trafficking is the ARF1-GNOM-mediated recycling of auxin carrier PIN FORMED 1 (PIN1), with GNOM being an ARF-GEF (Steinmann et al., 1999; Geldner et al., 2003). It raises the question if and how other ARF members take place in PM protein endomembrane trafficking.

TITAN 5 (TTN5), also known as HALLIMASCH (HAL), is an ARF-like (ARL) protein. It was identified in two independent screens for abnormal-embryo mutants. Analyzed *ttn5/hal* (from here on only called TTN5) seeds are disturbed in their embryo development and can only form few giant cells and the characteristic enlarged nuclei in embryo and endosperm which leads to embryo lethality (Mayer et al., 1999; McElver et al., 2000). Its function at the molecular level has not been described until now but sequence similarities revealed ADP-ribosylation factor-like 2 (HsARL2) as a close homolog. All conserved GTP-binding domains are also present in TTN5 (McElver et al., 2000). HsARL2 is known to play a role in the tubulin and microtubules development by interacting with cofactor D (TBCD), a homolog of TTN1/CHAMPIGNON in Arabidopsis (Bhamidipati et al., 2000; Tzafrir et al., 2002). Thereby it forms a high molecular weight complex with the cofactors TBCC, TBCD and TBCE (Nithianantham et al., 2015).This protein interaction or the microtubule connection was also reported for homologs in various organisms such as *Saccharomyces cerevisiae*, *Schizosaccharomyces pombe* or *Caenorhabditis elegans* (Fleming et al., 2000; Radcliffe et al., 2000; Antoshechkin and Han, 2002; Mori and Toda, 2013). A similar function for TTN5 is expected based on the *ttn5-1* phenotype (Mayer et al., 1999). Additionally, ARL2 can interact with Binder of ARL2 (BART) and the adenine nucleotide transporter ANT1 at mitochondria (Sharer et al., 2002). Next to this, ARL2 is able to release prenylated or myristoylated cargos by allosteric interaction with the cargo carrier PDE6δ (delta subunit of phosphodiesterase) (Ismail et al., 2011; Fansa and Wittinghofer, 2016). Interaction of ARL2 with PDE6δ leads to the narrowing of its hydrophobic binding pocket and the release of the lipid anchor (Ismail et al., 2011). These data indicate an involvement of TTN5 homologs in a diverse set of functions and signaling cascades associated to different interaction partners. Although few homologs of ARL2 interaction partners are present in Arabidopsis, it is exceedingly interesting to determine whether TTN5 performs similar functions or what other role it plays, making it an essential gene in embryo development.

We have recently described a strategy for identification of IRT1vr regulators using a yeast two-hybrid screen (Khan et al., 2019). We report here that with this same approach we retrieved the HsARL2 homolog and small putative GTPase TTN5. We validate protein interactions of TTN5 and IRT1vr and demonstrate that TTN5 is located in the endomembrane compartments, where it colocalizes partly with IRT1. We show new functions of TTN5 linking the endomembrane system with Fe regulation.

Results

TTN5 interacts with the variable region of IRT1

In an attempt to identify new proteins regulating IRT1, we had used the cytoplasmic loop with a variable region and subdomain of IRT1, IRTvr (residues 145-192), as bait against a cDNA expression library of Fe-deficient Arabidopsis roots (Khan et al., 2019). 25 of the colonies (representing 25 %) obtained in the yeast two-hybrid (Y2H) screen carried a fragment of the coding sequence of the gene AT2G18390, encoding the ARL-type small GTPase TTN5. We verified the interaction in a targeted Y2H test, with AD-TTN5 with BD-IRT1vr resulting in yeast growth on selection plates (Figure 1A). We further detected the protein interaction in plant cells via Bimolecular Fluorescence Complementation (BiFC) as a reconstitution of YFP by the combination of cYFP-TTN5 and nYFP-IRT1vr in positively transformed cells that expressed the control marker mRFP (Figure 1B). Similarly to other GTPases, TTN5 is likely to switch between a GTP-bound active or GDP-bound inactive conformation. We generated TTN5 variants with mutations of conserved amino acids in the GTP-binding pocket mimicking the inactive conformation, Thr30Asn (T30N), and the active conformation, Gln70Leu (Q70L) (Supplemental Figure 1). Both, the inactive (cYFP-TTN5^{T30N}, Figure 1C) and active (cYFP-TTN5^{Q70L}, Figure 1D) forms resulted in YFP complementation in the presence of nYFP-IRTvr, suggesting an interaction of the variants, similarly to the full-length cYFP-TTN5. The BiFC interactions were specific as neither cYFP-TTN5 nor nYFP-IRT1vr were able to complement YFP in the presence of non-interacting EHB1Δsig (defined in Rodriguez et al., 2014; Khan et al., 2019, Figure 1E, F). We further elucidated whether IRT1vr might discriminate between active and inactive TTN5 variant forms using a quantitative analysis of the interaction by Förster Resonance Energy Transfer-Acceptor Photobleaching (FRET-APB). This approach is based on close-proximity-dependent energy transfer of an excited GFP-tagged TTN5 donor to a mCherry acceptor, here IRT1vr-mCherry. Energy transfer was quantified as FRET efficiency (Figure 1G-I). FRET efficiencies between all GFP-TTN5 forms and mCherry-IRT1vr were significantly higher compared to the donor-only sample, confirming protein interactions between TTN5 forms and IRT1vr.

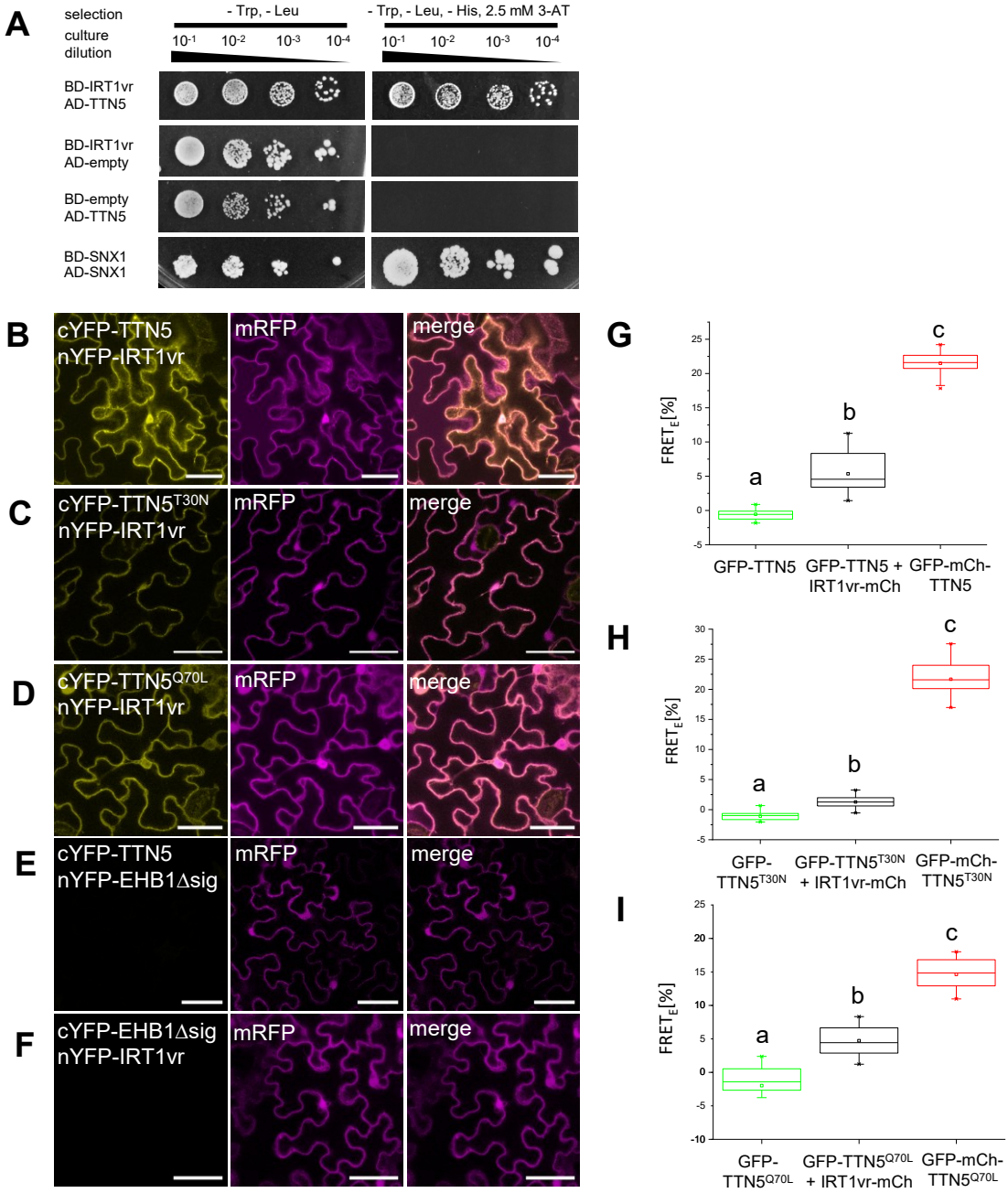

Figure 1. TTN5 interacts with IRT1vr in yeast and *planta*.
(A), Targeted Y2H screen between BD-IRT1vr (IRT1-variable region) and AD-TTN5. Yeast cotransformations were spotted in 10-fold dilution series (A_{600} = 10^{1}-10^{4}) on double selective (LW; control) and triple selective +0.5 mM 3-AT (LWH, selection for protein interactions) SD-plates. SNX1/SNX1, positive control (Pourcher et al., 2010), BD-IRT1vr/AD-empty and BD-empty/AD-TTN5 respective negative controls. (B-F), Verification of TTN5-IRT1vr interaction by BiFC. Genes of interest were fused either to the C- or N-terminal half of split-YFP. Potential interaction is indicated by a complemented YFP signal. mRFP serves as a transformation control. (B-D), nYFP-IRT1vr showed YFP complementation in combination with cYFP-TTN5 and its dominant inactive (cYFP-TTN5^{T30N}) and dominant active (cYFP-TTN5^{Q70L}) variant. The complementation takes place in nucleus and cytoplasm predominantly. (E, F), The combinations cYFP-TTN5/nYFP-EHB1Δsig and cYFP-EHB1Δsig/nYFP-IRT1vr served as negative controls. Each combination was tested a minimum of three times with comparable results. Scale bar 50 µm. (G-I), Confirmed interaction via FRET-APB. Significant increase of FRET-efficiency between IRT1vr-mcherry and GFP-TTN5 or its inactive or active variant indicate short protein distances. GFP-fusions are donor-only samples and serve as a negative control. GFP-mCherry-tagged constructs show intra-molecular FRET as a respective positive control. Each combination was tested a minimum of three times (n = 3) with comparable results. One-way ANOVA with Fisher-LSD post-hoc test was performed. Different letters indicate statistical significance ($p < 0.05$, $n \geq 10$).

Thus, we identified TTN5 as a novel interactor of IRT1vr and a potential missing link in the coordination of IRT1 regulation. Surprisingly, the GTP/GDP-binding conformations do not influence significantly the protein interaction in the case of TTN5.

TTN5 affects Fe homeostasis

Based on the IRT1-TTN5 interaction we assumed that TTN5 might affect the regulation of the Fe deficiency response. Homozygous TTN5 knock-outs are embryo-lethal (Mayer et al., 1999; McElver et al., 2000), and heterozygous plants (*ttn5-1*$^{+/-}$) show no obvious developmental defects (Figure 2A). However, when we selected specifically heterozygous seedlings we found that Fe reductase activity that is normally up-regulated under Fe-deficient conditions in WT and is an essential step of the Strategy I carried out by FRO2, was reduced in *ttn5-1*$^{+/-}$ seedlings (Figure 2B). FRO2 activity might have been reduced, because the IRT1-FRO2 complex is down-regulated in *ttn5-1*$^{+/-}$ seedlings. Consequently, IRT1 action might also be impaired in *ttn5-1*$^{+/-}$ seedlings. Loss of IRT1 leads to a severe Fe-deficient phenotype associated with low Fe amounts in the plant (Vert et al., 2002). Seeds from *ttn5-1*$^{+/-}$ plants, composed of 25 % aborted small homozygous seeds, 25 % WT seeds and 50 % *ttn5-1*$^{+/-}$ seeds, contained indeed lower amounts of Fe compared to 100 % WT seeds (Figure 2C), indicating that not only FRO2 but also IRT1 were less active in heterozygous plants.

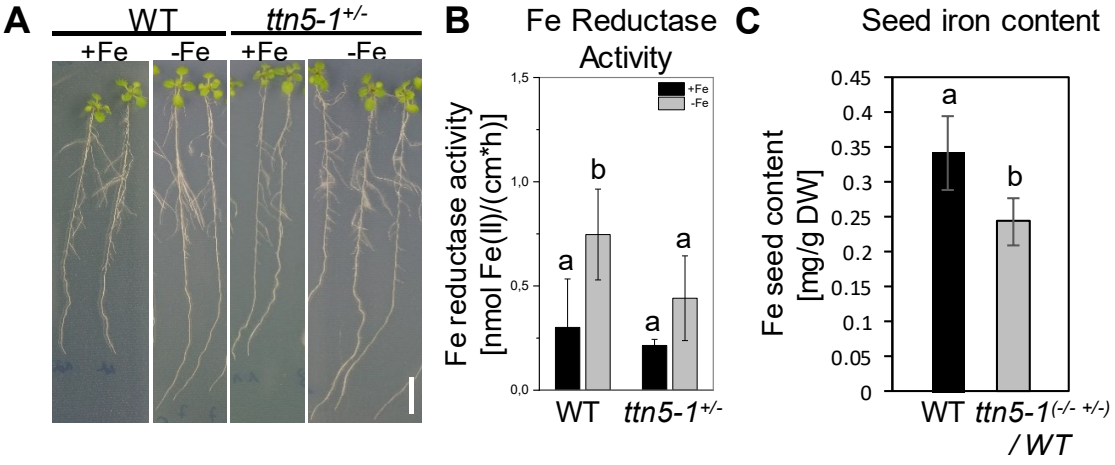

Figure 2. TTN5 in Fe deficiency.
Heterozygous *ttn5-1*$^{+/-}$ seedlings exhibited an Fe-dependent impact on the FIT-regulated Fe deficiency genes. (A), *ttn5-1*$^{+/-}$ seedlings grew phenotypically normal compared to WT. Seedlings were grown on +/- Fe Hoagland plates in the two-week system. Scale bar 1 cm. (B), Ferric reductase activity was measured as the complex formation-induced color change of ferrozine at 562 nm. *FRO2* is induced by Fe deficiency in WT seedlings indicated by an increase of reductase activity. Same is present in *ttn5-1*$^{+/-}$ seedlings under Fe deficiency but in statistical reduced amounts. Assay was performed with three biological replicates (n = 3). (C), Seed Fe content was determined by the specific absorbance of the Fe-chelator complex (BPDS) at 535 nm per dry weight. The Fe content of *ttn5-1*$^{(-/- +/-)}$*/ WT* (25 % WT / *ttn5-1*$^{-/-}$, 50 % *ttn5-1*$^{+/-}$) seeds is reduced compared to WT. Determination was performed with three biological replicates (n = 3). One-way ANOVA with Fisher-LSD as post-hoc test was performed. Different letters indicate statistical significance ($p < 0.05$).

Induction of several marker genes including *FRO2* and *IRT1* serves to quantify the responsiveness and sensitivity to Fe deficiency (Schwarz and Bauer, 2020). To assess whether

Fe deficiency responses were also affected in *ttn5-1*$^{+/-}$ plants, we analyzed gene expression data of known Strategy I players. *TTN5* expression served as a control and was nearly 50 % reduced in *ttn5-1*$^{+/-}$compared to WT, consistent with single allele presence. In WT we detected a 15 % decrease between Fe sufficiency and deficiency (Figure 3A). *FRO2* and *IRT1* genes showed low expression levels and no induction by Fe deficiency in *ttn5-1*$^{+/-}$ roots (Figure 3B, C).

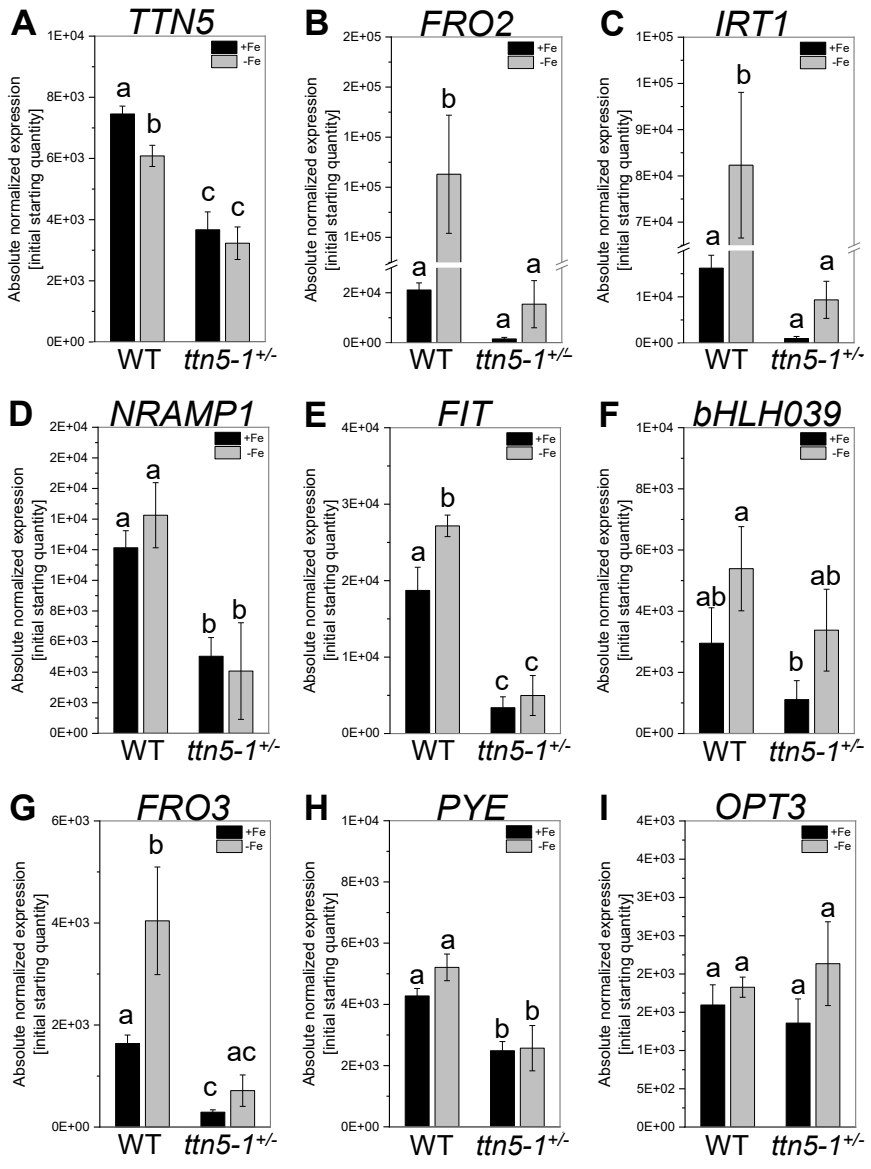

Figure 3. TTN5 effect on transcriptional level. (A-I), Gene expression data by RT-qPCR of Fe related genes in *ttn5-1*$^{+/-}$ roots compared to WT. Next to *TTN5* expression, genes of the FIT-dependent (*FIT*, *FRO2* and *IRT1*) and Fe homeostasis (FIT-independent) cluster (*bHLH039*, *FRO3*, *OPT3*, *PYE* and *NRAMP1*) were tested. Plants were grown in the two-week system in Fe-sufficient (+Fe, black bars) or -deficient (-Fe, grey bars) conditions. Data was obtained from three biological replicates (n = 3). One-way ANOVA with Fisher-LSD post-hoc test was performed. Different letters indicate statistical significance ($p < 0.05$).

This may partly explain the low Fe reductase level and Fe content of *ttn5-1*$^{+/-}$. However it was also unexpected because a Fe-deficient state should induce Fe acquisition responses. *NRAMP1* is coexpressed with *FRO2* and *IRT1* (Curie et al., 2000; Colangelo and Guerinot, 2004), and it was also expressed at lower levels in *ttn5-1*$^{+/-}$ (Figure 3D). These three marker genes are targets of FIT and bHLH subgroup Ib (e.g. bHLH039) transcription factors (Curie et al., 2000; Colangelo and Guerinot, 2004; Jakoby et al., 2004; Yuan et al., 2008). *FIT* is also coexpressed with its targets, and in our assay was found down-regulated in *ttn5-1*$^{+/-}$ (Figure 3E). *bHLH039*

was not found to be significantly changed in its expression compared to WT, however, it was not found significantly induced by Fe deficiency in this experiment (Figure 3F). *bHLH039* is normally induced by Fe deficiency by another layer of bHLH transcription factors (Zhang et al., 2015). Interestingly, several genes that are coexpressed with *bHLH039* were significantly reduced in their expression in *ttn5-1*$^{+/-}$ compared with WT, namely Fe homeostasis bHLH regulator gene *POPEYE* (*PYE*) and mitochondrial Fe reductase gene *FRO3* (Long et al., 2010; Ivanov et al., 2012) (Figure 3G, H). Only *FRO3* was also found induced by Fe deficiency in WT but not *PYE* (Figure 3G, H). *OPT3*, which encodes a phloem transporter for transmitting a shoot-to-root Fe signal is also coexpressed with *bHLH039* (Zhai et al., 2014). It was similarly expressed and not regulated like *bHLH039* in this experiment (Figure 3I).

Taken together, TTN5 has a positive effect on molecular and physiological Fe acquisition and Fe homeostasis responses in roots, besides root regulating transcript regulation was also account for it.

TTN5 localizes to different cellular compartments

ARF GTPases function in vesicle transport and are located at various membranous sites linked with the endomembrane compartments (Vernoud et al., 2003). IRT1 is located in endosomes and the PM. Considering our findings on protein interaction of TTN5 and IRT1vr, it was of great interest to analyze TTN5 cellular function and its dynamic localization.

YFP-TTN5 as well as both GTPase variants inactive YFP-TTN5^{T30N} and active YFP-TTN5^{Q70L} were localized in the nucleus and at or in close proximity to the PM and in many punctuate cytosolic vesicle-like structures (Figure 4, Supplemental Figure 2A-C). We performed colocalization with different fluorescent markers to more precisely identify the nature of YFP-TTN5-positive cellular compartments. At first, we investigated the endoplasmic reitculum (ER)-Golgi connection. ARF1 is for example a small GTPase like TTN5 known to be involved in COPI vesicle transport from Golgi to the ER (Just and Peränen, 2016). The soybean (*Glycine max*) protein α-1,2 mannosidase 1 (GmMan1) is a glycosidase that acts on glycoproteins at the *cis*-Golgi, facing the ER. GmMan1-mCherry-positive Golgi stacks are visible as almost round punctuate structures throughout the whole cell (Nelson et al., 2007; Wang et al., 2016). All three YFP-TTN5 variants partially colocalized with GmMan1-mCherry signals at the Golgi (Figure 4A-C). Further analysis confirmed the visible colocalization with the marker with 0.628 (TTN5), 0.653 (YFP-TTN5^{T30N}) and 0.677 (YFP-TTN5^{Q70L}) as Pearson coefficients (Supplemental Figure 2D). We detected 24 % overlapping YFP-TTN5 fluorescence with Golgi stacks (Supplemental Figure 2F). The GTPase variants YFP-TTN5^{T30N} and YFP-TTN5^{Q70L} signal shared 16 and 15 % with GmMan1-mCherry-positive stacks. Some YFP-TTN5 signals were not colocalized with the GmMan1 marker. This effect appeared more prominent

for inactive YFP-TTN5^{T30N} and less for active YFP-TTN5^{Q70L}, compared to the unmutated YFP-TTN5. Indeed, we identified 48 % GmMan1-mCherry signal overlapping with YFP-TTN5^{Q70L}-positive structures, whereas 43 and 31 % were present with YFP-TTN5 and YFP-TTN5^{T30N} respectively. We suggested that the active or WT TTN5 form is likely more present at Golgi stacks compared to inactive TTN5^{T30N}.

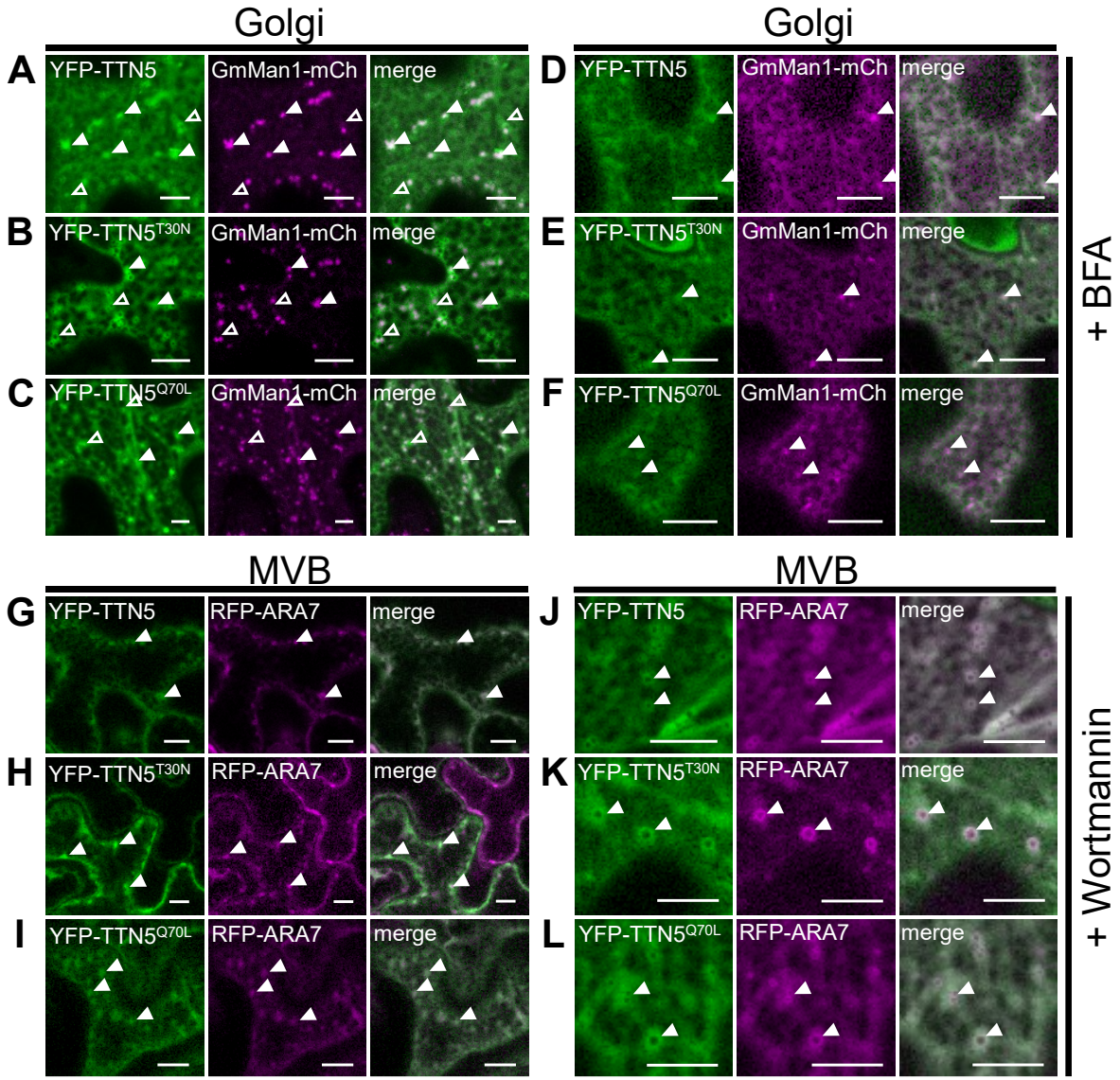

Figure 4. TTN5 localization in *N. benthamiana* leaf epidermal cells.
(A-L), YFP-tagged TTN5 and its dominant inactive (YFP-TTN5^{T30N}) and dominant active (YFP-TTN5^{Q70L}) variant were localized in *N. benthamiana* leaf epidermal cells with specific markers via fluorescent confocal microscopy. (A-F), Colocalization of YFP-TTN5s with the Golgi marker GmMan1-mCherry and (G-L), the multi vesicular body marker RFP-ARA7. (D-F), Redistribution of Golgi stacks was induced by BFA treatment. (J-L), MVB swelling was obtained by wortmannin treatment. Chemical treatment-induced changes were imaged after 25 min incubation. Colocalization is indicated with filled arrow heads, YFP-tagged construct expression alone with empty ones. Scale bar 10 µm

Next, we confirmed the Golgi localization by Brefeldin A (BFA) treatment, which is a commonly used tool in cell biology for preventing dynamic membrane trafficking events and vesicle transport involving the Golgi. BFA is a fungal macrocyclic lactone which leads to a loss

of *cis*-cisternae and accumulation of Golgi stacks, known as BFA-induced compartments, up to fusion of the Golgi with the ER. The action of BFA causes corresponding redistribution of GmMan1-mCherry (Ritzenthaler et al., 2002; Wang et al., 2016). We found that upon BFA treatment GmMan1-mCherry was present in the ER and in BFA-induced compartments. YFP-TTN5 proteins showed partially matching localization with GmMan1-mCherry upon BFA treatment proving the connection of TTN5 to Golgi localization, in addition to other cellular locations (Figure 4D-F).

Second, we tested localization to the endocytic compartments, endosomes of the TGN and multivesicular bodies (MVBs)/prevacuolar compartments (PVCs) using the marker RFP-ARA7 (RABF2B), a small RAB-GTPase present there (Kotzer et al., 2004; Lee et al., 2004; Stierhof and El Kasmi, 2010; Ito et al., 2016). These compartments play a role in sorting proteins between the endocytic and secretory pathways, with MVBs developing from the TGN and representing the final stage in transport to the vacuole (Valencia et al., 2016; Heucken and Ivanov, 2018). Colocalization studies revealed that YFP-TTN5 protein was present at RFP-ARA7-positive MVBs/PVCs (Figure 4G). Noticeable were lower obtained values for overlaps between RFP-ARA7 and inactive YFP-TTN5^{T30N} fluorescence signals (Figure 4H) by quantification (Supplemental Figure 2E, F). We obtained a Pearson coefficient for YFP-TTN5 and active YFP-TTN5^{Q70L} together with RFP-ARA7 of 0.781, whereas a coefficient of 0.586 was obtained with inactive YFP-TTN5^{T30N}. Additionally, RFP-ARA7-positive structures had a higher overlap with the active form. We identified an overlap of only 21 and 29 % with YFP-TTN5^{T30N} and YFP-TTN5, whereas 75 % of RFP-ARA7 signal was detectable at YFP-TTN5^{Q70L}-positive structures. Based on this we suggest a higher tendency of MVBs/PVCs localization for the active variant TTN5^{Q70L} and WT TTN5 than inactive TTN5^{T30N}. To prove MVB localization we treated plant cells with wortmannin, a common approach to study endocytosis events. Wortmannin is a fungal metabolite that inhibits phosphatidylinositol-3-kinase (PI3K) function and thereby causes swelling of the MVBs/PVCs (Cui et al., 2016). RFP-ARA7-expressing cells showed the expected typical wortmannin-induced formation of doughnut-like shaped MVBs/PVCs (Jaillais et al., 2008). The coexpressed YFP-TTN5 constructs partially colocalized with these structures (Figure 4J-L).

Finally, to investigate the connection of TTN5 with membranes we colocalized the YFP-TTN5 proteins with the dye FM4-64 that fluoresces in a lipophilic membrane environment and marks the PM (Bolte et al., 2004). All three forms of TTN5 localized together with FM4-64 at the PM (Figure 5A-C). To further prove PM localization, we performed mannitol-induced plasmolysis. All three YFP-TTN5 protein forms were located to FM4-64-stained Hechtian strands, which are threads of the PM that remain attached to the cell wall (Figure 5D-F). These

colocalization experiments showed that YFP-TTN5 locates to different membrane sites of the endomembrane system, including Golgi, MVBs/PVCs and PM. We figured that similar to other ARF proteins TTN5 might participate in a highly dynamic vesicle trafficking process. Indeed, detection of YFP-TTN5 protein colocalized with GmMan1-mCherry over time revealed high motion for WT and active TTN5 (video materials in Supplemental Movie 1-3). Taken together, we suggest that TTN5 has different functions in intracellular trafficking with dependence on activity status.

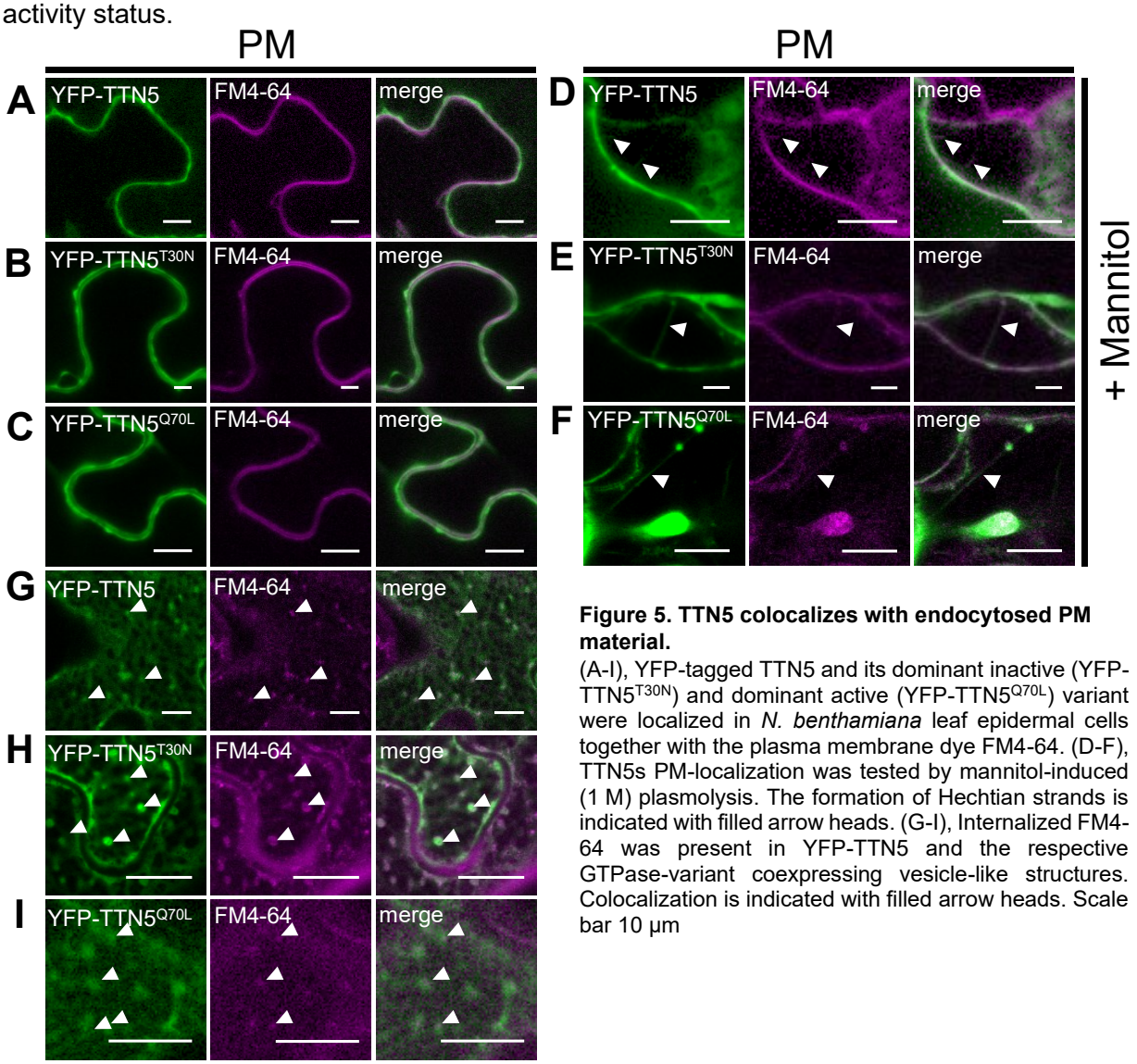

Figure 5. TTN5 colocalizes with endocytosed PM material.
(A-I), YFP-tagged TTN5 and its dominant inactive (YFP-TTN5^{T30N}) and dominant active (YFP-TTN5^{Q70L}) variant were localized in *N. benthamiana* leaf epidermal cells together with the plasma membrane dye FM4-64. (D-F), TTN5s PM-localization was tested by mannitol-induced (1 M) plasmolysis. The formation of Hechtian strands is indicated with filled arrow heads. (G-I), Internalized FM4-64 was present in YFP-TTN5 and the respective GTPase-variant coexpressing vesicle-like structures. Colocalization is indicated with filled arrow heads. Scale bar 10 µm

TTN5 colocalizes with IRT1 in endocytosed PM material

We further investigated TTN5 localization in late endosomal compartments that might be involved in the vacuolar targeting of IRT1. FM4-64 is used as marker for vacuolar degradation targeting, since following PM visualization FM4-64-stained endocytic vesicles become apparent at later stages as well as vacuolar membrane staining (Ueda et al., 2001; Emans et al., 2002; Dhonukshe et al., 2007; Ivanov and Vert, 2021). Hence, we colocalized YFP-TTN5

with FM4-64 and monitored dye degradation. Next to TTN5 colocalization with FM4-64 at the PM, we detected colocalization in vesicle-like structures in the cell, indicating dye degradation (Figure 5G-I). This indicates that TTN5 is involved in vacuolar targeting of PM material, and this might play a role in IRT1 endocytosis and degradation.

To further prove this idea, we checked colocalization of mCherry-TTN5, mCherry-TTN5^{T30N} and mCherry-TTN5^{Q70L} with IRT1-GFP at the PM. We approved the correct localization by PM staining with the FM4-64 dye (Supplement Figure 3A). IRT1-GFP is present at the PM and in fluorescent spots in close proximity to the PM (Supplement Figure 3A), consistent with previous reports (Barberon et al., 2011; Ivanov et al., 2014). As expected, we detected colocalization of IRT1-GFP and the three different mCherry-TTN5 constructs at the PM (Figure 6A-C).

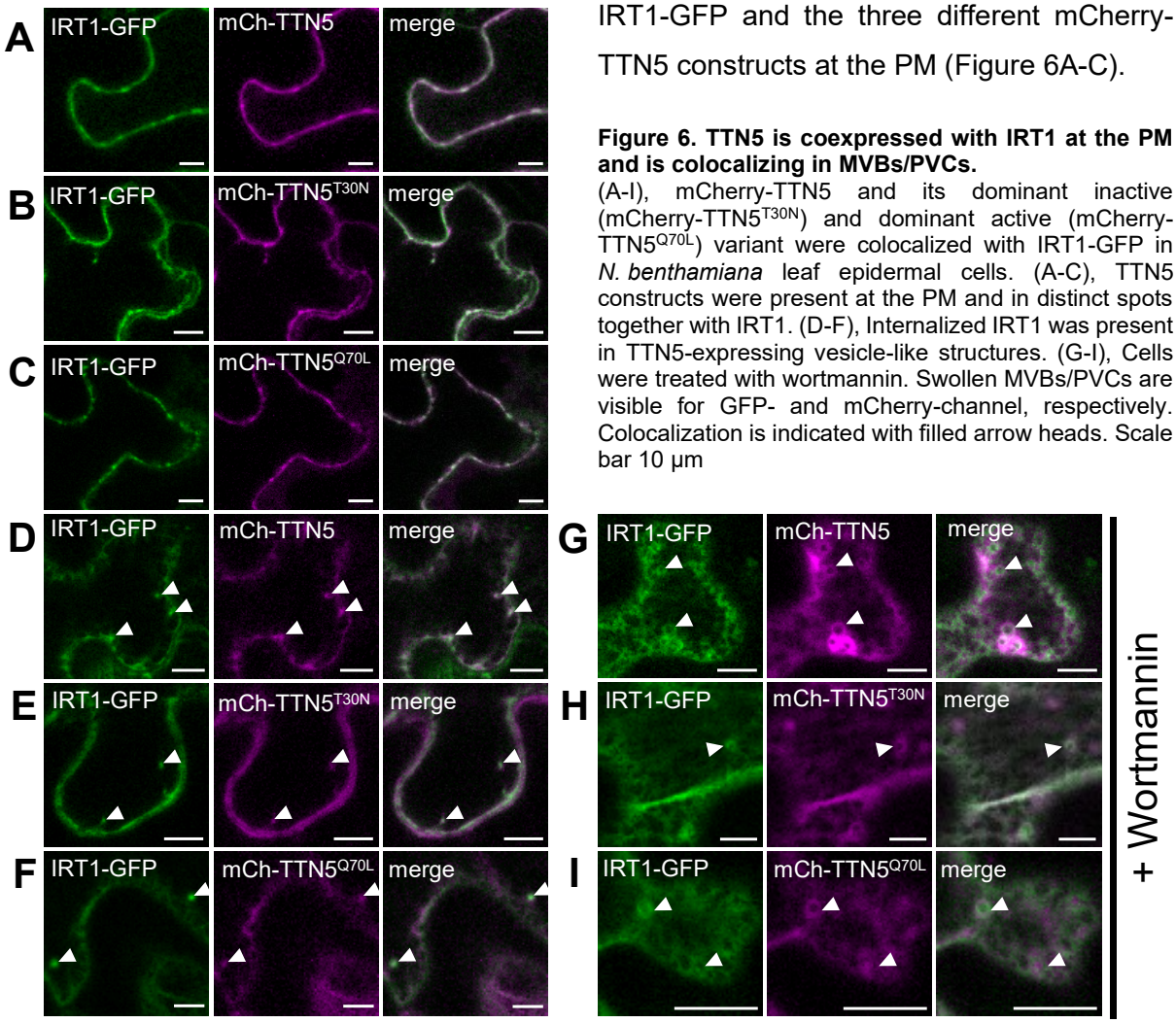

Figure 6. TTN5 is coexpressed with IRT1 at the PM and is colocalizing in MVBs/PVCs.
(A-I), mCherry-TTN5 and its dominant inactive (mCherry-TTN5^{T30N}) and dominant active (mCherry-TTN5^{Q70L}) variant were colocalized with IRT1-GFP in *N. benthamiana* leaf epidermal cells. (A-C), TTN5 constructs were present at the PM and in distinct spots together with IRT1. (D-F), Internalized IRT1 was present in TTN5-expressing vesicle-like structures. (G-I), Cells were treated with wortmannin. Swollen MVBs/PVCs are visible for GFP- and mCherry-channel, respectively. Colocalization is indicated with filled arrow heads. Scale bar 10 µm

Further investigation revealed a significant colocalization difference between the inactive and active variant of TTN5 with IRT1 (Supplemental Figure 3B). While Pearson coefficients of IRT1-GFP with mCherry-TTN5 and mCherry-TTN5^{Q70L} were 0.769 and 0.799 respectively, it was 0.902 for mCherry-TTN5^{T30N}. mCherry-TTN5s were also localized in IRT1-GFP-positive

structures close to the PM, suggesting the two proteins might colocalize in PM-derived vesicles (Figure 6D-F). Surprisingly, the Pearson coefficients changed when these structures were analyzed (Supplemental Figure 3C, D). While the values for mCherry-TTN5 (0.800) and mCherry-TTN5^{Q70L} (0.781) with IRT1-GFP remain relatively the same, we obtain with 0.778 now a similar coefficient with mCherry-TTN5^{T30N}. Similar results were achieved while checking the overlaps of mCherry-TTN5 signals with IRT1-GFP, with overlaps of 36-41 %. In contrast, only 54 % of IRT1-GFP-positive structures colocalized with mCherry-TTN5^{T30N}, whereas 61 % and up to 83 % colocalized with mCherry-TTN5 and mCherry-TTN5^{Q70L}, respectively. From this, we hypothesize that IRT1 along with inactive TTN5 is more likely to be localized at the PM while the active variant may play a role in cycling. In an attempt to identify the intracellular structures, we treated the cells with wortmannin. Structures positive for both IRT1-GFP and mCherry-TTN5 became doughnut-shaped suggesting IRT1-TTN5 colocalization in MVBs (Figure 6G-I). Presence of IRT1 in these late endosomal compartments has been observed previously, as part of the pathway to IRT1 vacuolar degradation (Dubeaux et al., 2018). Our findings emphasize the involvement of TTN5 in the endomembrane trafficking of the Fe transporter IRT1 towards the vacuole.

TTN5 interacts with IRT1 regulators EHB1 and SNX1

Since TTN5 binds to IRT1vr and acts in IRT1 cycling inside the cell, the question arose how this relates to other known regulatory and binding proteins of IRT1vr.

The IRT1vr interactor EHB1 was identified in the same Y2H screen as TTN5, and the sig domain of EHB1 is needed for interaction with IRT1vr (Khan et al., 2019). Interestingly, while EHB1Δsig does not interact with TTN5 in BiFC as shown above (Figure 1E, 7A), the intact EHB1 protein (Figure 7B) and the EHB1 sig domain alone (Figure 7C) allow YFP complementation in BiFC, indicating protein-protein interaction. On the other hand, no BiFC signals and interaction with EHB1 were detected for TTN5^{T30N} (Figure 7D) and TTN5^{Q70L} (Figure 7E). FRET-APB experiments were used for validation (Figure 7F) taking EHB1-GFP as the donor sample and all three TTN5 variants as the acceptor with a C-terminal mCherry-tag. EHB1-GFP with TTN5-mCherry yielded a significantly higher FRET efficiency compared to the donor-only sample. Surprisingly, the FRET pairs EHB1-GFP with TTN5^{T30N}-mCherry and TTN5^{Q70L}-mCherry resulted in an even higher FRET-efficiency in the nucleus compared to TTN5 WT. At first, this seems to be a contradiction to BiFC results. However, an explanation is that these two methods are dependent on the distance and orientation of the fluorescent tags. A potential hindrance can prevent BiFC or FRET.

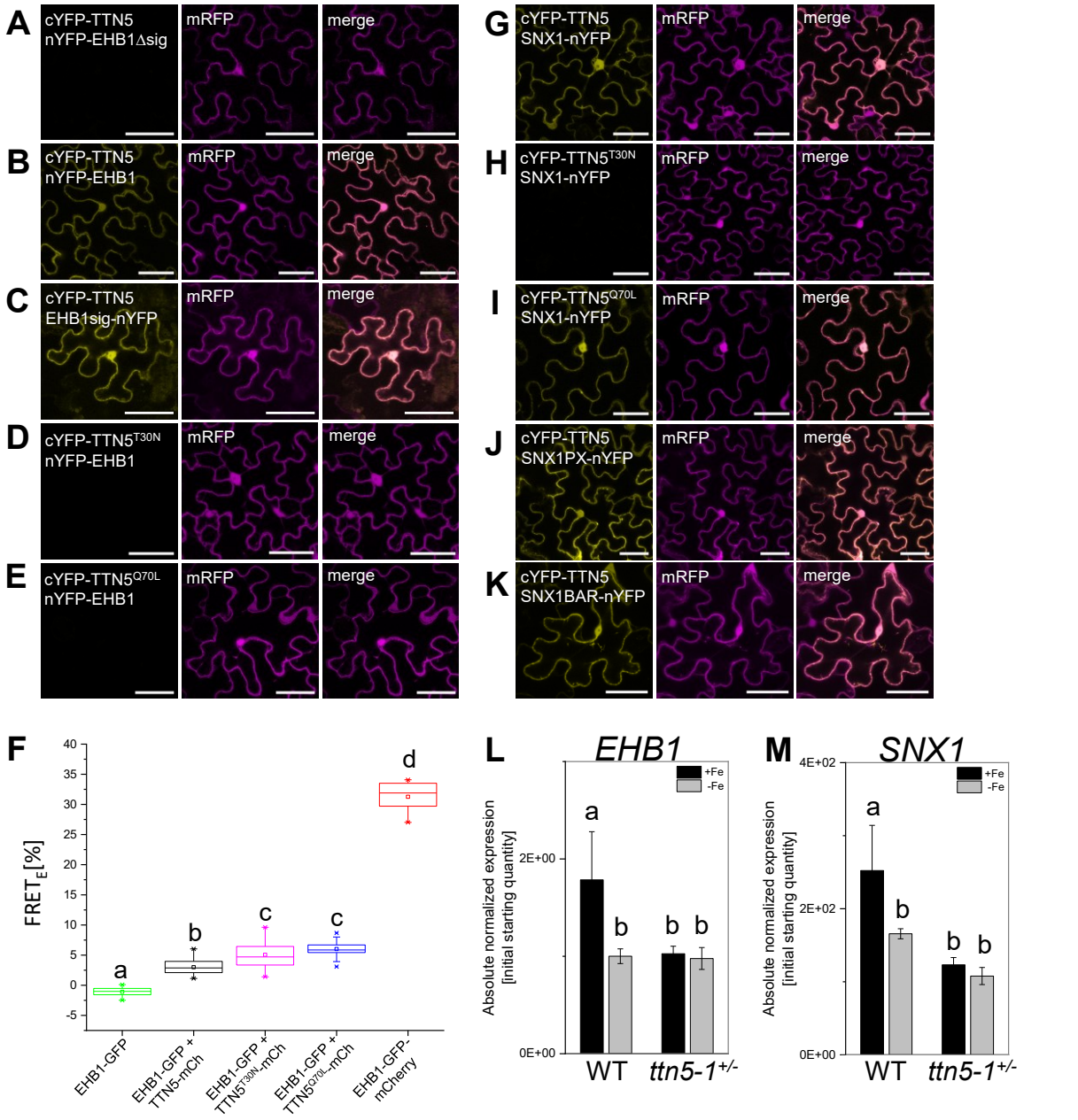

Figure 7. TTN5 interacts with IRT1 regulators EHB1 and SNX1.
(A-E), TTN5 interacts with IRT1 inhibitor EHB1 in BiFC experiments. Protein-protein interaction is visible by a complemented YFP signal. mRFP expression serves as a transformation control. (B, D, E), TTN5 and EHB1 showed complementation whereas inactive and active variant were not able to complement split-YFP with EHB1. (A, C), TTN5 was tested together with (EHB1sig) and without the EHB1 CAR signature domain (CAR domain defined in (Rodriguez et al., 2014), EHB1Δsig). Deletion of the domain lead to the loss of complementation. (F), Interaction between TTN5 and EHB1 was confirmed by FRET-APB. EHB1-GFP as donor-only sample (negative control), EHB1-GFP-mCherry for intra-molecular FRET (positive control). Each combination was tested a minimum of three times (n = 3) with comparable results. (G-K), TTN5 interacts with IRT1 positive regulator SNX1 in BiFC experiments. (G, I), TTN5 and TTN5^{Q70L} showed complemented YFP signal together with SNX1. (H), No YFP fluorescence was detectable for TTN5^{T30N} with SNX1. (J, K), An interaction took place between TTN5 and the PX or the BAR domain of SNX1. (L, M), Gene expression data was obtained by RT-qPCR of *EHB1* and *SNX1* in *ttn5-1*$^{+/-}$ roots compared to WT. Plants were grown in the two-week system in Fe-sufficient (+Fe, black bars) or -deficient (-Fe, grey bars) conditions. Data was obtained from three biological replicates (n = 3). One-way ANOVA was performed with Fisher-LSD post-hoc test. Different letters indicate statistical significance ($p < 0.05$). Scale bar 50 µm

SNX1 is a positive regulator of IRT1 recycling at the TGN (Ivanov et al., 2014). BiFC experiments, testing SNX1 together with WT TTN5 resulted in complemented YFP signal (Figure 7G). The same result was obtained for the active GTPase variant (Figure 7I), while the inactive mutant failed to complement the YFP signal (Figure 7H). Sorting nexins are classified by their characteristic domains. The human SNX family members contain either a Bin-Amphiphysin-Rvs (BAR) domain together with a PHOX-homology (PX) domain, a PX domain alone or in combination with a number of several other domains whereas the Arabidopsis sorting nexins exhibit both, BAR and PX domain (Heucken and Ivanov, 2018). A typical function by proteins with such a domain organization is membrane and phosphoinositide binding via the PX domain, whereas the BAR domain is involved in membrane curvature sensing and the formation of endosomal tubules (Peter et al., 2004; Frost et al., 2009). Interestingly, ARF-GAPs which are needed for the GTP hydrolysis, contain a BAR domain as well (Memon, 2004). We found evidence that TTN5 binds to the SNX1 PX and BAR domains using BiFC (Figure 7J, K). To test whether TTN5 is not only interacting with the known IRT1 regulators but also has a physiological effect, we analyzed their transcript levels in *ttn5-1*$^{+/-}$ seedlings (Figure 7L, M). Interestingly, both, *EHB1* and *SNX1*, were expressed at higher level under Fe-sufficient conditions than -deficient ones in WT, while transcript levels were low irrespective of Fe supply in *ttn5-1*$^{+/-}$.

In summary, we could show that TTN5 is not only interacting with the two IRT1 regulators but it is also influencing their expression under Fe-sufficient versus -deficient conditions.

Discussion

IRT1 is the main Fe transporter in Arabidopsis roots and is therefore responsible for balanced Fe acquisition to cope with the essential but also toxic nature of Fe (Balk and Schaedler, 2014; Brumbarova et al., 2015). The essential small GTPase TTN5 was identified through an embryo morphology screen nearly 20 years ago. Our finding that TTN5 links Fe acquisition with the endomembrane trafficking is highly exciting. Not only does it open up new possibilities to control the activity and localization of IRT1, but also does it shed light on ARL GTPase functions in plants. Binding of TTN5 directly to the cargo IRT1 indicates specificity of TTN5 function beyond housekeeping. TTN5 may play a fundamental role in Fe homeostasis already during seed formation.

TTN5 is part of the endomembrane system and targeting IRT1vr

The ARF family of small GTPases is well known for its involvement in vesicle trafficking and coat assembly with diverse localization patterns within the cell. We observed TTN5 to be localized at different cellular compartments which is typical for several members of this family

and emphasize its involvement in endomembrane trafficking (Memon, 2004; Sztul et al., 2019). A more detailed colocalization analysis showed that both *cis*-Golgi and endosomal/MVB-positive structures colocalize to a higher proportion with the active TTN5 variant compared with the inactive one. This could be an indicator of the site of action of TTN5, considering our knowledge of the activation of ARF GTPases and TTN5 homologs in other organisms. They are usually recruited or move to their place of action upon interacting with their specific GEF, which leads to GDP to GTP exchange-dependent activation (Sztul et al., 2019; Nielsen, 2020; Adarska et al., 2021). Most of GTPase interactions take place in their GTP-bound form (Sharer and Kahn, 1999; Hanzal-Bayer et al., 2002). One exception is the role of TTN5 homologs in microtubule dynamics. ARL2/Alp41-GDP is there interacting with Cofactor D/Alp1^{D} (Bhamidipati et al., 2000; Mori and Toda, 2013). The colocalization of TTN5 with ARA7-positive structures even still in the wortmannin-induced swollen state, triggered by homotypic fusion of prevacuolar compartments (Wang et al., 2009), may indicate that TTN5 performs similar functions in relation to ARA7. ARA7 is involved in cargo transport in the endocytic pathway to the vacuole, with a role, for example, in the endocytosis of FM4-64 (Ueda et al., 2001; Sohn et al., 2003; Kotzer et al., 2004; Ebine et al., 2011). Colocalization of TTN5 with FM4-64-labeled endocytosed vesicles leads to the assumption of a TTN5 involvement in endocytosis and the degradation pathway to the vacuole.

Of particular interest to us is ARF-signaling in PM protein trafficking. The auxin transporters PIN1 and PIN2 and the boron transporter BOR1, like IRT1, are polar localized in the PM and undergo a constant degradation-recycling cycle (Benková et al., 2003; Takano et al., 2010; Barberon et al., 2014). Not only vesicle formation as described for ARF1 or SAR1 plays a role but also other regulatory mechanisms of ARF-signaling through the GEFs and GAPs (Nielsen, 2020). GNOM and BIG5, two ARF-GEFs, and ARF1-regulators, are described to be involved in the proper localization of the PM transporter PIN1, functioning at different regulatory steps (Geldner et al., 2003; Anders et al., 2008; Kleine-Vehn et al., 2008; Tanaka et al., 2009). In addition, another ARF GTPase ARF1A1C may not only partially colocalize with GNOM, but modified activity also resulted in impaired localization of PIN1 to the PM and also altered vacuolar targeting of PIN2 (Tanaka et al., 2014). BOR1 PM localization depends on GNOM as well (Yoshinari et al., 2021), showing a good connection between ARF-GEFs and PM protein localization. We identified TTN5 as a novel IRT1vr interactor. Fluorescent localization of IRT1 with the TTN5 variants have revealed that the inactive variant tends to colocalize more at the PM with IRT1 while intracellular vesicle-like structures of IRT1 overlap more with the active TTN5 variant. This fits with our colocalization data with the different markers and reinforces our suggestion that TTN5 has functions in vesicle trafficking. The presence of TTN5 together with

IRT1 in wortmannin-induced swollen structures, probably indicating MVBs/PVCs, is supporting the idea of a role in transporter degradation. MVBs/PVCs are known to be the last step before vacuolar degradation or cargo recycling via the TGN (Kolb et al., 2015; Arora and Van Damme, 2021). This could indicate that TTN5 presence is a critical point of IRT1 sorting fate. We therefore propose here a role of TTN5 in targeting endocytosed IRT1 protein for vacuolar degradation. In this process, inactive TTN5 could be recruited to the PM, in the move of GTPase activation by nucleotide exchange, active TTN5 would play a role in IRT1 endocytosis.

Taken together, we could not only identify TTN5 as part of the endomembrane system but also uncover another link between ARF-signaling and PM protein trafficking with its interaction with IRT1vr. Identification of potential TTN5-GEF and -GAP proteins will be of greater interest to clarify the role of TTN5 in endomembrane trafficking with particular reference to IRT1 regulation.

TTN5 might play a general role in Fe nutrition

TTN5 does not only have an influence on IRT1 but rather potentially possess a general role in Fe nutrition. A partial lack of TTN5 results in decreased Fe reductase activity. It was already investigated that IRT1 can interact with FRO2 and AHA2 and potentially form a complex for a highly effective Fe uptake machinery (Martín-Barranco et al., 2020). Reduced Fe reductase activity could be both an indirect influence of IRT1 regulation by the complex formation or directly driven by TTN5. Gene expression analysis revealed a greater impact on Fe-related genes in *ttn5-1*$^{+/-}$ roots. Both FIT targets, *IRT1* and *FRO2* (Colangelo and Guerinot, 2004; Jakoby et al., 2004; Ivanov et al., 2012), exhibit transcriptional down-regulation, which was consistent with our expectations, as *FIT* itself also exhibited low gene expression compared with WT. Strategy I genes are up-regulated by FIT heterodimers with a bHLH transcription factor of group Ib (Yuan et al., 2008; Wang et al., 2013). Our first suggestion was a FIT-dependent down-regulation of Strategy I genes due to the constant expression levels of *bHLH039* compared to WT in *ttn5-1*$^{+/-}$ roots. Investigation of transcript levels of genes of the Fe homeostasis network, which are FIT-independent (Brumbarova et al., 2015; Brumbarova and Ivanov, 2019; Schwarz and Bauer, 2020) resulted in similar down-regulation. *FRO3* is induced by a bHLH IVc-bHLH121/URI heterodimer, but is repressed by PYE (Long et al., 2010; Kim et al., 2019). Based on the concomitant down-regulation of *PYE*, which is also induced by bHLH IVc-bHLH121/URI heterodimer (Kim et al., 2019), we suggested that there is impaired or complete absence of heterodimer up-regulation. However, *OPT3*, another target of these heterodimers (Kim et al., 2019) showed no altered gene expression compared with WT. One possible explanation could be that *PYE* and *FRO3* induction is dependent on the formation of a different bHLH IVc-bHLH121/URI heterodimer than that of *OPT3*. Our findings on a

physiological basis are pointing in a positive direction of TTN5 affecting plant Fe nutrition. We speculate that TTN5 may regulate an upstream target of the Fe homeostasis cascade, e.g. one of the bHLH transcription factors of subgroup IVc, bHLH034, bHLH104, bHLH105/ILR3 or bHLH115; however, this requires further investigation. A general role in Fe nutrition could give another explanation of embryo lethality in TTN5 loss of function seeds, as it is a known phenotype of disturbed Fe acquisition (Stacey et al., 2008; Jain et al., 2019) and *ttn5-1*$^{+/-}$ have a reduced seed Fe content.

A general positive impact on Fe homeostasis in combination with the TTN5-IRT1 colocalization in MVBs/PVCs could be an indicator for TTN5 being a regulator of independent cellular processes. Several interaction partners were already reported for the human homolog ARL2 with connection to distinct cellular functions. ARL2 together with Cofactor D is reported to be involved in tubulin folding and in more general in microtubule dynamics (Bhamidipati et al., 2000). Next to this, ARL2 was also detected in mitochondria. In a complex with its interactor BART, ARL2-GTP is able to interact with the adenine nucleotide translocase ANT1, an inner mitochondrial membrane protein. The deletion of ANT1 in mice, lead to an increased ARL2 concentration, pointing into a mitochondrial stress-induced regulation of ARL2 localization (Sharer et al., 2002). Based on these distinct locations and the associated function of ARL2, a role in higher order signaling was proposed making it a potential link between different cellular pathways on a regulatory basis (Francis et al., 2016). This can be also the case in Arabidopsis, to bridge TTN5 microtubule defective phenotype (Mayer et al., 1999) with our here found involvement in IRT1 regulation in a probably Fe deficiency stress-induced manner.

TTN5 interacts with EHB1 and SNX1 and may coordinate endocytosis

It is already known that IRT1 regulation is a process of high complexity which is not only influenced by Fe-sufficient or -deficient conditions, but also including other metals such as zinc and manganese or Ca^{2+}- and ROS-signaling among others (Dubeaux et al., 2018; Brumbarova and Ivanov, 2019; Khan et al., 2019; Gratz et al., 2021).

It was recently reported that Fe deficiency leads to an increase of cytosolic Ca^{2+} and promoting the Fe deficiency response (Gratz et al., 2019; Matthus et al., 2019). We could identify an interplay of CALCINEURIN B-LIKE PROTEIN 1/9 (CBL) and CIPK11 being responsible for transcription factor FIT activity by phosphorylation (Gratz et al., 2019). Additional physiological data indicate that CBL1/9-dependent CIPK23 activation is promoting an induction of the Fe reductase activity (Tian et al., 2016). Contrary to this, CBL1/9 are also responsible for potential IRT1 endocytosis by CIPK23-dependent phosphorylation and the transporter activity is inhibited by Ca^{2+}-induced recruiting of EHB1 to the PM (Dubeaux et al., 2018; Khan et al., 2019), proving opposing effects of Ca^{2+} in the Fe deficiency response. EHB1

is additionally interesting as a member of the CAR family. Several CAR proteins can interact with and recruit PYRABACTIN RESISTANCE 1 (PYR1)/PYR1-LIKE (PYL) abscisic acid (ABA) receptors to membranes. They can also initiate Ca^{2+}-dependent membrane curvature, which may provide a direct link to vesicle trafficking. We could show here that TTN5 is also able to interact with EHB1. Interestingly, Ca^{2+} is bound by EHB1 via its C2 domain, which is also a common feature of class III ARF-GAPs (Vernoud et al., 2003; Knauer et al., 2011). Crystallization experiments revealed a potential Ca^{2+}-binding site between HsARF6 and its GAP ASAP3. The GTP-hydrolysis was stimulated in the presence of Ca^{2+} proposing a linkage between Ca^{2+}- and ARF-signaling (Ismail et al., 2010). We consider the possibility of an interaction between TTN5 and EHB1 in a Ca^{2+}-dependent manner based on the published hypothesis and our findings.

Next to EHB1, we identified SNX1 as a positive regulator for IRT1 recycling to the PM in the sorting endosomes (Ivanov et al., 2014). In addition to IRT1, endosomal recycling of the auxin efflux carrier PIN2 is also dependent on SNX1 (Jaillais et al., 2006). SNX1 is therefore part of the recycling of specific PM proteins. Interestingly, deficiency of BLOS1 leads to accumulation of PIN1 and PIN2 at the PM (Cui et al., 2010). BLOS1 is one of the homologs to the mammalian biogenesis of lysosome-related organelles complex 1 (BLOC-1), which is responsible for vesicle transport from endosomes to lysosomes (Li et al., 2007; Raposo et al., 2007). BLOS1 could therefore perform a similar function to BLOC-1 in Arabidopsis. Interestingly, SNX1 can interact with both BLOS1 and BLOS2 and could therefore also play a role in vesicle-mediated transport through these interactions (Cui et al., 2010; Heucken and Ivanov, 2018). SNX1 possess a BAR domain which is also typical for class I ARF-GAPs (Vernoud et al., 2003; Heucken and Ivanov, 2018). A connection between the SNX1 BAR domain and an ARF6-GEF was identified in mouse by their interaction. This interaction was associated with a positive effect of ARF6 function (Fukaya et al., 2014). Colocalization analysis revealed overlapping expression in endosomes, which fits known SNX1 localization in Arabidopsis (Fukaya et al., 2014; Ivanov et al., 2014), this could be a possible interconnection between ARF-signaling and SNX1. Here, we identified an interaction between TTN5 and SNX1, which could be the critical link in the decision between SNX1-dependent recycling and degradation of IRT1. SNX1 could be also needed for a potential TTN5-GEF and subsequent TTN5 recruiting to membranes. Based on the opposing roles of EHB1 and SNX1 in IRT1 regulation and their here described connection to TTN5, we suggest a coordinating role of TTN5 in transporting IRT1 between PM and endosomes by interacting with its regulators such as EHB1 and SNX1. Their domain homology to ARF-GAPs, with a C2 or BAR domain, and SNX1 interaction with an ARF-GEF strengthen the interest in the identification of TTN5-GEFs and -GAPs.

In this study, we identified the ARF-like GTPase TTN5 as an interactor of the iron transporter IRT1 and two of its known regulators, SNX1 and EHB1. We detected TTN5 colocalization with IRT1 at the PM and late endosomes and a general involvement in the regulation of plant Fe homeostasis. The TTN5 involvement in vesicle trafficking and interaction with several IRT1 regulators with opposing functions suggests a coordinating role in IRT1 regulation.

Material & Methods

Yeast two-hybrid (Y2H)

The yeast two-hybrid screen for identification of IRT1vr interactors was performed previously and is described in Khan et al. (2019). Targeted Y2H interactions were tested using the GAL4 transcription factor system with histidine as selection marker. *TTN5* coding sequence was amplified using TITAN5 nter B1 and TITAN5 stop B2 primers (for primer sequences, see Supplemental Table 1). Primer pair I1LB1 and I1LB2 was used for *IRT1vr* coding sequence amplification. Obtained fragments were cloned into pDONR207 via Gateway BP reaction with following LR reactions into pGBKT7-GW (binding domain, BD) or pACT2-GW (activation domain, AD). Both vectors were a kind gift from Dr. Yves Jacob. The yeast strain AH109 was cotransformed with the corresponding AD- and BD-tagged expression vectors. The combination pACT2:SNX1 and pGBKT7:SNX1 (Pourcher et al., 2010) was used as a positive control. Negative controls were cotransformations with the respective non-recombined pACT2-GW or pGBKT7-GW. Drop test was performed with SD -Leu, -Trp-cultures at an OD_{600} of 0.1 and three additional 1:10 dilution steps (10^1-10^4) on SD -Leu, -Trp- and SD -Leu, -Trp, -His + 0,5 mM 3-amino-1,2,4-triazole-plates. One of each plate was incubated either at 30°C or at room temperature, wrapped in aluminum foil for up to two weeks.

Arabidopsis plant material and growth conditions

The Arabidopsis *ttn5-1* mutant was previously described (McElver et al., 2000). Heterozygous seedlings were selected by PCR on gDNA using the primer TTN5 intron1 fwd and pDAP101 LB1 (Supplemental Table 1). Arabidopsis seeds were sterilized with sodium hypochlorite solution (6 % Sodium hypochlorite and 0.1 % Triton X-100) and stored 24 hours at 4°C for stratification. Seedlings were grown upright on Hoagland media (1.5 mM $Ca(NO_3)_2$, 0.5 mM KH_2PO_4, 1.25 mM KNO_3, 0.75 mM $MgSO_4$, 1.5 µM $CuSO_4$, 50 µM H_3BO_3, 50 µM KCl, 10 µM $MnSO_4$, 0.075 µM $(NH_4)_6Mo_7O_{24}$, 2 µM $ZnSO_4$ and 1 % sucrose, pH 5.8, supplemented with 1.4 % Plant agar (Duchefa)] with sufficient (50 µM FeNaEDTA, + Fe) or deficient (0 µM FeNaEDTA, - Fe) Fe supply in growth chambers (CLF Plant Climatics) under long day condition (16 hours light at 21°C, 8 hours darkness at 19°C). Seedlings were grown in a two-week growth

system with plants growing 14 days on Fe-sufficient media and then transferred to either fresh Fe-sufficient or Fe-deficient media for additional three days.

Nicotiana benthamiana plants were grown on soil for 2-4 weeks in a greenhouse facility under long day conditions (16 hours light, 8 hours darkness).

Fe reductase activity assay

Fe reductase activity assay was performed as described in (Gratz et al., 2019). For Fe reductase activity plants were grown in the two-week system in Fe-sufficient or -deficient conditions. Two plants per replicate were washed in 100 mM $Ca(NO_3)_2$, then incubated for 1 hour in the dark in 1.5 ml Fe reductase solution (300 mM ferrozine and 100 mM FeNaEDTA). The Fe reductase activity-dependent color change was measured at 562 nm using Infinite 200® PRO (Tecan) plate reader. Activity calculation was done using the ferrozine extinction coefficient ε = 28.6 $mM^{-1}*cm^{-1}$ and was normalized to root length. The assay was performed with three replicates (n = 3), each consisting of a pool of two plants.

Seed Fe content

For seed Fe content determination, plants were grown on soil under long day conditions (16 hours light, 8 hours darkness, at 21°C). Seeds were dried for 16 hours at 100°C. Approximately 10 mg dried seeds were grinded in agate mortar and resuspended in 500 µl HNO_3 (3 %). Suspensions were incubated for 16 hours at 100°C followed by 5 min centrifugation at 14000*g*. 400 µl supernatant were transferred into a fresh tube. 160 µl sodium ascorbate (38 mg/ml), 320 µl bathophenanthrolinedisulfonic acid (BPDS) (1.7 mg/ml) and 126 µl ammonium acetate (1:3 dilution of saturated solution) were added. The specific absorbance of the iron-chelator complex was measured after 5 min at 535 nm. The non-specific absorbance at 680 nm was subtracted for an improved accuracy. An FeNaEDTA standard (3.125 µM – 50 µM) was recorded in parallel. The assay was performed in three biological replicates (n = 3).

Gene expression analysis by RT-qPCR

For gene expression analysis, plants were grown in the two-week system. Total RNA was isolated from roots using the peqGOLD Plant RNA kit (Peqlab) and cDNA synthesis was performed with the RevertAid RT Reverse Transcription Kit (ThermoFisher Scientific). The SFX96 Touch™Real-Time PCR Detection System (Bio-Rad) was used for RT-qPCR performance. Data processing was done with Bio-Rad SFX Manager™ (version3.1) software. Mass standard curve analysis was used for determination of the absolute gene expression and the elongation factor *EF1Bα* expression served as a reference for normalization. RT-qPCR was

performed in three biological replicates (n = 3) and two technical replicates each. All primer pairs used in this study are listed in Supplemental Table 1.

Nicotiana benthamiana leaf infiltration

N. benthamiana leaf infiltration was performed with the Agrobacterium (*Rhizobium radiobacter*) strain C58 (GV3101) carrying the respective constructs for confocal microscopy. Agrobacteria cultures were grown overnight at 28°C, centrifuged for 5 min at 4°C at 5000*g*, resuspended in infiltration solution (5 % sucrose, a pinch of glucose, 0.01 % Silwet Gold, 150 µM Acetosyringone) and incubated for 1 hour at room temperature. Bacterial suspension was set to an OD_{600}=0.4 and infiltrated into the abaxial side of *N. benthamiana* leaves.

Expression of pABind and pMDC7 (Bleckmann et al., 2010, Curtis and Grossniklaus, 2003) constructs was induced with a β-estradiol solution (20 µM β-estradiol, 0.1 % Tween 20) 16 hours before imaging.

Subcellular localization of fluorescent protein fusions

To create TTN5 inactive (T30N) and active (Q70L) constructs point mutations were introduced by site-directed mutagenesis. In a first step mutated CDS fragments were amplified with primer pairs TITAN5 n-ter B1 with T5T30Nr or T5Q70Lr and T5T30Nf or TQ70Lf with TITAN5 stop B2 respectively. In a second step the primer combination TITAN5 n-ter B1 with TITAN5 stop B2 was used with the previously obtained fragments as templates.

For YFP-tagged TTN5 constructs, *TTN5*, $TTN5^{Q70L}$ and $TTN5^{T30N}$ coding sequences with stop codon were amplified with B1 and B2 attachment sites for Gateway cloning (Life Technologies) using the primer TITAN5 n-ter B1 and TITAN5 stop B2. The obtained PCR fragments were cloned via BP reaction (Life Technologies) into pDONR207 (Invitrogen). The N-terminally YFP-tagged TTN5 constructs were created via LR reaction (Life Technologies) with the destination vector pH7WGY2 (Karimi et al., 2005). mCherry-tagged constructs were created via overlap-extension PCR. Fluorescent protein was amplified from pABind:mCherry (Bleckmann et al., 2010) using primer pair mCherry B1 and mCh R ns BIND. *TTN5*, $TTN5^{T30N}$ and $TTN5^{Q70L}$ CDS were amplified with a 20 bp overlap of mCherry using mCh to TTN5 and TITAN5 stop B2. In a third PCR mCherry-tagged TTN5 constructs were generated with the mCherry B1 and TITAN5 stop B2 primer pair. BP and LR reaction were performed as described above. As destination vector the XVE-driven β-estradiol inducible promoter driven vector pMDC7 (Curtis and Grossniklaus, 2003) was chosen. Agrobacteria were transformed with the obtained constructs and tested by *N. benthamiana* leaf infiltration after two days of expression.

Localization studies were carried out by laser-scanning confocal microscopy (LSM 780, Zeiss) with a 40x C-Apochromat water immersion objective. YFP constructs were excited at

488 nm and detected at 491-560 nm. mCherry or FM4-64 fluorescence was excited at 561 nm and detected at 570-633 nm.

RFP-ARA7 clones were a gift from Dr. Thierry Gaude.

Chemical treatments

Wortmannin (10 µM, Sigma-Aldrich), BFA (36 µM, Sigma-Aldrich) and plasma membrane dye FM4-64 (165 µM, ThermoFisher Scientific) were infiltrated into *N. benthamiana* leaves. FM4-64 was detected after five min incubation. Wortmannin and BFA were incubated for 25 min before checking the treatment effect. Plasmolysis was induced by incubating leaf discs in 1 M mannitol solution for 15 min.

JACoP based colocalization analysis

Colocalization analysis was performed with the ImageJ (Schneider et al., 2012) Plugin Just Another Colocalization Plugin (JACoP) (Bolte and Cordelières, 2006). A comparison of Pearson`s and Overlap coefficients and Li's intensity correlation quotient (ICQ) was done. Object-based analysis was performed for spotted-structures, adapted by (Ivanov et al., 2014). Percentage of colocalization for both channels was calculated based on distance between geometrical centers of signals. Analysis was conducted in three replicates each (n = 3).

Bimolecular Fluorescence Complementation (BiFC)

The interaction studies of TTN5 and the respective GTPase active ($TTN5^{Q70L}$) or inactive ($TTN5^{T30N}$) variants *in planta* were performed by using BiFC. *TTN5*, $TTN5^{Q70L}$ and $TTN5^{T30N}$ coding sequences with stop codon were amplified using the primers TITAN5 n-ter B1 and TITAN5 stop B4 (Supplemental Table 1).

IRT1vr coding sequence with stop codon was amplified using the primers I1L1B3 and I1LB2. Amplifying *EHB1* the primer pair EHB1 n-ter B3 and EHB1 stop B2 was used. *SNX1* coding sequence without stop codon for C-terminal fusion was amplified using the primer SNX1 B3 and SNX1 ns B2. Cloning of SNX1 deletion mutants SNX1PX and SNX1BAR was done using the primers SNX1 B3 and PXSNX1 rev and BARSNX1 fwd and SNX1 ns B2 respectively.

The amplified PCR products were cloned via Gateway BP reaction (Life Technologies) into pDONR221-P1P4 (Invitrogen) or pDONR221-P3P2 (Invitrogen). The obtained constructs were used in an LR reaction (Life Technologies) for cloning into pBiFCt-2in1 vectors (Grefen and Blatt, 2012). Agrobacteria were transformed with correct constructs and used for *N. benthamiana* leaf infiltration. After 48 hours, the mRFP expression control signal and YFP signals were detected by fluorescent microscopy (LSM 780, Zeiss) with a 40x C-Apochromat water immersion objective. YFP constructs were detected at 491-560 nm after exciting at

488 nm and mCherry fluorescence was excited at 561 nm and emission detected at 570-633 nm.

The BiFC constructs were tested in three independent replicates with three infiltrated leaves each. The vectors pBiFC-2in1-NN and pBiFC-2in1-CN were kindly provided by Dr. Christopher Grefen, Tübingen, Germany.

Förster-Resonance-Energy Transfer Acceptor Photo Bleaching (FRET-APB)

To verify protein-protein interactions of TTN5 and the corresponding GTPase active ($TTN5^{Q70L}$) and inactive ($TTN5^{T30N}$) variants the FRET-APB was used. The coding sequences without stop codon were amplified with the primers TITAN5 B1 and TITAN5 ns B2, and cloned into the pDONR207 (Invitrogen, BP reaction, Life Technologies). Coding sequences of *IRT1vr* and *EHB1* were cloned with the primer pairs I1LB1 and I1LnsB2 or EHB1 B1 and EHB1 nsB2 respectively. The obtained constructs were used for LR reactions (Life Technologies) with the pABind-GFP, pABind-mCherry and pABind-FRET for C-terminal tagging (Bleckmann et al., 2010). N-terminal GFP-TTN5 constructs were cloned via overlap extension PCR simultaneously with mCherry-TTN5 constructs (check paragraph 'Subcellular localization of fluorescent protein fusions'). In the first step the primer pairs GFP B1 with GFP R ns BIND and GFP to TTN5 with TITAN5 stop B2 were used with pABind-FRET (Bleckmann et al., 2010) as template for the fluorescent protein coding sequence. The final construct was obtained with the primer pair GFP B1 with TITAN5 stop B2. Constructs were cloned into pDONR207 for further cloning into pMDC7 via LR reactions. Agrobacteria were transformed and used for *N. benthamiana* leaf infiltration. FRET-APB was performed using laser-scanning confocal microscopy (LSM 780, Zeiss) with a 40x C-Apochromat water immersion objective. GFP was excited at 488 nm and detected at 491-560 nm and mCherry fluorescence was excited at 561 nm and detected at 570-633 nm. GFP and mCherry channels were recorded for five scans. The mCherry signal was then bleached with 70 iterations of maximum laser intensity in a specific region of interest (ROI) which was set to the nucleus. Both channels were detected for additional 20 post-bleaching scans. FRET-APB measurements were performed with a minimum of 10 repetitions ($n \geq 10$).

Structure prediction

TTN5 structure prediction was performed by AlphaFold (Jumper et al., 2021). Molecular graphic was edited with UCSF ChimeraX (1.2.5, Goddard et al., 2018), developed by the Resource for Biocomputing, Visualization, and Informatics at the University of California, San Francisco, with support from National Institutes of Health R01-GM129325 and the Office of Cyber Infrastructure and Computational Biology, National Institute of Allergy and Infectious Diseases.

Statistical analysis

One-way ANOVA was used for statistical analysis and performed in OriginPro 2019. Fisher LSD was chosen as post-hoc test with $p < 0.05$.

ACCESSION NUMBERS

Sequence data from this article can be found in the TAIR and GenBank data libraries under accession numbers: *bHLH039* (TAIR: AT3G56980), *FIT* (TAIR: AT2G28160), *FRO2* (TAIR: AT1G01580), *FRO3* (TAIR: AT1G23020), *EHB1* (TAIR: AT1G70800), *IRT1* (TAIR: AT4G19690), *NRAMP1* (TAIR: AT1G80830), *OPT3* (TAIR: AT4G16370), *PYE* (TAIR: AT3G47640), *TTN5* (TAIR: AT2G18390), and *SNX1* (TAIR: AT5G06140).

Acknowledgements

We thank Gintaute Matthäi and Elke Wieneke for excellent technical assistance. We thank Ksenia Trofimov for microscopic help and advice. We are thankful for the excellent assistance from Stefanie Weidtkamp-Peters and Sebastian Hänsch, members of the Center for Advanced Imaging (CAi) at the Heinrich Heine University.

This work was supported by the Deutsche Forschungsgemeinschaft (DFG, German Research Foundation Project no. 267205415–SFB 1208 and project B05 to P.B. and project Z02 to S.W.-P.)

References

Adarska P, Wong-Dilworth L, Bottanelli F (2021) ARF GTPases and Their Ubiquitous Role in Intracellular Trafficking Beyond the Golgi. Frontiers in cell and developmental biology **9:** 679046-679046

Anders N, Nielsen M, Keicher J, Stierhof YD, Furutani M, Tasaka M, Skriver K, Jürgens G (2008) Membrane association of the Arabidopsis ARF exchange factor GNOM involves interaction of conserved domains. Plant Cell **20:** 142-151

Antoshechkin I, Han M (2002) The *C. elegans* evl-20 Gene Is a Homolog of the Small GTPase ARL2 and Regulates Cytoskeleton Dynamics during Cytokinesis and Morphogenesis. Developmental Cell **2:** 579-591

Arora D, Van Damme D (2021) Motif-based endomembrane trafficking. Plant Physiology **186:** 221-238

Balk J, Schaedler TA (2014) Iron Cofactor Assembly in Plants. Annual Review of Plant Biology **65:** 125-153

Barberon M, Dubeaux G, Kolb C, Isono E, Zelazny E, Vert G (2014) Polarization of IRON-REGULATED TRANSPORTER 1 (IRT1) to the plant-soil interface plays crucial role in metal homeostasis. Proceedings of the National Academy of Sciences **111:** 8293-8298

Barberon M, Zelazny E, Robert S, Conéjéro G, Curie C, Friml J, Vert G (2011) Monoubiquitin-dependent endocytosis of the IRON-REGULATED TRANSPORTER 1 (IRT1) transporter controls iron uptake in plants. Proceedings of the National Academy of Sciences **108:** E450-E458

Bauer P (2016) Regulation of iron acquisition responses in plant roots by a transcription factor. Biochem Mol Biol Educ **44:** 438-449

Benková E, Michniewicz M, Sauer M, Teichmann T, Seifertová D, Jürgens G, Friml J (2003) Local, Efflux-Dependent Auxin Gradients as a Common Module for Plant Organ Formation. Cell **115:** 591-602

Bhamidipati A, Lewis SA, Cowan NJ (2000) ADP ribosylation factor-like protein 2 (Arl2) regulates the interaction of tubulin-folding cofactor D with native tubulin. Journal of Cell Biology **149:** 1087-1096

Bleckmann A, Weidtkamp-Peters S, Seidel CAM, Simon R (2010) Stem cell signaling in Arabidopsis requires CRN to localize CLV2 to the plasma membrane. Plant physiology **152:** 166-176

Bolte S, Cordelières FP (2006) A guided tour into subcellular colocalization analysis in light microscopy. J Microsc **224:** 213-232

Bolte S, Talbot C, Boutte Y, Catrice O, Read ND, Satiat-Jeunemaitre B (2004) FM-dyes as experimental probes for dissecting vesicle trafficking in living plant cells. Journal of Microscopy **214:** 159-173

Brumbarova T, Bauer P, Ivanov R (2015) Molecular mechanisms governing Arabidopsis iron uptake. Trends in Plant Science **20:** 124-133

Brumbarova T, Ivanov R (2019) The Nutrient Response Transcriptional Regulome of Arabidopsis. iScience **19:** 358-368

Cointry V, Vert G (2019) The bifunctional transporter-receptor IRT1 at the heart of metal sensing and signalling. New Phytologist **223:** 1173-1178

Colangelo EP, Guerinot ML (2004) The Essential Basic Helix-Loop-Helix Protein FIT1 Is Required for the Iron Deficiency Response. The Plant Cell **16:** 3400-3412

Cui Y, Li X, Chen Q, He X, Yang Q, Zhang A, Yu X, Chen H, Liu N, Xie Q, Yang W, Zuo J, Palme K, Li W (2010) BLOS1, a putative BLOC-1 subunit, interacts with SNX1 and modulates root growth in Arabidopsis. Journal of Cell Science **123:** 3727-3733

Cui Y, Shen J, Gao C, Zhuang X, Wang J, Jiang L (2016) Biogenesis of Plant Prevacuolar Multivesicular Bodies. Molecular Plant **9:** 774-786

Curie C, Alonso JM, Le Jean M, Ecker JR, Briat JF (2000) Involvement of NRAMP1 from *Arabidopsis thaliana* in iron transport. Biochem J **347 Pt 3:** 749-755

Curtis MD, Grossniklaus U (2003) A gateway cloning vector set for high-throughput functional analysis of genes in planta. Plant physiology **133:** 462-469

Dhonukshe P, Aniento F, Hwang I, Robinson DG, Mravec J, Stierhof Y-D, Friml J (2007) Clathrin-Mediated Constitutive Endocytosis of PIN Auxin Efflux Carriers in Arabidopsis. Current Biology **17:** 520-527

Dubeaux G, Neveu J, Zelazny E, Vert G (2018) Metal Sensing by the IRT1 Transporter-Receptor Orchestrates Its Own Degradation and Plant Metal Nutrition. Molecular Cell **69:** 953-964.e955

Ebine K, Fujimoto M, Okatani Y, Nishiyama T, Goh T, Ito E, Dainobu T, Nishitani A, Uemura T, Sato MH, Thordal-Christensen H, Tsutsumi N, Nakano A, Ueda T (2011) A membrane trafficking pathway regulated by the plant-specific RAB GTPase ARA6. Nat Cell Biol **13:** 853-859

Eide D, Broderius M, Fett J, Guerinot ML (1996) A novel iron-regulated metal transporter from plants identified by functional expression in yeast. Proceedings of the National Academy of Sciences of the United States of America **93:** 5624-5628

Emans N, Zimmermann S, Fischer R (2002) Uptake of a fluorescent marker in plant cells is sensitive to brefeldin A and wortmannin. Plant Cell **14:** 71-86

Fansa EK, Wittinghofer A (2016) Sorting of lipidated cargo by the Arl2/Arl3 system. Small GTPases **7:** 222-230

Fleming JA, Vega LR, Solomon F (2000) Function of tubulin binding proteins in vivo. Genetics **156:** 69-80

Foot N, Henshall T, Kumar S (2017) Ubiquitination and the Regulation of Membrane Proteins. Physiological Reviews **97:** 253-281

Francis JW, Turn RE, Newman LE, Schiavon C, Kahn RA (2016) Higher order signaling: ARL2 as regulator of both mitochondrial fusion and microtubule dynamics allows integration of 2 essential cell functions. Small GTPases **7:** 188-196

Frost A, Unger VM, De Camilli P (2009) The BAR Domain Superfamily: Membrane-Molding Macromolecules. Cell **137:** 191-196

Fukaya M, Fukushima D, Hara Y, Sakagami H (2014) EFA6A, a guanine nucleotide exchange factor for Arf6, interacts with sorting nexin-1 and regulates neurite outgrowth. Journal of Neurochemistry **129:** 21-36

Gaither LA, Eide DJ (2001) Eukaryotic zinc transporters and their regulation. Biometals **14:** 251-270

Geldner N, Anders N, Wolters H, Keicher J, Kornberger W, Muller P, Delbarre A, Ueda T, Nakano A, Jürgens G (2003) The Arabidopsis GNOM ARF-GEF mediates endosomal recycling, auxin transport, and auxin-dependent plant growth. Cell **112:** 219-230

Goddard TD, Huang CC, Meng EC, Pettersen EF, Couch GS, Morris JH, Ferrin TE (2018) UCSF ChimeraX: Meeting modern challenges in visualization and analysis. Protein Sci **27:** 14-25

Gratz R, Manishankar P, Ivanov R, Köster P, Mohr I, Trofimov K, Steinhorst L, Meiser J, Mai HJ, Drerup M, Arendt S, Holtkamp M, Karst U, Kudla J, Bauer P, Brumbarova T (2019) CIPK11-Dependent Phosphorylation Modulates FIT Activity to Promote Arabidopsis Iron Acquisition in Response to Calcium Signaling. Dev Cell **48:** 726-740.e710

Gratz R, von der Mark C, Ivanov R, Brumbarova T (2021) Fe acquisition at the crossroad of calcium and reactive oxygen species signaling. Curr Opin Plant Biol **63:** 102048

Grefen C, Blatt MR (2012) A 2in1 cloning system enables ratiometric bimolecular fluorescence complementation (rBiFC). Biotechniques **53:** 311-314

Grossoehme NE, Akilesh S, Guerinot ML, Wilcox DE (2006) Metal-Binding Thermodynamics of the Histidine-Rich Sequence from the Metal-Transport Protein IRT1 of *Arabidopsis thaliana*. Inorganic Chemistry **45:** 8500-8508

Guerinot ML (2000) The ZIP family of metal transporters. Biochimica et Biophysica Acta (BBA) - Biomembranes **1465:** 190-198

Hanzal-Bayer M, Renault L, Roversi P, Wittinghofer A, Hillig RC (2002) The complex of Arl2-GTP and PDEδ: from structure to function. The EMBO Journal **21:** 2095-2106

Heucken N, Ivanov R (2018) The retromer, sorting nexins and the plant endomembrane protein trafficking. J Cell Sci **131**

Ismail SA, Chen YX, Rusinova A, Chandra A, Bierbaum M, Gremer L, Triola G, Waldmann H, Bastiaens PI, Wittinghofer A (2011) Arl2-GTP and Arl3-GTP regulate a GDI-like transport system for farnesylated cargo. Nat Chem Biol **7:** 942-949

Ismail SA, Vetter IR, Sot B, Wittinghofer A (2010) The Structure of an Arf-ArfGAP Complex Reveals a Ca^{2+} Regulatory Mechanism. Cell **141:** 812-821

Ito E, Uemura T, Ueda T, Nakano A (2016) Distribution of RAB5-positive multivesicular endosomes and the *trans*-Golgi network in root meristematic cells of *Arabidopsis thaliana*. Plant biotechnology (Tokyo, Japan) **33:** 281-286

Ivanov R, Brumbarova T, Bauer P (2012) Fitting into the Harsh Reality: Regulation of Iron-deficiency Responses in Dicotyledonous Plants. Molecular Plant **5:** 27-42

Ivanov R, Brumbarova T, Blum A, Jantke A-M, Fink-Straube C, Bauer P (2014) SORTING NEXIN1 is required for modulating the trafficking and stability of the Arabidopsis IRON-REGULATED TRANSPORTER1. The Plant cell **26:** 1294-1307

Ivanov R, Vert G (2021) Endocytosis in plants: Peculiarities and roles in the regulated trafficking of plant metal transporters. Biology of the Cell **113:** 1-13

Jaillais Y, Fobis-Loisy I, Miège C, Gaude T (2008) Evidence for a sorting endosome in Arabidopsis root cells. The Plant Journal **53:** 237-247

Jaillais Y, Fobis-Loisy I, Miège C, Rollin C, Gaude T (2006) AtSNX1 defines an endosome for auxin-carrier trafficking in Arabidopsis. Nature **443:** 106-109

Jain A, Dashner ZS, Connolly EL (2019) Mitochondrial Iron Transporters (MIT1 and MIT2) Are Essential for Iron Homeostasis and Embryogenesis in *Arabidopsis thaliana*. Frontiers in plant science **10:** 1449-1449

Jakoby M, Wang H-Y, Reidt W, Weisshaar B, Bauer P (2004) FRU (BHLH029) is required for induction of iron mobilization genes in *Arabidopsis thaliana*. FEBS Letters **577:** 528-534

Jumper J, Evans R, Pritzel A, Green T, Figurnov M, Ronneberger O, Tunyasuvunakool K, Bates R, Žídek A, Potapenko A, Bridgland A, Meyer C, Kohl SAA, Ballard AJ, Cowie A, Romera-Paredes B, Nikolov S, Jain R, Adler J, Back T, Petersen S, Reiman D, Clancy E, Zielinski M, Steinegger M, Pacholska M, Berghammer T, Bodenstein S, Silver D, Vinyals O, Senior AW, Kavukcuoglu K, Kohli P, Hassabis D (2021) Highly accurate protein structure prediction with AlphaFold. Nature **596:** 583-589

Just WW, Peränen J (2016) Small GTPases in peroxisome dynamics. Biochimica et Biophysica Acta (BBA) - Molecular Cell Research **1863:** 1006-1013

Karimi M, De Meyer B, Hilson P (2005) Modular cloning in plant cells. Trends in Plant Science **10:** 103-105

Kerkeb L, Mukherjee I, Chatterjee I, Lahner B, Salt DE, Connolly EL (2008) Iron-Induced Turnover of the Arabidopsis IRON-REGULATED TRANSPORTER1 Metal Transporter Requires Lysine Residues Plant Physiology **146:** 1964-1973

Khan I, Gratz R, Denezhkin P, Schott-Verdugo SN, Angrand K, Genders L, Basgaran RM, Fink-Straube C, Brumbarova T, Gohlke H, Bauer P, Ivanov R (2019) Calcium-Promoted Interaction between the C2-Domain Protein EHB1 and Metal Transporter IRT1 Inhibits Arabidopsis Iron Acquisition. Plant Physiology **180:** 1564-1581

Kim SA, LaCroix IS, Gerber SA, Guerinot ML (2019) The iron deficiency response in *Arabidopsis thaliana* requires the phosphorylated transcription factor URI. Proceedings of the National Academy of Sciences **116:** 24933-24942

Klatte M, Schuler M, Wirtz M, Fink-Straube C, Hell Rd, Bauer P (2009) The Analysis of Arabidopsis Nicotianamine Synthase Mutants Reveals Functions for Nicotianamine in Seed Iron Loading and Iron Deficiency Responses Plant Physiology **150:** 257-271

Kleine-Vehn J, Dhonukshe P, Sauer M, Brewer PB, Wiśniewska J, Paciorek T, Benková E, Friml J (2008) ARF GEF-dependent transcytosis and polar delivery of PIN auxin carriers in Arabidopsis. Curr Biol **18:** 526-531

Knauer T, Dümmer M, Landgraf F, Forreiter C (2011) A negative effector of blue light-induced and gravitropic bending in Arabidopsis. Plant physiology **156:** 439-447

Kolb C, Nagel M-K, Kalinowska K, Hagmann J, Ichikawa M, Anzenberger F, Alkofer A, Sato MH, Braun P, Isono E (2015) FYVE1 is essential for vacuole biogenesis and intracellular trafficking in Arabidopsis. Plant physiology **167:** 1361-1373

Korshunova YO, Eide D, Clark WG, Guerinot ML, Pakrasi HB (1999) The IRT1 protein from *Arabidopsis thaliana* is a metal transporter with a broad substrate range. Plant Mol Biol **40:** 37-44

Kotzer AM, Brandizzi F, Neumann U, Paris N, Moore I, Hawes C (2004) AtRabF2b (Ara7) acts on the vacuolar trafficking pathway in tobacco leaf epidermal cells. Journal of Cell Science **117:** 6377-6389

Lee GJ, Sohn EJ, Lee MH, Hwang I (2004) The Arabidopsis rab5 homologs rha1 and ara7 localize to the prevacuolar compartment. Plant Cell Physiol **45:** 1211-1220

Li W, Feng Y, Hao C, Guo X, Cui Y, He M, He X (2007) The BLOC Interactomes Form a Network in Endosomal Transport. Journal of Genetics and Genomics **34:** 669-682

Long TA, Tsukagoshi H, Busch W, Lahner B, Salt DE, Benfey PN (2010) The bHLH transcription factor POPEYE regulates response to iron deficiency in Arabidopsis roots. The Plant cell **22:** 2219-2236

Martín-Barranco A, Spielmann J, Dubeaux G, Vert G, Zelazny E (2020) Dynamic Control of the High-Affinity Iron Uptake Complex in Root Epidermal Cells1. Plant Physiology **184:** 1236-1250

Matthus E, Wilkins KA, Davies JM (2019) Iron availability modulates the *Arabidopsis thaliana* root calcium signature evoked by exogenous ATP. Plant Signaling & Behavior **14:** 1640563

Mayer U, Herzog U, Berger F, Inzé D, Jürgens G (1999) Mutations in the PILZ group genes disrupt the microtubule cytoskeleton and uncouple cell cycle progression from cell division in Arabidopsis embryo and endosperm. European Journal of Cell Biology **78:** 100-108

McElver J, Patton D, Rumbaugh M, Liu C-m, Yang LJ, Meinke D (2000) The TITAN5 Gene of Arabidopsis Encodes a Protein Related to the ADP Ribosylation Factor Family of GTP Binding Proteins. The Plant Cell **12:** 1379-1392

McElver J, Tzafrir I, Aux G, Rogers R, Ashby C, Smith K, Thomas C, Schetter A, Zhou Q, Cushman MA, Tossberg J, Nickle T, Levin JZ, Law M, Meinke D, Patton D (2001) Insertional Mutagenesis of Genes Required for Seed Development in *Arabidopsis thaliana*. Genetics **159:** 1751-1763

Memon AR (2004) The role of ADP-ribosylation factor and SAR1 in vesicular trafficking in plants. Biochim Biophys Acta **1664:** 9-30

Mori R, Toda T (2013) The dual role of fission yeast Tbc1/cofactor C orchestrates microtubule homeostasis in tubulin folding and acts as a GAP for GTPase Alp41/Arl2. Molecular biology of the cell **24:** 1713-S1718

Mori R, Toda T (2013) The dual role of fission yeast Tbc1/cofactor C orchestrates microtubule homeostasis in tubulin folding and acts as a GAP for GTPase Alp41/Arl2. Mol Biol Cell **24:** 1713-1724, s1711-1718

Naranjo-Arcos MA, Maurer F, Meiser J, Pateyron S, Fink-Straube C, Bauer P (2017) Dissection of iron signaling and iron accumulation by overexpression of subgroup Ib bHLH039 protein. Scientific Reports **7:** 10911

Nelson BK, Cai X, Nebenführ A (2007) A multicolored set of *in vivo* organelle markers for co-localization studies in Arabidopsis and other plants. The Plant Journal **51:** 1126-1136

Nielsen E (2020) The Small GTPase Superfamily in Plants: A Conserved Regulatory Module with Novel Functions. Annual Review of Plant Biology **71:** 247-272

Nithianantham S, Le S, Seto E, Jia W, Leary J, Corbett KD, Moore JK, Al-Bassam J (2015) Tubulin cofactors and Arl2 are cage-like chaperones that regulate the soluble αβ-tubulin pool for microtubule dynamics. eLife **4:** e08811

Peter BJ, Kent HM, Mills IG, Vallis Y, Butler PJ, Evans PR, McMahon HT (2004) BAR domains as sensors of membrane curvature: the amphiphysin BAR structure. Science **303:** 495-499

Pourcher M, Santambrogio M, Thazar N, Thierry A-M, Fobis-Loisy I, Miège C, Jaillais Y, Gaude T (2010) Analyses of sorting nexins reveal distinct retromer-subcomplex functions in development and protein sorting in *Arabidopsis thaliana*. The Plant cell **22:** 3980-3991

Radcliffe PA, Vardy L, Toda T (2000) A conserved small GTP-binding protein Alp41 is essential for the cofactor-dependent biogenesis of microtubules in fission yeast. FEBS Letters **468:** 84-88

Raposo G, Marks MS, Cutler DF (2007) Lysosome-related organelles: driving post-Golgi compartments into specialisation. Current Opinion in Cell Biology **19:** 394-401

Ritzenthaler C, Nebenführ A, Movafeghi A, Stussi-Garaud C, Behnia L, Pimpl P, Staehelin LA, Robinson DG (2002) Reevaluation of the effects of brefeldin A on plant cells using tobacco Bright Yellow 2 cells expressing Golgi-targeted green fluorescent protein and COPI antisera. The Plant cell **14:** 237-261

Robinson NJ, Procter CM, Connolly EL, Guerinot ML (1999) A ferric-chelate reductase for iron uptake from soils. Nature **397:** 694-697

Rodriguez L, Gonzalez-Guzman M, Diaz M, Rodrigues A, Izquierdo-Garcia AC, Peirats-Llobet M, Fernandez MA, Antoni R, Fernandez D, Marquez JA, Mulet JM, Albert A, Rodriguez PL (2014) C2-domain abscisic acid-related proteins mediate the interaction of PYR/PYL/RCAR abscisic acid receptors with the plasma membrane and regulate abscisic acid sensitivity in Arabidopsis. Plant Cell **26:** 4802-4820

Rogers EE, Eide DJ, Guerinot ML (2000) Altered selectivity in an Arabidopsis metal transporter. Proceedings of the National Academy of Sciences **97:** 12356-12360

Römheld V, Marschner H (1986) Evidence for a specific uptake system for iron phytosiderophores in roots of grasses. Plant physiology **80:** 175-180

Santi S, Schmidt W (2009) Dissecting iron deficiency-induced proton extrusion in Arabidopsis roots. New Phytologist **183:** 1072-1084

Schneider CA, Rasband WS, Eliceiri KW (2012) NIH Image to ImageJ: 25 years of image analysis. Nature Methods **9:** 671-675

Schuler M (2011) The role of nicotianamine in the metal homeostasis of *Arabidopsis thaliana*. Dissertation. Universität des Saarlandes

Schwarz B, Bauer P (2020) FIT, a regulatory hub for iron deficiency and stress signaling in roots, and FIT-dependent and -independent gene signatures. Journal of Experimental Botany **71:** 1694-1705

Sharer JD, Kahn RA (1999) The ARF-like 2 (ARL2)-binding protein, BART. Purification, cloning, and initial characterization. J Biol Chem **274:** 27553-27561

Sharer JD, Shern JF, Van Valkenburgh H, Wallace DC, Kahn RA (2002) ARL2 and BART Enter Mitochondria and Bind the Adenine Nucleotide Transporter. Molecular Biology of the Cell **13:** 71-83

Shin L-J, Lo J-C, Chen G-H, Callis J, Fu H, Yeh K-C (2013) IRT1 degradation factor1, a ring E3 ubiquitin ligase, regulates the degradation of iron-regulated transporter1 in Arabidopsis. The Plant cell **25:** 3039-3051

Sohn EJ, Kim ES, Zhao M, Kim SJ, Kim H, Kim YW, Lee YJ, Hillmer S, Sohn U, Jiang L, Hwang I (2003) Rha1, an Arabidopsis Rab5 homolog, plays a critical role in the vacuolar trafficking of soluble cargo proteins. Plant Cell **15:** 1057-1070

Stacey MG, Patel A, McClain WE, Mathieu M, Remley M, Rogers EE, Gassmann W, Blevins DG, Stacey G (2008) The Arabidopsis AtOPT3 protein functions in metal homeostasis and movement of iron to developing seeds. Plant physiology **146:** 589-601

Steinmann T, Geldner N, Grebe M, Mangold S, Jackson CL, Paris S, Gälweiler L, Palme K, Jürgens G (1999) Coordinated polar localization of auxin efflux carrier PIN1 by GNOM ARF GEF. Science **286:** 316-318

Stierhof YD, El Kasmi F (2010) Strategies to improve the antigenicity, ultrastructure preservation and visibility of trafficking compartments in Arabidopsis tissue. Eur J Cell Biol **89:** 285-297

Sztul E, Chen P-W, Casanova JE, Cherfils J, Dacks JB, Lambright DG, Lee F-JS, Randazzo PA, Santy LC, Schürmann A, Wilhelmi I, Yohe ME, Kahn RA (2019) ARF GTPases and their GEFs and GAPs: concepts and challenges. Molecular biology of the cell **30:** 1249-1271

Takano J, Tanaka M, Toyoda A, Miwa K, Kasai K, Fuji K, Onouchi H, Naito S, Fujiwara T (2010) Polar localization and degradation of Arabidopsis boron transporters through distinct trafficking pathways. Proc Natl Acad Sci U S A **107:** 5220-5225

Tanaka H, Kitakura S, De Rycke R, De Groodt R, Friml J (2009) Fluorescence imaging-based screen identifies ARF GEF component of early endosomal trafficking. Curr Biol **19:** 391-397

Tanaka H, Nodzyński T, Kitakura S, Feraru MI, Sasabe M, Ishikawa T, Kleine-Vehn J, Kakimoto T, Friml J (2014) BEX1/ARF1A1C is Required for BFA-Sensitive Recycling of PIN Auxin Transporters and Auxin-Mediated Development in Arabidopsis. Plant and Cell Physiology **55:** 737-749

Tian Q, Zhang X, Yang A, Wang T, Zhang W-H (2016) CIPK23 is involved in iron acquisition of Arabidopsis by affecting ferric chelate reductase activity. Plant Science **246:** 70-79

Tzafrir I, McElver JA, Liu Cm C-m, Yang LJ, Wu JQ, Martinez A, Patton DA, Meinke DW (2002) Diversity of TITAN functions in Arabidopsis seed development. Plant physiology **128:** 38-51

Ueda T, Yamaguchi M, Uchimiya H, Nakano A (2001) Ara6, a plant-unique novel type Rab GTPase, functions in the endocytic pathway of *Arabidopsis thaliana*. The EMBO Journal **20:** 4730-4741

Valencia JP, Goodman K, Otegui MS (2016) Endocytosis and Endosomal Trafficking in Plants. Annual Review of Plant Biology **67:** 309-335

Vernoud V, Horton AC, Yang Z, Nielsen E (2003) Analysis of the small GTPase gene superfamily of Arabidopsis. Plant Physiol **131:** 1191-1208

Vert G, Grotz N, Dédaldéchamp F, Gaymard F, Guerinot ML, Briat J-F, Curie C (2002) IRT1, an Arabidopsis Transporter Essential for Iron Uptake from the Soil and for Plant Growth. The Plant Cell **14:** 1223-1233

Wang HY, Klatte M, Jakoby M, Bäumlein H, Weisshaar B, Bauer P (2007) Iron deficiency-mediated stress regulation of four subgroup Ib BHLH genes in *Arabidopsis thaliana*. Planta **226:** 897-908

Wang J, Cai Y, Miao Y, Lam SK, Jiang L (2009) Wortmannin induces homotypic fusion of plant prevacuolar compartments*. Journal of Experimental Botany **60:** 3075-3083

Wang N, Cui Y, Liu Y, Fan H, Du J, Huang Z, Yuan Y, Wu H, Ling H-Q (2013) Requirement and Functional Redundancy of Ib Subgroup bHLH Proteins for Iron Deficiency Responses and Uptake in *Arabidopsis thaliana*. Molecular Plant **6:** 503-513

Wang Y, Liu F, Ren Y, Wang Y, Liu X, Long W, Wang D, Zhu J, Zhu X, Jing R, Wu M, Hao Y, Jiang L, Wang C, Wang H, Bao Y, Wan J (2016) GOLGI TRANSPORT 1B Regulates Protein Export from the Endoplasmic Reticulum in Rice Endosperm Cells. The Plant Cell **28:** 2850-2865

Yoshinari A, Toda Y, Takano J (2021) GNOM-dependent endocytosis maintains polar localisation of the borate exporter BOR1 in Arabidopsis. Biology of the Cell **113:** 264-269

Yuan Y, Wu H, Wang N, Li J, Zhao W, Du J, Wang D, Ling H-Q (2008) FIT interacts with AtbHLH38 and AtbHLH39 in regulating iron uptake gene expression for iron homeostasis in Arabidopsis. Cell Research **18:** 385-397

Zhai Z, Gayomba SR, Jung H-i, Vimalakumari NK, Piñeros M, Craft E, Rutzke MA, Danku J, Lahner B, Punshon T, Guerinot ML, Salt DE, Kochian LV, Vatamaniuk OK (2014) OPT3 Is a Phloem-Specific Iron Transporter That Is Essential for Systemic Iron Signaling and Redistribution of Iron and Cadmium in Arabidopsis The Plant Cell **26:** 2249-2264

Zhang J, Liu B, Li M, Feng D, Jin H, Wang P, Liu J, Xiong F, Wang J, Wang H-B (2015) The bHLH Transcription Factor bHLH104 Interacts with IAA-LEUCINE RESISTANT3 and Modulates Iron Homeostasis in Arabidopsis. The Plant Cell **27:** 787-805

Supplemental Figures and Table

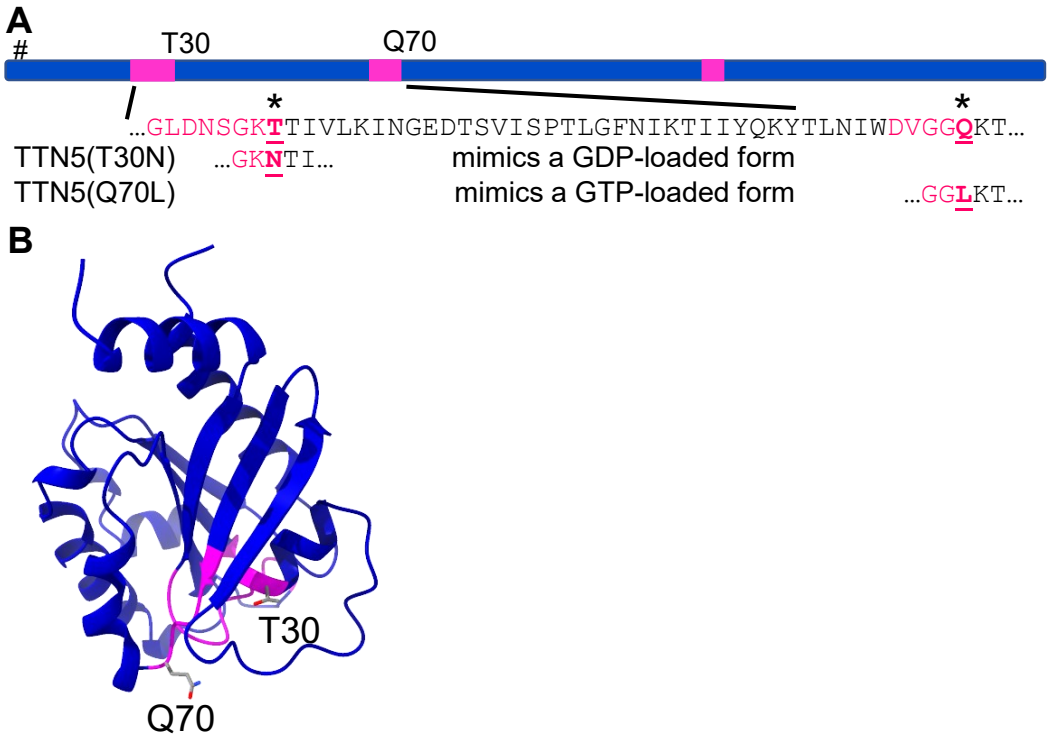

Supplemental Figure 1. TTN5 can switch between an inactive and active conformation.
(A), Schematic structure of TTN5 with highlighted GTP-binding pocket in magenta. Introduced point mutations to mimic an inactive (T30N) or active (Q70L) conformation are shown with the corresponding sequence part and are indicated with asterisks. Conserved Gly2 is marked by pound. AlphaFold (Jumper et al., 2021) structure prediction of TTN5 (Q9ZPX1) (B). GTP-binding pocket is highlighted in magenta and conserved amino acids, mutagenized for the GTPase variants are shown in sticks. Adaptation were done with UCSF ChimeraX 1.2.5 (Goddard et al., 2018).

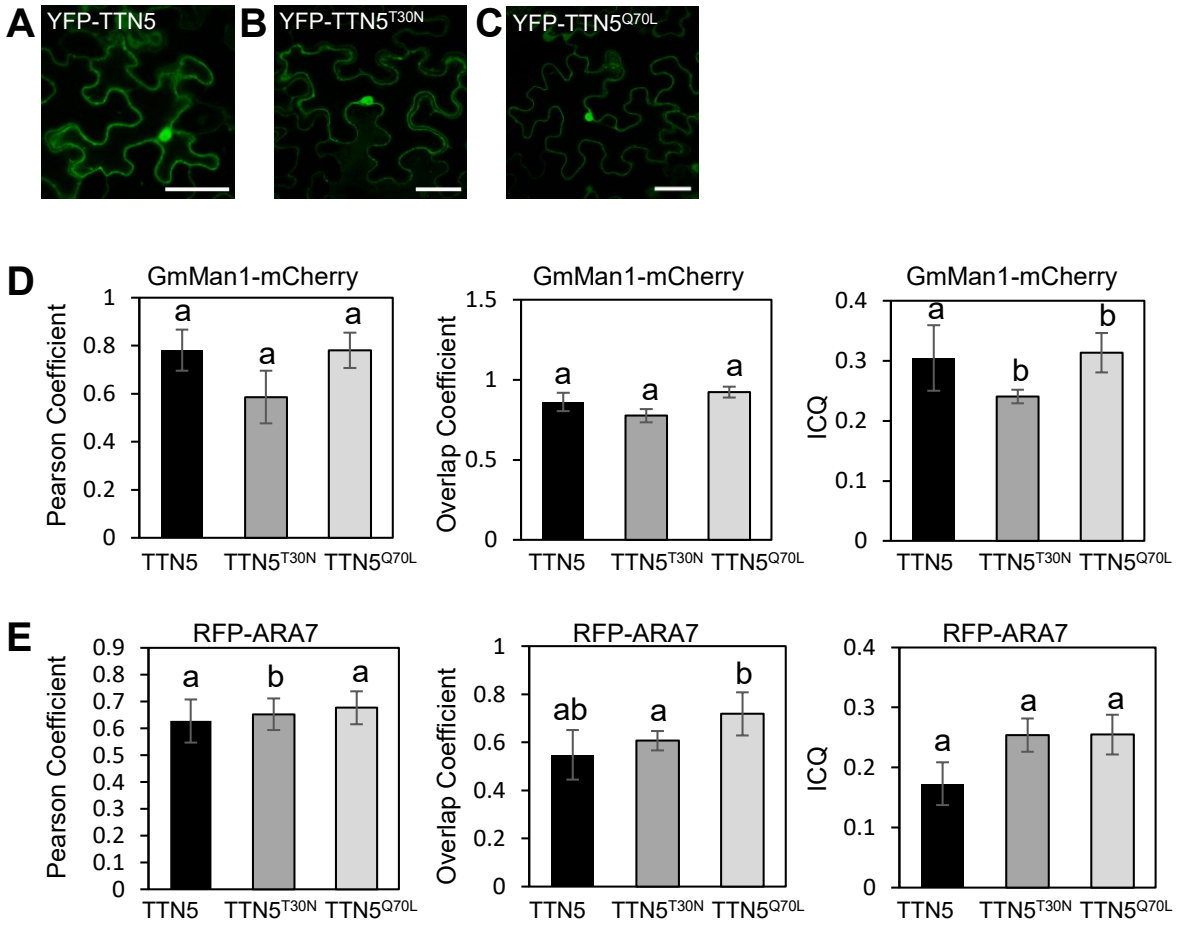

F

Channel		Colocalization	
GFP/YFP	mRFP/mCh	GFP/mRFP	mRFP/GFP
YFP-TTN5	GmMan1-mCherry	23.85±22.77	42.62±21.85
YFP-TTN5^{T30N}	GmMan1-mCherry	15.83±10.21	31.25±14.88
YFP-TTN5^{Q70L}	GmMan1-mCherry	14.81±6.79	47.82±35.04
YFP-TTN5	mRFP-ARA7	58.75±15.69	28.94±11.96
YFP-TTN5^{T30N}	mRFP-ARA7	51.79±8.12	21.21±11.76
YFP-TTN5^{Q70L}	mRFP-ARA7	64.90±6.15	75.05±10.66

Supplemental Figure 2. TTN5 is localized in the nucleus and close to the PM.
(A-C), YFP-TTN5 expression in *N. benthamiana* leaf epidermal cells. TTN5 and its two mutant variants are present in nucleus and cytoplasm and or in close proximity to the PM. Scale bar 50 µm. (B-D), JACoP-based colocalization analysis (Bolte and Cordelières, 2006). (B, C), Comparison of Pearson's and Overlap coefficients and Li's intensity correlation quotient (ICQ) for GmMan1-mCherry and RFP-ARA7 with the three mCherry-TTN5 variants in vesicle-like structures was done. (D), Object-based analysis was performed for spotted-structures based on distance between geometrical centers of signals. Analyses were conducted in three replicates each (n=3). One-way ANOVA with Fisher-LSD post-hoc test was performed. Different letters indicate statistical significance ($p < 0.05$).

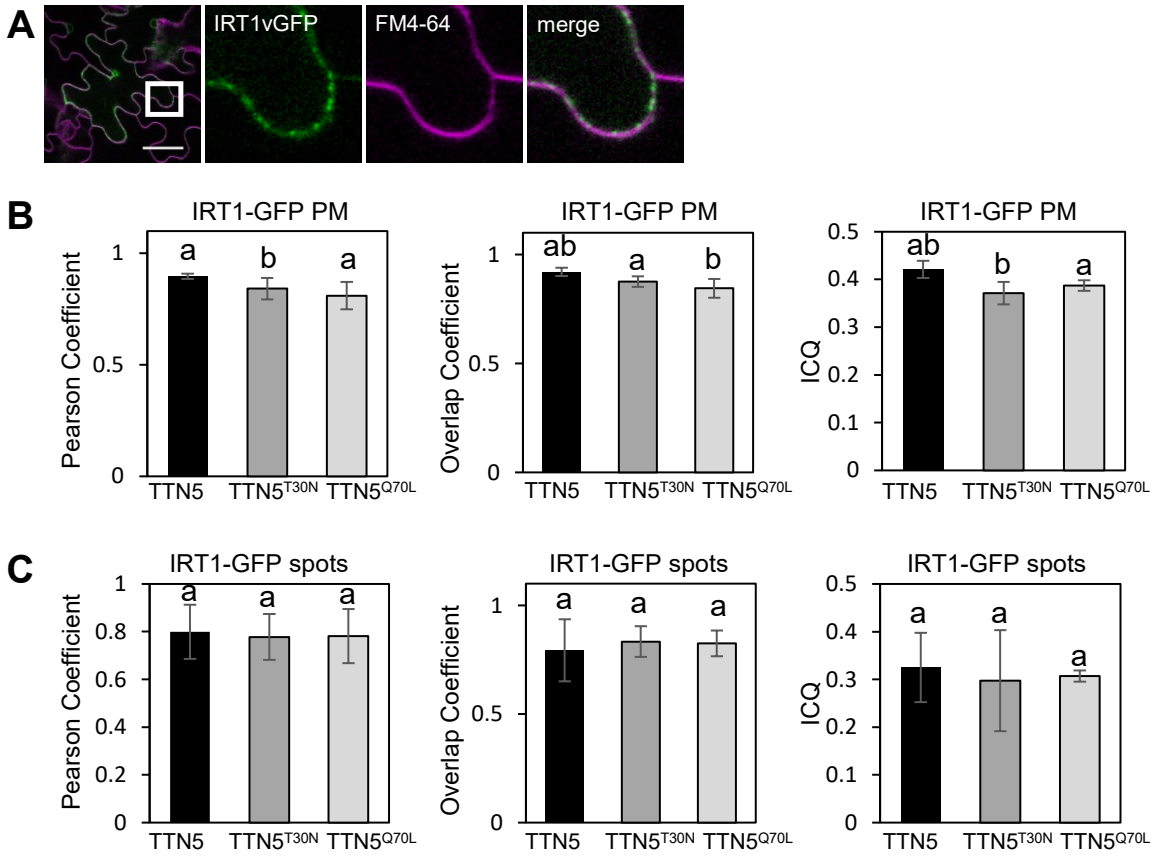

D

Channel		Colocalization spots	
GFP/YFP	mRFP/mCh	GFP/mRFP	mRFP/GFP
IRT1-GFP	mCh-TTN5	64.10±25.58	41.13±28.78
IRT1-GFP	mCh-TTN5^{T30N}	54.44±30.81	36.65±8.25
IRT1-GFP	mCh-TTN5^{Q70L}	82.59±12.71	36.34±9.66

Supplemental Figure 3. IRT1 colocalizes with FM4-64 at the PM.
(A), Plasma membrane dye FM4-64 confirmed IRT1-GFP expression at the PM. IRT1 is expressed in a spotted structure, indicating regions of higher transporter accumulation. Scale bar 50 µm. (B-D), JACoP-based colocalization analysis (Bolte and Cordelières, 2006). (B, C), Comparison of Pearson's and Overlap coefficients and Li's intensity correlation quotient (ICQ) for IRT1-GFP with the three mCherry-TTN5 variants at the PM and in vesicle-like structures was done. (D), Object-based analysis was performed for spotted-structures based on distance between geometrical centers of signals. Analyses were conducted in three replicates each (n=3). One-way ANOVA with Fisher-LSD post-hoc test was performed. Different letters indicate statistical significance ($p < 0.05$).

Supplemental Table 1. Primers used in this study.

Primer name	Primer sequence	Purpose	Origin
T5T30Nf	GATAATTCTGGGAAGAACACGATTG TTCTGAAA	Cloning of TTN5$^{T30N\ st\ CDS}$	this study
T5T30Nr	TTTCAGAACAATCGTGTTCTTCCCAG AATTATC	Cloning of TTN5$^{T30N\ st\ CDS}$	this study
TQ70Lf	TGGGATGTTGGTGGGCTAAAGACTAT AAGATCG	Cloning of TTN5$^{Q70L\ st\ CDS}$	this study
T5Q70Lr	CGATCTTATAGTCTTTAGCCCACCAA CATCCCA	Cloning of TTN5$^{Q70L\ st\ CDS}$	this study

TITAN5 nter B1	ggggacaagtttgtacaaaaaagcaggctttATGG GACTGTTAAGCATAA	Cloning of pDONR207:TTN5 st, pDONR221-P1P4 st and TTN5 RT-qPCR mass standard	this study
TITAN5 stop B2	ggggaccactttgtacaagaaagctgggtTTAGTC AAGCATG TAAATC	Cloning of pDONR207:TTN5 st and TTN5 RT-qPCR mass standard	this study
TITAN5 stop B4	ggggacaactttgtatagaaaagttgggtTTAGTCA AGCATGTAAATC	Cloning of pDONR221-P1P4:TTN5 st	this study
TITAN5 B1	ggggacaagtttgtacaaaaaagcaggctATGGGA CTGTTAAGCATAA	Cloning of pDONR207:TTN5s ns	this study
TITAN5 ns B2	ggggaccactttgtacaagaaagctgggttGTCAAG CATGTAAATCCTG	Cloning of pDONR207:TTN5s ns	this study
TTN5 intron1 fwd	CGTACATTATCATGTTGTGCT	Verification of *ttn5-1* T-DNA insertion	this study
pDAP101 LB1	GCCTTTTCAGAAATGGATAAATAGCCTT GCTTCC	Verification of *ttn5-1* T-DNA insertion	McElver et al., 2001
mCherry B1	ggggacaagtttgtacaaaaaagcaggctATGGTGA GCAAGGGCGAGGA	Cloning of pDONR207:mCherry-TTN5s st	this study
mCh to TTN5	cgagctgtacaagttaattaacATGGGACTGTTAA GCATAATCC	Cloning of pDONR207:mCherry-TTN5s st	this study
mCh R ns BIND	GTTAATTAACTTGTACAGCTCG	Cloning of pDONR207:mCherry-TTN5s st	this study
GFP B1	ggggacaagtttgtacaaaaaagcaggctATGAGTA AAGGAGAAGAACT	Cloning of pDONR207:GFP-TTN5s st	this study
GFP to TTN5	tggcatggatgaactatacaaaATGGGACTGTTAA GCATAATCC	Cloning of pDONR207:GFP-TTN5s st	this study
GFP R ns BIND	TTTGTATAGTTCATCCATGCCA	Cloning of pDONR207:GFP-TTN5s st	this study
TTN5 RT 5'	CGTGTATGCGCTGCAAC	TTN5 RT-qPCR	this study
TTN5 RT 3'	GCTAGCTGGTTCATCTTTG	TTN5 RT-qPCR	this study
I1Ln-terB1	ggggacaagtttgtacaaaaaagcaggctttTCCATG GCCACGAGCCTATA	Cloning of pDONR207:IRT1vr st	Khan et al., 2019
I1Ln-terB3	ggggacaactttgtataataaagttgtaTCCATGGCC ACGAGCCTATA	Cloning of pDONR221-P3P2:IRT1vr st	Khan et al., 2019
I1LB2	ggggaccactttgtacaagaaagctgggtTTATCGGT ATCGCAAGAGCTGTG	Cloning of pDONR207:IRT1vr st and pDONR221-P3P2:IRT1vr st	Khan et al., 2019
I1LB1	ggggacaagtttgtacaaaaaagcaggctTCCATGG CCACGAGCCTATA	Cloning of pDONR207:IRT1vr ns	Khan et al., 2019
I1LnsB2	GGGGACCACTTTGTACAAGAAAGCTGGG TTtcggtat	Cloning of pDONR207:IRT1vr ns	Khan et al., 2019
AtIRT1-temp-5'(898)	TAGCCATTGACTCCATGGC	IRT1 RT-qPCR mass standard	Klatte et al., 2008
AtIRT1-temp-3'(1910)	AGAAAACTATGAATCGTGGGG	IRT1 RT-qPCR mass standard	Klatte et al., 2008
AtIRT1-c-5'new	AAGCTTTGATCACGGTTGG	IRT1 RT-qPCR	Wang et al., 2007
AtIRT1-c-3' (1622)	TTAGGTCCCATGAACTCCG	IRT1 RT-qPCR	Wang et al., 2007
EHB1 n-ter B3	ggggacaactttgtataataaagttgtaATGGAGAAA	Cloning of pDONR221-P3P2:EHB1 st and EHB1 RT-qPCR mass standard	Khan et al., 2019
EHB1 stop B2	ggggaccactttgtacaagaaagctgggtTCAGAGTC CACTACCACCTGGAT	Cloning of pDONR221-P3P2:EHB1 st and EHB1 RT-qPCR mass standard	Khan et al., 2019
EHB1 B1	ggggacaagtttgtacaaaaaagcaggctATGGAGAA AACAGAGGAAGAG	Cloning of pDONR207:EHB1 ns	Khan et al., 2019

EHB1 nsB2	ggggaccactttgtacaagaaagctgggttGAGTCCACTACCACCTGGAT	Cloning of pDONR207:EHB1 ns	Khan et al., 2019
EHB1-sig nter B3	ggggacaactttgtataataaagttgtaGATATGAAACCGTTCCTAGACG	Cloning of pDONR221-P3P2:EHB1sig ns	Khan et al., 2019
EHB1-sig ns B2	ggggaccactttgtacaagaaagctgggttATTATCGGAGACGATTAT	Cloning of pDONR221-P3P2:EHB1sig ns	Khan et al., 2019
EHB1 RT1	GCTTGTCTGAAGATAGCATA	EHB1 RT-qPCR	Khan et al., 2019
EHB1 RT2	CGCATTCGACATTCTTCAACAG	EHB1 RT-qPCR	Khan et al., 2019
SNX1 B3	ggggacaactttgtataataaagttgATGGAGAGCACGGAGCAGC	Cloning of pDONR221-P3P2:SNX1 ns and pDONR221-P3P2:SNX1PX ns	Ivanov et al., 2014
SNX1 ns B2	ggggaccactttgtacaagaaagctgggttGACAGAATAAGAAGCTTCAAG	Cloning of pDONR221-P3P2:SNX1 ns and pDONR221-P3P2:SNX1BAR ns	Ivanov et al., 2014
PXSNX1 rev	ggggaccactttgtacaagaaagctgggtTACTAGTTTC	Cloning of pDONR221-P3P2:SNX1PX ns	this study
BARSNX1 fwd	ggggacaactttgtataataaagttgATGATATTCAAGA	Cloning of pDONR221-P3P2:SNX1BAR ns	this study
SNX1F-Std	AGGGCATTTTCATTCCTCCT	SNX1 RT-qPCR	Ivanov et al., 2014
SNX1R-Std	GGGAAGAAGGGATCTCCAAG	SNX1 RT-qPCR	Ivanov et al., 2014
SNX1F-RT	AAGTGAGGAAGCCACGAGAA	SNX1 RT-qPCR mass standard	Ivanov et al., 2014
SNX1-R-RT	GAGCTTGTCCTTTCGCAAAC	SNX1 RT-qPCR mass standard	Ivanov et al., 2014
STD-EF1Balpha2-5'	GCTGCTAAGAAGGACACCAAG	EF1Balpha (genomic) RT-qPCR mass standard	Bauer et al., 2016
STD-EF1Balpha2-3'	TGTTCTGTCCCTACTGGATCC	EF1Balpha (genomic) RT-qPCR mass standard	Bauer et al., 2016
AtEF-gen-5	TCCGAACAATACCAGAACTACG	EF1Balpha (genomic) RT-qPCR	Wang et al., 2007
AtEF-gen-3	CCGGGACATATGGAGGTAAG	EF1Balpha (genomic) RT-qPCR	Wang et al., 2007
EFc-5'	TATGGGATCAAGAAACTCACAAT	EF1Balpha RT-qPCR	Bauer et al., 2016
EFc-3'	CTGGATGTACTCGTTGTTAGGC	EF1Balpha RT-qPCR	Wang et al., 2007
STD-BHLH039-5'	AACCAAAGCAGCTTCCAAG	BHLH39 RT-qPCR mass standard	Naranjo Arcos et al., 2017
STD-BHLH039-3'	CGAAGAGAAAAAGGACGACA	BHLH39 RT-qPCR mass standard	Naranjo Arcos et al., 2017
bHLH039-RT 5'	GACGGTTTCTCGAAGCTTG	BHLH39 RT-qPCR	Wang et al., 2007
RT 3'bHLH39	GGTGGCTGCTTAACGTAACAT	BHLH39 RT-qPCR	Wang et al., 2007
STD-FIT-5'(MN)	AAGACATGACCAAAAATGTGTGT	FIT RT-qPCR mass standard	Naranjo Arcos et al., 2017
STD-FIT-3'(MN)	TGCATCTCCAACAATGGATGC	FIT RT-qPCR mass standard	Naranjo Arcos et al., 2017
FIT F (g166-187)	CCCTGTTTCATAGACGAGAACC	FIT RT-qPCR	Naranjo Arcos et al., 2017
RT-FIT-3'(MN)	ATCCTTCATACGCCCTCTCC	FIT RT-qPCR	Bauer et al., 2016
AtFRO2-temp-5'(3110)	CCATGCTCGATCTTGTCTTG	FRO2 RT-qPCR mass standard	Bauer et al., 2016

AtFRO2-temp-3'(4105)	ATTCCGGAACTTTTGAAAGG	FRO2 RT-qPCR mass standard	Bauer et al., 2016
FRO2-c5-RT5'	CTTGGTCATCTCCGTGAGC	FRO2 RT-qPCR	Wang et al., 2007
FRO2-c3-RT3'	AAGATGTTGGAGATGGACGG	FRO2 RT-qPCR	Wang et al., 2007
FRO3_stn fw	AATCAGATCGACCACCTTGC	FRO3 RT-qPCR mass standard	Schwarz et al., unpublished
FRO3_stn rev	TTCTTTTGGTGAGAAGATTTTGG	FRO3 RT-qPCR mass standard	Schwarz et al., unpublished
FRO3_qPCR fw	ATCGACCACCTTGCTGTTTC	FRO3 RT-qPCR	Schwarz et al., unpublished
FRO3_qPCR rev	TTATCCCACTGCCTCCACTC	FRO3 RT-qPCR	Schwarz et al., unpublished
NRAMP1 STD fwd	GGACGGTCTAATTCATTTC	NRAMP1 RT-qPCR mass standard	-
NRAMP1 STD rev	GACCAGAAGCAAGAAGCG	NRAMP1 RT-qPCR mass standard	-
NRAMP1 RT 5'	TAATCTTGGTGTTGTCACAG	NRAMP1 RT-qPCR	-
NRAMP1 RT3'	TAGGACTTCTCCTGGGTC	NRAMP1 RT-qPCR	-
PYE_stn fw	ACCGAAAAGGATCAACAAGG	PYE RT-qPCR mass standard	Schwarz et al., unpublished
PYE _stn rev	CCATCAAGGCCATAACTTCC	PYE RT-qPCR mass standard	Schwarz et al., unpublished
PYE _qPCR fw	GTTCCCAGGACTTCCCATTT	PYE RT-qPCR	Schwarz et al., unpublished
PYE _qPCR rev	GTGTCTGGGGATCAGGTTGT	PYE RT-qPCR	Schwarz et al., unpublished
OPT3 STD fwd	GGTCTGCAGTGAACACCACGA	OPT3 RT-qPCR mass standard	Schuler 2011
OPT3 STD rev	CAGGGCGAAGAACAAGAGCA	OPT3 RT-qPCR mass standard	Schuler 2011
OPT3 5end RT	CCCAAACAAGAAGTGGATCCC	OPT3 RT-qPCR	Schuler 2011
OPT3 3end RT	GTGACCAACCAGCTGGCAAT	OPT3 RT-qPCR	Schuler 2011

Author contribution to Manuscript II

Inga Mohr

Designed, performed and analyzed the following experiments: BiFC assays (Figures 1B-F, 7A-E, 7G-K) Fe reductase assay (Figure 2B), Seed Fe content measurement (Figure 2C), FRET-APB measurements (Figures 1G-I, 7F), (Co) localization studies (Figure 4, 5, 6, Supplemental Figure 2, 3, Supplemental Movie 1-3). Supervised and analyzed RT-qPCR (Figure 3, 7L+M). Prepared figures and tables, wrote and edited the manuscript.

Regina Gratz, Kalina Angrand, Tzvetina Brumbarova

Performed Y2H screen (Figure 1A).

Monique Eutebach

Performed RT-qPCR.

Lara Genders, Karolin Montag, Merina Rubek Basgaran

Contributed key materials.

Petra Bauer

Conceived and supervised the study, acquired funding, edited the manuscript.

Rumen Ivanov

Conceived and supervised the study, supervised and analyzed Y2H (Figure 1A), edited the manuscript.

8. Manuscript III

Interactomics of IRT1 regulators in the iron homeostasis

Interactomics of IRT1 regulators in the iron homeostasis

Inga Mohr[1], Pichaporn Chuenban[1], Monique Eutebach[1], Claudia von der Mark[1,3], Gereon Poschmann[2], Daniel Waldera-Lupa[2], Kai Stühler[2], Petra Bauer[1,4] and Rumen Ivanov[1]

[1]Institute of Botany, Heinrich Heine University, Universitätsstr. 1, 40225 Düsseldorf, Germany.
[2]Molecular Proteomics Laboratory (MPL), Biomedical Research Center (BMFZ), Heinrich Heine University, Universitätsstr. 1, 40225 Düsseldorf, Germany.
[3]Group of Plant Vascular Development, Swiss Federal Institute of Technology (ETH) Zurich, 8092 Zurich, Switzerland
[4]Cluster of Excellence on Plant Science (CEPLAS), Heinrich Heine University, 40225 Düsseldorf, Germany

Author contributions: P.B. and R.I. conceived the project; I.M., G.P., D.W.-L., K.S., P.B. and R.I. designed experiments and supervised the research; I.M., P.C., M.E., G.P. and D.W.-L. performed experiments and analyzed data; C.vdM. contributed key materials; I.M. wrote the manuscript; I.M., G.P., K.S., P.B. and R.I. edited the manuscript; P.B. acquired funding. P.B. and R.I. agreed to serve as the author responsible for contact and communication.

Highlights

- The H^+-ATPases AHA1 and AHA2 are novel interactors of small ARF-like GTPase TTN5
- TTN5 is a potential link in membrane protein trafficking
- Fe-related EHB1 and IDI1 interactome data reveal involvement in coumarin synthesis, Fe chelation and transport
- Link to prevention of Fe-induced lipid peroxidation by PATL2 interactome

Abstract

Identification of protein-protein interactions by immunoprecipitation-mass spectrometry-based interactome analysis is gaining importance with the increasing sensitivity of spectrometers. The advantage of *in vivo* interaction studies allows the inclusion of developmental or environmental changes in the analysis. Iron homeostasis is an elaborated system containing several subnetworks from iron uptake to intracellular transport and storage to cope with plant's sessile nature, concomitant with soil iron availability and iron essential but also toxic nature. Iron acquisition is tightly transcriptionally regulated but also depends on many direct protein-protein interactions. The small ARF-like GTPase is interacting with the main iron transporter IRT1 with additional impact on expression levels of many iron-related genes. Here we identified the H^+-ATPases AHA1 and AHA2 as novel interactors of the small ARF-like GTPase TITAN 5 (TTN5). AHA1 colocalizes with TTN5 at the plasma membrane and in vesicle-

like structures, proposing a TTN5-dependent AHA1 cycling in the endomembrane system. These data imply a role in plasma membrane protein turnover by TTN5. Additional IP-MS data reveal a strong connection of the iron-related proteins EHB1, PATL2 and IDI1 to iron homeostasis. The EHB1 and IDI1 interactomes contain proteins involved in the chelation and transport of iron, whereas the PATL2 interaction network leads to a suggested function in preventing ROS-induced lipid peroxidation by α-tocopherol recruiting. The revealed conjunctions in iron-related processes within our obtained interactomes deepen our knowledge in the iron homeostasis as an elaborated network.

Abbreviations

ABA	abscisic acid
ABCG37/PDR9	ATP-BINDING CASSETTE G37/PLEIOTROPIC DRUG RESISTANCE 9
ABI	ABSCISIC ACID INSENSITIVE
AHA	Arabidopsis H^+-ATPase
ANN	ANNEXIN
ARF-like / ARL	ADP-ribosylation factor-like
BGLU	BETA-GLUCOSIDASE
bHLH	basic helix-loop-helix
BiFC	Bimolecular Fluorescence Complementation
bZIP	basic leucine zipper
CAT	CATALASE
CIPK	CBL-INTERACTING PROTEIN KINASE
CYP	CYTOCHROME P450
EHB1	ENHANCED BENDING 1
F6'H1	FERULOYL-CoA 6'-HYDROXYLASE 1
FIT	FER-LIKE IRON DEFICIENCY-INDUCED TRANSCRIPTION FACTOR
FREE1	FYVE DOMAIN PROTEIN REQUIRED FOR ENDOSOMAL SORTING 1
FRET	Förster Resonance Energy Transfer
FRO2	FERRIC REDUCTION OXIDASE 2
GAP	GTPase-activating protein
GEF	guanine nucleotide exchange factor
GLL	GDSL LIPASE-LIKE PROTEIN
H_2O_2	hydrogen peroxide
HA_3	triple Hemagglutinin
HCT	HYDROXYCINNAMOYLTRANSFERASE
IDF1	IRT1 DEGRADATION FACTOR 1
IDI1	IRON DEFICIENCY-INDUCED 1
IP	immunoprecipitation
IRT1	IRON-REGULATED TRANSPORTER 1

ISR	induced systemic resistance
K-loop	K^+-binding loop
LEA	LATE EMBRYOGENESIS ABUNDANT
MDA	malondialdehyde
MS	mass spectrometry
NA	nicotianamine
NSP	NITRILE-SPECIFIER PROTEIN
PATL2	PATELLIN 2
PBP1	PYK10 BINDING PROTEIN 1
PPI	protein-protein interaction
PYR1/PYL	PYRABACTIN RESISTANCE 1 /-LIKE
REM1.2	REMORIN1.2
ROS	reactive oxygen species
SAM	*S*-adenosylmethionine
TBARS	thiobarbituric acid reactive substances
TTN5	TITAN 5
Y2H	yeast two-hybrid

Keywords: IRT1, TTN5, EHB1, PATL2, IDI1, AHA1, AHA2, IP-MS, interactome

Introduction

Protein-protein interactions (PPIs) are key points of nearly every biological process and essential for organism development and functionality. Formed complexes or interacting proteins are involved in the cytoskeleton formation, signaling and transporting pathways, gene regulation and nearly every other process. Though many processes and their underlying PPIs are already investigated, the majority remains elusive. There exists a broad range of different methods for identifying and analyzing PPIs, such as yeast two-hybrid (Y2H) and split-ubiquitin screens, co-immunoprecipitation (co-IP) with subsequent immunoblotting, fluorescent techniques like Bimolecular Fluorescence Complementation (BiFC) or Förster Resonance Energy Transfer (FRET), or computational predictions. Disadvantages here include the use of heterologous expression systems, the limited test set of pre-selected protein combinations, or the difficulty of considering stimuli or different developmental processes. With plants as origin the production of sufficient amount of material can be challenging. With the continuous improvement of mass spectrometry (MS) it became possible to analyze small amounts of plant material by immunoprecipitation- (IP) MS, producing interactomes (Xing et al., 2016; Bontinck et al., 2018).

We study the regulation of iron (Fe) uptake into Arabidopsis root epidermis cells, accomplished by an Fe reduction-based process, named Strategy I. Four main steps are performed in Arabidopsis (Römheld and Marschner, 1986; Brumbarova et al., 2015). Soil Fe is present mostly in insoluble ferric Fe (Fe^{3+}) complexes which can be solubilized by rhizosphere acidification via H^+-ATPase 2 (AHA2) through proton extrusion (Santi and Schmidt, 2009; Brumbarova et al., 2015) and chelation by secreted coumarins. The coumarins are transported into the rhizosphere by the ABC transporter ATP-BINDING CASSETTE G37/PLEIOTROPIC DRUG RESISTANCE 9 (ABCG37/PDR9) (Fourcroy et al., 2014). The FERRIC REDUCTION OXIDASE 2 (FRO2) is reducing the soluble Fe^{3+} to ferrous Fe (Fe^{2+}) for the uptake by the IRON-REGULATED TRANSPORTER 1 (IRT1) (Eide et al., 1996; Robinson et al., 1999; Vert et al., 2002). Most of the genes encoding these factors are transcriptionally induced by a heterodimer of the basic helix-loop-helix (bHLH) FER-LIKE IRON DEFICIENCY-INDUCED TRANSCRIPTION FACTOR (FIT) with a subgroup Ib bHLH protein upon Fe deficiency (Yuan et al., 2008; Wang et al., 2013; Schwarz and Bauer, 2020).

One of the most robustly induced genes upon Fe deficiency is the Kelch repeat protein AT3G07720, here called IRON DEFICIENCY-INDUCED 1 (IDI1) with high similarity to NITRILE-SPECIFIER PROTEINS (NSP) (Burow et al., 2008; Ivanov et al., 2012). NSPs can interact with myrosinases, β-glucosidases, in the pathogen defense response, by producing isothiocyanates or nitrile via glucosinolate hydrolysis (Wittstock et al., 2003; Burow et al., 2008). IDI1 coexpression network involves several genes of the Fe uptake, like *IRT1* and *FRO2*, and genes related to Fe chelation like nicotianamine (NA) with nicotianamine synthases (NAS) *NAS1* and *NAS2* or coumarin synthesis by *FERULOYL-CoA 6'-HYDROXYLASE 1* (*F6'H1*) or cytochrome P450 (CYP) *CYP82C4* (Schuler et al., 2012; Schmid et al., 2014; Obayashi et al., 2017; Rajniak et al., 2018). Like nitrile, coumarins play, next to Fe chelation, an important role in the defense response in a BETA-GLUCOSIDASE 42 (BGLU42)-dependent manner (Zamioudis et al., 2014).

Next to transcriptional regulation, protein modifications and PPI-based regulations play a key role in modulating the activity of the Fe uptake process. One aspect is the constant turnover of the membrane-located proteins between the plasma membrane (PM) and the degradation pathway to the vacuole. IRT1 evolved to a model system of root cell biology, with several regulators of IRT1 activity and its trafficking route being already identified (Ivanov and Vert, 2021). IRT1 large cytosolic loop with a variable region (IRT1vr) is important for protein-protein interactions. It is composed of several potential ubiquitination and phosphorylation sites (Kerkeb et al., 2008; Barberon et al., 2011; Shin et al., 2013; Dubeaux et al., 2018). The RING E3 ubiquitin ligase, IRT1 DEGRADATION FACTOR 1 (IDF1), is responsible for IRT1

ubiquitination, leading to its endocytosis (Shin et al., 2013). Under high non-iron metal conditions, the CBL-INTERACTING PROTEIN KINASE 23 (CIPK23) phosphorylates IRT1, resulting in IDF1 recruitment to the PM and K63-polyubiquitination-dependent degradation of IRT1 in the vacuole (Dubeaux et al., 2018). IRT1 function is inhibited by the interaction with ENHANCED BENDING 1 (EHB1) at the PM (Khan et al., 2019). Positive effects on IRT1 were identified by the phosphatidylinositol-3-phosphate (PI3P)-binding protein FYVE1 / FYVE DOMAIN PROTEIN REQUIRED FOR ENDOSOMAL SORTING 1 (FREE1), as well as the sorting nexin SNX1. Both are involved in IRT1 recycling from endosomes back to the PM. PATELLIN 2 (PATL2) interacts with IRT1vr and exhibits potential negative effects on IRT1 due to its presence at the PM (Hornbergs et al., Bauer lab, unpublished). The identified interactions demonstrate the scope and diversity of IRT1 regulation. Uncovering additional branches of the IRT1 network are of great interest, as they may also involve more universal transferable aspects of PM protein control.

We recently identified the small ADP-ribosylation factor-like (ARF-like) GTPase TITAN 5 (TTN5) as an IRT1 interactor with a suggested role in IRT1 trafficking and presented a new interesting component in ARF-mediated PM protein trafficking, comparable to PIN1 transport (Mohr et al., unpublished, Manuscript II, Tanaka et al., 2014). TTN5, also named HALLIMASCH, from here on only called TTN5, was originally identified in two separate screens for abnormal-embryo mutants (Mayer et al., 1999, McElver et al., 2000). *ttn5* seeds lack proper embryo development associated with the formation of only a few giant cells containing characteristic enlarged nuclei in embryo and endosperm which results in embryo lethality, demonstrating the importance of TTN5 function (McElver et al., 2000). TTN5 sequence contains the conserved GTP-binding domains and was identified as a close homolog of human ADP-ribosylation factor-like 2 (HsARL2) based on sequence similarities (McElver et al., 2000). TTN5 molecular function has not been well described but HsARL2 is interacting with cofactor D in microtubule polymerization, a conserved interaction in various organisms such as *Caenorhabditis elegans*, *Schizosaccharomyces pombe or Saccharomyces cerevisiae* (Fleming et al., 2000; Radcliffe et al., 2000; Antoshechkin and Han, 2002; Mori and Toda, 2013). The Arabidopsis cofactor D homolog, TTN1/CHAMPIGNON, exhibits a similar loss-of-function seed embryo phenotype compared to *ttn5* with a disturbed mitotic microtubule organization (Mayer et al., 1999; Bhamidipati et al., 2000; Tzafrir et al., 2002). Next to the interaction with IRT1, we additionally identified the IRT1 regulators, EHB1 and SNX1, as TTN5 interactors, promoting a coordinating role in IRT1 regulation by TTN5. Our current knowledge emphasize the importance of PPIs in the IRT1 regulation and demonstrate the need of further interactome data to unravel the regulatory network also with regard to common PM protein cycling. We

suggested that TTN5 may have a multitude of functions within the cell, a notion supported by the lethal phenotype of the *ttn5* mutants indicating its essentiality (Mohr et al., unpublished, Manuscript II).

Interactome data of an IP-MS approach on IRT1 roots revealed a potential complex formation with FRO2 and AHA2, the three main uptake genes indicating the tight interconnection in Fe uptake (Martín-Barranco et al., 2020). AHA2 together with AHA1 is one of the most prominent members of the family of Arabidopsis H^+-ATPase (AHA) family consisting of 11 proteins in total (Haruta and Sussman, 2012; Falhof et al., 2016). These two together make up to 80 % of the total mRNA transcript and protein level of the whole family expressed in whole plant tissue (Haruta and Sussman, 2012). Nevertheless, AHA1 is active mainly in the aerial parts and AHA2, in contrast, is more active in the roots (Harper et al., 1990; Haruta et al., 2010). AHA1 and AHA2 still show functional redundancy and homozygous T-DNA insertion mutants result in embryo lethality, pointing at a combined essential function (Haruta and Sussman, 2012).

TTN5 presence at different endomembrane compartments and colocalization with IRT1 in multivesicular bodies (MVBs) revealed a new link in IRT1 trafficking, but raising the question of missing key players in IRT1 degradation and recycling pathway (Mohr et al., unpublished, Manuscript II). The peripheral membrane proteins EHB1 and PATL2 and their three-way IRT1-TTN5-EHB1 and IRT1-PATL2 connection suggest a common link in IRT1 regulation and Fe homeostasis in the endomembrane system. We suspect IDI1 function being related to the Fe deficiency response via the coumarin secretion. IDI1 NSP-similarity could lead to interaction with β-glucosidases like BGLU42 or PYK10/BGLU23 which are both involved in scopolin, a coumarin, hydrolysis. Interestingly, BGLU23 is also the main component of ER-bodies, which form unique ER structures in the class of Brassicaceae and presumably also have a function in immune defense (Nakano et al., 2014). Here, we hypothesized overlapping functions of TTN5, EHB1, PATL2, and IDI1 in Fe homeostasis, based on our current knowledge regarding their associations in IRT1 regulation and Fe uptake. We used the advantage of IP-MS to reveal PPIs and protein complexes *in vivo* in a Fe-dependent fashion in root samples. The obtained interactomes included proteins of the Fe uptake machinery, Fe chelation and distribution as well as oxidative stress responses and more. Identified overlaps in the generated interactomes promote the idea of a regulated network containing the here investigated Fe-related genes.

Results

TTN5 interactome includes a PM ATPase and a potential GEF

We recently presented the interaction of TTN5 with IRT1. TTN5 together with IRT1 was present in membrane vesicles along the IRT1 degradation route towards the vacuole or the

corresponding recycling pathway. In addition, TTN5 interacted with EHB1 and SNX1, suggesting a coordinating role of TTN5 in regulation of IRT1 recycling and Fe acquisition (Mohr et al., unpublished, Manuscript II). Our next aim was the identification of further TTN5 interaction partners to get deeper knowledge of its function. Therefore, we created transgenic lines with *TTN5* expressed under the control of the constitutive 35S promoter tagged to a triple Hemagglutinin (HA_3-TTN5). The line was able to rescue *ttn5-1* embryo lethal seed phenotype (Supplemental Figure 1). We used this line in an IP experiment and subsequent interactome analysis by MS. IP was established and finally, the simultaneously performed IP on a WT control did not lead to any HA-related signal, suggesting that HA_3-TTN5 was specifically detected and enriched by IP (Figure 1A). 60 proteins were enriched in the IP-MS procedure using HA_3-TTN5 versus WT, 17 were enriched in Fe-sufficient, and 39 in Fe-deficient samples, while four were enriched under both Fe conditions (Figure 1B). The higher amount of detected proteins in roots grown under Fe starvation can be an indicator of induced TTN5 interaction activity in response to stress. Due to our recent findings and published data on TTN5, its homologues and the ARF family, we expected the TTN5 interactome to be related to cellular compartments of the endomembrane system and involved in cytoskeleton organization especially of microtubules. We checked whether any of the TTN5 protein interactors were coexpressed in the network of *TTN5* (created with ATTED-II Supplemental Figure 2) (Obayashi et al., 2017) finding coexpressed genes involved mainly in endocytosis and the connecting trafficking activities, the spliceosome function. Indeed, the MS data revealed an enrichment of proteins involved in the function of the endomembrane system with locations ranging from the PM to the vacuole (Figure 1C). The interactome also contained other members of the RAB and ARF small GTPase families, responsible for vesicular trafficking. Next to endomembrane proteins, we identified factors related to protein turnover, such as the proteasome and chaperone complexes. A deeper look at the enriched biological functions revealed the expected connection to microtubule organization (Figure 1D). Additionally, we could identify enrichment in stress responses, such as starvation, metal ions and oxidative stress due to the lack of Fe (All GO terms present in the Supplement).

The two most promising TTN5 interaction candidates were detected under Fe-sufficient conditions in comparison to the WT control (Figure 1E). They were represented in HA_3-TTN5 samples with highest intensity ratio. The first one was H^+-ATPase 1 (AHA1) one of the two prominent PM ATPases in Arabidopsis (Haruta and Sussman, 2012). Due to the functional redundancy between AHA1 and AHA2 and the involvement of AHA2 in the response to Fe deficiency (Santi and Schmidt, 2009; Haruta and Sussman, 2012), AHA1 represented an important target for further studies. The second one was the ER-membrane protein SEC12

which exhibits a guanine nucleotide exchange factor (GEF) activity for SAR1, a member of the ARF GTPase family, involved in COPII-vesicle formation (Barlowe and Schekman, 1993; De Craene et al., 2014; Brandizzi, 2018). The significance of this interaction lies in the fact that the TTN5 GTPase regulators like GEFs and GTPase-activating proteins (GAPs) are still unknown, and SAR1 activation represents an opportunity for understanding TTN5 function. Therefore, the two newly identified TTN5 interactors, AHA1 and SEC12, represent valuable opportunities for pinpointing the molecular functions of TTN5 and its biological role in stress response signaling.

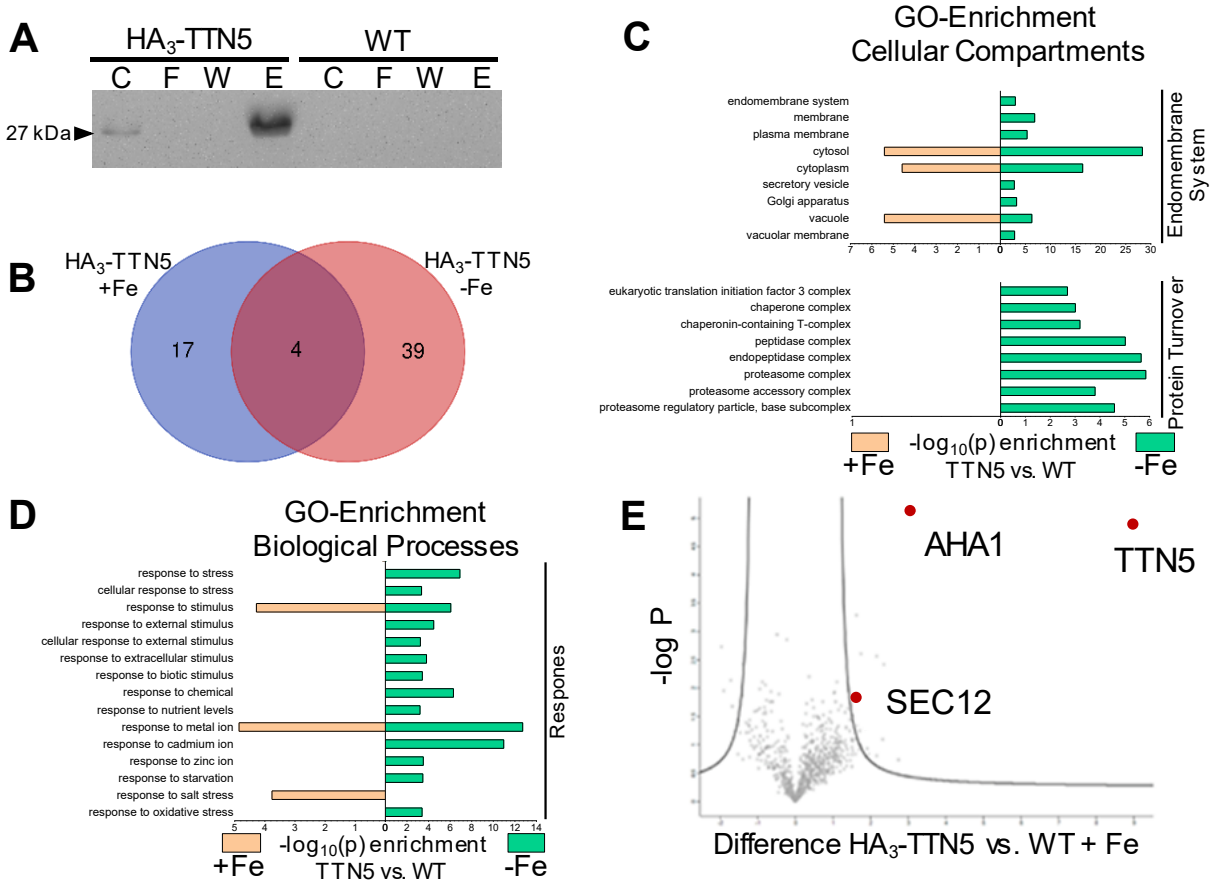

Figure 1. TTN5 interactome includes membrane proteins.
TTN5 interactome analysis carried out by immunoprecipitation (IP) with subsequent mass spectrometry (MS). IP was performed using HA_3-TTN5 roots grown under Fe-sufficient (+Fe) or -deficient (-Fe) conditions in the two-week system in comparison with WT control. (A), Immunoblot control of the performed IP. Abbreviations: C - crude extract, F - flow through, W - wash step I and E - elution sample. (B), Venn diagram (http://bioinformatics.psb.ugent.be/webtools/Venn/) of the coprecipitated proteins identified by MS. (C), GO-enrichment analysis of cellular compartments and (D), biological processes under Fe-sufficient (salmon bars) or -deficient (green bars) conditions compared to WT. (E), Volcano plot of enriched proteins in HA_3-TTN5 Fe-sufficient roots. TTN5, AHA1 and SEC12 are highlighted for better visualization. IP was performed in five biological replicates (n = 5).

H^+-ATPases, a favored TTN5 target

We were interested in potential interactome differences due to the GTPase activity state. With TTN5 as a GTPase we are able to mimic an active or inactive state by mutating specific amino acids in the GTP-binding pocket (Mohr et al., unpublished, Manuscript I and Manuscript

II, Dascher and Balch, 1994). Changing the Thr-30 to an Asn (TTN5^{T30N}) TTN5 is blocked in its GDP-loaded conformation. The GTP-loaded state is blocked by mutating Glu-70 to a Leu (TTN5^{Q70L}). Arabidopsis lines stably expressing inactive HA$_3$-TTN5^{T30N} and active HA$_3$-TTN5^{Q70L} were created and additional IP-MS was performed (Figure 2A). For the inactive GTPase, we identified 12 proteins in Fe-sufficient, 46 proteins in Fe-deficient roots und 17 proteins which were detected in both Fe conditions showing comparable amounts to the HA$_3$-TTN5 analysis (Figure 2B). In Fe-sufficient HA$_3$-TTN5^{Q70L} roots, nine proteins were identified, 65 under Fe deficiency and 22 were present in both set-ups (Figure 2C).

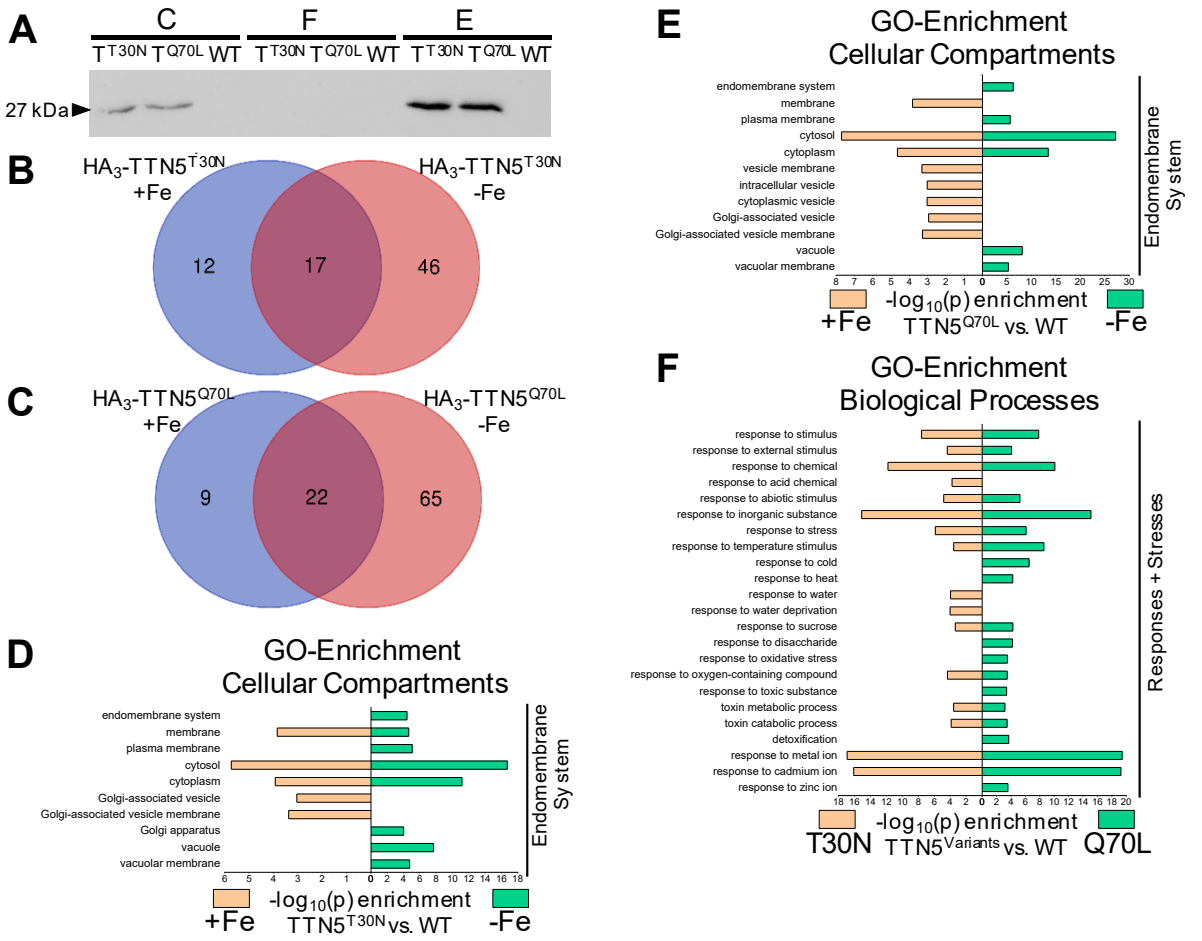

Figure 2. Interactome of GTPase activity variants.
TTN5 GTPase activity variants interactome analysis carried out by immunoprecipitation (IP) with subsequent mass spectrometry (MS). IP was performed using HA$_3$-TTN5^{T30N} and HA$_3$-TTN5^{Q70L} roots grown under Fe-sufficient (+Fe) or -deficient (-Fe) conditions in the two-week system in comparison with WT control. (A), Immunoblot control of the performed IP. Abbreviations: C - crude extract, F - flow through and E - elution sample. Venn diagrams (http://bioinformatics.psb.ugent.be/webtools/Venn/) of the coprecipitated proteins identified by MS of HA$_3$-TTN5^{T30N} (B) and HA$_3$-TTN5^{Q70L} (C) roots. (D) and (E), GO-enrichment analysis of cellular compartments in HA$_3$-TTN5^{T30N} (D) and HA$_3$-TTN5^{Q70L} (E) roots under Fe-sufficient (salmon bars) or -deficient (green bars) conditions compared to WT. (F), Comparison of GO-enrichment of biological processes of HA$_3$-TTN5^{T30N} (salmon bars) and HA$_3$-TTN5^{Q70L} (green bars) under Fe-deficient conditions compared to WT. IP was performed in five biological replicates (n = 5).

Both GTPase variants showed the same trend for more coprecipitated proteins when Fe is lacking, strengthen the idea of increasing interactions as a result of Fe stress. Interestingly,

slightly higher amounts of proteins were detected for active TTN5, consistent with published interaction data with a GTP-loaded GTPase (Sharer and Kahn, 1999; Hanzal-Bayer et al., 2002; Nie et al., 2018). This possibly reflects the different role between the GTP-loaded TTN5 and the GDP-loaded conformation in interaction-dependent cellular processes. Checking the interactomes for GO enrichments, we could identify comparable categories to unmutated TTN5, as expected. They consisted of proteins located in the endomembrane system with a connection to Golgi-associated vesicles (Figure 2D, E). We could identify RAB proteins, such as RABD2B or the clathrin vesicle coat protein CHC1. Due to the low number of proteins identified under Fe-sufficient conditions, we compared the biological function interactome enrichment of the GTPase variants in Fe deficiency (Figure 2F). Both were enriched for stress and stimuli responses as it was for the TTN5 interactome. Detected proteins were related to responses to metal ions and oxidative stress and leading to connections to detoxification processes for example the peroxidase PER16. Interestingly, we could identify AHA2 in HA_3-$TTN5^{T30N}$ roots under both Fe conditions. These findings make the H^+-ATPases strong candidates for further investigation.

TTN5 interacts with AHA1 and AHA2

To verify the identified TTN5-AHA interactions we performed Bimolecular Fluorescence Complementation (BiFC). It uses the split-YFP system with C-terminal half of the fluorescent protein fused to TTN5 and the N-terminal to AHA1. A potential interaction is hereby indicated by a complementation of the YFP. As expected based on the MS results, cYFP-TTN5 together with nYFP-AHA1 was able to complement the YFP (Figure 3A). The signal was visible only at the PM, the typical location of AHA1 as a PM ATPase. At the same time, we tested AHA2 due to its redundancy with AHA1 and its identification in the HA_3-$TTN5^{T30N}$ interactome. The combination of cYFP-TTN5 with nYFP-AHA2 led to a complementation of the fluorescence protein (Figure 3B). We tested if any preferences can be identified by testing the TTN5 variants in the BiFC set-up. In combination with nYFP-AHA1, both cYFP-$TTN5^{T30N}$ (Figure 3C) and cYFP-$TTN5^{Q70L}$ (Figure 3E) led to YFP complementation. Interestingly, only cYFP-$TTN5^{Q70L}$ with nYFP-AHA2 revealed an YFP signal (Figure 3F). The inactive TTN5 variant failed to complement the split halves (Figure 3D), this can occur due to several reasons e.g. the distance- and orientation of the fluorescent tags. For this reason, we cannot exclude from a negative BiFC result that the interaction occurs. The BiFC signals were specific, the cYFP-TTN5/nYFP-EHB1Δsig (Figure 3G) combination failed complementation as a previously investigated negative control (Mohr et al., unpublished, Manuscript II) showing the dependency of AHA1 or AHA2 for complementation. nYFP-AHA1 together with cYFP-EHB1Δsig was also

not able to complement split-YFP (Figure 3H). We confirmed the interactions and identified the two H$^+$-ATPases AHA1 and AHA2 as novel interactors of TTN5.

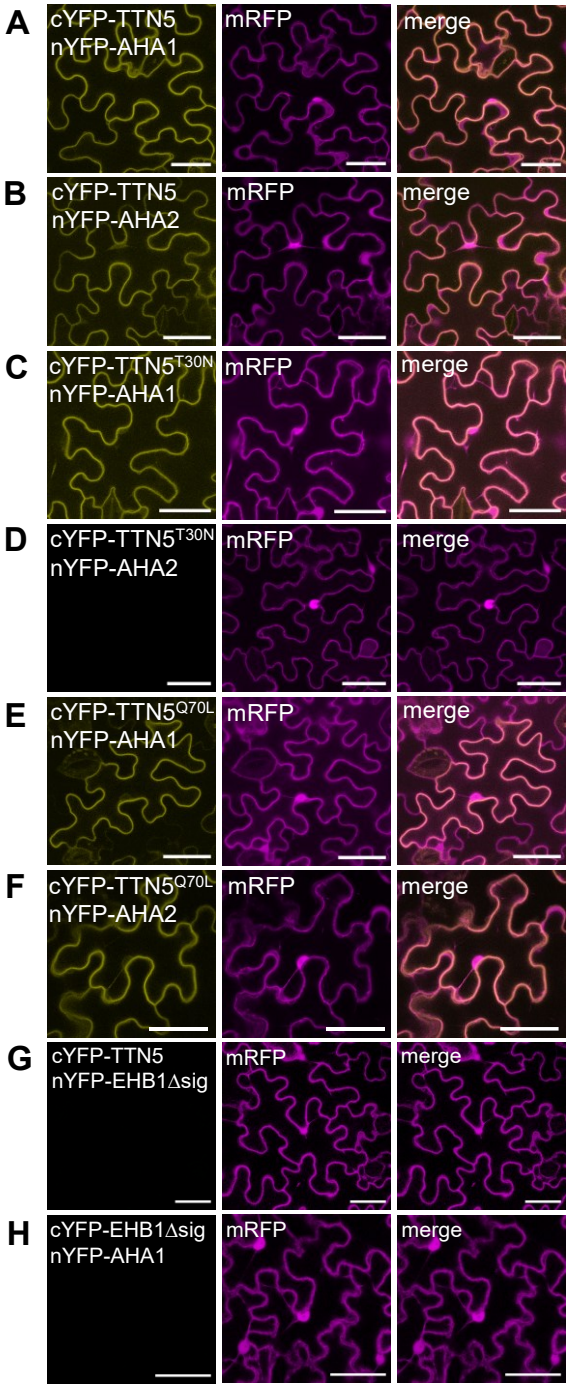

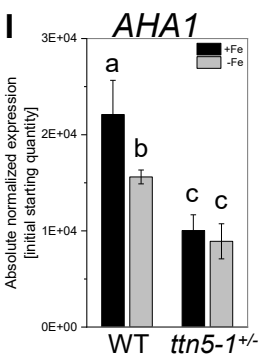

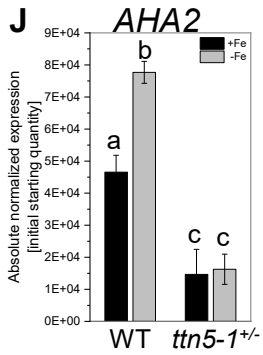

Figure 3. TTN5 interacts with PM ATPases. (A-H), Confirmation of IP-MS identified TTN5 interaction with H$^+$-ATPases AHA1 and AHA2 by BiFC in *N. benthamiana* leaf epidermal cells. C-terminal half of YFP was fused to TTN5 and the N-terminal to AHA1 or AHA2 respectively. Complemented YFP signal indicates a potential interaction. mRFP serves as a transformation control. (A), nYFP-tagged AHA1 showed complemented YFP signal with N-terminally-tagged cYFP-TTN5. (B), nYFP-tagged AHA2 showed complemented YFP signal together with cYFP-TTN5. (C) nYFP-tagged AHA1 showed complemented YFP signal with N-terminally-tagged dominant inactive cYFP-TTN5^{T30N}. (D) nYFP-tagged AHA2 and N-terminally-tagged dominant inactive cYFP-TTN5^{T30N} produced no complemented YFP signal. (E) nYFP-tagged AHA1 showed complemented YFP signal with N-terminally-tagged dominant active cYFP-TTN5^{Q70L}. (F) nYFP-tagged AHA2 showed complemented YFP signal with N-terminally-tagged dominant active cYFP-TTN5^{Q70L}. (G, H), Negative controls cYFP-TTN5 and nYFP-EHB1Δsig (G) and cYFP-EHB1Δsig and nYFP-AHA1 (H) produced no YFP signal. The YFP signals were predominantly observed at the PM. Every construct was tested a minimum of three times (n ≥ 3) with similar results. Scale bar 50 µm. (I and J), Gene expression data by RT-qPCR of *AHA1* (I) and *AHA2* (J) in *ttn5-1*$^{+/-}$ roots compared to WT. Plants were grown in the two-week system under Fe-sufficient (+Fe, black bars) or -deficient (-Fe, grey bars) conditions. Three biological replicates were tested (n = 3). One-way ANOVA with Fisher-LSD post-hoc test was performed. Different letters indicate statistical significance ($p < 0.05$).

We reported recently an effect of TTN5 on the expression of Fe acquisition genes (Mohr et al., unpublished, Manuscript II). To test whether TTN5 is not only interacting with the PM H$^+$-ATPases but also affecting their transcript levels, we checked the gene expression of both. Due to the embryonal lethality in homozygous *ttn5-1* line, we could not study the effect of full TTN5 loss of function on Fe deficiency. For this reason, we analyzed gene expression levels of the PM ATPases in heterozygous *ttn5-1* knock-out (designated *ttn5-1*$^{+/-}$) roots by RT-qPCR. *AHA1* expression (Figure 3I) was here down-

regulated under Fe-deficient conditions in WT roots whereas *AHA2* (Figure 3J) was induced as part of the Fe deficiency response (Santi and Schmidt, 2009; Ivanov et al., 2012). Interestingly, the partial lack of *TTN5* led to significant decrease in transcript levels for both *AHA1* and *AHA2* irrespective of the Fe status. The effect is similar to the reduced expression for several Fe-related genes, including *IRT1* and *FRO2* in *ttn5-1*$^{+/-}$ compared to WT (Mohr et al., unpublished, Manuscript II). Though AHA1 is not predicted to be part of Fe uptake, we suggest a positive effect of the ATPase on Fe uptake, due to functional redundancy with AHA2. We cannot exclude a more Fe-independent role of TTN5-AHA1 interaction, because *AHA1* expression is less dependent of the Fe status (Santi and Schmidt, 2009).

TTN5 colocalizes with AHA1 in cytoplasmic vesicles

Activity of H^+-ATPases is dependent on their correct PM localization. They undergo a degradation and recycling process typical for membrane proteins (Ivanov and Vert, 2021) but can be also differently regulated including post-translational modifications (Haruta et al., 2015; Falhof et al., 2016; Xue et al., 2018). To identify the place of interaction we used YFP-tagged constructs of TTN5 and the active GTPase variant TTN5^{Q70L} and coexpressed them with AHA1-RFP (Caesar et al., 2011) in *N. benthamiana* leaf epidermal cells. We focused here just on the two TTN5 variants, as we expected a TTN5 function mostly in its GTP-loaded form based on literature of homologs (Sharer and Kahn, 1999; Hanzal-Bayer et al., 2002; Nie et al., 2018) or a recruitment of TTN5-GDP and further activation, presented by YFP-TTN5, which is able to switch from its GDP- to GTP-bound conformation. AHA1-RFP expression was detectable at the PM, consistent with our BiFC data. Both YFP-TTN5 constructs showed a colocalizing signal at the PM (Figure 4A, B). Mannitol-induced plasmolysis confirmed the identified location. The formation of Hechtian strands, PM which stays in contact with the cell wall, was visible for AHA1-RFP together with YFP-TTN5 (Figure 4C) and the YFP-tagged active variant (Figure 4D). Further analysis confirmed the colocalization with comparable Pearson coefficients for the two YFP-TTN5 constructs (Figure 4E). We recently obtained similar localization results for TTN5 with its interactor the Fe transporter IRT1 (Mohr et al., unpublished, Manuscript II). IRT1 cycles inside the cell, being internalized for degradation in the vacuole, or recycled back to the membrane (Ivanov and Vert, 2021). We identified TTN5 together with IRT1 expression in MVBs, suggesting a role in the IRT1 trafficking (Mohr et al., unpublished, Manuscript II). In *patrol1* plants, AHA1 was also expressed in vesicle-like structures, indicating a PATROL1-dependent PM localization in stomatal cells (Hashimoto-Sugimoto et al., 2013). Based on these data, we suspected a similar AHA1 vesicle-like occurrence with TTN5. Indeed, we could detect AHA1-RFP expression in vesicle-like structures inside the cell. Coexpression of both YFP-TTN5 variants (Figure 4F, G) showed some overlapping localization of these spots leading to

the assumption of TTN5 being involved in AHA1 trafficking as already shown for IRT1. Taken together, we were able to identify interaction of TTN5 with IRT1 and AHA1, two PM-located proteins. Additionally, TTN5 colocalized with both in vesicle-like structures. Hence, we propose a universal role of the small GTPase in the transport of membrane proteins within the cell. It has to be further clarified whether TTN5 acts in trafficking of newly synthesized proteins or in the degradation and recycling pathway.

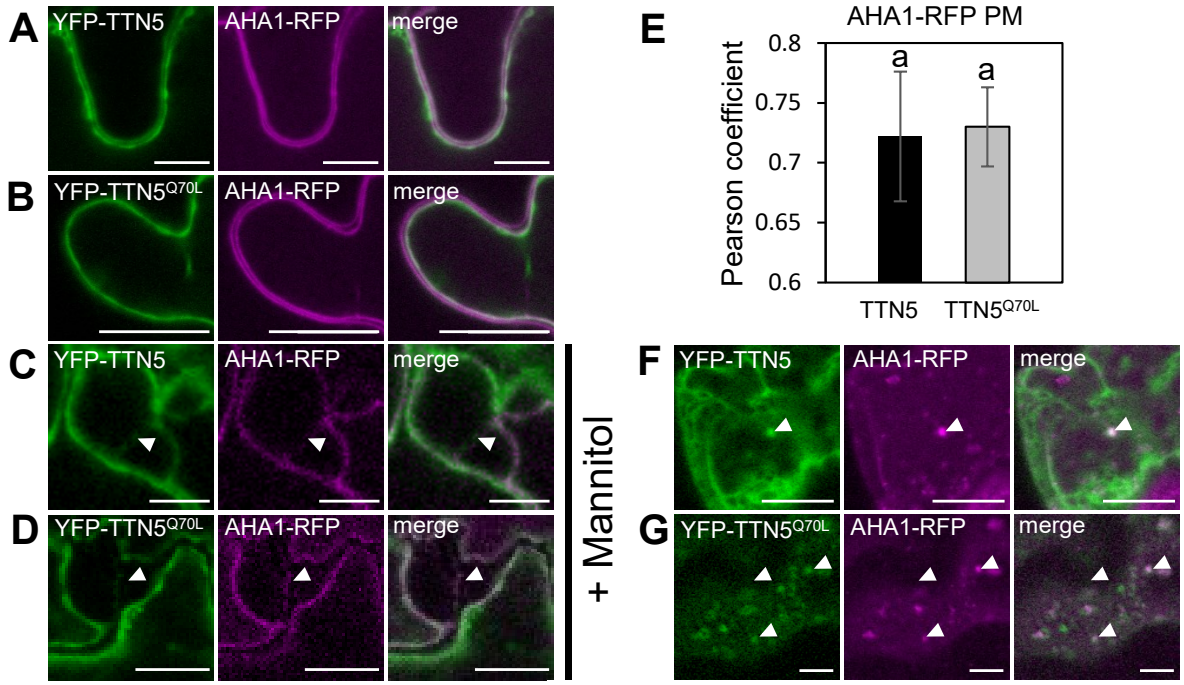

Figure 4. TTN5 colocalizes with AHA1 at the PM and in vesicle-like structures.
(A, C, F), AHA1-RFP coexpression with YFP-TTN5 in epidermal *N. benthamiana* cells. (B, D, G) AHA1-RFP coexpression with the active variant YFP-TTN5^{Q70L}. (A, B), AHA1 is located at the PM and colocalizes with both TTN5 variants. (C, D), PM localization was proven by mannitol-induced plasmolysis. Hechtian strands, PM which is still attached to the cell wall, are marked with arrow heads. (E), Comparison of Pearson coefficient using ImageJ Plugin JACoP (Bolte and Cordelières, 2006). (F, G), Colocalization of YFP-TTN5 (F) and YFP-TTN5^{Q70L} (G) with AHA1-RFP in internalized vesicle-like structures, highlighted with arrowheads. Scale bar 10 µm

Interactome Data of Fe-related genes

The TTN5 interactome did not only reveal a potential new function and regulatory relation, but also strengthened its connection with IRT1. To obtain further knowledge of the IRT1-related interactome, we also tested other IRT1 interactors or proteins with a specific role in the Fe response. Therefore, we used triple HA-tagged transgenic plant lines of the C2-domain CAR protein EHB1 (Khan et al., 2019), the SEC14-like protein PATL2 (Hornbergs et al., Bauer lab, unpublished) and the Kelch-repeat protein IDI1 (von der Mark et al., Bauer lab, unpublished) and performed IP with subsequent MS analysis.

Due to the three-way IRT1-TTN5-EHB1 connection (Mohr et al., unpublished, Manuscript II, Khan et al., 2019), EHB1 was a natural candidate for extending the interactome study by IP-MS (Figure 5A). 135 proteins were present in the EHB1 Fe-sufficient interactome, 153 proteins

in Fe-deficient roots und only 13 proteins were detected for both Fe conditions compared with non-transgenic WT controls (Figure 5B). *EHB1* coexpression network showed a connection, to calcium-related proteins, such as abiotic stress-related proteins, with responses to light, water or temperature (Supplemental Figure 3, Obayashi et al., 2017). One gene coexpressed with *EHB1* encodes a protein detected in the EHB1 IP-MS experiment, LATE EMBRYOGENESIS ABUNDANT 14 (LEA14). *LEA14* expression is induced in response to salt stress and has a suggested protective activity under this condition (Jia et al., 2014).

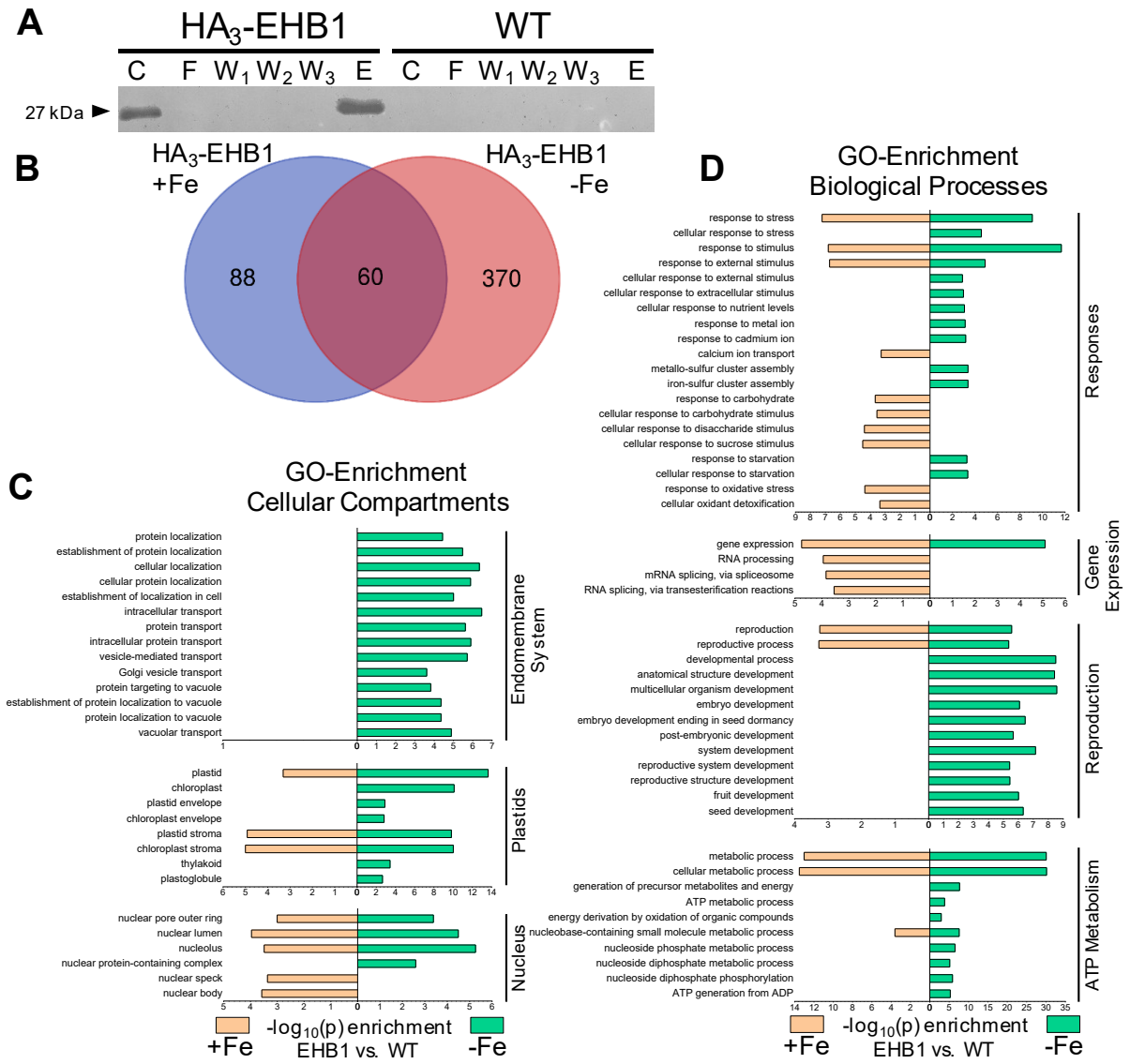

Figure 5. EHB1 interactome is related to Fe homeostasis maintenance.
EHB1 interactome analysis carried out by immunoprecipitation (IP) with subsequent mass spectrometry (MS). IP was performed using HA_3-EHB1 roots grown under Fe-sufficient (+Fe) or -deficient (-Fe) conditions in the two-week system in comparison with WT control. (A), Immunoblot control of the performed IP. Abbreviations: C - crude extract, F - flow through, W_1-W_3 - wash steps I to III and E - elution sample. (B), Venn diagram (http://bioinformatics.psb.ugent.be/webtools/Venn/) of the coprecipitated proteins identified by MS. (C), GO-enrichment analysis of cellular compartments and (D), biological processes under Fe-sufficient (salmon bars) or -deficient (green bars) conditions compared to WT. IP was performed in five biological replicates (n = 5).

The GO enrichment analysis (Figure 5C) of the MS-based identified proteins showed again a good connection to the localization of endomembrane compartments from the PM via endosomes and Golgi to the vacuole and the trafficking machinery, in form of vesicles, under both Fe conditions. Interestingly, enrichment in the direct transporting categories were only present under Fe-deficient conditions. We found several proteins expressed in different parts of the nucleus and nuclear body forming proteins in Fe-sufficient root samples, occurred by RNA splicing-related proteins. Biological processes such as the generation of metabolites and energy with ATP metabolism and glycolytic processes appeared and giving a link to electron-transfer systems and cytochromes (Figure 5D). We identified several cytochromes such as CYP82C4 which is up-regulated under Fe deficiency in a FIT-dependent manner and is a member of the core Fe acquisition gene coexpression module (Colangelo and Guerinot, 2004; Brumbarova and Ivanov, 2019). Reproduction and developmental processes are also more present in EHB1-enriched Fe-deficient roots. Interestingly, we detected AHA7 in these samples, which is important for root hair growth under Fe deficiency (Santi and Schmidt, 2009). This data additionally strengthens the position of EHB1 as an Fe response regulator and shows that its function is not limited to the Fe import step alone but also to coordinating developmental adaptations under Fe deficiency.

PATL2 is a GOLD domain-carrying SEC14-like phosphatidylinositol transfer protein with affinity to phosphoinositides. PATL2 is present at the PM and an interactor of IRT1 (Hornbergs et al., Bauer lab, unpublished, Montag et al., 2020). The loss of *PATL2* leads to an increase in Fe reductase activity and thiobarbituric acid reactive substances (TBARS), byproducts of lipid peroxidation, promoting a positive impact in alleviating Fe^{2+}-induced oxidative stress (Hornbergs et al., Bauer lab, unpublished). Tight connections between Fe homeostasis and reactive oxygen species (ROS) metabolism have been extensively studied in the last several years (Le et al., 2015; Reyt et al., 2015; von der Mark et al., 2020; Gratz et al., 2021). In addition to this, PATL2 has provided us with the opportunity to explore the direct link between oxidative stress and Fe acquisition at the PM. We used HA_3-PATL2-expressing plants (Hornbergs et al., Bauer lab, unpublished) for IP-MS analysis of PATL2 interacting proteins (Figure 6A). The detected PATL2 interactome consisted out of 28 proteins in Fe-sufficient roots, 171 proteins under Fe deficiency and an overlap of 54 proteins for both set-ups (Figure 6B). The coexpression network (Supplemental Figure 4, Obayashi et al., 2017) revealed a connection to steroid biosynthesis, embryogenesis and developmental processes and lipids, especially phosphatidylinositol with a link to cytoskeletal filaments. In our interactome data set, we found the coexpressed calcium (Ca^{2+}) - and copper (Cu^{2+})-binding protein PCaP1 in the Fe-deficient root samples. PCaP1 is PM located due to its strong interactions with phosphatidylinositol

(Nagata et al., 2016). Further analysis revealed an enrichment of proteins related to endomembrane trafficking, with vesicle-associations under Fe deficiency (Figure 6C). Also, cytoskeleton connected proteins, linked to microtubules, are enriched at Fe deficiency.

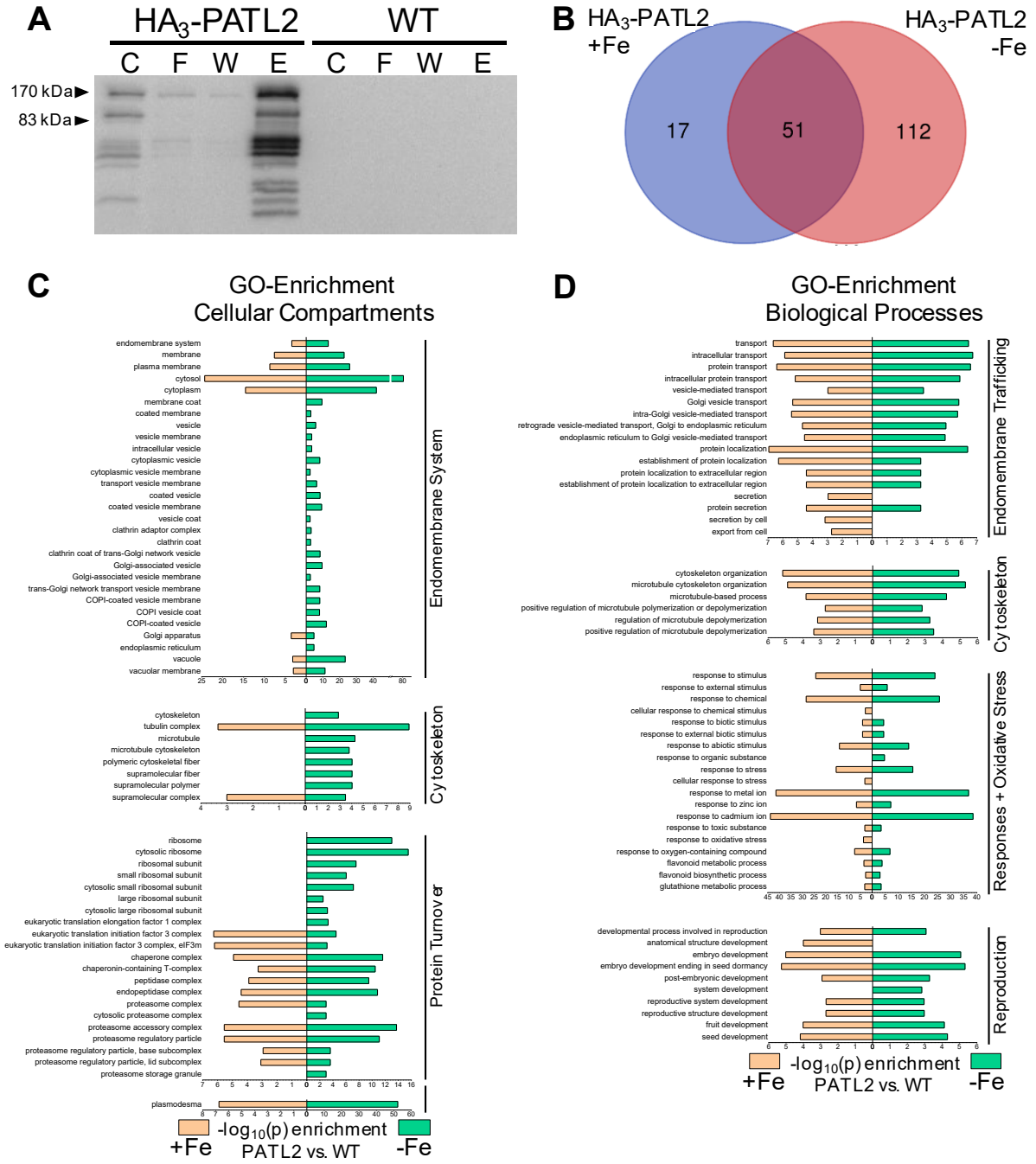

Figure 6. PATL2 interactome is involved in ROS-induced responses.
PATL2 interactome analysis carried out by immunoprecipitation (IP) with subsequent mass spectrometry (MS). IP was performed using HA_3-PATL2 roots grown under Fe-sufficient (+Fe) or -deficient (-Fe) conditions in the two-week system in comparison with WT control. (A), Immunoblot control of the performed IP. Abbreviations: C - crude extract, F - flow through, W - wash step I and E - elution sample. (B), Venn diagram (http://bioinformatics.psb.ugent.be/webtools/Venn/) of the coprecipitated proteins identified by MS. (C), GO-enrichment analysis of cellular compartments and (D), biological processes under Fe-sufficient (salmon bars) or -deficient (green bars) conditions compared to WT.
IP was performed in five biological replicates (n = 5).

We detected a drastic increase in plasmodesmata located proteins, like REMORIN1.2 (REM1.2) compared to Fe-sufficient conditions. We could also identify GO categories of protein synthesis and degradation with locations at ribosomes, chaperone complexes or the proteasome. Interestingly, the enrichment of stimuli and stresses, such as oxidative stress (Figure 6D), was consistent with our previous observations linking PATL2 to the prevention of membrane oxidative damage (Hornbergs et al., Bauer lab, unpublished). Oxidative stress can occur due to the Fenton reaction, with Fe^{2+} as catalyst. Fe^{2+} is reacting with hydrogen peroxide (H_2O_2) and producing hydroxyl radicals. Catalases, like CAT3, identified in Fe-deficient PATL2-enriched root samples, can lower the concentration of H_2O_2 by its breakdown to oxygen and water and prevent oxidative damage (Gratz et al., 2021). This would represent a second mode of action for PATL2, which can also deliver α-tocopherol to membranes for limiting the formation of lipid radicals (Hornbergs et al., Bauer lab, unpublished). PATL2 interactome revealed enrichment and specific candidates connected to oxidative stress suggesting an involvement in stress responses to ROS-induced membrane damage by lipid peroxidation.

We chose IDI1 as a candidate because of its stable up-regulation under Fe-deficient conditions in several screens concomitant with a strong correlation in its coexpression network (Supplemental Figure 5, Obayashi et al., 2017) to Fe-related genes (Ivanov et al., 2012; Mai et al., 2016). Next, to the Strategy I genes *FRO2* and *IRT1* and the transcription factor *FIT*, *IDI1* is coexpressed with other metal transporters or related to Fe transport, potentially independent from the Fe^{2+} import by IRT1 (Obayashi et al., 2017). IP-MS-based IDI1 interactome list was created in a way similar to that for TTN5 variants, EHB1 and PATL2 using a HA_3-IDI1-expressing Arabidopsis line (Figure 7A, von der Mark et al., Bauer lab, unpublished). We detected 94 proteins only present under Fe sufficiency, 473 proteins for Fe-deficient IDI1 roots and 153 proteins which were present for both Fe statuses (Figure 7B). In Fe-sufficient roots, the phloem protein PP2-A8 was detected, while two nicotianamine synthases NAS1 and NAS2, producing the Fe chelator NA involved in Fe redistribution within the plant, were present in both set-ups, giving a connection between coexpression network and interactome and topically to plant Fe transport. The GO analysis showed again a strong connection to the endomembrane system, with a lot of categories linked directly to vesicle trafficking (Figure 7C). Indeed, we identified in the interactome several RAB proteins but also ARF-GEFs and -GAPs, like GNOM and BIGs. Next to this, enrichment was detectable in categories like stress responses and immune system reactions, as well as cytoskeletal organization, with regard to cell cycle control and developmental processes (Figure 7D). We could identify proteins of the phenylpropanoid pathway like another cytochrome P450, CYP98A3, or the hydroxycinnamoyl-Coenzyme A

shikimate/quinate hydroxycinnamoyltransferase (HCT) pointing in the direction of coumarin synthesis which is reinforced by the detection of BGLU42 (Zamioudis et al., 2014).

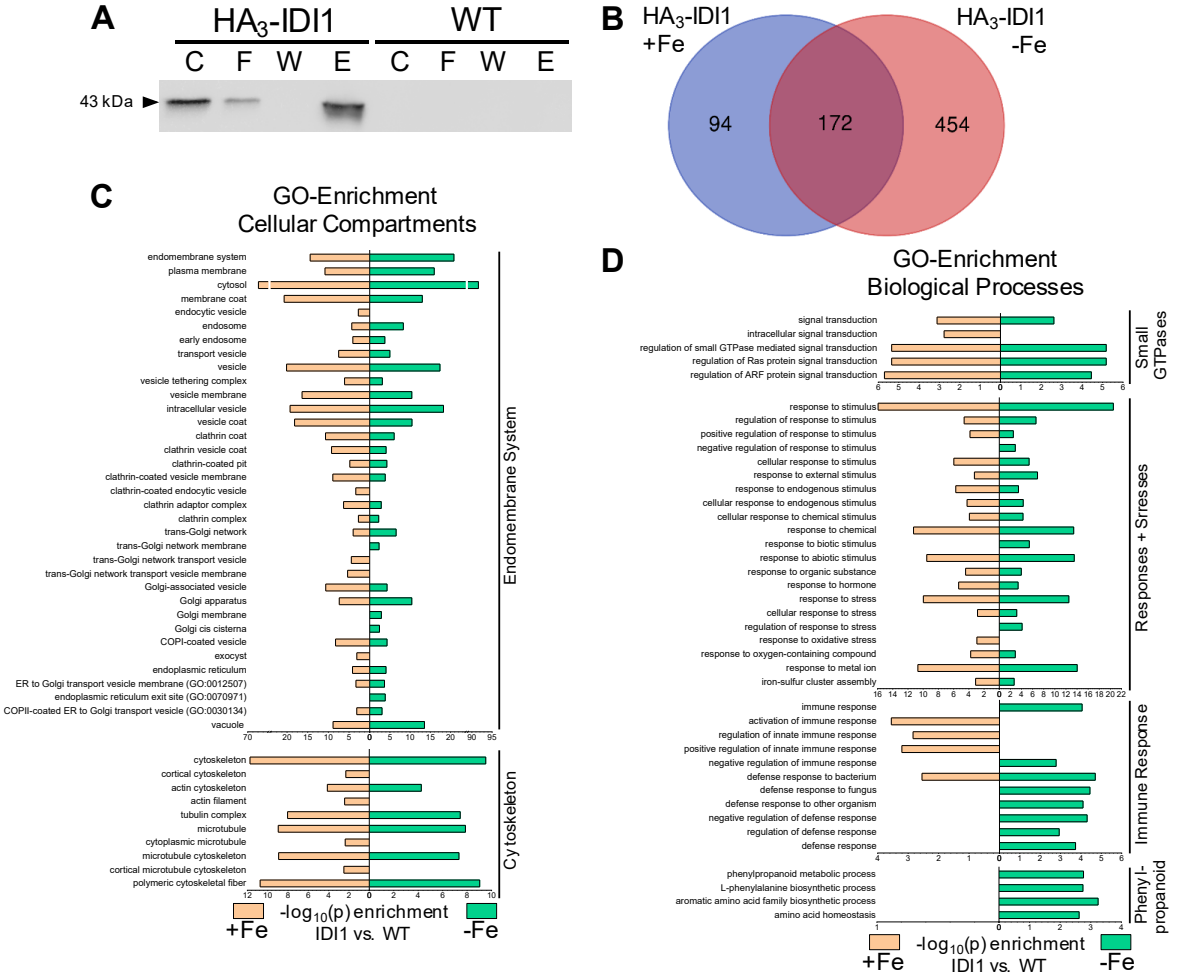

Figure 7. IDI1 interactome is linked to Fe-chelation.
IDI1 interactome analysis carried out by immunoprecipitation (IP) with subsequent mass spectrometry (MS). IP was performed using HA_3-IDI1 roots grown under Fe-sufficient (+Fe) or -deficient (-Fe) conditions in the two-week system in comparison with WT control. (A), Immunoblot control of the performed IP. Abbreviations: C - crude extract, F - flow through, W - wash step I and E - elution sample. (B), Venn diagram (http://bioinformatics.psb.ugent.be/webtools/Venn/) of the coprecipitated proteins identified by MS. (C), GO-enrichment analysis of cellular compartments and (D), biological processes under Fe-sufficient (salmon bars) or -deficient (green bars) conditions compared to WT.
IP was performed in five biological replicates (n = 5).

Taken together, the idea of IDI1 involvement in Fe homeostasis based on its stable up-regulation under Fe deficiency is supported by the interactome data. Identified proteins reveal a link to coumarin-based Fe chelation.

Interactomes overlap in Fe-related processes

Finally, we were interested in the connection of our Fe-related genes to identify functional overlaps in Fe homeostasis. Hence, we compared the obtained enriched proteins of our IP-MS-based root interactomes (Figure 8, Table 1). We could not detect any match between all compared interactomes, but several smaller overlaps between selections of two to three

interactomes. The IDI1 interactome displays the most intersections in our comparison. It exhibits a large overlap with the EHB1 interactome with 369 in total. PATL2 and TTN5

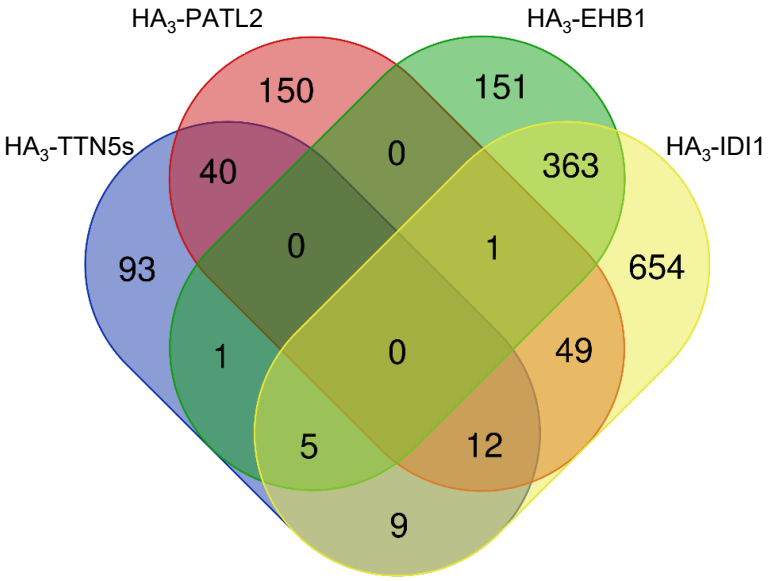

Figure 8. Overlaps in interactome comparison.
Venn diagram (http://bioinformatics.psb.ugent.be/webtools/Venn/) of interactomes carried out by immunoprecipitation (IP) with subsequent mass spectrometry (MS) under summed up Fe-sufficient and -deficient conditions. For visualization, the TTN5 interactome was combined (HA_3-TTN5s) with the two interactomes of its inactive ($TTN5^{T30N}$) and active ($TTN5^{Q70L}$) variant.

interactomes still share an overlap of 62 and 26 of enriched proteins with IDI1 and 52 between each other. The intersections of EHB1 interactome with PATL2 and TTN5 are low with only one and six proteins. Nevertheless, when viewed in detail, the data show some interesting correlations between interactomes. All interactomes share proteins connected to the cytoskeleton with several tubulins (TUBA3, TUBA5-6, TUBB1-3, TUBB5, TUBB8) or the endomembrane trafficking with different coatomer subunits (α2, β2, γ, ε1). The latter is regulated by ARF-signaling. EHB1 and IDI1 interactomes exhibit the ARF-GAPs AGD5 and AGD12, as well as ARF-GEFs GNOM and GNL1. GNOM and GNL1 play a role in ER-Golgi trafficking. We identified several ER body-related intersections in our data sets. We detected the NAI1-regulated genes, *NAI2* and *GLL23*. ER body formation can be induced by wounding as a defense response. Another pathogen defense response leads to the secretion of coumarins and is regulated by BGLU42. We identified overlaps in proteins involved in coumarin precursor synthesis, like the *S*-adenosylmethionine synthase 1 and 4 (SAM1/METK4) or NAS1. We identified the annexin proteins 1-3 (ANN1-3) potential Ca^{2+}- and ROS-dependent membrane-binding proteins and another catalase CAT1, as oxidative stress-related interactome overlaps. We propose an interplay of our here investigated Fe-related genes based on the identified overlaps in the interactomes.

TTN5 interacts with PATL2

We recently reported the interaction of TTN5 with IRT1 and its regulators EHB1 and SNX1 suggesting a modulating function of TTN5 in Fe acquisition (Mohr et al., unpublished,

Manuscript II). Based on this, we were also interested in a potential interaction between TTN5 and PATL2. Therefore, we tested cYFP-TTN5 with nYFP-PATL2 in BiFC experiments.

Table 1. Overlaps in interactome comparison.
Comparison (http://bioinformatics.psb.ugent.be/webtools/Venn/) of interactomes carried out by immunoprecipitation (IP) with subsequent mass spectrometry (MS) under summed up Fe-sufficient and -deficient conditions**.** Obtained intersections were grouped into specific categories. The appearance of a gene in the interactomes is indicated by +.

		TTN5	TTN5^{T30N}	TTN5^{Q70L}	PATL2	EHB1	IDI1
Oxidative stress	Fe chelation	SAM1	+		+	+		+
		METK4				+		+
		NAS1					+	+
		BGLU42					+	+
		HST					+	+
		CSE	+			+		
		CCR1				+		+
	ER bodies / Vesicles	PAL1;PAL2		+	+			
		DHS1		+	+			
		Actin-11;Actin-12;Actin-4		+	+			
		TUBA3;TUBA5				+		+
		TUBA6				+		+
		TUBB1				+		+
		TUBB3;TUBB2		+		+		+
		TUBB5				+		+
		TUBB8				+		+
		TFCB					+	+
		CHC1		+	+	+		+
		EPSIN1					+	+
		Coatomer subunit alpha-2		+	+	+		+
		Coatomer subunit beta-2				+		+
		Coatomer subunit gamma				+		+
		Coatomer subunit epsilon-1				+		+
		SEC31B				+		+
		Sec24-like					+	+
		NAI2		+	+	+		
		GLL23		+	+			+
		MEBL					+	+
		BGLU21				+		+
	ARF-signaling	GN					+	+
		GNL1					+	+
		AGD5					+	+
		AGD12					+	+
		ARLA1C	+					+
		ANN1		+	+			+
		ANN2			+	+		
		ANN3					+	+
		CAT1					+	+
		PCAP1				+		+
		LEA14					+	+

Complemented YFP was visible at the PM, which fit the localization studies of both PATL2 and TTN5 (Figure 9A, Mohr et al., unpublished, Manuscript II, Montag et al., 2020). We were not able to observe complementation for the combination of PATL2 and any of the two GTPase variants TTN5^{T30N} (Figure 9B) and TTN5^{Q70L} (Figure 9C). It is possible that the TTN5 switching mechanism is essential for a potential interaction between these two proteins. To further identify

the place of interaction, we tested already published deletion mutants of PATL2. The N-terminal part of PATL2 is needed for the interaction with the variable region of IRT1 (Montag et al., 2020). We used the PATL2 deletion mutants nYFP-PATL2ΔC lacking the three named domains, CTN, SEC14 and GOLD domain, and nYFP-PATL2ΔN with all domains present but without the N-terminal part. Together with cYFP-TTN5, the N-terminus of PATL2 complemented YFP (Figure 9D), whereas no signal was obtained in combination with just the C-terminal domain region of PATL2 (Figure 9E).Interestingly, the fluorescent complementation signal between cYFP-TTN5 and nYFP-PATL2ΔC was shifted to the ER, proving the PM localization being dependent on C-terminal PATL2 domain region (Montag et al., 2020). Additionally, we checked TTN5 influence on *PATL2* gene expression (Figure 9F). *PATL2* transcript levels did not change in an Fe-dependent manner in WT roots. In *ttn5-1*$^{+/-}$ we detected again a decreased gene expression under both conditions with a statistical difference to WT for Fe-deficient root samples. We could therefore identify another IRT1-related interactor of TTN5 and the obtained data strengthen our idea of TTN5 being a coordinator in Fe acquisition.

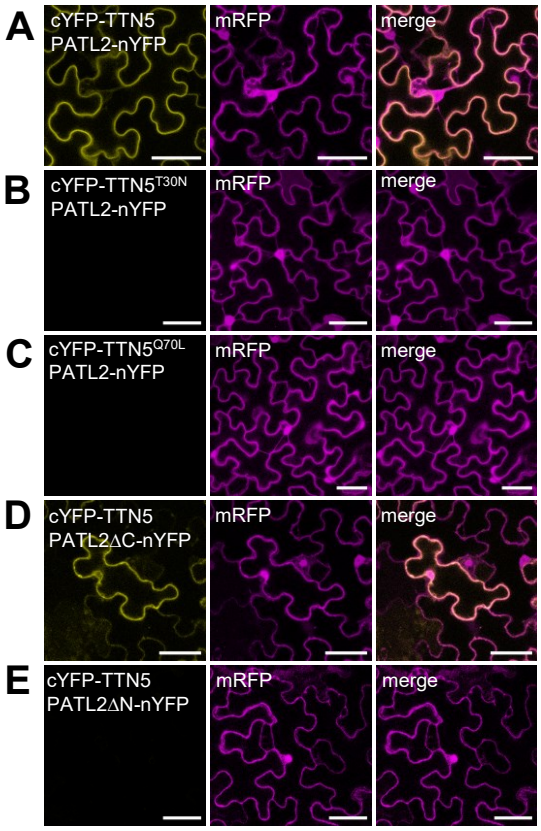

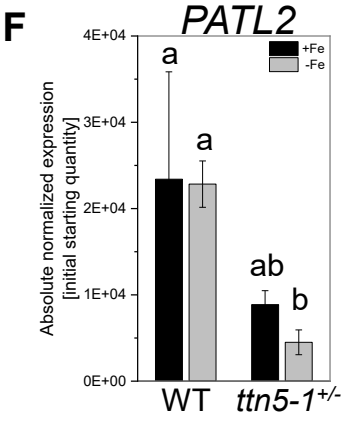

Figure 9. TTN5 can interact with PATL2 in leaf epidermal cells.
(A-F), TTN5 interaction studies with PATL2 by BiFC in *N. benthamiana* leaf epidermal cells. C-terminal half of YFP was fused to TTN5 and the N-terminal to PATL2. Complemented YFP signal indicated a potential interaction. mRFP served as a transformation control. (A), nYFP-tagged PATL2 showed complemented YFP signal with N-terminally-tagged cYFP-TTN5. (B), cYFP-TTN5^{T30N} and PATL2-nYFP do not complement YFP. (C), cYFP-TTN5^{Q70L} and PATL2-nYFP do not complement YFP. (D, E), Deletion mutants of PATL2 showed dependency of the N-terminus for complementation with TTN5. YFP signal in the ER is visible for PATL2 N-terminus (PATL2ΔC, D). C-terminus alone (PATL2ΔN, E) has no detectable YFP. Every construct was tested a minimum of three times (n ≥ 3) with similar results. Scale bar 50 µm. (F), Gene expression data by RT-qPCR of *PATL2* in *ttn5-1*$^{+/-}$ roots compared to WT. Plants were grown in the two-week system under Fe-sufficient (+Fe, black bars) or -deficient (-Fe, grey bars) conditions. Three biological replicates were tested (n = 3). One-way ANOVA with Fisher-LSD post-hoc test was performed. Different letters indicate statistical significance ($p < 0.05$).

SEC12 interacts with TTN5

We detected SEC12 in the IP-MS approach opening a possibility of being a GEF for TTN5. The identified interaction between TTN5 and SEC12 was also verified using BiFC. We observed a complementation of the split YFP located to the ER, fitting the localization of SEC12

as an ER membrane protein (Figure 10A). nYFP-SEC12 together with the two GTPase variants cYFP-TTN5^{T30N} (Figure 10B) and cYFP-TTN5^{Q70L} (Figure 10C) was also able to give a complemented signal, thus providing no indication for a GTPase structural preference. However, we should point out that BiFC shows whether the proteins can interact or not. Our previous experience with TTN5 shows that sometimes the differences in interaction strength might be more subtle and might require quantitative methods to reveal (Mohr et al., unpublished, Manuscript II). We used again the combination cYFP-TTN5-nYFP-EHB1Δsig (Figure 10D) as a negative control. The same result was obtained with cYFP-EHB1Δsig and nYFP-SEC12 (Figure 10E). Thus, we could confirm the IP-MS-based interaction and suggested TTN5-GEF activity of SEC12, based on its function on SAR1 (d'Enfert et al., 1992; Barlowe and Schekman, 1993; Brandizzi, 2018). Due to this, we did not expect *SEC12* to be transcriptionally regulated by TTN5. Additional qPCR data approved our hypothesis (Figure 10F). The Fe status had no impact on *SEC12* gene expression in WT samples and similar values were obtained in *ttn5-1*$^{+/-}$. Taken together, our data confirmed the IP-MS data and leaves the possibility open that SEC12 might have a GEF activity on TTN5.

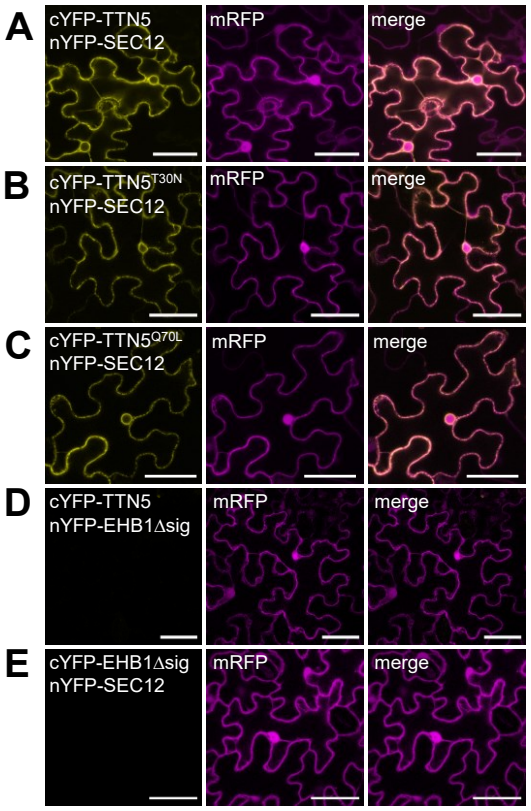

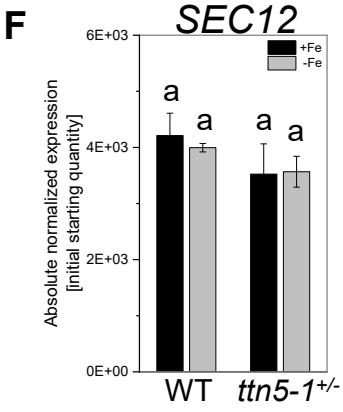

Figure 10. TTN5-SEC12 can interact in leaf epidermal cells.
(A-F), Confirmation of IP-MS identified TTN5 interaction with SEC12 by BiFC in *N. benthamiana* leaf epidermal cells. C-terminal half of YFP was fused to TTN5 and the N-terminal to SEC12. Complemented YFP signal indicated a potential interaction. mRFP served as a transformation control. (A), nYFP-tagged SEC12 showed complemented YFP signal with N-terminally-tagged cYFP-TTN5. (B), nYFP-SEC12 complemented split-YFP with cYFP-TTN5^{T30N}. (C), nYFP-SEC12 complemented split-YFP with cYFP-TTN5^{Q70L}. Interaction took place at the ER. (D, E), The negative controls cYFP-TTN5 and nYFP-EHB1Δsig (D), and cYFP-EHB1Δsig/nYFP-SEC12 (E) produced no YFP signal. Every construct was tested a minimum of three times (n ≥ 3) with similar results. Scale bar 50 µm. (F), Gene expression data by RT-qPCR of *SEC12* in *ttn5-1*$^{+/-}$ roots compared to WT. Plants were grown in the two-week system under Fe-sufficient (+Fe, black bars) or -deficient (-Fe, grey bars) conditions. Three biological replicates were tested (n = 3). One-way ANOVA with Fisher-LSD post-hoc test was performed. Different letters indicate statistical significance ($p < 0.05$).

Discussion

The regulation of Fe deficiency-induced Fe uptake, the internal Fe transport and related processes are just one good example of a mechanistic interplay showing the importance of

PPIs. Many proteins and their function in Fe homeostasis are already elaborated but a lot of processes are still unclear and are probably based on unknown PPIs. Therefore, the identification of novel proteins and interactors in Fe-related processes is of great interest to fill the gaps in our knowledge. Here, we presented new interactors of the Fe-related genes *TTN5*, *EHB1*, *PATL2* and *IDI1* identified by IP-MS and described their potential role in Fe homeostasis. We detected proteins of the Fe uptake machinery and involvement in Fe distribution as well as oxidative stress responses. Identified overlaps in the generated interactomes promoted the idea of a regulated network containing the here investigated Fe-related genes.

Principal role of TTN5 in PM protein trafficking

The ARF family of small GTPases functions in vesicle trafficking and is part of the endomembrane system. We could recently identify the ARF-like protein TTN5 as an interactor of the main Fe root transporter IRT1 with a proposed role in its intracellular cycling process. With the additional connection to IRT1 regulators it became clear that a deeper insight into the TTN5 interactome was needed to obtain a better understanding of its function (Mohr et al., unpublished, Manuscript II). We could identify here the two H^+-ATPases AHA1 and AHA2 as novel TTN5 interactors in an IP-MS approach. These findings open two main directions of TTN5 activity. Firstly, we suggest a role of TTN5 in the Fe deficiency response. AHA2 is, next to FRO2 and IRT1, one of the three main proteins involved in Fe uptake of Strategy I. The proton pump is needed for the acidification of the rhizosphere and leads to the solubilization of complexed Fe^{3+} (Santi and Schmidt, 2009; Brumbarova et al., 2015). Partial lack of TTN5 has a negative impact on the Fe deficiency response by a reduced Fe reductase activity and seed Fe content (Mohr et al., unpublished, Manuscript II). The down-regulation on transcript levels of Fe-related genes can also be observed for both H^+-ATPases fitting the suggested role in the Fe deficiency response. A second option is independent of the plant Fe status but focusses on PM proteins in general, especially their constant turnover. The detailed process of H^+-ATPases cycling between the PM and the vacuole is not well established. We could colocalize AHA1 with TTN5 at the PM and in intracellular vesicles promoting the idea of TTN5 being involved in the transport of AHA1 in the endomembrane system to the vacuole or back to the PM. We hypothesize similar colocalization with AHA2, implying TTN5-affected PM protein cycling of already three identified interactors. An Fe-independent role of TTN5 in PM trafficking can be proposed by the fact that we identified AHA1 only in Fe-sufficient HA_3-TTN5 roots leading to the assumption of a stronger interaction under these conditions. TTN5 is of great importance due to its effects on many gene transcript levels, including *AHA1* and *AHA2* and its embryo lethal phenotype implying a multitude of diverse functions making both hypotheses possible.

With the identification of SEC12 as a potential TTN5-GEF we can open up further functional studies of the GTPase. We hypothesize a role of SEC12 in TTN5 activation based on its SAR1 interaction in COPII, ER to Golgi, transport (d'Enfert et al., 1992; Barlowe and Schekman, 1993; Brandizzi, 2018). We recently detected TTN5 localization connected to the *cis*-Golgi site, the site which is receiving ER-derived vesicles (Mohr et al., unpublished, Manuscript II). SEC12 differs in structure from the typical ARF-GEFs. It is a β-propeller ER transmembrane protein lacking the Sec7 domain, typical for ARF-GEFs (McMahon et al., 2012; Joiner and Fromme, 2021). Crystal structures of the SEC12-SAR1 complex revealed an atypical conformational change in SAR1 switch region. An extended K^+-binding loop (K-loop) of SEC12, essential for GEF-activity, is disrupting SAR1 nucleotide-binding site via displacement of a conserved Asp (McMahon et al., 2012; Joiner and Fromme, 2021). SAR1 sequence differs from most ARF and ARF-like by lacking the usually n-myristoylated Gly-2 (Memon, 2004). TTN5 and its homolog ARL2 possess the Gly residue, but are not myristoylated as well (Sharer et al., 2002; Boisson et al., 2003) supporting our hypothesis, but future studies have to be done for clarification. Of greater interest will be the investigation of a connection between SEC12-dependent TTN5 activation and our proposed function in PM trafficking. TTN5-SEC12 interaction could lead to the formation of vesicles at the ER to transport newly synthesized proteins to their cell destination. We were not surprised by the unaltered gene expression levels of *SEC12* in *ttn5-1*$^{+/-}$ roots as ARF GTPase activity is dependent on the GEF-recruitment. The unequal ratio of more than 20 ARF GTPases to only eight ARF-GEFs (Vernoud et al., 2003) suggests that one GEF can activate multiple GTPases. Therefore, transcriptional regulation of *SEC12* by TTN5, although not excluded, would be unlikely.

MS interactome data reveal an elaborated network of Fe homeostasis

With the revealed interactions of TTN5, EHB1 and PATL2 with IRT1 and the revealed interactions of EHB1 and PATL2 with TTN5 we already have a strong connection between these proteins and in the IRT1-related Fe deficiency response (Hornbergs et al., Bauer lab, unpublished, Mohr et al., unpublished, Manuscript II, Khan et al., 2019). The performed IP-MS experiments elucidated the link in an Fe interactome, strengthened by IDI1 investigation.

All data sets contained a higher number of proteins under Fe-deficient conditions, indicating the initiation of an elaborated machinery due to Fe stress. Based on transcriptomic root data it is known, that more than 2000 genes are regulated upon Fe deficiency (Schwarz et al., 2020). For all selected proteins, we identified an interactome enrichment in the processes of endomembrane trafficking, like vesicle transport. Especially the IDI1 data set had a strong correlation with several ARF-GEFs and -GAPs presenting a potential link to TTN5.

EHB1 and IDI1 interactomes reveal interplay related to coumarin synthesis

Vesicle formation becomes also very interesting with the CAR protein involvement in Ca^{2+}-dependent membrane curvature initiation (Rodriguez et al., 2014; Diaz et al., 2016). Several CAR proteins are able to interact with the PYRABACTIN RESISTANCE 1 (PYR1)/PYR1-LIKE (PYL) abscisic acid (ABA)-receptors and recruit them to membranes. Based on the IRT1-EHB1 interaction, similar to CAR-PYR/PYL interactions at membranes, we suggested the tubulation of IRT1-containing membranes, promoted by EHB1 in a Ca^{2+}-dependent manner (Diaz et al., 2016; Khan et al., 2019). The detected proteins, such as ARA6/RABF1, RABE1D or RABA4B can be the link in the formation of IRT1-containing vesicles or in the direct transport inside the cell. Tested *car* mutants were less ABA-sensitive and in combination with the PYR1/PYL interactions, CAR proteins are expected to take place in ABA-signaling (Rodriguez et al., 2014; Diaz et al., 2016). Additionally, the coexpressed and in the EHB1 interactome detected *LEA14* is a stress-related marker for drought or salt stress and directly induced by ABSCISIC ACID INSENSITIVE 3 (ABI3) (Galau et al., 1993; Jia et al., 2014; Tian et al., 2020). This detection presents another link of ABA-signaling to EHB1 and to Fe homeostasis. Connections between ABA and Fe are presented for example by CIPK11-phosphorylation-dependent activation of FIT and basic leucine zipper (bZIP) transcription factor ABI5 (Zhou et al., 2015; Gratz et al., 2019). The EHB1 interactome revealed several links to Fe homeostasis. *AHA7* and *CYP82C4* present in the interactome data set, are two genes, well known to be up-regulated under Fe deficiency (Ivanov et al., 2012). While AHA7 probably does not have a direct function in Fe uptake it is necessary for the Fe deficiency-dependent root hair growth (Santi and Schmidt, 2009). *CYP82C4* strongly correlates with *FIT* and *IRT1* and it is up-regulated in a FIT-dependent manner (Colangelo and Guerinot, 2004; Murgia et al., 2011). Next to it, it also highly correlates with the expression of several genes of metal uptake and transport (Murgia et al., 2011). CYP82C4 raised interest due to its activity in hydroxylating 8-methoxypsoralen a furanocoumarin with structural similarity to scopoletin (Kruse et al., 2008). Scopoletin is produced in the phenylpropanoid metabolism by the oxoglutarate-dependent oxidase F6′H1, which is an important component of Fe acquisition (Schmid et al., 2013). Of note is the large overlap of EHB1 and IDI1 interactomes and in addition with regard to *IDI1* coexpression network we suspect an interplay of EHB1 and IDI1 in Fe homeostasis.

The function of IDI1 is still not investigated, but its expression strongly correlates with Fe-related genes. In the IDI1 interactome, we detected two nicotianamine synthases, NAS1 and NAS2, with NAS1 also present in EHB1 interactome and both coexpressed with *IDI1* at transcriptional level. This provides a strong indication of an IDI1 function in Fe homeostasis. NAS1 and NAS2 are catalyzing the production of NA, which can form complexes with metals,

such as Fe, enabling metal transport in the plant (Schuler and Bauer, 2011). NA is produced from SAM the product of *S*-adenosylmethionine synthetases, like SAM1 and SAM2 and METK4, which also appeared in the IDI1 interactome. Strikingly, METK4 is also part of the PATL2 interactome, and SAM1 was even enriched in both TTN5, TTN5^{Q70L}, and PATL2 root samples, providing a link in Fe chelation in our combined data sets. *NAS1*, *NAS2*, *IDI1* and *CYP82C4* appear together in a coexpression network (Ivanov et al., 2012; Brumbarova and Ivanov, 2019) suggesting a link between NA-dependent Fe chelation and transport and the phenylpropanoid pathway opening the direction into Fe uptake. Arabidopsis is releasing fluorescent phenolics such as scopoletin, sideretin and fraxetin via ABCG37 into the rhizosphere (Rodríguez-Celma et al., 2013; Schmid et al., 2013; Fourcroy et al., 2014). As mentioned, scopoletin is produced by F6'H1 and can be further processed to fraxetin and subsequently to sideretin, two cargos of ABCG37. The last hydroxylation step is catalyzed by CYP82C4 (Rajniak et al., 2018). A connection between the phenylpropanoid pathway and NA synthesis is carried out by SAM, which serves as a methyl donor. Taking a deeper look in the interactome data sets, we could identify several genes involved in the shikimate, phenylpropanoid and NA biosynthetic pathways, which are essential for the production of Fe chelators such as NA and coumarins (Zamioudis et al., 2014). We detected BGLU42 in EHB1 and IDI1 interactome, which is regulated by the Fe-responsive transcription factors MYB10 and MYB72, both highly induced in Fe-deficient plants and also regulating NAS expression (Colangelo and Guerinot, 2004; Dinneny et al., 2008; Palmer et al., 2013). MYB72 has a dual function in induced systemic resistance (ISR) but also in Fe uptake with a role in phenolic biosynthesis, promoting the same for its target genes (Van der Ent et al., 2008; Zamioudis et al., 2014). Indeed, next to BGLU42 importance in ISR response, *bglu42* seedlings are described with a lower amount of fluorescent phenolics in the root compared to wild type, promoting MYB72-regulated secretion induction by BGLU42 (Zamioudis et al., 2014). Recent data draw a connection between the secretion of coumarins and the root microbiota in Fe-deficient soil for plant development, suggesting an interplay of the immune and Fe deficiency response (Harbort et al., 2020). In conclusion, we identified a strong correlation of genes involved in Fe chelation, coumarin biosynthesis and their extrusion, in the EHB1 and most prominently the IDI1 interactome. It is not surprising, that knockout seedlings of IDI1 have a reduced concentration of phenolic compounds in the root exudate under alkaline pH, proposing a role of IDI1 in phenolic-based Fe chelation (von der Mark et al., Bauer lab, unpublished). Such a strong coordination might suggest that the newer connection to immune responses and the root microbiota can be detected in our data sets as well. Other BGLU, next to BGLU42, are involved in the defense response. Of greater interest are BGLU23/PYK10 and its close

homolog BGLU21, which are present in special endomembrane compartments, the ER bodies, unique to Brassicaceae (Matsushima et al., 2003; Nakano et al., 2014). The body formation could be induced in non-Brassicaceae by expressing *BGLU23* together with *NAI2* (Yamada et al., 2020). IDI1 interactome contains next to the defense response associated coumarin connection also an ER body link with BGLU21 and NAI1-induced *GDSL LIPASE-LIKE PROTEIN 23* (GLL23) and *PYK10-BINDING PROTEIN 1* (*PBP1*). Additionally, we identified NAI2 and GLL23 in both TTN5 variants and NAI2 and BGLU21 in the PATL2 interactome, strengthen our Fe-related network in ER body-related content as well.

PATL2 interactome suggests a role in prevention of Fe-induced oxidative damage

In the PATL2 interactome, we could identify an enrichment in oxidative stress-related proteins and connection to antioxidants biosynthetic pathways. Oxidative stress can occur by the production of ROS, such as radicals like superoxide or hydroxyl radical or H_2O_2. Prolonged Fe deficiency leads to a FIT-dependent increase in H_2O_2 concentration as well as an activity increase of catalase CAT2 (Le et al., 2015; von der Mark et al., 2020; Gratz et al., 2021). We previously reported that loss-of-function *cat2-1* roots show an induction of *CAT1* and *CAT3* expression under Fe deficiency, as a potential compensation approach (Gratz et al., 2021). Oxidative stress can also be caused by Fe. IRT1 is importing Fe^{2+} into the cell which can then also be part of the Fenton reaction. In the presence of H_2O_2, Fe^{2+} can be oxidized, and hydroxyl radicals are formed. These radicals can oxidize a broad range of organic compounds such as unsaturated membrane lipids, starting a chain reaction of lipid peroxidation and causing membrane damages. As already mentioned, this reaction can be prevented by catalases, like the identified CAT1-CAT3 in the PATL2, EHB1 or IDI1 interactomes, which lower the H_2O_2 concentration again (Gratz et al., 2021). Next to it, the already triggered lipid peroxidation can be blocked by antioxidants, such as α-tocopherol. It can interact with the radicals and form tocopherol-radicals which are not toxic to the cell. These tocopherol-radicals can further neutralize present lipid radicals as well. Interestingly, a SEC14-GOLD protein in tomato, a homolog of the Arabidopsis PATL6, is able to bind α-tocopherol (Bermúdez et al., 2018). We observed a similar possibility for PATL2 by applying modeling approaches (Hornbergs et al., Bauer lab, unpublished). Due to this, we hypothesize that PATL2 is able to recruit α-tocopherol to the membrane where it interrupts the lipid radical chain reaction. We detected an increase of malondialdehyde (MDA) in *patl2* knock-out lines. MDA is a result of lipid peroxidation, hence a marker of oxidative stress and strengthen PATL2 role in Arabidopsis' oxidative stress response (Hornbergs et al., Bauer lab, unpublished). In the PATL2 and IDI1 interactomes detected PCaP1 interacts and competes with the also coexpressed REM1.2 for actin filaments at plasmodesmata in *Tobacco mosaic virus* movement (Cheng et al., 2020). Many REMs are

described to be components of plasmodesmata-PM sub compartments and functioning in cell-to-cell movement via plasmodesmata opening-size regulation (Raffaele et al., 2009; Fernandez-Calvino et al., 2011; Huang et al., 2019). The here identified link between PATL2 coexpression network and interactome could be a potential regulating step of PATL2-dependent α-tocopherol recruitment due to ROS-induced lipid peroxidation. We suggest an effect on REM1.2-dependent plasmodesmata regulation via PATL2 interaction with PCaP1 to facilitate α-tocopherol recruitment. PCaP1 was also detected as IDI1 interactor, providing intersections with PATL2 role in oxidative stress responses, together with the CAT1 and CAT2 overlap. ANN proteins 1-3, of which at least one is present in nearly every our interactomes, also come to the fore. They are typical oxidative stress-induced proteins with Ca^{2+}-dependence (Demidchik, 2018). It was proposed that ANN proteins can form ROS-regulated Ca^{2+}-carriers (Laohavisit et al., 2009; Baucher et al., 2012) or being mediator and membrane anchor of Ca^{2+}-channels (Konopka-Postupolska and Clark, 2017). Mammalian ANN is suggested to be involved in membrane fusions, playing a role in vesicle trafficking, by interacting with SNARE proteins (Gerelsaikhan et al., 2012). During Fe deficiency, intracellular Ca^{2+}-concentration increases and activates potential Ca^{2+}-signaling cascades (Tian et al., 2016; Gratz et al., 2019). Ca^{2+} takes place in IRT1 regulation through interactions with EHB1 or CIPK23 (Dubeaux et al., 2018; Khan et al., 2019). We demonstrated that Ca^{2+} is also of particular importance in the transcriptional control of the iron response, through the interaction of CIPK11 with FIT and the positive influence on FIT activity (Gratz et al., 2019). ROS also play a major role in Fe homeostasis. H_2O_2 levels increase under prolonged Fe deficiency and possibly these ROS levels could be important for FIT activity (Le et al., 2015; Gratz et al., 2021). In addition, H_2O_2-dependent induction of transcription factor *ZAT12*, resulting in FIT inactivation by interaction and thereby preventing dimerization with bHLHs Ib (Davletova et al., 2005; Le et al., 2015). In this context, ANN1-3 membrane binding could be induced by ROS and interactions with our Fe-related genes to act as a Ca^{2+}-carrier, providing a link in Ca^{2+}-ROS-signaling.

Taken together, we could show here, that IP-MS is not only a good approach to identify new interactors in a broad range *in vivo* but can also give a potential overview of regulatory pathways and open ideas for further functions. Compared to the still excessively used Y2H screens, IP-MS approaches have the crucial advantage of working in the own organism. In addition, certain conditions can be created, such as Fe deficiency in our case. However, a major disadvantage is the production of material, especially in plant research. Although MS is also becoming more and more sensitive, a suitable amount of protein must be present in the samples. The cultivation of plants is not only a time consuming but also a much more space consuming task compared to cell culture or bacterial expression. We have therefore taken

constitutively expressing transgenic plant lines to ensure sufficient expression of our target gene. However, overexpression can of course also lead to altered behavior in the cell, so the use of the endogenous promoter should be considered. Especially the last years approved that IP-MS approaches are a good alternative in PPI identification and confirmation, as well as in the detection of regulatory networks.

We revealed many interconnections in our obtained data sets and highlighted here some of them. The stated hypotheses have to be proven in future studies. The study presents a broad overview of the biological processes and signaling events related to plant Fe homeostasis, provides a database for Fe-related PPIs and opens up a variety of opportunities for further understanding the mechanistic details of plant signaling and stress responses.

Materials & Methods

Arabidopsis plant growth

Arabidopsis plants were grown in a two-week growth system. Seed sterilization was performed in sodium hypochlorite solution (6 % Sodium hypochlorite and 0.1 % Triton X-100) with a 24 hours storage at 4°C for stratification. Seedlings were grown upright for two weeks on Hoagland media plates (1.5 mM $Ca(NO_3)_2$, 0.5 mM KH_2PO_4, 1.25 mM KNO_3, 0.75 mM $MgSO_4$, 1.5 µM $CuSO_4$, 50 µM H_3BO_3, 50 µM KCl, 10 µM $MnSO_4$, 0.075 µM $(NH_4)_6Mo_7O_{24}$, 2 µM $ZnSO_4$ and 1 % sucrose, pH 5.8, supplemented with 1.4 % Plant agar (Duchefa)] with sufficient (50 µM FeNaEDTA, + Fe) Fe supply in growth chambers (CLF Plant Climatics) under long day condition (16 hours light at 21°C, 8 hours darkness at 19°C). After 14 days, seedlings were transferred to either fresh Fe-sufficient or Fe-deficient media (Hoagland media with (0 µM FeNaEDTA, - Fe) for additional three days.

Generation of HA_3-tagged constitutively expressing lines

TTN5, *TTN5*^{Q70L} and *TTN5*^{T30N} coding sequences with stop codons were amplified using TITAN5 n-ter B1 and TITAN5 stop B2 primer to create a Gateway-compatible (Life Technology) insert. The PCR fragment was cloned into pDONR207 (Invitrogen) via BP reaction (Life Technology). To create triple HA-tagged TTN5, plasmid pALLIGATOR2 (Bensmihen et al., 2004) was used (LR reaction, Life Technology). For generating HA_3-PATL2, *PATL2* coding sequence was amplified using primer pair PAT2 nter B1 and PAT2 stop B2. *IDI1* CDS was amplified using Kelch fw N-attB1 and Kelch bw N-attB2. The cloning strategies followed the same steps as for TTN5 constructs. Agrobacteria were transformed with pALLIGATOR2:HA_3-TTN5, pALLIGATOR2:HA_3-TTN5^{Q70L}, pALLIGATOR2:HA_3-TTN5^{T30N}, HA_3-PATL2 or HA_3-IDI1 and used for stable Arabidopsis transformation (adapted by Clough and Bent, 1998).

2 ml YEB media were inoculated with a tested colony and grown overnight at 28°C while shaking. Overnight culture was used to inoculate a 200 ml YEB culture and grown again overnight at 28°C while shaking. The culture was centrifuged for 30 min at 5000*g* at 4°C. The supernatant was removed and the pellet was resuspended in 800 ml Arabidopsis transformation buffer (5 % sucrose, 10 mM $MgCl_2*6H_2O$, 0.05 % Silwet Gold). Col-0 plants were immersed with their flower buds in the Arabidopsis transformation buffer for 2 min and stored for 24 hours in a plastic bag. Plants were grown under long day conditions until they produced seeds.

Generation of HA_3-EHB1 line and is described in (Khan et al., 2019).

All primer pairs used in this study are listed in Supplemental Table 1.

Gene expression analysis by RT-qPCR

Plants were grown in the two-week system and roots were chosen for gene expression analysis using absolute transcript quantification via mass standard curve analysis as described in (Mohr et al., unpublished, Manuscript II). RT-qPCR was performed in three biological replicates (n = 3) with two technical replicates each. All primer pairs used in this study are listed in Supplemental Table 1.

***Nicotiana benthamiana* leaf infiltration**

Agrobacterium (*Rhizobium radiobacter*) strain C58 (GV3101) was used for *N. benthamiana* leaf infiltration and subsequent confocal microscopy. The designated constructs were transferred into Agrobacteria. For leaf infiltration cultures were grown at 28°C overnight, centrifuged for 5 min at 5000*g* and 4°C, followed by resuspension in infiltration solution (5 % sucrose, a pinch of glucose, 0.01 % Silwet Gold, 150 µM Acetosyringone) and incubated for 1 hour at RT. The abaxial sides of *N. benthamiana* leaves were infiltrated with bacterial suspension with an OD_{600}=0.4.

Bimolecular Fluorescence Complementation (BiFC)

The interaction studies of TTN5 and the respective GTPase active ($TTN5^{Q70L}$) or inactive ($TTN5^{T30N}$) variants *in planta* were performed by using BiFC. TTN5 constructs are described in (Mohr et al., unpublished, Manuscript II) and the used PATL2 constructs are described in (Hornbergs et al., Bauer lab, unpublished). *SEC12*, *AHA1* and *AHA2* coding sequences with stop codon were amplified using the primer SEC12 n-ter B3 and SEC12 stop B2, AHA1 n-ter B3 and AHA1 stop B2 and AHA2 n-ter B3 and AHA2 stop B2 respectively. The amplified PCR products were cloned via Gateway BP reaction (Life Technologies) into pDONR221-P3P2 (Invitrogen). The obtained constructs were used in an LR reaction (Life Technologies) for cloning into pBiFCt-2in1-NN vectors (Grefen and Blatt, 2012). Agrobacteria transformed with

the indicated constructs were used for *N. benthamiana* leaf infiltration. After 48 hours, the mRFP expression control signal and YFP signals were detected by fluorescence microscopy. The BiFC constructs were tested in three independent replicates (n = 3) with three infiltrated leaves each.

The vectors pBiFC-2in1-NN and pBiFC-2in1-NC were kindly provided by Dr. Christopher Grefen, Tübingen, Germany.

Subcellular localization of fluorescent protein fusions

YFP-TTN5, YFP-TTN5^{T30N} and YFP-TTN5^{Q70L} were created via Gateway cloning into destination vector pH7WGY2 (Karimi et al., 2005). Detailed description in (Mohr et al., unpublished, Manuscript II). AHA1-mRFP is described in (Caesar et al., 2011). Constructs were used for localization in *N. benthamiana* leaf epidermal cells via agrobacteria transformation.

JACoP based colocalization analysis

The ImageJ (Schneider et al., 2012) Plugin 'Just Another Colocalization Plugin' (JACoP, Bolte and Cordelières, 2006) was used to determine Pearson coefficient for further colocalization analysis. Analysis was performed in three replicates each (n = 3).

Immunoprecipitation

Immunoprecipitation with following mass spectrometry analysis was performed with Arabidopsis seedlings grown in the two-week growth system under Fe-sufficient and -deficient conditions. The TTN5 constitutively expressing lines HA_3-TTN5, HA_3-TTN5^{T30N} and HA_3-TTN5^{Q70L}, HA_3-PATL2, HA_3-EHB1 and HA_3-IDI1, were analyzed in comparison with a WT control line. Roots of approximately 150 seedlings (TTN5, TTN5^{T30N}, TTN5^{Q70L} and PATL2) or 75 seedlings (EHB1 and IDI1) were separated from the shoots and flash frozen in liquid nitrogen. The frozen roots were grinded using the Precellys® 24 with Cryolys® cooling unit (VWR) in the presence of 1.4 mm Precellys® zirconium oxide beads (Bertin Corp.) three times for 20 sec. Grinded material was solubilized in 1 ml IP Buffer (50 mM Tris-HCl, 150 mM NaCl, 1 mM EDTA, 1 % Triton X-100 and cOmpete Mini Protease Inhibitor, pH 9 (TTN5, TTN5^{T30N} and TTN5^{Q70L}), pH 8 (EHB1, IDI), pH 7.4 (PATL2). Solution was incubated for 10 min at room temperature followed by a 10 min centrifugation at 4°C and 17.000*g* (max speed). The supernatant was transferred into a fresh 1.5 ml reaction tube. The centrifugation step was repeated until all cellular debris were removed. 50 µl were taken as Crude Extract (CE) aliquot. 25 µl anti-HA magnetic beads (Thermo Scientific, Pierce) were added to the solution and reaction was incubated overnight at 4°C while rotating. A magnet was used to collect the beads at the side of the reaction tube and solution was transferred to a fresh 1.5 ml reaction tube (Flow through). 1 ml IP buffer was added to wash beads (Wash I). Collection of supernatant

and washing procedure was repeated for a total number of five washing steps. Each IP was performed in five replicates each (n = 5).

Mass Spectrometry

IP samples were processed for further MS analysis by in-gel digestion, described in (Grube et al., 2018). Briefly, samples were shortly separated (~5 mm running distance) in Bis-Tris buffered 4–12 % acrylamide gels (Thermo Fisher Scientific, Waltham, MA, USA). After silver staining and band processing, in-gel digest was performed using trypsin. Peptides were extracted from the gel and finally processed for MS. Obtained peptide samples were separated on an Ultimate 3000 rapid separation liquid chromatography system (RSLS, Thermo Fisher Scientific) by a 1 hour (TTN5, TTN5^{T30N}, TTN5^{Q70L}, PATL2) or 2 hour gradient (EHB1, IDI1). The separated peptides were detected by a coupled QExactive plus quadrupole/orbitrap mass spectrometer (Thermo Fisher Scientific) (EHB1, IDI1, TTN5, TTN5^{T30N}, TTN5^{Q70L}) or Orbitrap Fusion Lumos Tribrid mass spectrometer (Thermo Fisher Scientific) (PATL2). Mass spectrometers were operated in data-dependent positive mode. Firstly, resolution 70,000 (EHB1, IDI1, TTN5, TTN5^{T30N}, TTN5^{Q70L}) or 120,000 (PATL2) over a scan range of 350-2000 m/z (EHB1) or 200-2000 m/z (IDI1, TTN5, TTN5^{T30N}, TTN5^{Q70L}, PATL2). Then, up to 10 twofold- and threefold- (EHB1, IDI1, TTN5^{T30N}, TTN5^{Q70L}), twofold- to fivefold- (TTN5), or twofold- to sevenfold-charged (PATL2) precursors were isolated by the build in quadrupole (isolation window: 2 m/z (EHB1, IDI1), 4 m/z (TTN5, TTN5^{T30N}, TTN5^{Q70L}) or 1.6 m/z (PATL2)) and fragmented via higher-energy collisional dissociation. The fragment spectra were recorded with an available scan range of 200-2000 m/z (EHB1, IDI1, TTN5, TTN5^{T30N}, TTN5^{Q70L}) or in the ‘auto’-mode (PATL2) at a resolution of 17,500. For 10 sec (TTN5, TTN5^{T30N}, TTN5^{Q70L}), 60 sec (PATL2) or 100 sec (EHB1, IDI1), already fragmented precursors were excluded from fragmentation.

Recorded MS data was further analyzed using MaxQuant software (version 1.5.3.30 (EHB1, IDI1), 1.6.1.0 (TTN5), 1.6.6.0 (PATL2) and 1.6.17.0 (TTN5^{T30N}, TTN5^{Q70L}), Max Planck Institute of Biochemistry, Martinsried, Germany) with standard parameters. Searches were based on entries of the *Arabidopsis thaliana* proteome set (UP000006548, downloaded on 05.09.2017 (EHB1, IDI1), 05.07.2018 (TTN5), 04.11.2019 (PATL2) and 03.08.2021 (TTN5^{T30N}, TTN5^{Q70L})) from the UniProt Knowledgebase. Label-free quantification (LFQ) was enabled and proteins had to be detected by at least two different peptides and four valid values in at least one group. Perseus (version 1.6.1.1 (TTN5) 1.6.6.0 (PATL2, TTN5^{T30N}, TTN5^{Q70L}), 1.6.2.2 (EHB1, IDI1) Max Planck Institute of Biochemistry, Martinsried, Germany) was used for further processing. Detected intensities were log2 transformed and missing values were imputed by replacement with randomized values from the normal distribution (width 0.3 SD, downshift 1.8 SD).

Statistical enrichment compared to WT was identified by two-tailed two-sample Student's t-tests (S0 0.1, FDR 0.05 [EHB1, IDI1, PATL2], S0 0.6, FDR 0.05 [TTN5], S0 0.05, FDR 0.05 [$TTN5^{T30N}$, $TTN5^{Q70L}$]).

One n of each replicate set was removed from TTN5 analysis (n = 4), because of lacking similarity to the other samples based on principle component analysis. For the PATL2 set-up one n (WT, +Fe) was removed (n = 4). As an additional cut-off, proteins had to appear at least three times in the HA_3-TTN5 (HA_3-$TTN5_{T30N}$, HA_3-$TTN5_{Q70L}$, HA_3-PATL2, HA_3-EHB1) samples and less than three times in WT control samples.

Statistical Analysis

Statistical analysis was performed in OriginPro 2019 via one-way ANOVA with subsequent Fisher LSD post-hoc test ($p < 0.05$).

ACCESSION NUMBERS

Sequence data from this article can be found in the TAIR and GenBank data libraries under accession numbers:

AHA1 TAIR: (AT2G18960), *AHA2* TAIR: (AT4G30190), *EHB1* (TAIR: AT1G70800), *IDI1* TAIR (AT3G07720), *IRT1* (TAIR: AT4G19690), *PATL2* (TAIR: AT1G22530), *SEC12* (TAIR: AT2G01470), *TTN5* (TAIR: AT2G18390).

Acknowledgements

We thank Gintaute Matthäi and Elke Wieneke for excellent technical assistance. We acknowledge the contribution of the students Sam Seidel and Katharina Jürgens. We thank Ksenia Trofimov for the microscopic help and advice. We are thankful for the excellent assistance from Stefanie Weidtkamp-Peters, Miriam Bäumers and Sebastian Hänsch, members of the Center for Advanced Imaging (CAi) at the Heinrich Heine University.

This work was supported by the Deutsche Forschungsgemeinschaft (DFG, German Research Foundation Project no. 267205415–SFB 1208 and project B05 to P.B., project Z01 to K.S. and project Z02 to S.W.-P.)

References

Antoshechkin I, Han M (2002) The *C. elegans* evl-20 Gene Is a Homolog of the Small GTPase ARL2 and Regulates Cytoskeleton Dynamics during Cytokinesis and Morphogenesis. Developmental Cell **2:** 579-591

Barberon M, Zelazny E, Robert S, Conéjéro G, Curie C, Friml J, Vert G (2011) Monoubiquitin-dependent endocytosis of the IRON-REGULATED TRANSPORTER 1 (IRT1) transporter

controls iron uptake in plants. Proceedings of the National Academy of Sciences **108:** E450-E458

Barlowe C, Schekman R (1993) SEC12 encodes a guanine-nucleotide-exchange factor essential for transport vesicle budding from the ER. Nature **365:** 347-349

Baucher M, Pérez-Morga D, El Jaziri M (2012) Insight into plant annexin function. Plant Signaling & Behavior **7:** 524-528

Bensmihen S, To A, Lambert G, Kroj T, Giraudat J, Parcy F (2004) Analysis of an activated ABI5 allele using a new selection method for transgenic Arabidopsis seeds. FEBS Lett **561:** 127-131

Bermúdez L, del Pozo T, Silvestre Lira B, de Godoy F, Boos I, Romanò C, Previtali V, Almeida J, Bréhélin C, Asis R, Quadrana L, Demarco D, Alseekh S, Salinas Gamboa R, Pérez-Flores L, Dominguez PG, Rothan C, Fernie AR, González M, Stocker A, Hemmerle A, Clausen MH, Carrari F, Rossi M (2018) A Tomato Tocopherol-Binding Protein Sheds Light on Intracellular α-Tocopherol Metabolism in Plants. Plant and Cell Physiology **59:** 2188-2203

Bhamidipati A, Lewis SA, Cowan NJ (2000) ADP ribosylation factor-like protein 2 (Arl2) regulates the interaction of tubulin-folding cofactor D with native tubulin. Journal of Cell Biology **149:** 1087-1096

Boisson B, Giglione C, Meinnel T (2003) Unexpected Protein Families Including Cell Defense Components Feature in the N-Myristoylome of a Higher Eukaryote*. Journal of Biological Chemistry **278:** 43418-43429

Bolte S, Cordelières FP (2006) A guided tour into subcellular colocalization analysis in light microscopy. J Microsc **224:** 213-232

Bontinck M, Van Leene J, Gadeyne A, De Rybel B, Eeckhout D, Nelissen H, De Jaeger G (2018) Recent Trends in Plant Protein Complex Analysis in a Developmental Context. Frontiers in plant science **9:** 640-640

Brandizzi F (2018) Transport from the endoplasmic reticulum to the Golgi in plants: Where are we now? Semin Cell Dev Biol **80:** 94-105

Brumbarova T, Bauer P, Ivanov R (2015) Molecular mechanisms governing Arabidopsis iron uptake. Trends Plant Sci **20:** 124-133

Brumbarova T, Ivanov R (2019) The Nutrient Response Transcriptional Regulome of Arabidopsis. iScience **19:** 358-368

Burow M, Losansky A, Müller R, Plock A, Kliebenstein DJ, Wittstock U (2008) The Genetic Basis of Constitutive and Herbivore-Induced ESP-Independent Nitrile Formation in Arabidopsis Plant Physiology **149:** 561-574

Caesar K, Elgass K, Chen Z, Huppenberger P, Witthöft J, Schleifenbaum F, Blatt MR, Oecking C, Harter K (2011) A fast brassinolide-regulated response pathway in the plasma membrane of *Arabidopsis thaliana*. The Plant Journal **66:** 528-540

Cheng G, Yang Z, Zhang H, Zhang J, Xu J (2020) Remorin interacting with PCaP1 impairs Turnip mosaic virus intercellular movement but is antagonised by VPg. New Phytologist **225:** 2122-2139

Clough SJ, Bent AF (1998) Floral dip: a simplified method for Agrobacterium-mediated transformation of *Arabidopsis thaliana*. Plant J **16:** 735-743

Colangelo EP, Guerinot ML (2004) The Essential Basic Helix-Loop-Helix Protein FIT1 Is Required for the Iron Deficiency Response. The Plant Cell **16:** 3400-3412

d'Enfert C, Gensse M, Gaillardin C (1992) Fission yeast and a plant have functional homologues of the Sar1 and Sec12 proteins involved in ER to Golgi traffic in budding yeast. The EMBO journal **11:** 4205-4211

Dascher C, Balch WE (1994) Dominant inhibitory mutants of ARF1 block endoplasmic reticulum to Golgi transport and trigger disassembly of the Golgi apparatus. J Biol Chem **269:** 1437-1448

Davletova S, Rizhsky L, Liang H, Shengqiang Z, Oliver DJ, Coutu J, Shulaev V, Schlauch K, Mittler R (2005) Cytosolic Ascorbate Peroxidase 1 Is a Central Component of the Reactive Oxygen Gene Network of Arabidopsis. The Plant Cell **17:** 268-281

De Craene J-O, Courte F, Rinaldi B, Fitterer C, Herranz MC, Schmitt-Keichinger C, Ritzenthaler C, Friant S (2014) Study of the Plant COPII Vesicle Coat Subunits by Functional Complementation of Yeast *Saccharomyces cerevisiae* Mutants. PLOS ONE **9:** e90072

Demidchik V (2018) ROS-Activated Ion Channels in Plants: Biophysical Characteristics, Physiological Functions and Molecular Nature. International journal of molecular sciences **19:** 1263

Diaz M, Sanchez-Barrena MJ, Gonzalez-Rubio JM, Rodriguez L, Fernandez D, Antoni R, Yunta C, Belda-Palazon B, Gonzalez-Guzman M, Peirats-Llobet M, Menendez M, Boskovic J,

Marquez JA, Rodriguez PL, Albert A (2016) Calcium-dependent oligomerization of CAR proteins at cell membrane modulates ABA signaling. Proc Natl Acad Sci U S A **113:** E396-405

Dinneny JR, Long TA, Wang JY, Jung JW, Mace D, Pointer S, Barron C, Brady SM, Schiefelbein J, Benfey PN (2008) Cell Identity Mediates the Response of Arabidopsis Roots to Abiotic Stress. Science **320:** 942-945

Dubeaux G, Neveu J, Zelazny E, Vert G (2018) Metal Sensing by the IRT1 Transporter-Receptor Orchestrates Its Own Degradation and Plant Metal Nutrition. Molecular Cell **69:** 953-964.e955

Eide D, Broderius M, Fett J, Guerinot ML (1996) A novel iron-regulated metal transporter from plants identified by functional expression in yeast. Proceedings of the National Academy of Sciences **93:** 5624-5628

Falhof J, Pedersen Jesper T, Fuglsang Anja T, Palmgren M (2016) Plasma Membrane H^+-ATPase Regulation in the Center of Plant Physiology. Molecular Plant **9:** 323-337

Fernandez-Calvino L, Faulkner C, Walshaw J, Saalbach G, Bayer E, Benitez-Alfonso Y, Maule A (2011) Arabidopsis Plasmodesmal Proteome. PLOS ONE **6:** e18880

Fleming JA, Vega LR, Solomon F (2000) Function of tubulin binding proteins *in vivo*. Genetics **156:** 69-80

Fourcroy P, Sisó-Terraza P, Sudre D, Savirón M, Reyt G, Gaymard F, Abadía A, Abadia J, Álvarez-Fernández A, Briat J-F (2014) Involvement of the ABCG37 transporter in secretion of scopoletin and derivatives by Arabidopsis roots in response to iron deficiency. New Phytologist **201:** 155-167

Galau GA, Wang HY, Hughes DW (1993) Cotton Lea5 and Lea14 encode atypical late embryogenesis-abundant proteins. Plant Physiol **101:** 695-696

Gerelsaikhan T, Vasa PK, Chander A (2012) Annexin A7 and SNAP23 interactions in alveolar type II cells and *in vitro*: A role for Ca^{2+} and PKC. Biochimica et Biophysica Acta (BBA) - Molecular Cell Research **1823:** 1796-1806

Gratz R, Manishankar P, Ivanov R, Köster P, Mohr I, Trofimov K, Steinhorst L, Meiser J, Mai HJ, Drerup M, Arendt S, Holtkamp M, Karst U, Kudla J, Bauer P, Brumbarova T (2019) CIPK11-Dependent Phosphorylation Modulates FIT Activity to Promote Arabidopsis Iron Acquisition in Response to Calcium Signaling. Dev Cell **48:** 726-740.e710

Gratz R, von der Mark C, Ivanov R, Brumbarova T (2021) Fe acquisition at the crossroad of calcium and reactive oxygen species signaling. Curr Opin Plant Biol **63:** 102048

Grefen C, Blatt MR (2012) A 2in1 cloning system enables ratiometric bimolecular fluorescence complementation (rBiFC). Biotechniques **53:** 311-314

Grube L, Dellen R, Kruse F, Schwender H, Stühler K, Poschmann G (2018) Mining the Secretome of C2C12 Muscle Cells: Data Dependent Experimental Approach To Analyze Protein Secretion Using Label-Free Quantification and Peptide Based Analysis. J Proteome Res **17:** 879-890

Hanzal-Bayer M, Renault L, Roversi P, Wittinghofer A, Hillig RC (2002) The complex of Arl2-GTP and PDEδ: from structure to function. The EMBO Journal **21:** 2095-2106

Harbort CJ, Hashimoto M, Inoue H, Niu Y, Guan R, Rombolà AD, Kopriva S, Voges MJEEE, Sattely ES, Garrido-Oter R, Schulze-Lefert P (2020) Root-Secreted Coumarins and the Microbiota Interact to Improve Iron Nutrition in Arabidopsis. Cell Host & Microbe **28:** 825-837.e826

Harper JF, Manney L, DeWitt ND, Yoo MH, Sussman MR (1990) The *Arabidopsis thaliana* plasma membrane $H(^+)$-ATPase multigene family. Genomic sequence and expression of a third isoform. Journal of Biological Chemistry **265:** 13601-13608

Haruta M, Burch HL, Nelson RB, Barrett-Wilt G, Kline KG, Mohsin SB, Young JC, Otegui MS, Sussman MR (2010) Molecular Characterization of Mutant Arabidopsis Plants with Reduced Plasma Membrane Proton Pump Activity Journal of Biological Chemistry **285:** 17918-17929

Haruta M, Gray WM, Sussman MR (2015) Regulation of the plasma membrane proton pump (H^+-ATPase) by phosphorylation. Current Opinion in Plant Biology **28:** 68-75

Haruta M, Sussman MR (2012) The effect of a genetically reduced plasma membrane protonmotive force on vegetative growth of Arabidopsis. Plant physiology **158:** 1158-1171

Hashimoto-Sugimoto M, Higaki T, Yaeno T, Nagami A, Irie M, Fujimi M, Miyamoto M, Akita K, Negi J, Shirasu K, Hasezawa S, Iba K (2013) A Munc13-like protein in Arabidopsis mediates H^+-ATPase translocation that is essential for stomatal responses. Nature Communications **4:** 2215

Huang D, Sun Y, Ma Z, Ke M, Cui Y, Chen Z, Chen C, Ji C, Tran TM, Yang L, Lam SM, Han Y, Shui G, Wei Z, Tan S, Liao K, Friml J, Miao Y, Jiang L, Chen X (2019) Salicylic acid-mediated plasmodesmal closure via Remorin-dependent lipid organization. Proceedings of the National Academy of Sciences **116:** 21274-21284

Ivanov R, Brumbarova T, Bauer P (2012) Fitting into the Harsh Reality: Regulation of Iron-deficiency Responses in Dicotyledonous Plants. Molecular Plant **5:** 27-42

Ivanov R, Vert G (2021) Endocytosis in plants: Peculiarities and roles in the regulated trafficking of plant metal transporters. Biology of the Cell **113:** 1-13

Jia F, Qi S, Li H, Liu P, Li P, Wu C, Zheng C, Huang J (2014) Overexpression of Late Embryogenesis Abundant 14 enhances Arabidopsis salt stress tolerance. Biochemical and Biophysical Research Communications **454:** 505-511

Joiner AMN, Fromme JC (2021) Structural basis for the initiation of COPII vesicle biogenesis. Structure **29:** 859-872.e856

Karimi M, De Meyer B, Hilson P (2005) Modular cloning in plant cells. Trends in Plant Science **10:** 103-105

Kerkeb L, Mukherjee I, Chatterjee I, Lahner B, Salt DE, Connolly EL (2008) Iron-induced turnover of the Arabidopsis IRON-REGULATED TRANSPORTER1 metal transporter requires lysine residues. Plant Physiol **146:** 1964-1973

Khan I, Gratz R, Denezhkin P, Schott-Verdugo SN, Angrand K, Genders L, Basgaran RM, Fink-Straube C, Brumbarova T, Gohlke H, Bauer P, Ivanov R (2019) Calcium-Promoted Interaction between the C2-Domain Protein EHB1 and Metal Transporter IRT1 Inhibits Arabidopsis Iron Acquisition. Plant Physiology **180:** 1564-1581

Konopka-Postupolska D, Clark G (2017) Annexins as Overlooked Regulators of Membrane Trafficking in Plant Cells. International Journal of Molecular Sciences **18:** 863

Kruse T, Ho K, Yoo H-D, Johnson T, Hippely M, Park J-H, Flavell R, Bobzin S (2008) In Planta Biocatalysis Screen of P450s Identifies 8-Methoxypsoralen as a Substrate for the CYP82C Subfamily, Yielding Original Chemical Structures. Chemistry & Biology **15:** 149-156

Laohavisit A, Mortimer JC, Demidchik V, Coxon KM, Stancombe MA, Macpherson N, Brownlee C, Hofmann A, Webb AAR, Miedema H, Battey NH, Davies JM (2009) Zea mays Annexins Modulate Cytosolic Free Ca^{2+} and Generate a Ca^{2+}-Permeable Conductance. The Plant Cell **21:** 479-493

Le CTT, Brumbarova T, Ivanov R, Stoof C, Weber E, Mohrbacher J, Fink-Straube C, Bauer P (2015) ZINC FINGER OF ARABIDOPSIS THALIANA12 (ZAT12) Interacts with FER-LIKE IRON DEFICIENCY-INDUCED TRANSCRIPTION FACTOR (FIT) Linking Iron Deficiency and Oxidative Stress Responses Plant Physiology **170:** 540-557

Mai H-J, Pateyron S, Bauer P (2016) Iron homeostasis in *Arabidopsis thaliana:* transcriptomic analyses reveal novel FIT-regulated genes, iron deficiency marker genes and functional gene networks. BMC Plant Biology **16:** 211

Martín-Barranco A, Spielmann J, Dubeaux G, Vert G, Zelazny E (2020) Dynamic Control of the High-Affinity Iron Uptake Complex in Root Epidermal Cells1. Plant Physiology **184:** 1236-1250

Matsushima R, Kondo M, Nishimura M, Hara-Nishimura I (2003) A novel ER-derived compartment, the ER body, selectively accumulates a β-glucosidase with an ER-retention signal in Arabidopsis. The Plant Journal **33:** 493-502

Mayer U, Herzog U, Berger F, Inzé D, Jürgens G (1999) Mutations in the PILZ group genes disrupt the microtubule cytoskeleton and uncouple cell cycle progression from cell division in Arabidopsis embryo and endosperm. European Journal of Cell Biology **78:** 100-108

McElver J, Patton D, Rumbaugh M, Liu C-m, Yang LJ, Meinke D (2000) The TITAN5 Gene of Arabidopsis Encodes a Protein Related to the ADP Ribosylation Factor Family of GTP Binding Proteins. The Plant Cell **12:** 1379-1392

McMahon C, Studer SM, Clendinen C, Dann GP, Jeffrey PD, Hughson FM (2012) The structure of Sec12 implicates potassium ion coordination in Sar1 activation. J Biol Chem **287:** 43599-43606

Memon AR (2004) The role of ADP-ribosylation factor and SAR1 in vesicular trafficking in plants. Biochim Biophys Acta **1664:** 9-30

Montag K, Hornbergs J, Ivanov R, Bauer P (2020) Phylogenetic analysis of plant multi-domain SEC14-like phosphatidylinositol transfer proteins and structure–function properties of PATELLIN2. Plant Molecular Biology **104:** 665-678

Mori R, Toda T (2013) The dual role of fission yeast Tbc1/cofactor C orchestrates microtubule homeostasis in tubulin folding and acts as a GAP for GTPase Alp41/Arl2. Molecular biology of the cell **24:** 1713-S1718

Murgia I, Tarantino D, Soave C, Morandini P (2011) Arabidopsis CYP82C4 expression is dependent on Fe availability and circadian rhythm, and correlates with genes involved in the early Fe deficiency response. J Plant Physiol **168:** 894-902

Nagata C, Miwa C, Tanaka N, Kato M, Suito M, Tsuchihira A, Sato Y, Segami S, Maeshima M (2016) A novel-type phosphatidylinositol phosphate-interactive, Ca-binding protein PCaP1 in *Arabidopsis thaliana*: stable association with plasma membrane and partial involvement in stomata closure. Journal of Plant Research **129:** 539-550

Nakano RT, Yamada K, Bednarek P, Nishimura M, Hara-Nishimura I (2014) ER bodies in plants of the Brassicales order: biogenesis and association with innate immunity. Frontiers in plant science **5:** 73-73

Nie C, Wang H, Wang R, Ginsburg D, Chen X-W (2018) Dimeric sorting code for concentrative cargo selection by the COPII coat. Proceedings of the National Academy of Sciences of the United States of America **115:** E3155-E3162

Obayashi T, Aoki Y, Tadaka S, Kagaya Y, Kinoshita K (2017) ATTED-II in 2018: A Plant Coexpression Database Based on Investigation of the Statistical Property of the Mutual Rank Index. Plant and Cell Physiology **59:** e3-e3

Palmer CM, Hindt MN, Schmidt H, Clemens S, Guerinot ML (2013) MYB10 and MYB72 Are Required for Growth under Iron-Limiting Conditions. PLOS Genetics **9:** e1003953

Radcliffe PA, Vardy L, Toda T (2000) A conserved small GTP-binding protein Alp41 is essential for the cofactor-dependent biogenesis of microtubules in fission yeast. FEBS Letters **468:** 84-88

Raffaele S, Bayer E, Lafarge D, Cluzet Sp, German Retana S, Boubekeur T, Leborgne-Castel N, Carde J-P, Lherminier J, Noirot E, Satiat-Jeunemaître Ba, Laroche-Traineau J, Moreau P, Ott T, Maule AJ, Reymond P, Simon-Plas Fo, Farmer EE, Bessoule J-J, Mongrand Sb (2009) Remorin, a Solanaceae Protein Resident in Membrane Rafts and Plasmodesmata, Impairs Potato virus X Movement. The Plant Cell **21:** 1541-1555

Rajniak J, Giehl RFH, Chang E, Murgia I, von Wirén N, Sattely ES (2018) Biosynthesis of redox-active metabolites in response to iron deficiency in plants. Nature Chemical Biology **14:** 442-450

Reyt G, Boudouf S, Boucherez J, Gaymard F, Briat J-F (2015) Iron- and Ferritin-Dependent Reactive Oxygen Species Distribution: Impact on Arabidopsis Root System Architecture. Molecular Plant **8:** 439-453

Robinson NJ, Procter CM, Connolly EL, Guerinot ML (1999) A ferric-chelate reductase for iron uptake from soils. Nature **397:** 694-697

Rodríguez-Celma J, Lin W-D, Fu G-M, Abadía J, López-Millán A-F, Schmidt W (2013) Mutually Exclusive Alterations in Secondary Metabolism Are Critical for the Uptake of Insoluble Iron Compounds by Arabidopsis and *Medicago truncatula* Plant Physiology **162:** 1473-1485

Rodriguez L, Gonzalez-Guzman M, Diaz M, Rodrigues A, Izquierdo-Garcia AC, Peirats-Llobet M, Fernandez MA, Antoni R, Fernandez D, Marquez JA, Mulet JM, Albert A, Rodriguez PL (2014) C2-domain abscisic acid-related proteins mediate the interaction of PYR/PYL/RCAR abscisic acid receptors with the plasma membrane and regulate abscisic acid sensitivity in Arabidopsis. Plant Cell **26:** 4802-4820

Römheld V, Marschner H (1986) Evidence for a Specific Uptake System for Iron Phytosiderophores in Roots of Grasses 1. Plant Physiology **80:** 175-180

Santi S, Schmidt W (2009) Dissecting iron deficiency-induced proton extrusion in Arabidopsis roots. New Phytologist **183:** 1072-1084

Schmid NB, Giehl RFH, Döll S, Mock H-P, Strehmel N, Scheel D, Kong X, Hider RC, von Wirén N (2013) Feruloyl-CoA 6′-Hydroxylase1-Dependent Coumarins Mediate Iron Acquisition from Alkaline Substrates in Arabidopsis Plant Physiology **164:** 160-172

Schmid NB, Giehl RFH, Döll S, Mock H-P, Strehmel N, Scheel D, Kong X, Hider RC, von Wirén N (2014) Feruloyl-CoA 6′-Hydroxylase1-Dependent Coumarins Mediate Iron Acquisition from Alkaline Substrates in Arabidopsis. Plant Physiology **164:** 160-172

Schneider CA, Rasband WS, Eliceiri KW (2012) NIH Image to ImageJ: 25 years of image analysis. Nature Methods **9:** 671-675

Schuler M, Bauer P (2011) Heavy Metals Need Assistance: The Contribution of Nicotianamine to Metal Circulation Throughout the Plant and the Arabidopsis NAS Gene Family. Frontiers in plant science **2:** 69-69

Schuler M, Rellán-Álvarez R, Fink-Straube C, Abadía J, Bauer P (2012) Nicotianamine functions in the Phloem-based transport of iron to sink organs, in pollen development and pollen tube growth in Arabidopsis. The Plant cell **24:** 2380-2400

Schwarz B, Azodi CB, Shiu S-H, Bauer P (2020) Putative *cis*-Regulatory Elements Predict Iron Deficiency Responses in Arabidopsis Roots1. Plant Physiology **182:** 1420-1439

Schwarz B, Bauer P (2020) FIT, a regulatory hub for iron deficiency and stress signaling in roots, and FIT-dependent and -independent gene signatures. Journal of Experimental Botany **71:** 1694-1705

Sharer JD, Kahn RA (1999) The ARF-like 2 (ARL2)-binding Protein, BART: PURIFICATION, CLONING, AND INITIAL CHARACTERIZATION. Journal of Biological Chemistry **274:** 27553-27561

Sharer JD, Shern JF, Van Valkenburgh H, Wallace DC, Kahn RA (2002) ARL2 and BART Enter Mitochondria and Bind the Adenine Nucleotide Transporter. Molecular Biology of the Cell **13:** 71-83

Shin L-J, Lo J-C, Chen G-H, Callis J, Fu H, Yeh K-C (2013) IRT1 degradation factor1, a ring E3 ubiquitin ligase, regulates the degradation of iron-regulated transporter1 in Arabidopsis. The Plant cell **25:** 3039-3051

Tanaka H, Nodzyłski T, Kitakura S, Feraru MI, Sasabe M, Ishikawa T, Kleine-Vehn J, Kakimoto T, Friml J (2014) BEX1/ARF1A1C is required for BFA-sensitive recycling of PIN auxin transporters and auxin-mediated development in Arabidopsis. Plant Cell Physiol **55:** 737-749

Tian Q, Zhang X, Yang A, Wang T, Zhang W-H (2016) CIPK23 is involved in iron acquisition of Arabidopsis by affecting ferric chelate reductase activity. Plant Science **246:** 70-79

Tian R, Wang F, Zheng Q, Niza VMAGE, Downie AB, Perry SE (2020) Direct and indirect targets of the arabidopsis seed transcription factor ABSCISIC ACID INSENSITIVE3. The Plant Journal **103:** 1679-1694

Tzafrir I, McElver JA, Liu C-m, Yang LJ, Wu JQ, Martinez A, Patton DA, Meinke DW (2002) Diversity of TITAN Functions in Arabidopsis Seed Development. Plant Physiology **128:** 38-51

Van der Ent S, Verhagen BWM, Van Doorn R, Bakker D, Verlaan MG, Pel MJC, Joosten RG, Proveniers MCG, Van Loon LC, Ton J, Pieterse CMJ (2008) MYB72 Is Required in Early Signaling Steps of Rhizobacteria-Induced Systemic Resistance in Arabidopsis Plant Physiology **146:** 1293-1304

Vernoud V, Horton AC, Yang Z, Nielsen E (2003) Analysis of the small GTPase gene superfamily of Arabidopsis. Plant Physiol **131:** 1191-1208

Vert G, Grotz N, Dédaldéchamp F, Gaymard F, Guerinot ML, Briat JF, Curie C (2002) IRT1, an Arabidopsis transporter essential for iron uptake from the soil and for plant growth. Plant Cell **14:** 1223-1233

von der Mark C, Ivanov R, Eutebach M, Maurino VG, Bauer P, Brumbarova T (2020) Reactive oxygen species coordinate the transcriptional responses to iron availability in Arabidopsis. Journal of Experimental Botany **72:** 2181-2195

Wang N, Cui Y, Liu Y, Fan H, Du J, Huang Z, Yuan Y, Wu H, Ling H-Q (2013) Requirement and Functional Redundancy of Ib Subgroup bHLH Proteins for Iron Deficiency Responses and Uptake in *Arabidopsis thaliana*. Molecular Plant **6:** 503-513

Wittstock U, Kliebenstein DJ, Lambrix V, Reichelt M, Gershenzon J (2003) Chapter five Glucosinolate hydrolysis and its impact on generalist and specialist insect herbivores. *In* JT Romeo, ed, Recent Advances in Phytochemistry, Vol 37. Elsevier, pp 101-125

Xing S, Wallmeroth N, Berendzen KW, Grefen C (2016) Techniques for the Analysis of Protein-Protein Interactions *in Vivo*. Plant physiology **171:** 727-758

Xue Y, Yang Y, Yang Z, Wang X, Guo Y (2018) VAMP711 Is Required for Abscisic Acid-Mediated Inhibition of Plasma Membrane H^+-ATPase Activity1[OPEN]. Plant Physiology **178:** 1332 - 1343

Yamada K, Goto-Yamada S, Nakazaki A, Kunieda T, Kuwata K, Nagano AJ, Nishimura M, Hara-Nishimura I (2020) Endoplasmic reticulum-derived bodies enable a single-cell chemical defense in Brassicaceae plants. Communications Biology **3:** 21

Yuan Y, Wu H, Wang N, Li J, Zhao W, Du J, Wang D, Ling HQ (2008) FIT interacts with AtbHLH38 and AtbHLH39 in regulating iron uptake gene expression for iron homeostasis in Arabidopsis. Cell Res **18:** 385-397

Zamioudis C, Hanson J, Pieterse CMJ (2014) β-Glucosidase BGLU42 is a MYB72-dependent key regulator of rhizobacteria-induced systemic resistance and modulates iron deficiency responses in Arabidopsis roots. New Phytologist **204:** 368-379

Zhou X, Hao H, Zhang Y, Bai Y, Zhu W, Qin Y, Yuan F, Zhao F, Wang M, Hu J, Xu H, Guo A, Zhao H, Zhao Y, Cao C, Yang Y, Schumaker KS, Guo Y, Xie CG (2015) SOS2-LIKE PROTEIN KINASE5, an SNF1-RELATED PROTEIN KINASE3-Type Protein Kinase, Is Important for Abscisic Acid Responses in Arabidopsis through Phosphorylation of ABSCISIC ACID-INSENSITIVE5 Plant Physiology **168:** 659-676

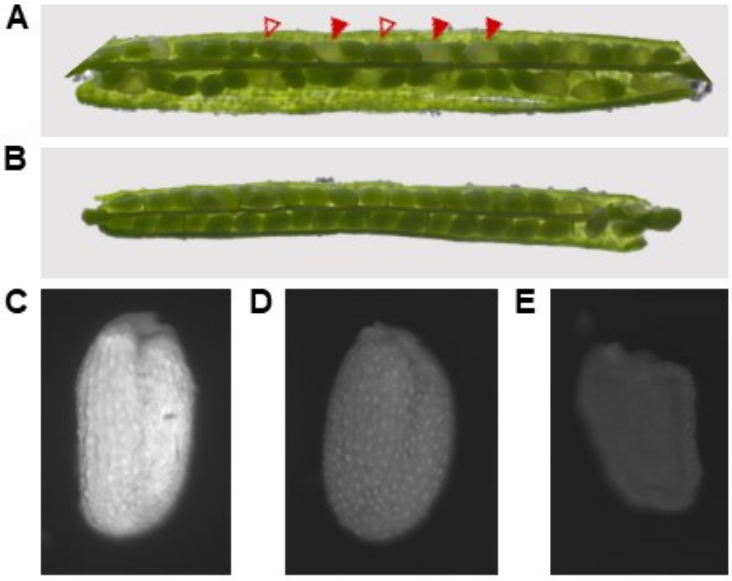

Supplemental Figure 1. HA_3-TTN5 can complement *ttn5-1*$^{+/-}$ embryonal seed phenotype.
(A), Siliques of heterozygous *ttn5-1*$^{+/-}$ plants contain 25 % of white seeds (highlighted by filled arrow heads) indicating aborted embryo development of homozygotes, heterozygotes develop similar to WT, visible as green seeds (highlighted by empty arrow head). (B), HA_3-TTN5 line crossed to *ttn5-1*$^{+/-}$ can rescue embryo lethal seed phenotype. (C-E), Representation of HA_3-TTN5-positive seed visible by its green fluorescence (C), HA_3-TTN5-negative seed (D) and an aborted one (E).

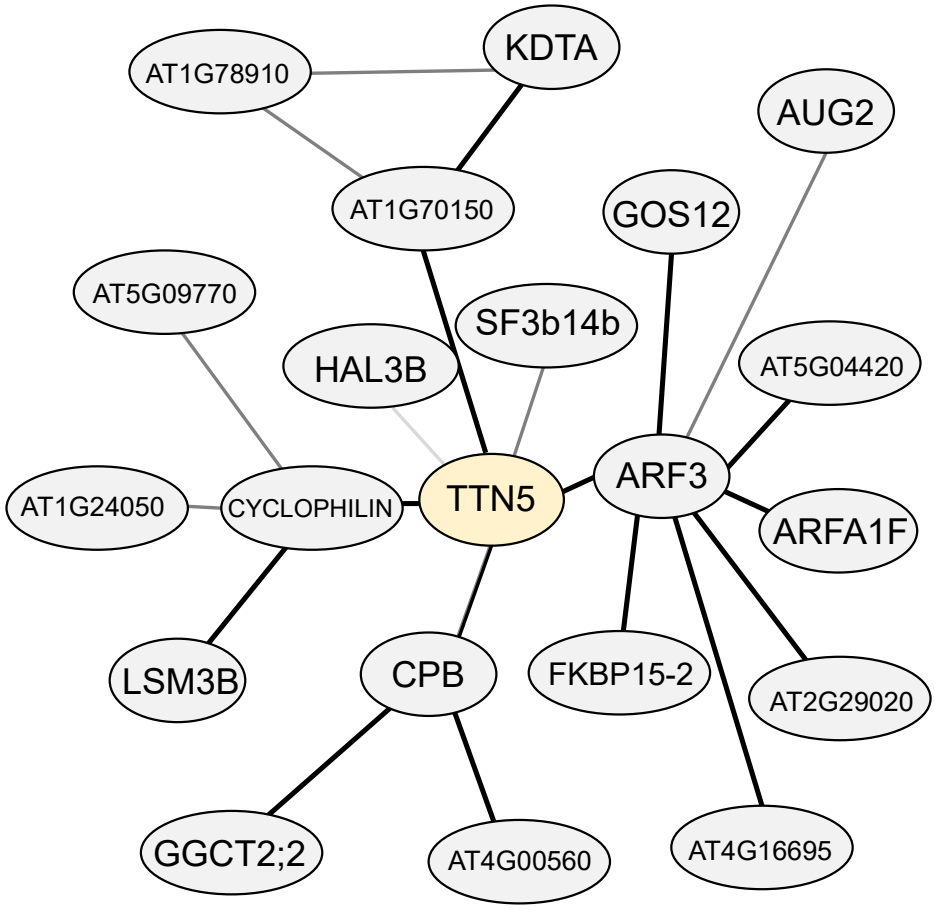

Supplemental Figure 2. TTN5 coexpression network.
TTN5 coexpression network was obtained using ATTED-II (Obayashi et al., 2017). It contains genes involved in endocytosis and spliceosome function.

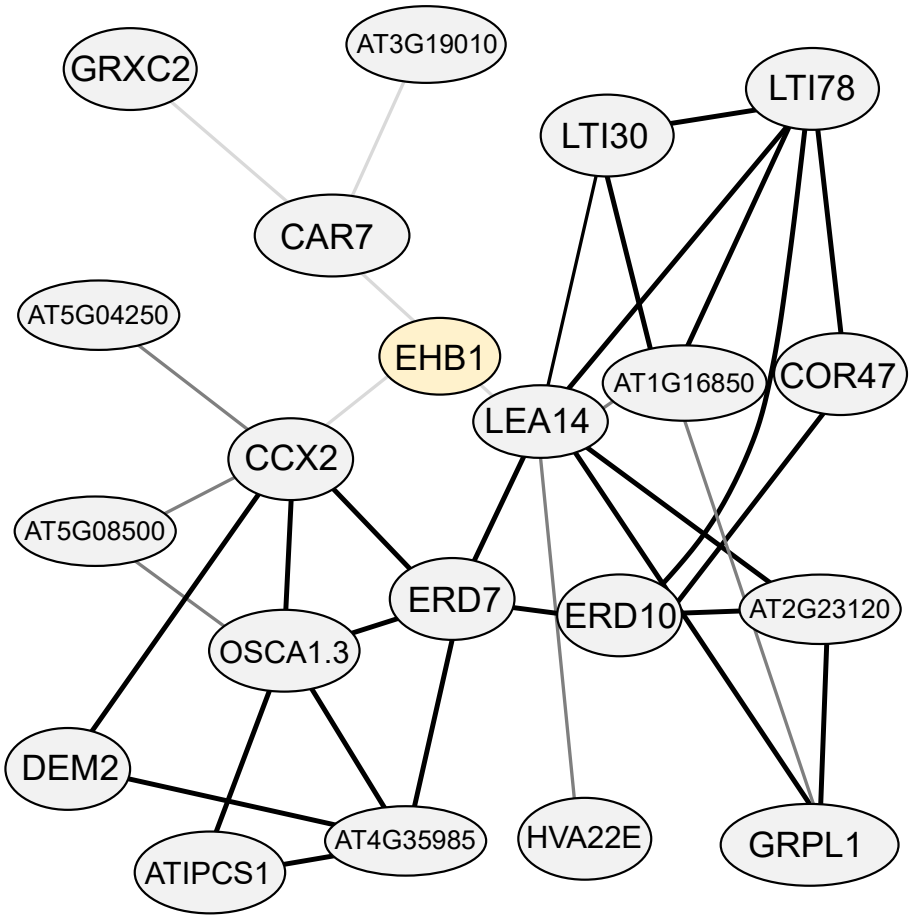

Supplemental Figure 3. EHB1 coexpression network.
EHB1 coexpression network was obtained using ATTED-II (Obayashi et al., 2017). Coexpressed genes are involved in stress-related processes, such as light, water and temperature or regulated by calcium.

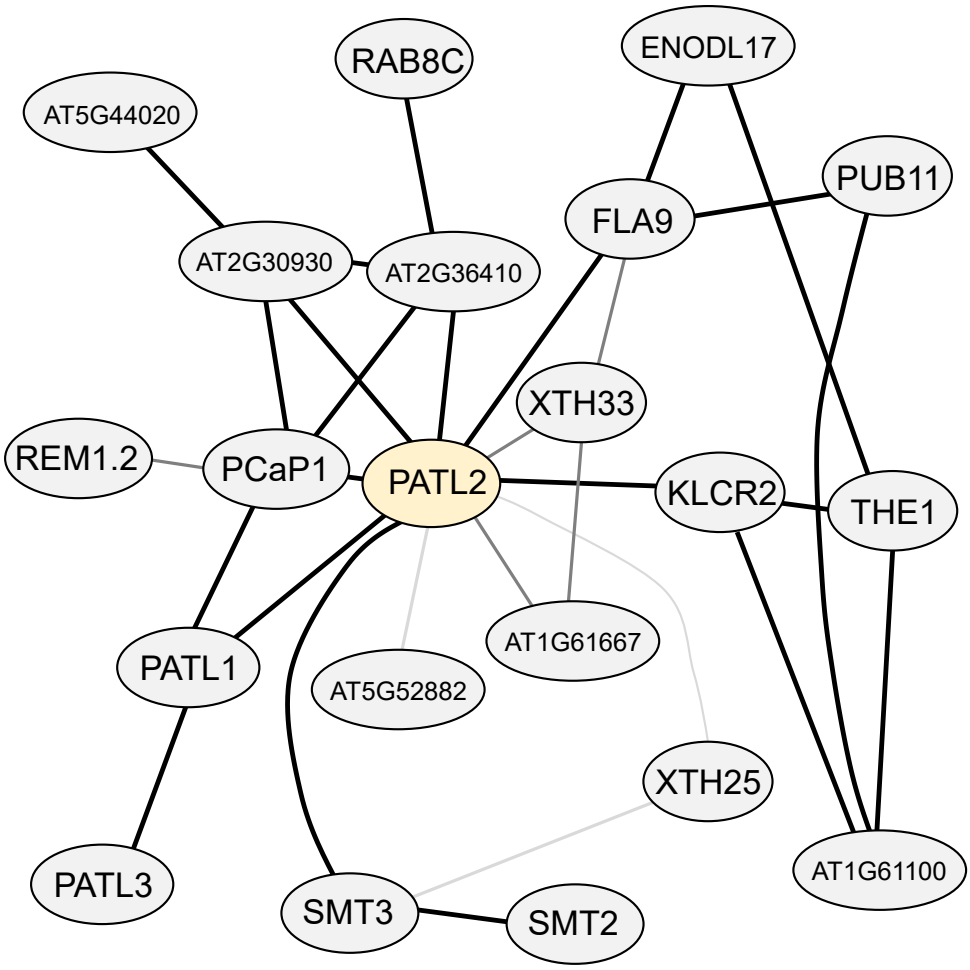

Supplemental Figure 4. PATL2 coexpression network.
PATL2 coexpression network was obtained using ATTED-II (Obayashi et al., 2017). Connected processes of coexpressed genes are widely spread, including among others steroid biosynthesis, embryogenesis with developmental processes and lipids.

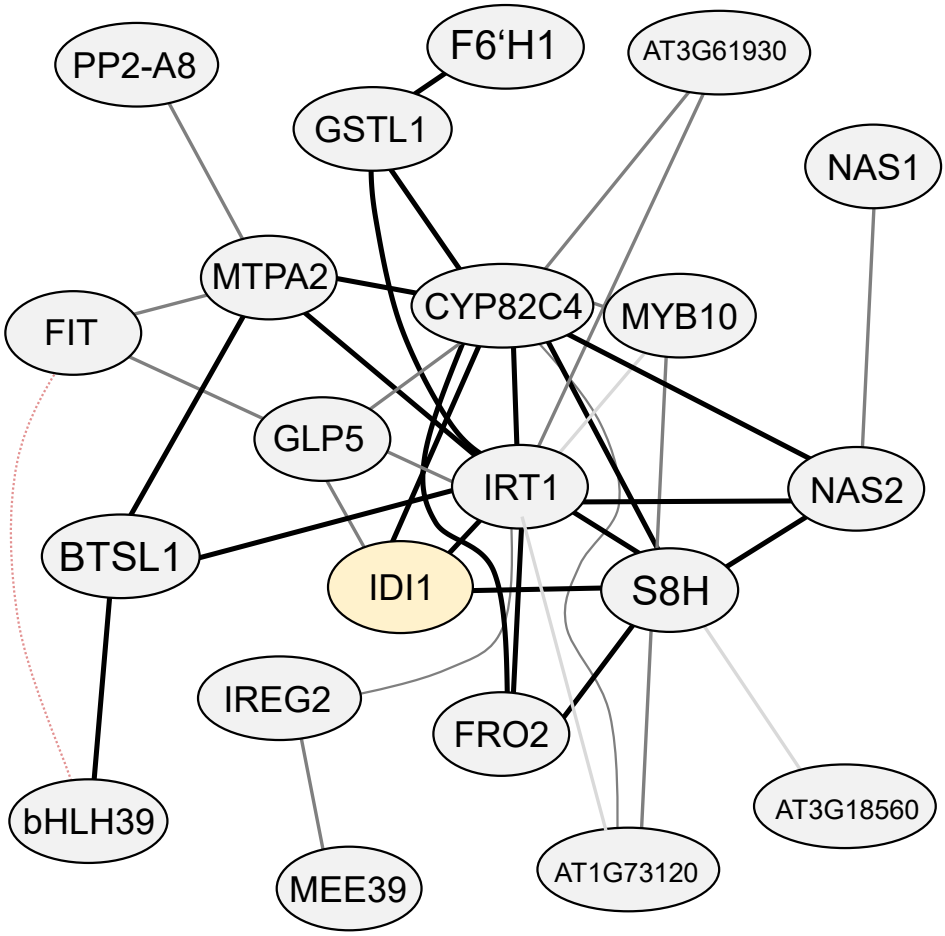

Supplemental Figure 5. IDI1 coexpression network.
IDI1 coexpression network was obtained using ATTED-II (Obayashi et al., 2017). IDI1 is stable up-regulated in Fe-deficient conditions as well as many of the coexpressed genes. Fe-related genes are for example involved Strategy I or Fe transport.

Supplemental Table 1. Primers used in this study.

Primer name	Primer sequence	Purpose	Origin
TITAN5 n-ter B1	ggggacaagtttgtacaaaaaagcaggcttt ATGGGACTGTTAAGCATAA	Cloning of pDONR207:TTN5s stop	Mohr et al., unpublished, MII
TITAN5 stop B2	ggggaccactttgtacaagaaagctgggt TTAGTCAAGCATGTAAATC	Cloning of pDONR207:TTN5s stop	Mohr et al., unpublished, MII
TITAN5 stop B4	ggggacaactttgtatagaaaagttgggt TTAGTCAAGCATGTAAATC	Cloning of pDONR221-P1P4:TTN5 st	this study
PATL2B1F _N	ggggacaagtttgtacaaaaaagcaggcttt ATGGCTCAAGAAGAGATACA	Cloning of pDONR207:PATL2 st and PATL2 RT-qPCR mass standard	Montag et al., 2020
PATL2B2stopR	ggggaccactttgtacaagaaagctgggt TTATGCTTGGGTTTTGGACC	Cloning of pDONR207:PATL2 st and PATL2 RT-qPCR mass standard	Montag et al., 2020
PAT2B3	ggggacaactttgtataataaagttg ATGGCTCAAGAAGAGATACAG	Cloning of pDONR221-P3P2:PATL2 ns and PATL2ΔN ns	Hornbergs et al., Bauer lab, unpublished
PAT2 ns B2	ggggaccactttgtacaagaaagctgggtt TGCTTGGGTTTTGGACCTGTAG	Cloning of pDONR221-P3P2:PATL2 ns and PATL2ΔC ns	Hornbergs et al., Bauer lab, unpublished
PATL2Δndr	ggggacaactttgtataataaagttg ATGCTTCTAGAGGACGAAAGATCC	Cloning of pDONR221-P3P2:PATL2 ns and PATL2ΔN ns	Hornbergs et al., Bauer lab, unpublished

PAT2Δdo	ggggaccactttgtacaagaaagctgggtt TGGGATTCCCCAGATTGAGAC	Cloning of pDONR221-P3P2:PATL2 ns and PATL2ΔC ns	Hornbergs et al., Bauer lab, unpublished
PATL2-RT-F	ACCGTTGAAGCAGTCGAAGA	PATL2 RT-qPCR	Hornbergs et al., Bauer lab, unpublished
PATL2-RT-R	GAGGAGGATCACGTCGGATCT	PATL2 RT-qPCR	Hornbergs et al., Bauer lab, unpublished
KELCH_B1 fw	ggggacaagtttgtacaaaaaagcaggcttc ATGGCAGCGACTCCAATG	Cloning of pDONR207:IDI1 st	Schwarz et al., unpublished
KELCHs_B2 rev	ggggaccactttgtacaagaaagctgggt CTCACTTGAGTAGAGTGTTGG	Cloning of pDONR207:IDI1 st	Schwarz et al., unpublished
AHA1 n-ter B3	ggggacaactttgtataataaagttgta ATGTCAGGTCTCGAAGATATCAAG	Cloning of pDONR221-P3P2:AHA1 stop	this study
AHA1 stop B2	ggggaccactttgtacaagaaagctgggtt CTACACAGTGTAGTGATGTCCTG	Cloning of pDONR221-P3P2:AHA1 stop	this study
AHA1 STD fwd	GGACAAGTTCGGTGTGAGGT	AHA1 RT-qPCR mass standard	this study
AHA1 STD rev	GGCCATTAAAAAGCAAAGTGC	AHA1 RT-qPCR mass standard	this study
AHA1 RT fwd	CACAAACATTTACCGAAAACCA	AHA1 RT-qPCR	Santi et al., 2009
AHA1 RT rev	CAAATTTGCAAAGCTCATATCG	AHA1 RT-qPCR	Santi et al., 2009
AHA2 n-ter B3	ggggacaactttgtataataaagttgta ATGTCGAGTCTCGAAGATAT	Cloning of pDONR221-P3P2:AHA2 stop	this study
AHA2 stop B2	ggggaccactttgtacaagaaagctgggt CTACACAGTGTAGTGACTGG	Cloning of pDONR221-P3P2:AHA2 stop	this study
AHA2 STD fwd	TGCTCAAAGGACACTTCACG	AHA2 RT-qPCR mass standard	this study
AHA2 STD rev	TTGCACGTGTCTCACAGTCA	AHA2 RT-qPCR mass standard	this study
AHA2 RT fwd	TGACTGATCTTCGATCCTCTCA	AHA2 RT-qPCR	Santi et al., 2009
AHA2 RT rev	GAGAATGTGCATGTGCCAAA	AHA2 RT-qPCR	Santi et al., 2009
SEC12 n-ter B3	ggggacaactttgtataataaagttgta ATGGCGAATCAGAGTACAGAG	Cloning of pDONR221-P3P2:SEC12 st	this study
SEC12 stop B2	ggggaccactttgtacaagaaagctgggtt CTAAGGTATGATACCCTTTGCC	Cloning of pDONR221-P3P2:SEC12 st	this study
SEC12 STD fwd	TTTTTGCGTAGAACGTGGTG	SEC12 RT-qPCR mass standard	this study
SEC12 STD rev	TGTTGAAAGAGTCTTACTGATCCA	SEC12 RT-qPCR mass standard	this study
SEC12 RT fwd	GATACAGCGGAATGGCTTGT	SEC12 RT-qPCR	this study
SEC12 RT rev	GGAAACAAATTGTAACTTTTGCTG	SEC12 RT-qPCR	this study

Author contributions to manuscript III

Inga Mohr

Designed, performed and analyzed the following experiments: Immunoprecipitations (Figure 1A, 2A, 5A, 6A, 7A), BiFC assays (Figures 3A-H, 9A-E, 10A-E), (Co) localization studies (Figure 4). Supervised and analyzed RT-qPCR (Figure 3I+J, 9F, 10F). Performed interactome analysis and GO enrichment analysis (Fig 1B-E, 2B-F, 5B-D, 6B-D, 7B-D, 8, Table 1). Prepared stable transgenic lines HA_3-TTN5, HA_3-TTN5^{T30N}, HA_3-TTN5^{Q70L}, HA_3-TTN5/*ttn5-1.* Prepared figures and tables, wrote and edited the manuscript.

Pichaporn Chuenban

Performed complementing seed phenotype analysis (Supplemental figure 1A+B).

Monique Eutebach

Performed RT-qPCR.

Claudia von der Mark

Prepared stable transgenic lines HA_3-IDI1.

Gereon Poschmann, Daniel Waldera-Lupa, Kai Stühler

Designed, performed and analyzed mass spectrometry experiments.

Petra Bauer

Conceived and supervised the study, acquired funding, reviewed/edited the manuscript.

Rumen Ivanov

Conceived and supervised the study, reviewed/edited the manuscript.

9. Concluding Remarks

The iron homeostasis with its included processes such as iron uptake, transport and storage is an already well-understood field. It is regulated by a broad range of different stimuli such as hormone-, calcium (Ca^{2+})- or reactive oxygen species (ROS)-signaling, transcriptional und post-translational regulation or direct protein-protein interactions. Though well-studied, many aspects of actual mechanisms or the interaction partners remain still elusive (Brumbarova and Ivanov, 2019; Gao et al., 2019; Gratz et al., 2021; Riaz and Guerinot, 2021).

The ADP-ribosylation factor (ARF) family of Ras small GTPases has a well-conserved function in vesicle trafficking especially in vesicle-coat formation (Vernoud et al., 2003). We identified the small ARF-like GTPase TITAN 5 (TTN5) as a novel interactor of IRON-REGULATED TRANSPORT 1 (IRT1). We were able to localize TTN5 to several sites, from the plasma membrane (PM), to the Golgi, to the *trans*-Golgi network (TGN) and multi vesicular bodies (MVBs), consistent with a role in vesicle transport. We identified IRT1 together with TTN5 in vesicle-like structures which were wortmannin-sensitive, indicating sorting endosomes and MVBs. In addition, we found interactions with the already known IRT1 regulators, ENHANCED BENDING 1 (EHB1) and SORTING NEXIN 1 (SNX1). EHB1 has an inhibitory role on IRT1 activity at the PM whereas SNX1 is involved in the sorting and recycling of the transporter back to the PM (Ivanov et al., 2014; Khan et al., 2019). The resulting network leads to the hypothesis that TTN5 has a coordinating role in IRT1 sorting fate, through interaction with IRT1 regulators. An influence of TTN5 on iron reductase activity and expression levels of several iron-regulated genes, suggests a general role in iron homeostasis, with a positive impact. The additional interaction found with plasma membrane H^+-ATPase AHA2 strengthens this assumption. To IRT1-similar colocalization data of TTN5 together with AHA1 promotes a hypothetical general involvement of TTN5 in intracellular transport of membrane proteins.

To date, no TTN5-guanine nucleotide exchange factor (GEF) is known and similar is the case for the well-studied homolog HsARL2. It was assumed that ARL2 does not need any help in the exchange, as it exhibits relatively weak binding of GDP and GTP (Fansa and Wittinghofer, 2016). Recent data, however, suggest a co-GEF activity of BINDER OF ARL2 (BART) on HsARL3 with the potential to act on HsARL2 in the same way. In this context, BART should help with the nucleotide exchange, which is complicated due to the lack of a myristoylated anchor of the HsARL3 (ElMaghloob et al., 2021). HsARL2 as well as TTN5 are also not myristoylated (Boisson et al., 2003; Kahn et al., 2006). The identification of SEC12, a SECRETION ASSOCIATED AND RAS-RELATED 1 (SAR1)-GEF in COPII, endoplasmic reticulum (ER) to Golgi, transport may play a similar role. SEC12 does not have the typical

Sec7 domain but is a β-propeller, ER transmembrane protein. Although SAR1 is a member of the ARF family, it does not have the conserved Gly-2, resulting in a not myristoylated N-terminus. Based on these prerequisites, we suspect a possible role of SEC12 as TTN5-GEF with further TTN5 function in ER-derived vesicle transport.

The use of immunoprecipitation-mass spectrometry-based (IP-MS) interactome analyses have distinct advantages over other protein-protein interaction methods. On the one hand, it allows working in the actual organism *in vivo*, and additional, the identification of different interaction partners at once is possible. A large-scale screen or a defined set of specific potential interacting proteins is not needed (Xing et al., 2016; Bontinck et al., 2018).

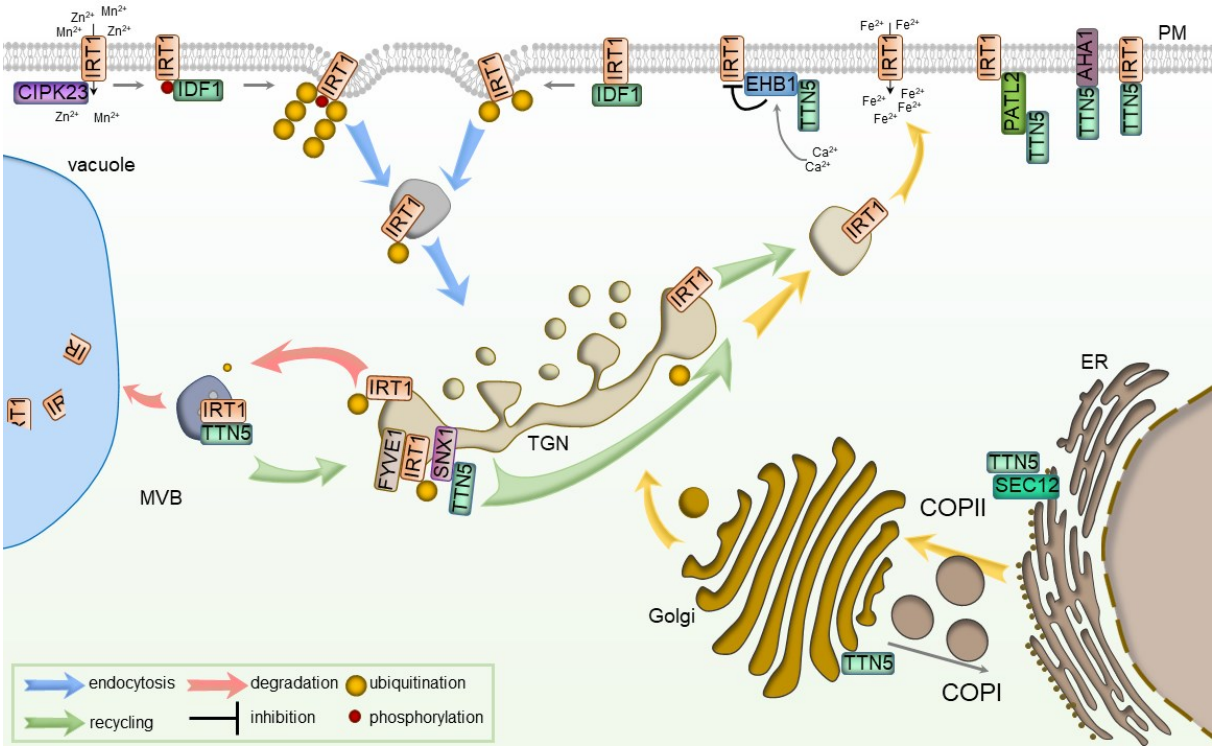

Figure 1. TTN5 within the endomembrane system.
TTN5 localized to different compartments within the endomembrane system. It was colocalizing with compartment markers at the plasma membrane (PM), the *cis*-Golgi and in multivesicular bodies (MVB). TTN5 interacted with IRT1 and together they colocalized at the PM and in MVBs. TTN5 interacted with AHA1 and together they were present at the PM and in MVBs, similarly to IRT1, promoting TTN5 involvement in intracellular cycling of the PM proteins. TTN5 interacted with IRT1 regulators, EHB1, SNX1 and PATL2 and thereby potentially influencing IRT1 regulation. The ER membrane-anchored SEC12 is a GEF protein and interacted with TTN5. SEC12 potentially possess TTN5-GEF activity.

By using IP-MS-based interactome analyses we could reveal and highlight connections between our known IRT1 regulators and iron-related genes. We could detect an enrichment for PATELLIN 2 (PATL2) related to oxidative damage. This fits very well with our hypothesis that PATL2 plays a role in the oxidative stress response, based on our data, indicating an increase of MDA in the absence of PATL2 (Hornbergs et al., Bauer lab, unpublished). An identified

interaction related to plasmodesmata regulation promotes our suggestion of PATL2-dependent α-tocopherol recruitment to prevent membrane damage due to ROS-induced lipid peroxidation

Of greater interest was the revealed connection of the EHB1 and IRON-DEFICIENCY INDUCED 1 (IDI1) interactome to iron chelation in particular to coumarins. We identified several proteins involved in the coumarin synthesis, its secretion and regulation and intracellular iron chelation. Additional data indicate an IDI1-dependent accumulation of phenolic compounds in the root exudate (von der Mark et al., Bauer lab, unpublished).

Taken together, the here presented studies reveal novel insights in iron homeostasis by the identification of protein-protein interactions with a focus on the iron uptake machinery by IRT1 regulation. In particular, the generation of IP-MS-based interactomes has opened up a range of possibilities in the understanding of iron-regulated processes, its related signaling and stress responses.

References

Boisson B, Giglione C, Meinnel T (2003) Unexpected Protein Families Including Cell Defense Components Feature in the N-Myristoylome of a Higher Eukaryote*. Journal of Biological Chemistry **278:** 43418-43429

Bontinck M, Van Leene J, Gadeyne A, De Rybel B, Eeckhout D, Nelissen H, De Jaeger G (2018) Recent Trends in Plant Protein Complex Analysis in a Developmental Context. Frontiers in Plant Science **9**

Brumbarova T, Ivanov R (2019) The Nutrient Response Transcriptional Regulome of Arabidopsis. iScience **19:** 358-368

ElMaghloob Y, Sot B, McIlwraith MJ, Garcia E, Yelland T, Ismail S (2021) ARL3 activation requires the co-GEF BART and effector-mediated turnover. eLife **10:** e64624

Fansa EK, Wittinghofer A (2016) Sorting of lipidated cargo by the Arl2/Arl3 system. Small GTPases **7:** 222-230

Gao F, Robe K, Gaymard F, Izquierdo E, Dubos C (2019) The Transcriptional Control of Iron Homeostasis in Plants: A Tale of bHLH Transcription Factors? Frontiers in Plant Science **10**

Gratz R, von der Mark C, Ivanov R, Brumbarova T (2021) Fe acquisition at the crossroad of calcium and reactive oxygen species signaling. Curr Opin Plant Biol **63:** 102048

Ivanov R, Brumbarova T, Blum A, Jantke A-M, Fink-Straube C, Bauer P (2014) SORTING NEXIN1 is required for modulating the trafficking and stability of the Arabidopsis IRON-REGULATED TRANSPORTER1. The Plant cell **26:** 1294-1307

Kahn RA, Cherfils J, Elias M, Lovering RC, Munro S, Schurmann A (2006) Nomenclature for the human Arf family of GTP-binding proteins: ARF, ARL, and SAR proteins. The Journal of cell biology **172:** 645-650

Khan I, Gratz R, Denezhkin P, Schott-Verdugo SN, Angrand K, Genders L, Basgaran RM, Fink-Straube C, Brumbarova T, Gohlke H, Bauer P, Ivanov R (2019) Calcium-Promoted Interaction between the C2-Domain Protein EHB1 and Metal Transporter IRT1 Inhibits Arabidopsis Iron Acquisition. Plant Physiology **180:** 1564-1581

Riaz N, Guerinot ML (2021) All together now: regulation of the iron deficiency response. Journal of Experimental Botany **72:** 2045-2055

Vernoud V, Horton AC, Yang Z, Nielsen E (2003) Analysis of the small GTPase gene superfamily of Arabidopsis. Plant Physiol **131:** 1191-1208

Xing S, Wallmeroth N, Berendzen KW, Grefen C (2016) Techniques for the Analysis of Protein-Protein Interactions *in Vivo*. Plant physiology **171:** 727-758

Acknowledgements

First of all, I would like to thank Prof. Petra Bauer. Thank you for giving me the opportunity to work on this interesting and challenging topic and for your support over the past years.

I would also like to thank Prof. Kai Stühler for being my mentor during this time and for giving me the opportunity to integrate mass spectrometry into my topic.
I am especially grateful to Daniel and Gereon for their great help and support in my analyses.

A very special thank you goes to the entire Bauer lab with all the colleagues who have accompanied me over the past years.
Especially to Rumen and Tzvetina, thank you for always supporting me with scientific and personal advice. Thank you Ginte for your help and small distractions besides work. A thank you to Ksenia, especially for her magic hands but also our brainstorming sessions. Thanks Jannik for our teamwork and all the little things besides and thanks to Picha, Moni and Elke for your support especially in the last time. Thanks to "my" students, Sam, Katharina and Natalie, who also taught me a lot.
A thank you also to Dani, Anna, Birte, Regina, Sieglinde, Hansi and of course to everyone I may not have mentioned here but definitely not forgotten, for the great time, the productive but also very funny moments, our celebrations, the successes and failures and much more.

A big thank you also to the “SFBers” who let me think outside the box and provided many great memories outside my own work group.

Mein größter Dank gilt meiner Familie und Patrick, die sich immer mit mir für meine Arbeit begeistern konnten. Danke für eure Unterstützung und euer Verständnis in all den Jahren ohne euch wäre dies alles so nicht möglich gewesen.

„Wir alle leben geistig von dem, was uns Menschen in bedeutungsvollen Stunden unseres Lebens gegeben haben.“
Albert Schweitzer